JAERI-M
83-043

EXPERIMENT DATA OF ROSA-III INTEGRAL TEST RUN 7341

(SINGLE FAILURE SERIES TEST NO. 4; FULL ECCS)

February 1983

Yoshinari ANODA, Kunihisa SODA, Kanji TASAKA,
Hideo MURATA, Mitsuhiro SUZUKI, Yasuo KOIZUMI,
Hiroshige KUMAMARU, Motoaki OKAZAKI, Isao TAKESHITA
and Masayoshi SHIBA

日本原子力研究所
Japan Atomic Energy Research Institute

JAERI-Mレポートは，日本原子力研究所が不定期に公刊している研究報告書です。
入手の問合わせは，日本原子力研究所技術情報部情報資料課（〒319-11茨城県那珂郡東海村）あて，お申しこしください。なお，このほかに財団法人原子力弘済会資料センター（〒319-11 茨城県那珂郡東海村日本原子力研究所内）で複写による実費頒布をおこなっております。

JAERI-M reports are issued irregularly.
Inquiries about availability of the reports should be addressed to Information Section, Division of Technical Information, Japan Atomic Energy Research Institute, Tokai-mura, Naka-gun, Ibaraki-ken 319-11, Japan.

編集兼発行　日本原子力研究所
印　　刷　いばらき印刷㈱

JAERI-M 83-043

Experiment Data of ROSA-III Integral Test Run 7341
(Single Failure Series Test No.4; Full ECCS)

Yoshinari ANODA, Kunihisa SODA, Kanji TASAKA,
Hideo MURATA, Mitsuhiro SUZUKI, Yasuo KOIZUMI,
Hiroshige KUMAMARU, Motoaki OKAZAKI, Isao TAKESHITA
and Masayoshi SHIBA

Division of Nuclear Safety Research,
Tokai Research Establishment, JAERI

(Received February 1, 1983)

This report presents the test data of Run 7341 in the single failure test series of the ROSA-III program to conduct the system effect test concerning the response of a BWR during a LOCA with the ECC injection. The ROSA-III test facility is a volumetrically scaled (1/424) system of the BWR/6 with an electrically heated core and the scaled ECCS. Run 7341 is a double-ended break test at the reciculation pump inlet with the assumption that all ECCS function as designed. The test is initiated with the steam dome pressure of 7.28 MPa, the lower plenum subcooling of 11.0 K, the core inlet flow rate of 15.3 kg/s, and the core heat generation rate of 3.55 MW and proceeded as planned. The whole core is quenched after the ECCS actuation and the maximum fuel cladding temperature is 810 K. The effectiveness of ECC injection has been clarified from the comparison of the test results with those of the other test in the series without ECCS.

Keywords; BWR, LOCA, ECCS, Integral Test, ROSA-III Program, Double-ended Break, Recirculation Loop, Data Report

JAERI －M 83－043

ROSA －Ⅲ実験データレポート；Run 7341
（単一故障シリーズ実験№4，全ECCS作動）

日本原子力研究所東海研究所安全工学部
安濃田良成・早田　邦久・田坂　完二・村田　秀男
鈴木　光弘・小泉　安郎・熊丸　博滋・岡崎　元昭
竹下　　功・斯波　正誼

（1983年2月1日受理）

本報は，ROSA－Ⅲ実験装置によるBWR LOCA模擬実験のうち，単一故障実験シリーズのRun 7341の実験データレポートである。ROSA－Ⅲ実験装置は炉心を電気加熱ヒータで模擬した実炉比1／424（体積比）の装置である。Run 7341は，再循環ポンプ吸込側配管の両端破断実験で，全ECCSを作動させた場合のものである。主な初期条件は，蒸気ドーム圧力7.28 MPa，下部プレナム未飽和度11.0 K，炉心入口流量15.3 kg／s，炉心発熱量3.55 MWである。実験は，予定通り行なわれた。ECCS作動後，炉心はクエンチし，最高被覆管表面温度は810 Kであった。ECCS不作動の実験結果との比較から，ECCS注入効果が明らかとなった。

Contents

目　　次

LIST OF TABLES

LIST OF FIGURES

ABBREVIATIONS

ADS	Automatic Depressurization System
AT	Air Tank
AV	Air Actuation Valve
(2)B	(2) inches Pipe of Schedule 80
BN	Boron Nitride
BWR	Boiling Water Reactor
CA	Chromel-Alumel
CHV	Check Valve
CV	Control Valve
CWT	Cooling Water Tank
D	Differential Pressure
DF	Density of Fluid
DL(+100)	Elevation (+100 mm) from the bottom of PV
ECCS	Emergency Core Cooling System
ESF	Engineered Safety Features
F	Flow Rate
Fig.	Figure
FS	Full Scale
FWP	Feed Water Pump
FWT	Feed Water Tank
HPCS	High Pressure Core Spray
HPCSP	High Pressure Core Spray Pump
HPCST	High Pressure Core Spray Tank
HPWP	High Pressure Water Pump
ID	Inner diameter
INC 600	Inconel 600
JP	Jet Pump
K	Kelvin

kg	Kilogram
kPa	Kilopascal
kW	Kilowatt
L	Liquid Level
ℓ	Liter
LB	Liquid Level in Channel Box
LBWR	Large Boiling Water Reactor
LL	Liquid Level in the Lower Plenum
LOCA	Loss-of-Coolant Accident
LOCE	Loss-of-Coolant Experiment
LP	Lower Plenum
LPCI	Low Pressure Coolant Injection
LPCIP	Low Pressure Coolant Injection Pump
LPCIT	Low Pressure Coolant Injection Tank
LPCS	Low Pressure Core Spray
LPCSP	Low Pressure Core Spray Pump
LPCST	Low Pressure Core Spray Tank
M	Momentum Flux
m	Meter
mm	Milimeter
MLHR	Maximum Linear Heat Rate
MPa	Megapascal
MRP	Main Recirculation Pump
MW	Megawatt
N	Rotation Speed
OR	Orifice
P	Pressure
PV	Pressure Vessel
PWT	Pure Water Tank

QOBV	Quick Opening Blowdown Valve
QSV	Quick Shut-off Valve
RCN	Rapid Condencer
ROSA	Rig of Safety Assessment
rpm	Revolution per Minute
S	Signal
s	Second
Sch	Schedule
SUS	Stainless Steel
T	Temperature
T/C	Thermocouple
TC	Temperature of Fluid
TF	Temperature of Fuel
TS	Temperature of Structure Material
V	Valve
VF	Void Fraction
W	Power
W	Watt
WL	Water Level
WSP	Water Supply Pump

1. Introduction

The ROSA(Rig of Safety Assessment)-III program is to study thermal hydraulic response of a BWR (boiling water reactor) during a postulated LOCA (loss-of-coolant accident) with the ECC (emergency core cooling) injection and to provide base data to evaluate the predictability of computer codes developed for LOCA/ECC analysis. The program has been carried out since 1978 at JAERI (Japan Atomic Energy Research Institute) to conduct the system effect testes using the ROSA-III test facility. The ROSA-III test facility consists of the volumetrically scaled primary system of a 1100MW electric BWR/6-251 with an electrically heated core and the scaled ECCS (emergency core cooling system). The objectives of the ROSA-III experimental program are:

(1) To provide data required to evaluate the adequacy and improve the analytical methods currently used to predict the LOCA response of large BWRs. The performance of the ESFs (engineered safety features),with particular emphasis on ECCS (emergency core cooling systems), and the quantitative magins of safety inherent in performance of the ESF are of primary interest.

(2) To identify and investigate any unexpected event(s) or threshold(s) in the response of either the plant or the ESF and develop analytical techniques that adequately describe and account for such unexpected behavior.

The information acquired from LOCEs (loss-of-coolant experiments) is thus used for evaluation and development of LOCA analytical methods and assessment for the quantitative margins of safety of ESFs in response to a LOCA.

Run 7341, conducted on March 28, 1980, is the fourth test in the single failure test series. The test simulates a double-ended break at the recirculation pump inlet side with the assumption that all ECCS function as designed. The primary objectives of the test are to :

(1) Provide reference data to evaluate coolant behavior during a posturated design basis accident LOCA with full ECCS operation.
(2) Evaluate ECCS behavior during a design basis accident conditions and compare the results with those in the single failure tests.

The purpose of this report is to present the data of Run 7341 in an uninterpreted but readily usable form for use by the nuclear community in advance of detailed analysis and interpretation. Section 2 briefly describes the ROSA-III facility configuration; Section 3 discusses the ROSA-III instrumentation system and the methods of obtaining certain physical quantities; and Section 4 summarizes Run 7341 initial conditions and test procedures. Section 5 presents the data with supporting information for data interpretation. Section 6 describes concluding remarks.

2. ROSA-III Test Facility

The ROSA-III facility is a volumetrically scaled (1/424) BWR system with electrically heated core designed to study the response of the primary system, the core, and the ECCS during the postulated LOCA. The facility is instrumented such that various thermal-hydraulic parameters are measured and recoreded during the test. Details of the instrumentations are described in Section 3.

The test facility consists of four major subsystems. These subsystems are: (a) the pressure vessel, (b) the steam line and the feedwater line, (c) the recirculation loops, and (d) the ECCS. Figures 2.1 and 2.2 illustrate configuration of the facility and the pressure vessel internals, respectively. The ROSA-III piping system is shown in Figure 2.3. Table 2.1 compares the major dimensions of the ROSA-III facility to the corresponding dimensions of the large BWR.

The ROSA-III pressure vessel includes various compornents in it simulating the internal structures of the reactor vessel in the BWR system as shown in Fig. 2.4. The interior of the vessel is divided into the core, the lower plenum, the upper plenum, the downcomer annulus, the steam separator, the steam dome, and the steam dryer. The core is consisted of four model fuel assemblies of half length and a

(1) Provide reference data to evaluate coolant behavior during a posturated design basis accident LOCA with full ECCS operation.
(2) Evaluate ECCS behavior during a design basis accident conditions and compare the results with those in the single failure tests.

The purpose of this report is to present the data of Run 7341 in an uninterpreted but readily usable form for use by the nuclear community in advance of detailed analysis and interpretation. Section 2 briefly describes the ROSA-III facility configuration; Section 3 discusses the ROSA-III instrumentation system and the methods of obtaining certain physical quantities; and Section 4 summarizes Run 7341 initial conditions and test procedures. Section 5 presents the data with supporting information for data interpretation. Section 6 describes concluding remarks.

2. ROSA-III Test Facility

The ROSA-III facility is a volumetrically scaled (1/424) BWR system with electrically heated core designed to study the response of the primary system, the core, and the ECCS during the postulated LOCA. The facility is instrumented such that various thermal-hydraulic parameters are measured and recoreded during the test. Details of the instrumentations are described in Section 3.

The test facility consists of four major subsystems. These subsystems are: (a) the pressure vessel, (b) the steam line and the feedwater line, (c) the recirculation loops, and (d) the ECCS. Figures 2.1 and 2.2 illustrate configuration of the facility and the pressure vessel internals, respectively. The ROSA-III piping system is shown in Figure 2.3. Table 2.1 compares the major dimensions of the ROSA-III facility to the corresponding dimensions of the large BWR.

The ROSA-III pressure vessel includes various compornents in it simulating the internal structures of the reactor vessel in the BWR system as shown in Fig. 2.4. The interior of the vessel is divided into the core, the lower plenum, the upper plenum, the downcomer annulus, the steam separator, the steam dome, and the steam dryer. The core is consisted of four model fuel assemblies of half length and a

control rod simulator. Each fuel assembly contains 62 heater rods (Fig.2.5) and two supporting rods which are spaced and supported in a square (8x8) array by lower and upper tie plates. The heater rod is heated electrically with chopped-cosine power distribution along the axis as shown in Fig.2.6. The effective heated length is 1880 mm, one half of the active length of a BWR fuel rod. The electric power supplied to the model fuel assembly "A" is 1.4 times larger than the power suplied to each of the other assemblies (Fig.2.7). Radial power distribution within an assembly is uniform. The orifice plates are inserted at the core inlet to control the core inlet flow.

The steam line is connected to the steam dome of the pressure vessel. The steam line has three branches. The first branch has a control valve to control the steady-state steam dome pressure before blowdown. The second branch simulates the ADS (automatic depressurization system). The third branch has an orifice to simulate the flow resistance of a steam turbine-generator. Immediately after the blowdown initiation, the steam line is changed from the first branch to the third one. The feed water is supplied from the FWT (feed water tank) through the feed water line and feed water sparger in the downcomer annulus.

Figure 2.8 shows the recirculation system consisted of two loops. Each loop is furnished with a recirculation pump and two jet pumps. The jet pumps are installed outside the pressure vessel to simulate the relative volume and the relative hight to the core. Two break simulators and a quick shut-off valve are installed in one of these loops to simulate the various break conditions. Each break simulator consists of an orifice or a nozzle to determine the break size and a blowdown valve to initiate the test. The break mode (the double-ended or split), the break size, and the break location can be changed. The standard break condition is a 200% double-ended shear break at the recirculation pump inlet side with the nozzle diameter of 26.2 mm. Several nozzles of different size are prepared to vary the break size (Fig.2.9).

The ROSA-III facility is furnished with all kinds of the ECCS avilable in the BWR system, i.e., the HPCS (high pressure core spray), the LPCS (low pressure core spray), the LPCI (low pressure coolant injection), and the ADS (automatic depressurization system). The HPCS

and the LPCS provide the cooling water from the top of the core. The LPCI injects the cooling water into the core bypass. Each ECCS consists of a pump, a tank, piping, and a control system.

More detailed information of the facility design is available in Reference (1).

3. Instrumentation

The instrumentation of the ROSA-III is designed to obtain thermo-hydraulic data during the simulated BWR LOCE. The data obtained from the experiment will contribute to the assessment of the analytical computer code. Table 3.1 summerizes instrumentation used in Run 7341.

Instrumentation locations are shown in Fig.3.1 through Fig.3.7. Typical measured parameters in the ROSA-III are pressure, differential pressure, flow rate, electric power, pump speed, fluid and metal temperatures, liquid level, coolant fluid density, on-off type signals and so on.

Pressure and differential pressure transducers are two-wire, direct-current type which convert diaphram displacement to electric capacitance. The pressure lead pipes are either the standard single cylindrical pipes used with condensate pots or, dual concentric cylinders allowing for the circulation of cooling water to prevent flashing of the fluid.

Flow rate is measured by eithe orifice or venturi type flow meters depending on the fluid condition and measurement location.

The temperatures of the fluid, structural materials and heater rod surface are measured with Chromel-Alumel thermocouples (CA T/C) of 1.6 mm dia. or 0.5 mm dia.

Liquid levels are measured by either differential pressure transducers, of the type descrived above, or needle type electrical conductivity probes developed in the ROSA-III program. The probe is distributed along the vessel hight to detect the existance of water or vapor at each level.

Electric power for the simulated fuel rods is controlled to predetermined function of time and it is measured by a fast response electric power meter.

and the LPCS provide the cooling water from the top of the core. The LPCI injects the cooling water into the core bypass. Each ECCS consists of a pump, a tank, piping, and a control system.

More detailed information of the facility design is available in Reference (1).

3. Instrumentation

The instrumentation of the ROSA-III is designed to obtain thermo-hydraulic data during the simulated BWR LOCE. The data obtained from the experiment will contribute to the assessment of the analytical computer code. Table 3.1 summerizes instrumentation used in Run 7341.

Instrumentation locations are shown in Fig.3.1 through Fig.3.7. Typical measured parameters in the ROSA-III are pressure, differential pressure, flow rate, electric power, pump speed, fluid and metal temperatures, liquid level, coolant fluid density, on-off type signals and so on.

Pressure and differential pressure transducers are two-wire, direct-current type which convert diaphram displacement to electric capacitance. The pressure lead pipes are either the standard single cylindrical pipes used with condensate pots or, dual concentric cylinders allowing for the circulation of cooling water to prevent flashing of the fluid.

Flow rate is measured by eithe orifice or venturi type flow meters depending on the fluid condition and measurement location.

The temperatures of the fluid, structural materials and heater rod surface are measured with Chromel-Alumel thermocouples (CA T/C) of 1.6 mm dia. or 0.5 mm dia.

Liquid levels are measured by either differential pressure transducers, of the type descrived above, or needle type electrical conductivity probes developed in the ROSA-III program. The probe is distributed along the vessel hight to detect the existance of water or vapor at each level.

Electric power for the simulated fuel rods is controlled to predetermined function of time and it is measured by a fast response electric power meter.

Pump speed is measured by a pulse generator integral to the pump. On-off signals such as selected valve positions, power control and pump coastdown simulation initiations are detected in order to record the exact signal actuation time.

Fluid density in the pipe is measured by means of gamma densitometers. Preliminary studies indicate three-beam densitometers should be used to determine the flow regime. The gamma source is ^{137}Cs and the detector is a water cooled NaI (Tl) scintillation type.

The data acquisition system (DATAC 2000B, Iwasaki Tsushinki Co.) scans all the 500 channel signals with the frequency up to 30 kHz. The data recorded on magnetic tape is processed by the FACOM M200 system at JAERI. After evaluation, for example by comparing the initial and final pressure values with standard values, the data is reprocessed using the correct conversion factors as determined from the consistency examination.

More detailed information on the instrumentation and the data processing procedure are available in Reference (2).

4. Test Conditions and Experiment Procedure

Run 7341 simulates a 200 % double-ended shear break at the recirculation pump inlet in the recirculation line. The break area is determined by inserting nozzles upstream of the QOBVs (quick opening blowdown valves).

The initial conditions of the test are as follows : The steam dome pressure is 7.28 MPa, the steam dome temperature is 562 K at saturation condition, the core inlet flow rate is 15.3 kg/s, the recirculation flow rate in each of the two recirclation loops is 0.0101 m^3/s, the estimated quality at the core outlet is 13.6 % and the core heat generating rate is 3.55 MW. The detailed conditions are summarized in Table 4.1.

To conduct the test, make-up water is pumped into the primary system of the test facility and electric power is supplied to the core to heat the water in the system and to achieve the saturation condition in the upper portion of the pressure vessel. The core power is 3.55 MW befor the initiation of the test and it is 40 % of the BWR

Pump speed is measured by a pulse generator integral to the pump. On-off signals such as selected valve positions, power control and pump coastdown simulation initiations are detected in order to record the exact signal actuation time.

Fluid density in the pipe is measured by means of gamma densitometers. Preliminary studies indicate three-beam densitometers should be used to determine the flow regime. The gamma source is ^{137}Cs and the detector is a water cooled NaI (Tl) scintillation type.

The data acquisition system (DATAC 2000B, Iwasaki Tsushinki Co.) scans all the 500 channel signals with the frequency up to 30 kHz. The data recorded on magnetic tape is processed by the FACOM M200 system at JAERI. After evaluation, for example by comparing the initial and final pressure values with standard values, the data is reprocessed using the correct conversion factors as determined from the consistency examination.

More detailed information on the instrumentation and the data processing procedure are available in Reference (2).

4. Test Conditions and Experiment Procedure

Run 7341 simulates a 200 % double-ended shear break at the recirculation pump inlet in the recirculation line. The break area is determined by inserting nozzles upstream of the QOBVs (quick opening blowdown valves).

The initial conditions of the test are as follows : The steam dome pressure is 7.28 MPa, the steam dome temperature is 562 K at saturation condition, the core inlet flow rate is 15.3 kg/s, the recirculation flow rate in each of the two recirclation loops is 0.0101 m^3/s, the estimated quality at the core outlet is 13.6 % and the core heat generating rate is 3.55 MW. The detailed conditions are summarized in Table 4.1.

To conduct the test, make-up water is pumped into the primary system of the test facility and electric power is supplied to the core to heat the water in the system and to achieve the saturation condition in the upper portion of the pressure vessel. The core power is 3.55 MW befor the initiation of the test and it is 40 % of the BWR

core power based on the power to volume ratio which is taken the same in the BWR and in the test facility. The core power is changed during the transient after the break initiation as shown in Fig.4.1. The power is kept constant for the first 12.9 seconds and reduced along the curve shown in the figure which simulated the heat transfer rate in a BWR core, composed of the delayed neutron fission power, the decay power of fission products and actinides and stored heat in the fuel pin. There is a high power channel in the core as introduced in the preceding section. The maximum heat generation rate is 13.6 kW/m before the initiation of the test.

The steam line and feedwater line are independent open loops for the present test. The steam line has steady and transient lines as shown in Fig.2.3. The steady line is switched to the transient line at the initiation of the break. The closure of the valves in the steam line and feedwater line is initiated by timer setting. It takes a few seconds to close completely as shown in Table 4.2. The initiating time to close the feedwater line is specified by the evaluation guide for BWR safety. The coolant recirculation pumps are tripped to start coasting down at the break initiation.

Emergency core coolant is injected to the upper plenum during blowdown. Injection from HPCS is started at 27.0 s by timmer setting. Injection from LPCS bigins at a system pressure of 2.26 MPa. The LPCI flow is initiated by experimental control 13.0 s after LPCS initiation. The ADS valve is opened at 120.0 s after the break. The orifice with diameter of 6.0 mm is inserted in ADS line to simulate a typical ADS line flow of a BWR.

The data acquisition is terminated at about 900 s.

5. Data Presentation

Run 7341 is proceeded as previously planned, started by opening two QOBVs (quick opening blowdown valves) and closing the quick shut-off valve between the two break locations. The sequence of major events is shown in Table 5.1.

The feedwater line valve begins to close at 2.0 s and completely closes at 3.2 s. The steam discharge line valve begins to close at 5.0

core power based on the power to volume ratio which is taken the same in the BWR and in the test facility. The core power is changed during the transient after the break initiation as shown in Fig.4.1. The power is kept constant for the first 12.9 seconds and reduced along the curve shown in the figure which simulated the heat transfer rate in a BWR core, composed of the delayed neutron fission power, the decay power of fission products and actinides and stored heat in the fuel pin. There is a high power channel in the core as introduced in the preceding section. The maximum heat generation rate is 13.6 kW/m before the initiation of the test.

The steam line and feedwater line are independent open loops for the present test. The steam line has steady and transient lines as shown in Fig.2.3. The steady line is switched to the transient line at the initiation of the break. The closure of the valves in the steam line and feedwater line is initiated by timer setting. It takes a few seconds to close completely as shown in Table 4.2. The initiating time to close the feedwater line is specified by the evaluation guide for BWR safety. The coolant recirculation pumps are tripped to start coasting down at the break initiation.

Emergency core coolant is injected to the upper plenum during blowdown. Injection from HPCS is started at 27.0 s by timmer setting. Injection from LPCS bigins at a system pressure of 2.26 MPa. The LPCI flow is initiated by experimental control 13.0 s after LPCS initiation. The ADS valve is opened at 120.0 s after the break. The orifice with diameter of 6.0 mm is inserted in ADS line to simulate a typical ADS line flow of a BWR.

The data acquisition is terminated at about 900 s.

5. Data Presentation

Run 7341 is proceeded as previously planned, started by opening two QOBVs (quick opening blowdown valves) and closing the quick shut-off valve between the two break locations. The sequence of major events is shown in Table 5.1.

The feedwater line valve begins to close at 2.0 s and completely closes at 3.2 s. The steam discharge line valve begins to close at 5.0

s and completely closes at 6.5 s. Jet pump suction lines are uncovered at 8.3 s and recirculation pump suction lines are uncovered at 14.0 s in the downcomer. Core power is reduced after 12.9 s to simulate decay heat and stored heat of a nuclear fuel rod. The lower plenum fluid is saturated and initiates flashing at 16.0 s. The liquid level gradually decreased in the core and the core is completely dried out at 54.0 s. Injection from HPCS, LPCS and LPCI initiates at 27.0 s, 63.5 s and 76.5 s, respectively. The feedwater line fluid is saturated and initiates flashing at 61.5 s. ADS valve is opened at 120.0 s. The whole core is quenched by reflooding at 160.0 s. The maximum fuel cladding temperature is 810 K occured at Position 2 (352.5 mm above the mid-plane of the core) in the high power channel.

The test data are presented in Figs. 5.1 through 5.181. In these figures, the each measured quantity is identified by the channel number and the alphabetic characters (See Table 3.1).

Figures 5.1 through 5.7 show the pressures in the pressure vessel and in the recirculation loops. Figures 5.8 through 5.40 show the differential pressures between various positions in the pressure vessel and loops. Figures 5.41 through 5.45 show the flow rates. Figure 5.46 shows the power supplies to the core with the maximum capacities of 550,1800 and 2100 kW. The revolution speeds of the recirculation pumps are shown in Fig 5.47. On-off signals such as the break initiation signal and the valve positioning signals are shown in Figs. 5.48 and 5.49. Figures 5.50 through 5.54 show the fluid temperatures at the various positions in the loops. The cladding temperatures is shown in Figs. 5.55 through 5.103. Figures 5.104 and 5.105 show the fluid temperatures in the core. The wall surface temperatures of the channel box and core support are shown in Figs. 5.106 through 5.112. The fluid temperatures in the lower plenum and guide tube are shown in Figs. 5.113 and 5.114. Figures 5.115 through 5.124 show the fluid temperatures in the upper tie plate. The cladding temperatures and the surface temperatures of channel box are shown in Figs. 5.125 through 5.159, comparing the data at the same elevation. The liquid level signals in the core, the downcomer and the lower plenum are shown in Figs. 5.160 through 5.169. Figures 5.170 and 5.171 show the void fraction in the core, however, these data are not reliable. Figures 5.172 through 5.181 show the fluid densities

measured by the gamma densitometer. Figure 5.182 shows the estimated liquid level in the pressure vessel obtained from the conductivity probe signals in Figs. 5.160 through 5.169. Figures 5.183 and 5.184 show the dryout front and quench front transients in the core.

Figures 5.185 through 5.188 show the average densities. The average density is calculated from the data measured by the three-beam or two-beam gamma densiometers. The beam configurations of gamma densitometers installed in the ROSA-III facility are shown in Figs. 3.8 and 3.9. The average density is calculated as an arithmetric meam of the densities in two or three directions with the weight of the cord length.

For a three beam densitometer,

$$\rho_{av}=0.3221\rho_A+0.43\rho_B+0.2479\rho_C \tag{5.1}$$

where,

ρ_{av}: average density obtained from three-beam gamma densitometer,

ρ_A : density measured by A beam (bottom),

ρ_B : density measured by B beam (middle),

ρ_C : density measured by C beam (top).

For a two-beam densitometer,

$$\rho_{av}=0.5863\rho_A+0.4137\rho_B \tag{5.2}$$

where,

ρ_{av}: average density obtained from a two-beam gamma densitometer,

ρ_A : density measured by A beam (bottom),

ρ_B : density measured by B beam (top).

Fig.5.189 and Fig.190 show the collapsed water levels outside and inside the shroud. The collapsed water level is obtained from the differential pressure in the pressure vessel. The differential pressure may include the flow resistance effect, however, the flow resistance becomes negligible after completion of the recirculation pump coastdown in a short time after break.

Figures. 5.191, 5.192 and 5.193 show the fluid mass inventories in the pressure vessel. The fluid mass inventory is determined from the density and the volumes of liquid outside and inside the shroud,

$$M=\rho_l . Q \tag{5.3}$$

where,

M : fluid mass inventry,

ρ_l: liquid density estimated from the saturation temprature and/or pressure,

Q : liquid volume calculated from the liquid level.

The volume $Q(m^3)$ outside the shroud is given below as a function of hight L(m).

$$\begin{aligned}
Q &= 0 && (\quad L< 0.494) \\
Q &= 0.0225\ L - 0.0111 && (0.494 < L< 1.384) \\
Q &= 0.0697\ L - 0.0769 && (1.384 < L< 1.519) \\
Q &= 0.0225\ L - 0.0048 && (1.519 < L< 3.355) \\
Q &= 0.0801\ L - 0.1980 && (3.355 < L< 4.250) \\
Q &= 0.2443\ L - 0.8959 && (4.250 < L< 4.413) \\
Q &= 0.2611\ L - 0.9700 && (4.413 < L< 4.578) \\
Q &= 0.2504\ L - 0.9211 && (4.578 < L< 4.654) \\
Q &= 0.2375\ L - 0.8610 && (4.654 < L< 4.815) \\
Q &= 0.2866\ L - 1.0974 && (4.815 < L< 4.915) \\
Q &= 0.3396\ L - 1.3580 && (4.915 < L< 5.143) \\
Q &= 0.3607\ L - 1.4665 && (5.143 < L< 5.365) \\
Q &= 0.3848\ L - 1.5960 && (5.365 < L< 5.955) \\
Q &= 0.7111 && (5.955 < L\quad\ )
\end{aligned} \tag{5.4}$$

The volume $Q(m^3)$ inside the shroud is given below as a function of hight L(m).

$$\begin{aligned}
Q &= 0 && (\quad L< 0.0\ ) \\
Q &= 0.2350\ L && (0.0\ < L< 0.497) \\
Q &= 0.1245\ L + 0.0549 && (0.497 < L< 1.354) \\
Q &= 0.0698\ L + 0.1290 && (1.354 < L< 3.589)
\end{aligned}$$

$$
\begin{aligned}
Q &= 0.1648\ L - 0.2120 \quad && (3.589 < L < 3.744) \\
Q &= 0.1963\ L - 0.3299 \quad && (3.744 < L < 4.243) \\
Q &= 0.0196\ L + 0.4199 \quad && (4.243 < L < 4.578) \\
Q &= 0.0186\ L + 0.4244 \quad && (4.578 < L < 4.654) \\
Q &= 0.0410\ L + 0.3201 \quad && (4.654 < L < 5.099) \\
Q &= 0.0196\ L + 0.4292 \quad && (5.099 < L < 5.365) \\
Q &= 0.5344 \quad && (5.365 < L\ \ \ \ )
\end{aligned}
\tag{5.5}
$$

The total fluid mass inventory in the pressure vessel is obtained as the summation of the mass inventories outside and inside the shroud.

The mass decrease by the fluid discharge from the steam line and the fluid mass increase by ECCS water and feedwater injection is shown in Fig. 5.194. The variation of fluid mass inventory with time can be calculated by the following equation.

$$M = \int_0^t \{G + \rho_1 \cdot (W_A + W_B + W_C) + \rho_2 \cdot W_D\}\, dt \tag{5.6}$$

where,

M : mass accumulation,

G : steam discharge flow rate,

ρ_1: density of saturated liquid at 315 K,

ρ_2: density of saturated liquid at 489 K,

W_A: volumetric flow rate of the HPCS,

W_B: volumetric flow rate of the LPCS,

W_C: volumetric flow rate of the LPCI,

W_D: volumetric flow rate of the feedwater.

Fig.5.195 shows the fluid mass discharged from the break. The fluid mass discharge is calculated as follows.

$$M_B = (M_P)_{initial} - M_P + M_F \tag{5.7}$$

where,

M_B: fluid mass discharged from the break,

M_P: fluid mass inventory in the pressure vessel,

M_F: fluid mass increase by the ECCS and the feedwater flow and the decrease by the steam discharge flow

There is a considerable error in the evaluation of the mass inventory M_P in the pressure vessel during a short time after break due to considerable momentum term in the differential pressure data. Therefore, the fluid mass discharge M_B from the break becomes negative during a short time after the break.

Fig.5.196 show the break flow calculated from the integrated break flow given in Fig. 5.195. The break flow is estimated from the mass by differetiation as follows,

$$G_B=\frac{d}{dt}M_B \tag{5.8}$$

where,

G_B: break flow,

M_B: integrated fluid mass discharged from the break.

6. Concluding Remarks

The conduct of ROSA-III Run 7341 and the experimental data acquired for integral systems phenomena during a LOCA following a 200 % double-ended break at the recieculation pump suction with full ECCS actuation are considered to have met the objectives as described in Section 1.

The ROSA-III facility and its instrumentation worked well, and the obtained experimental data are useful for assessing the computer codes for BWR LOCA/ECCS analysis.

Acknowledgment

The authors are grateful to H. Asahi, T. Odaira, S. Sekiguchi, M. Tokoi and J. Tamura of Nuclear Engineering Corporation for their assistance in conducting the experiment. They are also indebted to K. Yamano of Information System Laboratory Corporation for preparing the data plots.

There is a considerable error in the evaluation of the mass inventory M_P in the pressure vessel during a short time after break due to considerable momentum term in the differential pressure data. Therefore, the fluid mass discharge M_B from the break becomes negative during a short time after the break.

Fig.5.196 show the break flow calculated from the integrated break flow given in Fig. 5.195. The break flow is estimated from the mass by differetiation as follows,

$$G_B = -\frac{d}{dt} M_B \tag{5.8}$$

where,

G_B: break flow,

M_B: integrated fluid mass discharged from the break.

6. Concluding Remarks

The conduct of ROSA-III Run 7341 and the experimental data acquired for integral systems phenomena during a LOCA following a 200 % double-ended break at the recieculation pump suction with full ECCS actuation are considered to have met the objectives as described in Section 1.

The ROSA-III facility and its instrumentation worked well, and the obtained experimental data are useful for assessing the computer codes for BWR LOCA/ECCS analysis.

Acknowledgment

The authors are grateful to H. Asahi, T. Odaira, S. Sekiguchi, M. Tokoi and J. Tamura of Nuclear Engineering Corporation for their assistance in conducting the experiment. They are also indebted to K. Yamano of Information System Laboratory Corporation for preparing the data plots.

There is a considerable error in the evaluation of the mass inventory M_P in the pressure vessel during a short time after break due to considerable momentum term in the differential pressure data. Therefore, the fluid mass discharge M_B from the break becomes negative during a short time after the break.

Fig.5.196 show the break flow calculated from the integrated break flow given in Fig. 5.195. The break flow is estimated from the mass by differetiation as follows,

$$G_B=\frac{d}{dt}M_B \tag{5.8}$$

where,

G_B: break flow,

M_B: integrated fluid mass discharged from the break.

6. Concluding Remarks

The conduct of ROSA-III Run 7341 and the experimental data acquired for integral systems phenomena during a LOCA following a 200 % double-ended break at the recieculation pump suction with full ECCS actuation are considered to have met the objectives as described in Section 1.

The ROSA-III facility and its instrumentation worked well, and the obtained experimental data are useful for assessing the computer codes for BWR LOCA/ECCS analysis.

Acknowledgment

The authors are grateful to H. Asahi, T. Odaira, S. Sekiguchi, M. Tokoi and J. Tamura of Nuclear Engineering Corporation for their assistance in conducting the experiment. They are also indebted to K. Yamano of Information System Laboratory Corporation for preparing the data plots.

References

(1) ANODA,Y. et.al., " ROSA-III System Description ", JAERI-M 9243 (1980).

(2) SOBAJIMA,M. et.al., " Instrumentation and Data Processing for ROSA-III Test ", JAERI-M 8499 (1979) (in Japanese).

Table 2.1 Primary Characteristics of BWR/6 and ROSA-III

	BWR-6	ROSA-III	BWR/ROSA
No. of Recirculation Loops	2	2	1
No. of Jet Pumps	24	4	6
No. of Separators	251	1	251
No. of Fuel Assemblies	848	4	212
Active Fuel Length (m)	3.76	1.88	2
Total Volume (m^3)	621	1.42	437
Power (MW)	3800	4.4	864
Pressure (MPa)	7.23	7.23	1
Core Flow (kg/s)	1.54×10^4	36.4	424
Recirculation Flow (ℓ/s)	2970	7.01	424
Feedwater Flow (kg/s)	2060	4.86	424
Feedwater Temperature (K)	489	489	1

Table 3.1 ROSA-III Measurement List

** MEASUREMENT LIST **

1CH.- 50CH.

CH.	ITEM	SYMBOL	ID.		LOCATION	FIG.NO.	RANGE				ACCURACY
1	PRESS.	P- 1	PA	1	LOWER PLENUM	AMPLIFIER FAILED	0.100	-	10.0	MPA	1.08%FS
2	PRESS.	P- 2	PA	2	UPPER PLENUM	FIG.5.1	0.100	-	10.0	MPA	1.08%FS
3	PRESS.	P- 3	PA	3	STEAM DOME	FIG.5.1	0.100	-	10.0	MPA	1.08%FS
4	PRESS.	P- 4	PA	4	DOWNCOMER BOTTOM	FIG.5.1	0.100	-	10.0	MPA	1.08%FS
5	PRESS.	P- 5	PA	5	JP-3 DRIVE	FIG.5.2	0.100	-	10.0	MPA	1.08%FS
6	PRESS.	P- 6	PA	6	JP-4 DRIVE	FIG.5.2	0.100	-	10.0	MPA	1.08%FS
7	PRESS.	P- 7	PA	7	JP-3 SUCTION	FIG.5.2	0.100	-	10.0	MPA	1.08%FS
8	PRESS.	P- 8	PA	8	JP-4 SUCTION	FIG.5.2	0.100	-	10.0	MPA	1.08%FS
9	PRESS.	P- 9	PA	9	MRP-1 SUCTION	FIG.5.3	0.100	-	10.0	MPA	1.08%FS
10	PRESS.	P-10	PA	10	MRP-2 SUCTION	FIG.5.4	0.100	-	10.0	MPA	1.08%FS
11	PRESS.	P-11	PA	11	MRP-2 DELIVERY	FIG.5.4	0.100	-	10.0	MPA	1.08%FS
12	PRESS.	P-12	PA	12	BREAK A UPSTREAM	FIG.5.5	0.100	-	10.0	MPA	1.08%FS
13	PRESS.	P-13	PA	13	BREAK A DOWNSTREAM	FIG.5.5	0.100	-	10.0	MPA	1.08%FS
14	PRESS.	P-14	PA	14	BREAK B UPSTREAM	FIG.5.6	0.100	-	10.0	MPA	1.08%FS
15	PRESS.	P-15	PA	15	BREAK B DOWNSTREAM	FIG.5.6	0.100	-	10.0	MPA	1.08%FS
16	PRESS.	P-16	PA	16	STEAM LINE	FIG.5.7	0.100	-	10.0	MPA	1.08%FS
17	PRESS.	P-17	PA	17	JP-1,2 OUTLET SPOOL	NOT MEASURED	0.100	-	10.0	MPA	1.08%FS
18	PRESS.	P-18	PA	18	JP-3,4 OUTLET SPOOL	NOT MEASURED	0.100	-	10.0	MPA	1.08%FS
19	PRESS.	P-19	PA	19	BREAK A SPOOL PIECE	NOT MEASURED	0.100	-	10.0	MPA	1.08%FS
20	PRESS.	P-30	PA	20	BREAK B SPOOL PIECE	NOT MEASURED	0.100	-	10.0	MPA	1.08%FS
21	DIFF.P.	D- 1	PD	21	LOWER PL.-UPPER PL.	FIG.5.8	-50.0	-	350.	KPA	0.63%FS
22	DIFF.P.	D- 2	PD	22	UPPER PL.-STEAM DOME	FIG.5.9	-10.0	-	90.0	KPA	0.63%FS
23	DIFF.P.	D- 3	PD	23	LOWER PLNUM HEAD	NOT MEASURED	0.0	-	150.	KPA	0.63%FS
24	DIFF.P.	D- 4	PD	24	DOWNCOMER HEAD	FIG.5.10	0.0	-	100.	KPA	0.63%FS
25	DIFF.P.	D- 5	PD	25	PV BOTTOM-TOP	FIG.5.11	-100.	-	900.	KPA	0.63%FS
26	DIFF.P.	D- 6	PD	26	JP-1 DISCH.-SUCTION	FIG.5.12	-100.	-	300.	KPA	0.63%FS
27	DIFF.P.	D- 7	PD	27	JP-1 DRIVE -SUCTION	FIG.5.13	0.0	-	2.50	MPA	0.63%FS
28	DIFF.P.	D- 8	PD	28	JP-2 DISCH.-SUCTION	FIG.5.12	-100.	-	300.	KPA	0.63%FS
29	DIFF.P.	D- 9	PD	29	JP-2 DRIVE -SUCTION	FIG.5.13	0.0	-	2.50	MPA	0.63%FS
30	DIFF.P.	D-10	PD	30	JP-3 DISCH.-SUCTION	FIG.5.14	-100.	-	300.	KPA	0.63%FS
31	DIFF.P.	D-11	PD	31	JP-3 DRIVE -SUCTION	FIG.5.15	-1.00	-	2.00	MPA	0.63%FS
32	DIFF.P.	D-12	PD	32	JP-4 DISCH.-SUCTION	FIG.5.14	-100.	-	300.	KPA	0.63%FS
33	DIFF.P.	D-13	PD	33	JP-4 DRIVE -SUCTION	FIG.5.15	-0.500	-	2.50	MPA	0.63%FS
34	DIFF.P.	D-14	PD	34	MRP-1 DELIV.-SUCTION	FIG.5.16	-0.100	-	2.50	MPA	0.63%FS
35	DIFF.P.	D-15	PD	35	MRP-2 DELIV.-SUCTION	FIG.5.17	-0.100	-	2.50	MPA	0.63%FS
36	DIFF.P.	D-16	PD	36	DC BOTTOM- MRP-1 SUC.	FIG.5.18	-50.0	-	50.0	KPA	0.63%FS
37	DIFF.P.	D-17	PD	37	MRP1 DELIV.-JP1 DRIVE	FIG.5.19	0.0	-	250.	KPA	0.63%FS
38	DIFF.P.	D-18	PD	38	MRP1 DELIV.-JP2 DRIVE	FIG.5.20	0.0	-	250.	KPA	0.63%FS
39	DIFF.P.	D-19	PD	39	DC MIDDLE-JP1 SUCTION	FIG.5.21	0.0	-	250.	KPA	0.63%FS
40	DIFF.P.	D-20	PD	40	DC MIDDLE-JP2 SUCTION	FIG.5.22	0.0	-	250.	KPA	0.63%FS
41	DIFF.P.	D-21	PD	41	JP1 DISCH.-LOWER PL.	FIG.5.23	-100.	-	100.	KPA	0.63%FS
42	DIFF.P.	D-22	PD	42	JP2 DISCH.-LOWER PL.	FIG.5.24	-100.	-	100.	KPA	0.63%FS
43	DIFF.P.	D-23	PD	43	DC BOTTOM- BREAK B	FIG.5.25	0.0	-	2.00	MPA	0.63%FS
44	DIFF.P.	D-24	PD	44	BREAK B- BREAK A	FIG.5.26	0.0	-	100.	KPA	0.63%FS
45	DIFF.P.	D-25	PD	45	BREAK A- MRP2 SUCTION	FIG.5.27	-500.	-	100.	KPA	0.63%FS
46	DIFF.P.	D-26	PD	46	MRP2 DELIV.-JP3 DRIVE	FIG.5.28	-500.	-	500.	KPA	0.63%FS
47	DIFF.P.	D-27	PD	47	MRP2 DELIV.-JP4 DRIVE	FIG.5.29	-500.	-	500.	KPA	0.63%FS
48	DIFF.P.	D-28	PD	48	DC MIDDLE-JP3 SUCTION	FIG.5.30	-250.	-	250.	KPA	0.63%FS
49	DIFF.P.	D-29	PD	49	DC MIDDLE-JP4 SUCTION	FIG.5.31	-250.	-	250.	KPA	0.63%FS
50	DIFF.P.	D-30	PD	50	JP3 DISCH.-BELOW Y	FIG.5.32	-100.	-	100.	KPA	0.63%FS

Table 3.1 (Continued)

** MEASUREMENT LIST **

51CH.- 100CH.

CH.	ITEM	SYMBOL	ID.		LOCATION	FIG.NO.	RANGE				ACCURACY
51	DIFF.P.	D-31	PD	51	JP4 DISCH.-BELOW Y	FIG.5.33	-100.	-	100.	KPA	0.63%FS
52	DIFF.P.	D-32	PD	52	BELOW Y -LOWER PLENUM	FIG.5.34	-50.0	-	50.0	KPA	0.63%FS
53	DIFF.P.	D-33	PD	53	LOWER PL.-DC MIDDLE	FIG.5.35	-250.	-	250.	KPA	0.63%FS
54	DIFF.P.	D-34	PD	54	LOWER PL.-DC BOTTOM	FIG.5.36	-250.	-	250.	KPA	0.63%FS
55	DIFF.P.	D-35	PD	55	DC BOTTOM-DC MIDDLE	FIG.5.37	-50.0	-	50.0	KPA	0.63%FS
56	DIFF.P.	D-36	PD	56	DC MIDDLE-STEAM DOME	FIG.5.38	-50.0	-	50.0	KPA	0.63%FS
57	DIFF.P.	D-37	PD	57	LOWER PL.MID-UPPER PL	FIG.5.39	0.0	-	250.	KPA	0.63%FS
58	DIFF.P.	D-38	PD	58	LOWER PL.BOTTOM-MID.	FIG.5.40	0.0	-	50.0	KPA	0.63%FS
59	DIFF.P.	D-39	PD	59	UPPER PLENUM HEAD	NOT MEASURED	0.0	-	20.0	KPA	0.63%FS
60	DIFF.P.	D-40	PD	60	CHANNEL ORIFICE A	NOT MEASURED	0.0	-	100.	KPA	0.63%FS
61	DIFF.P.	D-41	PD	61	CHANNEL ORIFICE B	NOT MEASURED	0.0	-	100.	KPA	0.63%FS
62	DIFF.P.	D-42	PD	62	CHANNEL ORIFICE C	NOT MEASURED	0.0	-	100.	KPA	0.63%FS
63	DIFF.P.	D-43	PD	63	CHANNEL ORIFICE D	NOT MEASURED	0.0	-	100.	KPA	0.63%FS
64	DIFF.P.	D-44	PD	64	BYPASS HOLE	NOT MEASURED	0.0	-	200.	KPA	0.63%FS
65	MASS.F.	F- 1	FM	65	MAIN STEAM LINE	SENSOR FAILED	0.0	-	15.0	KG/S	0.92%FS
66	MASS.F.	F- 2	FM	66	ADS STEAM LINE	FIG.5.41	0.0	-	3.00	KG/S	0.92%FS
67	MASS.F.	F- 3	FM	67	RCN A CONDENSED WATER	NOT MEASURED	0.0	-	250.	KG/S	1.40%FS
68	MASS.F.	F- 4	FM	68	RCN A COOLING WATER	NOT MEASURED	0.0	-	250.	KG/S	1.40%FS
69	MASS.F.	F- 5	FM	69	RCN B CONDENSED WATER	NOT MEASURED	0.0	-	250.	KG/S	1.40%FS
70	MASS.F.	F- 6	FM	70	RCN B COOLING WATER	NOT MEASURED	0.0	-	250.	KG/S	1.40%FS
71	VOL.F.	F- 7	FV	71	HPCS (UPPER PLENUM)	FIG.5.42	0.0	-	0.250E-02	M3/S	0.79%FS
72	VOL.F.	F- 9	FV	72	LPCS (UPPER PLENUM)	FIG.5.42	0.0	-	0.250E-02	M3/S	0.79%FS
73	VOL.F.	F-11	FV	73	LPCI (IN-SHROUD)	FIG.5.42	0.0	-	0.830E-02	M3/S	0.79%FS
74	VOL.F.	F-15	FV	74	FEED WATER	FIG.5.43	0.0	-	0.100E-01	M3/S	0.79%FS
75	VOL.F.	F-17	FV	75	JP1 DISCHARGE	FIG.5.44	0.0	-	0.170E-01	M3/S	0.88%FS
76	VOL.F.	F-18	FV	76	JP2 DISCHARGE	FIG.5.44	0.0	-	0.170E-01	M3/S	0.88%FS
77	VOL.F.	F-19	FV	77	JP3 DISCH. POSITIVE	FIG.5.45	0.0	-	0.170E-01	M3/S	0.92%FS
78	VOL.F.	F-20	FV	78	JP3 DISCH. NEGATIVE	NOT PRESENTED	0.0	-	0.500E-02	M3/S	0.92%FS
79	VOL.F.	F-21	FV	79	JP4 DISCH. POSITIVE	FIG.5.45	0.0	-	0.170E-01	M3/S	0.92%FS
80	VOL.F.	F-22	FV	80	JP4 DISCH. NEGATIVE	NOT PRESENTED	0.0	-	0.500E-02	M3/S	0.92%FS
81	MASS.F.	F-23	FM	81	JP1,2 OUTLET SPOOL	NOT MEASURED	0.0	-	30.0	KG/S	1.40%FS
82	MASS.F.	F-24	FM	82	JP3,4 OUTLET SPOOL	NOT MEASURED	0.0	-	30.0	KG/S	1.40%FS
83	MASS.F.	F-25	FM	83	BREAK A SPOOL PIECE	NOT MEASURED	0.0	-	30.0	KG/S	1.40%FS
84	MASS.F.	F-26	FM	84	BREAK B SPOOL PIECE	NOT MEASURED	0.0	-	30.0	KG/S	1.40%FS
85	POWER	W- 1	WE	85	550 KW POWER SUPPLIER	FIG.5.46	0.0	-	550.	KW	1.00%FS
86	POWER	W- 2	WE	86	1800 KW POWER SUPPLIER	FIG.5.46	0.0	-	0.170E+04	KW	1.00%FS
87	POWER	W- 3	WE	87	2100 KW POWER SUPPLIER	FIG.5.46	0.0	-	0.210E+04	KW	1.00%FS
88	REV.	N- 1	SR	88	MRP-1	FIG.5.47	0.0	-	0.500E+04	RPM	1.08%FS
89	REV.	N- 2	SR	89	MRP-2	FIG.5.47	0.0	-	0.500E+04	RPM	1.08%FS
90	SIGNAL	S- 1	EV	90	BREAK SIGNAL A	FIG.5.48					
91	SIGNAL	S- 2	EV	91	BREAK SIGNAL B	FIG 5.48					
92	SIGNAL	S- 3	EV	92	QSV SIGNAL	FIG 5.48					
93	SIGNAL	S-10	EV	93	MSIV SIGNAL	FIG 5.48					
94	SIGNAL	S-11	EV	94	STEAM LINE VALVE	FIG.5.48					
95	SIGNAL	S-12	EV	95	ADS VALVE	FIG.5.49					
96	FLUID T.	T- 1	TE	96	LOWER PLENUM	FIG.5.50	273.	-	673.	K	0.64%FS
97	FLUID T.	T- 2	TE	97	UPPER PLENUM	FIG.5.50	273.	-	673.	K	0.64%FS
98	FLUID T.	T- 3	TE	98	STEAM DOME	FIG.5.50	273.	-	673.	K	0.64%FS
99	FLUID T.	T- 4	TE	99	UPPER DOWNCOMER	FIG.5.50	273.	-	673.	K	0.64%FS
100	FLUID T.	T- 5	TE	100	LOWER DOWNCOMER	FIG.5.50	273.	-	673.	K	0.64%FS

Table 3.1 (Continued)

** MEASUREMENT LIST **　　101CH.- 150CH.

CH.	ITEM	SYMBOL	ID.	LOCATION	FIG.NO.	RANGE	ACCURACY
101	FLUID T.	T- 6	TE 101	JP-1 DRIVE	FIG.5.51	273. - 673. K	0.64%FS
102	FLUID T.	T- 7	TE 102	JP-2 DRIVE	FIG.5.51	273. - 673. K	0.64%FS
103	FLUID T.	T- 8	TE 103	JP-3 DRIVE	FIG.5.52	273. - 673. K	0.64%FS
104	FLUID T.	T- 9	TE 104	JP-4 DRIVE	FIG.5.52	273. - 673. K	0.64%FS
105	FLUID T.	T-10	TE 105	JP-1 DISCHARGE	FIG.5.51	273. - 673. K	0.64%FS
106	FLUID T.	T-11	TE 106	JP-2 DISCHARGE	FIG.5.51	273. - 673. K	0.64%FS
107	FLUID T.	T-12	TE 107	JP-3 DISCHARGE	FIG.5.52	273. - 673. K	0.64%FS
108	FLUID T.	T-13	TE 108	JP-4 DISCHARGE	FIG.5.52	273. - 673. K	0.64%FS
109	FLUID T.	T-14	TE 109	MRP-1 SUCTION	FIG.5.51	273. - 673. K	0.64%FS
110	FLUID T.	T-15	TE 110	MRP-1 DELIVERY	FIG.5.51	273. - 673. K	0.64%FS
111	FLUID T.	T-16	TE 111	MRP-2 SUCTION	FIG.5.52	273. - 673. K	0.64%FS
112	FLUID T.	T-17	TE 112	MRP-2 DELIVERY	FIG.5.52	273. - 673. K	0.64%FS
113	FLUID T.	T-18	TE 113	BREAK A UPSTREAM	FIG.5.53	273. - 673. K	0.64%FS
114	FLUID T.	T-19	TE 114	BREAK B UPSTREAM	FIG.5.53	273. - 673. K	0.64%FS
115	FLUID T.	T-20	TE 115	RCN A CONDENSED WATER	NOT MEASURED	273. - 673. K	0.64%FS
116	FLUID T.	T-21	TE 116	RCN B CONDENSED WATER	NOT MEASURED	273. - 673. K	0.64%FS
117	FLUID T.	T-22	TE 117	DISCHARGED STEAM	FIG.5.54	273. - 673. K	0.64%FS
118	FLUID T.	T-24	TE 118	JP-1,2 OUTLET SPOOL	NOT MEASURED	273. - 673. K	0.64%FS
119	FLUID T.	T-25	TE 119	JP-3,4 OUTLET SPOOL	NOT MEASURED	273. - 673. K	0.64%FS
120	FLUID T.	T-26	TE 120	BREAK A SPOOL PIECE	NOT MEASURED	273. - 673. K	0.64%FS
121	FLUID T.	T-37	TE 121	BREAK B SPOOL PIECE	NOT MEASURED	273. - 673. K	0.64%FS
122	TEMP.	TF- 1	TE 122	A11 FUEL ROD POS.1	FIG.5.55, 125	273. - 0.147E+04 K	0.64%FS
123	TEMP.	TF- 2	TE 123	A11 FUEL ROD POS.2	FIG.5.55, 126	273. - 0.147E+04 K	0.64%FS
124	TEMP.	TF- 3	TE 124	A11 FUEL ROD POS.3	FIG.5.55, 127	273. - 0.147E+04 K	0.64%FS
125	TEMP.	TF- 4	TE 125	A11 FUEL ROD POS.4	FIG.5.55, 128	273. - 0.147E+04 K	0.64%FS
126	TEMP.	TF- 5	TE 126	A11 FUEL ROD POS.5	FIG.5.55, 129	273. - 0.147E+04 K	0.64%FS
127	TEMP.	TF- 6	TE 127	A11 FUEL ROD POS.6	FIG.5.55, 130	273. - 0.147E+04 K	0.64%FS
128	TEMP.	TF- 7	TE 128	A11 FUEL ROD POS.7	FIG.5.55, 131	273. - 0.147E+04 K	0.64%FS
129	TEMP.	TF- 8	TE 129	A12 FUEL ROD POS.1	FIG.5.56	273. - 0.147E+04 K	0.64%FS
130	TEMP.	TF- 9	TE 130	A12 FUEL ROD POS.2	FIG.5.56	273. - 0.147E+04 K	0.64%FS
131	TEMP.	TF- 10	TE 131	A12 FUEL ROD POS.3	FIG.5.56	273. - 0.147E+04 K	0.64%FS
132	TEMP.	TF- 11	TE 132	A12 FUEL ROD POS.4	FIG.5.56	273. - 0.147E+04 K	0.64%FS
133	TEMP.	TF- 12	TE 133	A12 FUEL ROD POS.5	FIG.5.56	273. - 0.147E+04 K	0.64%FS
134	TEMP.	TF- 13	TE 134	A12 FUEL ROD POS.6	FIG.5.56	273. - 0.147E+04 K	0.64%FS
135	TEMP.	TF- 14	TE 135	A12 FUEL ROD POS.7	FIG.5.56	273. - 0.147E+04 K	0.64%FS
136	TEMP.	TF- 15	TE 136	A13 FUEL ROD POS.1	FIG.5.57	273. - 0.147E+04 K	0.64%FS
137	TEMP.	TF- 16	TE 137	A13 FUEL ROD POS.2	FIG.5.57	273. - 0.147E+04 K	0.64%FS
138	TEMP.	TF- 17	TE 138	A13 FUEL ROD POS.3	FIG.5.57	273. - 0.147E+04 K	0.64%FS
139	TEMP.	TF- 18	TE 139	A13 FUEL ROD POS.4	FIG.5.57	273. - 0.147E+04 K	0.64%FS
140	TEMP.	TF- 19	TE 140	A13 FUEL ROD POS.5	FIG.5.57	273. - 0.147E+04 K	0.64%FS
141	TEMP.	TF- 20	TE 141	A13 FUEL ROD POS.6	FIG.5.57	273. - 0.147E+04 K	0.64%FS
142	TEMP.	TF- 21	TE 142	A13 FUEL ROD POS.7	FIG.5.57	273. - 0.147E+04 K	0.64%FS
143	TEMP.	TF- 22	TE 143	A14 FUEL ROD POS.1	FIG.5.58, 125	273. - 0.147E+04 K	0.64%FS
144	TEMP.	TF- 23	TE 144	A14 FUEL ROD POS.2	FIG.5.58, 126	273. - 0.147E+04 K	0.64%FS
145	TEMP.	TF- 24	TE 145	A14 FUEL ROD POS.3	FIG.5.58, 127	273. - 0.147E+04 K	0.64%FS
146	TEMP.	TF- 25	TE 146	A14 FUEL ROD POS.4	FIG.5.58, 128	273. - 0.147E+04 K	0.64%FS
147	TEMP.	TF- 26	TE 147	A14 FUEL ROD POS.5	FIG.5.58, 129	273. - 0.147E+04 K	0.64%FS
148	TEMP.	TF- 27	TE 148	A14 FUEL ROD POS.6	FIG.5.58, 130	273. - 0.147E+04 K	0.64%FS
149	TEMP.	TF- 28	TE 149	A14 FUEL ROD POS.7	FIG.5.58, 131	273. - 0.147E+04 K	0.64%FS
150	TEMP.	TF- 29	TE 150	A15 FUEL ROD POS.1	FIG.5.74	273. - 0.147E+04 K	0.64%FS

Table 3.1 (Continued)

** MEASUREMENT LIST ** 151CH.- 200CH.

CH.	ITEM	SYMBOL	ID.	LOCATION	FIG.NO.	RANGE	ACCURACY
151	TEMP.	TF- 30	TE 151	A15 FUEL ROD POS.4	FIG.5.74	273. - 0.147E+04 K	0.64%FS
152	TEMP.	TF- 31	TE 152	A17 FUEL ROD POS.1	FIG.5.75	273. - 0.147E+04 K	0.64%FS
153	TEMP.	TF- 32	TE 153	A17 FUEL ROD POS.4	FIG.5.75	273. - 0.147E+04 K	0.64%FS
154	TEMP.	TF- 33	TE 154	A22 FUEL ROD POS.1	FIG.5.59, 125	273. - 0.147E+04 K	0.64%FS
155	TEMP.	TF- 34	TE 155	A22 FUEL ROD POS.2	FIG.5.59, 126	273. - 0.147E+04 K	0.64%FS
156	TEMP.	TF- 35	TE 156	A22 FUEL ROD POS.3	FIG.5.59, 127	273. - 0.147E+04 K	0.64%FS
157	TEMP.	TF- 36	TE 157	A22 FUEL ROD POS.4	FIG.5.59, 128	273. - 0.125E+04 K	0.64%FS
158	TEMP.	TF- 37	TE 158	A22 FUEL ROD POS.5	CHANNEL FAILED	273. - 0.125E+04 K	0.64%FS
159	TEMP.	TF- 38	TE 159	A22 FUEL ROD POS.6	CHANNEL FAILED	273. - 0.125E+04 K	0.64%FS
160	TEMP.	TF- 39	TE 160	A22 FUEL ROD POS.7	CHANNEL FAILED	273. - 0.125E+04 K	0.64%FS
161	TEMP.	TF- 40	TE 161	A23 FUEL ROD POS.1	FIG.5.60	273. - 0.125E+04 K	0.64%FS
162	TEMP.	TF- 41	TE 162	A23 FUEL ROD POS.2	FIG.5.60	273. - 0.125E+04 K	0.64%FS
163	TEMP.	TF- 42	TE 163	A23 FUEL ROD POS.3	FIG.5.60	273. - 0.125E+04 K	0.64%FS
164	TEMP.	TF- 43	TE 164	A23 FUEL ROD POS.4	FIG.5.60	273. - 0.125E+04 K	0.64%FS
165	TEMP.	TF- 44	TE 165	A23 FUEL ROD POS.5	FIG.5.60	273. - 0.125E+04 K	0.64%FS
166	TEMP.	TF- 45	TE 166	A23 FUEL ROD POS.6	FIG.5.60	273. - 0.125E+04 K	0.64%FS
167	TEMP.	TF- 46	TE 167	A23 FUEL ROD POS.7	FIG.5.60	273. - 0.125E+04 K	0.64%FS
168	TEMP.	TF- 47	TE 168	A24 FUEL ROD POS.1	FIG.5.61, 125	273. - 0.125E+04 K	0.64%FS
169	TEMP.	TF- 48	TE 169	A24 FUEL ROD POS.2	FIG.5.61, 126	273. - 0.125E+04 K	0.64%FS
170	TEMP.	TF- 49	TE 170	A24 FUEL ROD POS.3	FIG.5.61, 127	273. - 0.125E+04 K	0.64%FS
171	TEMP.	TF- 50	TE 171	A24 FUEL ROD POS.4	FIG.5.61, 128	273. - 0.125E+04 K	0.64%FS
172	TEMP.	TF- 51	TE 172	A24 FUEL ROD POS.5	FIG.5.61, 129	273. - 0.125E+04 K	0.64%FS
173	TEMP.	TF- 52	TE 173	A24 FUEL ROD POS.6	FIG.5.61, 130	273. - 0.125E+04 K	0.64%FS
174	TEMP.	TF- 53	TE 174	A24 FUEL ROD POS.7	FIG.5.61, 131	273. - 0.125E+04 K	0.64%FS
175	TEMP.	TF- 54	TE 175	A26 FUEL ROD POS.1	FIG.5.76	273. - 0.125E+04 K	0.64%FS
176	TEMP.	TF- 55	TE 176	A26 FUEL ROD POS.4	FIG.5.76	273. - 0.125E+04 K	0.64%FS
177	TEMP.	TF- 56	TE 177	A28 FUEL ROD POS.1	FIG.5.77	273. - 0.125E+04 K	0.64%FS
178	TEMP.	TF- 57	TE 178	A28 FUEL ROD POS.4	FIG.5.77	273. - 0.125E+04 K	0.64%FS
179	TEMP.	TF- 58	TE 179	A31 FUEL ROD POS.1	FIG.5.78	273. - 0.125E+04 K	0.64%FS
180	TEMP.	TF- 59	TE 180	A31 FUEL ROD POS.4	FIG.5.78	273. - 0.125E+04 K	0.64%FS
181	TEMP.	TF- 60	TE 181	A33 FUEL ROD POS.1	FIG.5.62, 125, 139	273. - 0.125E+04 K	0.64%FS
182	TEMP.	TF- 61	TE 182	A33 FUEL ROD POS.2	FIG.5.62, 126, 140	273. - 0.125E+04 K	0.64%FS
183	TEMP.	TF- 62	TE 183	A33 FUEL ROD POS.3	FIG.5.62, 127, 141	273. - 0.125E+04 K	0.64%FS
184	TEMP.	TF- 63	TE 184	A33 FUEL ROD POS.4	FIG.5.62, 128, 142	273. - 0.125E+04 K	0.64%FS
185	TEMP.	TF- 64	TE 185	A33 FUEL ROD POS.5	FIG.5.62, 129, 143	273. - 0.125E+04 K	0.64%FS
186	TEMP.	TF- 65	TE 186	A33 FUEL ROD POS.6	FIG.5.62, 130, 144	273. - 0.125E+04 K	0.64%FS
187	TEMP.	TF- 66	TE 187	A33 FUEL ROD POS.7	FIG.5.62, 131, 145	273. - 0.125E+04 K	0.64%FS
188	TEMP.	TF- 67	TE 188	A34 FUEL ROD POS.1	FIG.5.63, 125	273. - 0.125E+04 K	0.64%FS
189	TEMP.	TF- 68	TE 189	A34 FUEL ROD POS.2	FIG.5.63, 126	273. - 0.125E+04 K	0.64%FS
190	TEMP.	TF- 69	TE 190	A34 FUEL ROD POS.3	FIG.5.63, 127	273. - 0.125E+04 K	0.64%FS
191	TEMP.	TF- 70	TE 191	A34 FUEL ROD POS.4	FIG.5.63, 128	273. - 0.125E+04 K	0.64%FS
192	TEMP.	TF- 71	TE 192	A34 FUEL ROD POS.5	FIG.5.63, 129	273. - 0.125E+04 K	0.64%FS
193	TEMP.	TF- 72	TE 193	A34 FUEL ROD POS.6	FIG.5.63, 130	273. - 0.125E+04 K	0.64%FS
194	TEMP.	TF- 73	TE 194	A34 FUEL ROD POS.7	FIG.5.63, 131	273. - 0.125E+04 K	0.64%FS
195	TEMP.	TF- 74	TE 195	A35 FUEL ROD POS.1	FIG.5.79	273. - 0.125E+04 K	0.64%FS
196	TEMP.	TF- 75	TE 196	A35 FUEL ROD POS.4	FIG.5.79	273. - 0.125E+04 K	0.64%FS
197	TEMP.	TF- 76	TE 197	A37 FUEL ROD POS.1	FIG.5.80	273. - 0.125E+04 K	0.64%FS
198	TEMP.	TF- 77	TE 198	A37 FUEL ROD POS.4	FIG.5.80	273. - 0.125E+04 K	0.64%FS
199	TEMP.	TF- 78	TE 199	A42 FUEL ROD POS.1	FIG.5.81	273. - 0.125E+04 K	0.64%FS
200	TEMP.	TF- 79	TE 200	A42 FUEL ROD POS.4	FIG.5.81	273. - 0.125E+04 K	0.64%FS

Table 3.1 (Continued)

** MEASUREMENT LIST **

201CH.- 250CH.

CH.	ITEM	SYMBOL	ID.	LOCATION	FIG.NO.	RANGE	ACCURACY
201	TEMP.	TF- 80	TE 201	A45 FUEL ROD POS.1	FIG.5.82	273. - 0.125E+04 K	0.64%FS
202	TEMP.	TF- 81	TE 202	A45 FUEL ROD POS.4	FIG.5.82	273. - 0.125E+04 K	0.64%FS
203	TEMP.	TF- 82	TE 203	A46 FUEL ROD POS.1	FIG.5.83	273. - 0.125E+04 K	0.64%FS
204	TEMP.	TF- 83	TE 204	A46 FUEL ROD POS.4	FIG.5.83	273. - 0.125E+04 K	0.64%FS
205	TEMP.	TF- 84	TE 205	A48 FUEL ROD POS.1	FIG.5.84	273. - 0.125E+04 K	0.64%FS
206	TEMP.	TF- 85	TE 206	A48 FUEL ROD POS.4	FIG.5.84	273. - 0.125E+04 K	0.64%FS
207	TEMP.	TF- 86	TE 207	A51 FUEL ROD POS.1	FIG.5.85	273. - 0.125E+04 K	0.64%FS
208	TEMP.	TF- 87	TE 208	A51 FUEL ROD POS.4	FIG.5.85	273. - 0.125E+04 K	0.64%FS
209	TEMP.	TF- 88	TE 209	A53 FUEL ROD POS.1	FIG.5.86	273. - 0.125E+04 K	0.64%FS
210	TEMP.	TF- 89	TE 210	A53 FUEL ROD POS.4	FIG.5.86	273. - 0.125E+04 K	0.64%FS
211	TEMP.	TF- 90	TE 211	A54 FUEL ROD POS.1	FIG.5.87	273. - 0.125E+04 K	0.64%FS
212	TEMP.	TF- 91	TE 212	A57 FUEL ROD POS.1	FIG.5.88	273. - 0.125E+04 K	0.64%FS
213	TEMP.	TF- 92	TE 213	A57 FUEL ROD POS.4	FIG.5.88	273. - 0.125E+04 K	0.64%FS
214	TEMP.	TF- 93	TE 214	A62 FUEL ROD POS.1	FIG.5.89	273. - 0.125E+04 K	0.64%FS
215	TEMP.	TF- 94	TE 215	A62 FUEL ROD POS.4	FIG.5.89	273. - 0.125E+04 K	0.64%FS
216	TEMP.	TF- 95	TE 216	A64 FUEL ROD POS.1	FIG.5.90	273. - 0.125E+04 K	0.64%FS
217	TEMP.	TF- 96	TE 217	A64 FUEL ROD POS.4	FIG.5.90	273. - 0.125E+04 K	0.64%FS
218	TEMP.	TF- 97	TE 218	A67 FUEL ROD POS.1	FIG.5.91	273. - 0.125E+04 K	0.64%FS
219	TEMP.	TF- 98	TE 219	A67 FUEL ROD POS.4	FIG.5.91	273. - 0.125E+04 K	0.64%FS
220	TEMP.	TF- 99	TE 220	A68 FUEL ROD POS.1	FIG.5.92	273. - 0.125E+04 K	0.64%FS
221	TEMP.	TF-100	TE 221	A68 FUEL ROD POS.4	FIG.5.92	273. - 0.125E+04 K	0.64%FS
222	TEMP.	TF-101	TE 222	A71 FUEL ROD POS.1	FIG.5.93	273. - 0.125E+04 K	0.64%FS
223	TEMP.	TF-102	TE 223	A71 FUEL ROD POS.4	FIG.5.93	273. - 0.125E+04 K	0.64%FS
224	TEMP.	TF-103	TE 224	A73 FUEL ROD POS.1	FIG.5.94	273. - 0.125E+04 K	0.64%FS
225	TEMP.	TF-104	TE 225	A73 FUEL ROD POS.4	FIG.5.94	273. - 0.125E+04 K	0.64%FS
226	TEMP.	TF-105	TE 226	A75 FUEL ROD POS.1	FIG.5.95	273. - 0.125E+04 K	0.64%FS
227	TEMP.	TF-106	TE 227	A75 FUEL ROD POS.4	FIG.5.95	273. - 0.125E+04 K	0.64%FS
228	TEMP.	TF-107	TE 228	A77 FUEL ROD POS.1	FIG.5.96	273. - 0.125E+04 K	0.64%FS
229	TEMP.	TF-108	TE 229	A77 FUEL ROD POS.4	FIG.5.96	273. - 0.125E+04 K	0.64%FS
230	TEMP.	TF-109	TE 230	A82 FUEL ROD POS.1	FIG.5.97	273. - 0.125E+04 K	0.64%FS
231	TEMP.	TF-110	TE 231	A82 FUEL ROD POS.4	FIG.5.97	273. - 0.125E+04 K	0.64%FS
232	TEMP.	TF-111	TE 232	A84 FUEL ROD POS.1	FIG.5.98	273. - 0.125E+04 K	0.64%FS
233	TEMP.	TF-112	TE 233	A84 FUEL ROD POS.4	FIG.5.98	273. - 0.125E+04 K	0.64%FS
234	TEMP.	TF-113	TE 234	A86 FUEL ROD POS.1	FIG.5.99	273. - 0.125E+04 K	0.64%FS
235	TEMP.	TF-114	TE 235	A86 FUEL ROD POS.4	FIG.5.99	273. - 0.125E+04 K	0.64%FS
236	TEMP.	TF-115	TE 236	A88 FUEL ROD POS.1	FIG.5.100	273. - 0.125E+04 K	0.64%FS
237	TEMP.	TF-116	TE 237	A88 FUEL ROD POS.4	FIG.5.100	273. - 0.125E+04 K	0.64%FS
238	TEMP.	TF-117	TE 238	B11 FUEL ROD POS.4	NOT PRESENTED	273. - 0.125E+04 K	0.64%FS
239	TEMP.	TF-118	TE 239	B13 FUEL ROD POS.4	NOT PRESENTED	273. - 0.125E+04 K	0.64%FS
240	TEMP.	TF-119	TE 240	B15 FUEL ROD POS.1	FIG.5.64, 132	273. - 0.125E+04 K	0.64%FS
241	TEMP.	TF-120	TE 241	B15 FUEL ROD POS.2	FIG.5.64, 133	273. - 0.125E+04 K	0.64%FS
242	TEMP.	TF-121	TE 242	B15 FUEL ROD POS.3	FIG.5.64, 134	273. - 0.125E+04 K	0.64%FS
243	TEMP.	TF-122	TE 243	B15 FUEL ROD POS.4	FIG.5.64, 135	273. - 0.125E+04 K	0.64%FS
244	TEMP.	TF-123	TE 244	B15 FUEL ROD POS.5	FIG.5.64, 136	273. - 0.125E+04 K	0.64%FS
245	TEMP.	TF-124	TE 245	B15 FUEL ROD POS.6	FIG.5.64, 137	273. - 0.125E+04 K	0.64%FS
246	TEMP.	TF-125	TE 246	B15 FUEL ROD POS.7	FIG.5.64, 138	273. - 0.125E+04 K	0.64%FS
247	TEMP.	TF-126	TE 247	B31 FUEL ROD POS.4	FIG.5.101	273. - 0.125E+04 K	0.64%FS
248	TEMP.	TF-127	TE 248	B33 FUEL ROD POS.4	FIG.5.101	273. - 0.125E+04 K	0.64%FS
249	TEMP.	TF-128	TE 249	B35 FUEL ROD POS.4	FIG.5.101	273. - 0.125E+04 K	0.64%FS
250	TEMP.	TF-129	TE 250	B51 FUEL ROD POS.4	FIG.5.101	273. - 0.125E+04 K	0.64%FS

Table 3.1 (Continued)

** MEASUREMENT LIST **

251CH.- 300CH.

CH.	ITEM	SYMBOL	ID.	LOCATION	FIG.NO.	RANGE	ACCURACY
251	TEMP.	TF-130	TE 251	B53 FUEL ROD POS.4	FIG.5.101	273. - 0.125E+04 K	0.64%FS
252	TEMP.	TF-131	TE 252	B85 FUEL ROD POS.1	FIG.5.65, 132	273. - 0.125E+04 K	0.64%FS
253	TEMP.	TF-132	TE 253	B85 FUEL ROD POS.2	FIG.5.65, 133	273. - 0.125E+04 K	0.64%FS
254	TEMP.	TF-133	TE 254	B85 FUEL ROD POS.3	FIG.5.65, 134	273. - 0.125E+04 K	0.64%FS
255	TEMP.	TF-134	TE 255	B85 FUEL ROD POS.4	FIG.5.65, 135	273. - 0.125E+04 K	0.64%FS
256	TEMP.	TF-135	TE 256	B85 FUEL ROD POS.5	FIG.5.65, 136	273. - 0.125E+04 K	0.64%FS
257	TEMP.	TF-136	TE 257	B85 FUEL ROD POS.6	FIG.5.65, 137	273. - 0.125E+04 K	0.64%FS
258	TEMP.	TF-137	TE 258	B85 FUEL ROD POS.7	FIG.5.65, 138	273. - 0.125E+04 K	0.64%FS
259	TEMP.	TF-138	TE 259	C11 FUEL ROD POS.4	FIG.5.102	273. - 0.125E+04 K	0.64%FS
260	TEMP.	TF-139	TE 260	C13 FUEL ROD POS.4	FIG.5.102	273. - 0.125E+04 K	0.64%FS
261	TEMP.	TF-140	TE 261	C15 FUEL ROD POS.4	FIG.5.102	273. - 0.125E+04 K	0.64%FS
262	TEMP.	TF-141	TE 262	C31 FUEL ROD POS.4	FIG.5.102	273. - 0.125E+04 K	0.64%FS
263	TEMP.	TF-142	TE 263	C33 FUEL ROD POS.1	FIG.5.66, 132	273. - 0.125E+04 K	0.64%FS
264	TEMP.	TF-143	TE 264	C33 FUEL ROD POS.2	FIG.5.66, 133	273. - 0.125E+04 K	0.64%FS
265	TEMP.	TF-144	TE 265	C33 FUEL ROD POS.3	FIG.5.66, 134	273. - 0.125E+04 K	0.64%FS
266	TEMP.	TF-145	TE 266	C33 FUEL ROD POS.4	FIG.5.66, 135	273. - 0.125E+04 K	0.64%FS
267	TEMP.	TF-146	TE 267	C33 FUEL ROD POS.5	FIG.5.66, 136	273. - 0.125E+04 K	0.64%FS
268	TEMP.	TF-147	TE 268	C33 FUEL ROD POS.6	FIG.5.66, 137	273. - 0.125E+04 K	0.64%FS
269	TEMP.	TF-148	TE 269	C33 FUEL ROD POS.7	FIG.5.66, 138	273. - 0.125E+04 K	0.64%FS
270	TEMP.	TF-149	TE 270	C35 FUEL ROD POS.4	FIG.5.102	273. - 0.125E+04 K	0.64%FS
271	TEMP.	TF-150	TE 271	C51 FUEL ROD POS.4	FIG.5.102	273. - 0.125E+04 K	0.64%FS
272	TEMP.	TF-151	TE 272	C53 FUEL ROD POS.4	FIG.5.102	273. - 0.125E+04 K	0.64%FS
273	TEMP.	TF-152	TE 273	C77 FUEL ROD POS.1	FIG.5.67, 132	273. - 0.125E+04 K	0.64%FS
274	TEMP.	TF-153	TE 274	C77 FUEL ROD POS.2	FIG.5.67, 133	273. - 0.125E+04 K	0.64%FS
275	TEMP.	TF-154	TE 275	C77 FUEL ROD POS.3	FIG.5.67, 134	273. - 0.125E+04 K	0.64%FS
276	TEMP.	TF-155	TE 276	C77 FUEL ROD POS.4	FIG.5.67, 135	273. - 0.125E+04 K	0.64%FS
277	TEMP.	TF-156	TE 277	C77 FUEL ROD POS.5	FIG.5.67, 136	273. - 0.125E+04 K	0.64%FS
278	TEMP.	TF-157	TE 278	C77 FUEL ROD POS.6	FIG.5.67, 137	273. - 0.125E+04 K	0.64%FS
279	TEMP.	TF-158	TE 279	C77 FUEL ROD POS.7	FIG.5.67, 138	273. - 0.125E+04 K	0.64%FS
280	TEMP.	TF-159	TE 280	D11 FUEL ROD POS.4	FIG.5.103	273. - 0.125E+04 K	0.64%FS
281	TEMP.	TF-160	TE 281	D13 FUEL ROD POS.4	FIG.5.103	273. - 0.125E+04 K	0.64%FS
282	TEMP.	TF-161	TE 282	D27 FUEL ROD POS.1	FIG.5.68, 132	273. - 0.125E+04 K	0.64%FS
283	TEMP.	TF-162	TE 283	D27 FUEL ROD POS.2	FIG.5.68, 133	273. - 0.125E+04 K	0.64%FS
284	TEMP.	TF-163	TE 284	D27 FUEL ROD POS.3	FIG.5.68, 134	273. - 0.125E+04 K	0.64%FS
285	TEMP.	TF-164	TE 285	D27 FUEL ROD POS.4	FIG.5.68, 135	273. - 0.125E+04 K	0.64%FS
286	TEMP.	TF-165	TE 286	D27 FUEL ROD POS.5	FIG.5.68, 136	273. - 0.125E+04 K	0.64%FS
287	TEMP.	TF-166	TE 287	D27 FUEL ROD POS.6	FIG.5.68, 137	273. - 0.125E+04 K	0.64%FS
288	TEMP.	TF-167	TE 288	D27 FUEL ROD POS.7	FIG.5.68, 138	273. - 0.125E+04 K	0.64%FS
289	TEMP.	TF-168	TE 289	D31 FUEL ROD POS.4	FIG.5.103	273. - 0.125E+04 K	0.64%FS
290	TEMP.	TF-169	TE 290	D33 FUEL ROD POS.4	FIG.5.103	273. - 0.125E+04 K	0.64%FS
291	TEMP.	TF-170	TE 291	D35 FUEL ROD POS.4	FIG.5.103	273. - 0.125E+04 K	0.64%FS
292	TEMP.	TF-171	TE 292	D51 FUEL ROD POS.4	FIG.5.103	273. - 0.125E+04 K	0.64%FS
293	TEMP.	TF-172	TE 293	D53 FUEL ROD POS.4	FIG.5.103	273. - 0.125E+04 K	0.64%FS
294	TEMP.	TF-173	TE 294	D88 FUEL ROD POS.1	FIG.5.69, 132	273. - 0.125E+04 K	0.64%FS
295	TEMP.	TF-174	TE 295	D88 FUEL ROD POS.2	FIG.5.69, 133	273. - 0.125E+04 K	0.64%FS
296	TEMP.	TF-175	TE 296	D88 FUEL ROD POS.3	FIG.5.69, 134	273. - 0.125E+04 K	0.64%FS
297	TEMP.	TF-176	TE 297	D88 FUEL ROD POS.4	FIG.5.69, 135	273. - 0.125E+04 K	0.64%FS
298	TEMP.	TF-177	TE 298	D88 FUEL ROD POS.5	FIG.5.69, 136	273. - 0.125E+04 K	0.64%FS
299	TEMP.	TF-178	TE 299	D88 FUEL ROD POS.6	FIG.5.69, 137	273. - 0.125E+04 K	0.64%FS
300	TEMP.	TF-179	TE 300	D88 FUEL ROD POS.7	FIG.5.69, 138	273. - 0.125E+04 K	0.64%FS

Table 3.1 (Continued)

** MEASUREMENT LIST **

301CH.- 350CH.

CH.	ITEM	SYMBOL	ID.	LOCATION	FIG.NO.	RANGE	ACCURACY
301	FLUID T.	TF-180	TE 301	A44 TIE ROD POS.1	FIG.5.70, 146	273. - 0.125E+04 K	0.64%FS
302	FLUID T.	TF-181	TE 302	A44 TIE ROD POS.2	FIG.5.70, 147	273. - 0.125E+04 K	0.64%FS
303	FLUID T.	TF-182	TE 303	A44 TIE ROD POS.3	FIG.5.70, 148	273. - 0.125E+04 K	0.64%FS
304	FLUID T.	TF-183	TE 304	A44 TIE ROD POS.4	FIG.5.70, 149	273. - 0.125E+04 K	0.64%FS
305	FLUID T.	TF-184	TE 305	A44 TIE ROD POS.5	FIG.5.70, 150	273. - 0.125E+04 K	0.64%FS
306	FLUID T.	TF-185	TE 306	A44 TIE ROD POS.6	AMPLIFIER FAILED	273. - 0.125E+04 K	0.64%FS
307	FLUID T.	TF-186	TE 307	A44 TIE ROD POS.7	FIG.5.70, 152	273. - 0.125E+04 K	0.64%FS
308	FLUID T.	TF-187	TE 308	B44 TIE ROD POS.1	FIG.5.71, 146	273. - 0.125E+04 K	0.64%FS
309	FLUID T.	TF-188	TE 309	B44 TIE ROD POS.2	FIG.5.71, 147	273. - 0.125E+04 K	0.64%FS
310	FLUID T.	TF-189	TE 310	B44 TIE ROD POS.3	FIG.5.71, 148	273. - 0.125E+04 K	0.64%FS
311	FLUID T.	TF-190	TE 311	B44 TIE ROD POS.4	FIG.5.71, 149	273. - 0.125E+04 K	0.64%FS
312	FLUID T.	TF-191	TE 312	B44 TIE ROD POS.5	FIG.5.71, 150	273. - 0.125E+04 K	0.64%FS
313	FLUID T.	TF-192	TE 313	B44 TIE ROD POS.6	FIG.5.71, 151	273. - 0.125E+04 K	0.64%FS
314	FLUID T.	TF-193	TE 314	B44 TIE ROD POS.7	FIG.5.71, 152	273. - 0.125E+04 K	0.64%FS
315	FLUID T.	TF-194	TE 315	C44 TIE ROD POS.1	FIG.5.72, 146	273. - 0.125E+04 K	0.64%FS
316	FLUID T.	TF-195	TE 316	C44 TIE ROD POS.2	FIG.5.72, 147	273. - 0.125E+04 K	0.64%FS
317	FLUID T.	TF-196	TE 317	C44 TIE ROD POS.3	FIG.5.72, 148	273. - 0.125E+04 K	0.64%FS
318	FLUID T.	TF-197	TE 318	C44 TIE ROD POS.4	FIG.5.72, 149	273. - 0.125E+04 K	0.64%FS
319	FLUID T.	TF-198	TE 319	C44 TIE ROD POS.5	FIG.5.72, 150	273. - 0.125E+04 K	0.64%FS
320	FLUID T.	TF-199	TE 320	C44 TIE ROD POS.6	FIG.5.72, 151	273. - 0.125E+04 K	0.64%FS
321	FLUID T.	TF-200	TE 321	C44 TIE ROD POS.7	FIG.5.72, 152	273. - 0.125E+04 K	0.64%FS
322	FLUID T.	TF-201	TE 322	D44 TIE ROD POS.1	FIG.5.73, 146	273. - 0.125E+04 K	0.64%FS
323	FLUID T.	TF-202	TE 323	D44 TIE ROD POS.2	FIG.5.73, 147	273. - 0.125E+04 K	0.64%FS
324	FLUID T.	TF-203	TE 324	D44 TIE ROD POS.3	FIG.5.73, 148	273. - 0.125E+04 K	0.64%FS
325	FLUID T.	TF-204	TE 325	D44 TIE ROD POS.4	FIG.5.73, 149	273. - 0.125E+04 K	0.64%FS
326	FLUID T.	TF-205	TE 326	D44 TIE ROD POS.5	FIG.5.73, 150	273. - 0.125E+04 K	0.64%FS
327	FLUID T.	TF-206	TE 327	D44 TIE ROD POS.6	FIG.5.73, 151	273. - 0.125E+04 K	0.64%FS
328	FLUID T.	TF-207	TE 328	D44 TIE ROD POS.7	FIG.5.73, 152	273. - 0.125E+04 K	0.64%FS
329	FLUID T.	TC- 1	TE 329	CHANNEL BOX A OUTLET	FIG.5.104	273. - 0.125E+04 K	0.64%FS
330	FLUID T.	TC- 2	TE 330	CHANNEL BOX A INLET	FIG.5.105	273. - 0.125E+04 K	0.64%FS
331	FLUID T.	TC- 3	TE 331	CHANNEL BOX B OUTLET	FIG.5.104	273. - 0.125E+04 K	0.64%FS
332	FLUID T.	TC- 4	TE 332	CHANNEL BOX B INLET	FIG.5.105	273. - 0.125E+04 K	0.64%FS
333	FLUID T.	TC- 5	TE 333	CHANNEL BOX C OUTLET	FIG.5.104	273. - 0.125E+04 K	0.64%FS
334	FLUID T.	TC- 6	TE 334	CHANNEL BOX C INLET	FIG.5.105	273. - 0.125E+04 K	0.64%FS
335	FLUID T.	TC- 7	TE 335	CHANNEL BOX D OUTLET	FIG.5.104	273. - 0.125E+04 K	0.64%FS
336	FLUID T.	TC- 8	TE 336	CHANNEL BOX D INLET	FIG.5.105	273. - 0.125E+04 K	0.64%FS
337	SLAB T.	TB- 1	TE 337	C.B.INNER SURFACE A-1	FIG.5.106, 153	273. - 0.125E+04 K	0.64%FS
338	SLAB T.	TB- 2	TE 338	C.B.INNER SURFACE A-2	FIG.5.106, 154	273. - 0.125E+04 K	0.64%FS
339	SLAB T.	TB- 3	TE 339	C.B.INNER SURFACE A-3	FIG.5.106, 155	273. - 0.125E+04 K	0.64%FS
340	SLAB T.	TB- 4	TE 340	C.B.INNER SURFACE A-4	FIG.5.106, 156	273. - 0.125E+04 K	0.64%FS
341	SLAB T.	TB- 5	TE 341	C.B.INNER SURFACE A-5	FIG.5.106, 157	273. - 0.125E+04 K	0.64%FS
342	SLAB T.	TB- 6	TE 342	C.B.INNER SURFACE A-6	AMPLIFIER FAILED	273. - 0.125E+04 K	0.64%FS
343	SLAB T.	TB- 7	TE 343	C.B.INNER SURFACE A-7	FIG.5.106, 159	273. - 0.125E+04 K	0.64%FS
344	SLAB T.	TB- 8	TE 344	C.B.INNER SURFACE A-8	FIG.5.107, 153	273. - 0.125E+04 K	0.64%FS
345	SLAB T.	TB- 9	TE 345	C.B.INNER SURFACE A-9	FIG.5.107, 154	273. - 0.125E+04 K	0.64%FS
346	SLAB T.	TB-10	TE 346	C.B.INNER SURFACE A-10	FIG.5.107, 155	273. - 0.125E+04 K	0.64%FS
347	SLAB T.	TB-11	TE 347	C.B.INNER SURFACE A-11	AMPLIFIER FAILED	273. - 0.125E+04 K	0.64%FS
348	SLAB T.	TB-12	TE 348	C.B.INNER SURFACE A-12	FIG.5.107, 157	273. - 0.125E+04 K	0.64%FS
349	SLAB T.	TB-13	TE 349	C.B.INNER SURFACE A-13	FIG.5.107, 158	273. - 0.125E+04 K	0.64%FS
350	SLAB T.	TB-14	TE 350	C.B.INNER SURFACE A-14	FIG.5.107, 159	273. - 0.125E+04 K	0.64%FS

Table 3.1 (Continued)

** MEASUREMENT LIST **

351CH.- 400CH.

CH.	ITEM	SYMBOL	ID.	LOCATION	FIG.NO.	RANGE	ACCURACY
351	SLAB T.	TB-15	TE 351	C.B.INNER SURFACE B-1	FIG.5.108, 153	273. - 0.125E+04 K	0.64%FS
352	SLAB T.	TB-16	TE 352	C.B.INNER SURFACE B-2	FIG.5.108, 154	273. - 0.125E+04 K	0.64%FS
353	SLAB T.	TB-17	TE 353	C.B.INNER SURFACE B-3	FIG.5.108, 155	273. - 0.125E+04 K	0.64%FS
354	SLAB T.	TB-18	TE 354	C.B.INNER SURFACE B-4	FIG.5.108, 156	273. - 0.125E+04 K	0.64%FS
355	SLAB T.	TB-19	TE 355	C.B.INNER SURFACE B-5	FIG.5.108, 157	273. - 0.125E+04 K	0.64%FS
356	SLAB T.	TB-20	TE 356	C.B.INNER SURFACE B-6	FIG.5.108, 158	273. - 0.125E+04 K	0.64%FS
357	SLAB T.	TB-21	TE 357	C.B.INNER SURFACE B-7	FIG.5.108, 159	273. - 0.125E+04 K	0.64%FS
358	SLAB T.	TB-22	TE 358	C.B.INNER SURFACE C-1	FIG.5.109, 153	273. - 0.125E+04 K	0.64%FS
359	SLAB T.	TB-23	TE 359	C.B.INNER SURFACE C-2	FIG.5.109, 154	273. - 0.125E+04 K	0.64%FS
360	SLAB T.	TB-24	TE 360	C.B.INNER SURFACE C-3	FIG.5.109, 155	273. - 0.125E+04 K	0.64%FS
361	SLAB T.	TB-25	TE 361	C.B.INNER SURFACE C-4	FIG.5.109, 156	273. - 0.125E+04 K	0.64%FS
362	SLAB T.	TB-26	TE 362	C.B.INNER SURFACE C-5	FIG.5.109, 157	273. - 0.125E+04 K	0.64%FS
363	SLAB T.	TB-27	TE 363	C.B.INNER SURFACE C-6	FIG.5.109, 158	273. - 0.125E+04 K	0.64%FS
364	SLAB T.	TB-28	TE 364	C.B.INNER SURFACE C-7	FIG.5.109, 159	273. - 0.125E+04 K	0.64%FS
365	SLAB T.	TB-29	TE 365	C.B.INNER SURFACE D-1	FIG.5.110, 153	273. - 0.125E+04 K	0.64%FS
366	SLAB T.	TB-30	TE 366	C.B.INNER SURFACE D-2	FIG.5.110, 154	273. - 0.125E+04 K	0.64%FS
367	SLAB T.	TB-31	TE 367	C.B.INNER SURFACE D-3	FIG.5.110, 155	273. - 0.125E+04 K	0.64%FS
368	SLAB T.	TB-32	TE 368	C.B.INNER SURFACE D-4	FIG.5.110, 156	273. - 0.125E+04 K	0.64%FS
369	SLAB T.	TB-33	TE 369	C.B.INNER SURFACE D-5	FIG.5.110, 157	273. - 0.125E+04 K	0.64%FS
370	SLAB T.	TB-34	TE 370	C.B.INNER SURFACE D-6	FIG.5.110, 158	273. - 0.125E+04 K	0.64%FS
371	SLAB T.	TB-35	TE 371	C.B.INNER SURFACE D-7	FIG.5.110, 159	273. - 0.125E+04 K	0.64%FS
372	SLAB T.	TP- 1	TE 372	LOWER PL.NORTH HIGH	FIG.5.111	273. - 0.125E+04 K	0.64%FS
373	SLAB T.	TP- 2	TE 373	LOWER PL.NORTH MIDDLE	FIG.5.111	273. - 0.125E+04 K	0.64%FS
374	SLAB T.	TP- 3	TE 374	LOWER PL.NORTH LOW	FIG.5.111	273. - 0.125E+04 K	0.64%FS
375	SLAB T.	TP- 4	TE 375	LOWER PL.SOUTH HIGH	FIG.5.112	273. - 0.125E+04 K	0.64%FS
376	SLAB T.	TP- 5	TE 376	LOWER PL.SOUTH MIDDLE	FIG.5.112	273. - 0.125E+04 K	0.64%FS
377	SLAB T.	TP- 6	TE 377	LOWER PL.SOUTH LOW	FIG.5.112	273. - 0.125E+04 K	0.64%FS
378	FLUID T.	TP- 7	TE 378	LOWER PL.CENTER LOW	FIG.5.113	273. - 0.125E+04 K	0.64%FS
379	FLUID T.	TP- 8	TE 379	LOWER PL.CENTER BOTTOM	FIG.5.113	273. - 0.125E+04 K	0.64%FS
380	FLUID T.	TP- 9	TE 380	L.P.GUIDE TUBE HIGH	FIG.5.114	273. - 0.125E+04 K	0.64%FS
381	FLUID T.	TP-11	TE 381	L.P.GUIDE TUBE LOW	FIG.5.114	273. - 0.125E+04 K	0.64%FS
382	FLUID T.	TG- 1	TE 382	UPPER TIEPLATE A UP.1	FIG.5.115	273. - 0.125E+04 K	0.64%FS
383	FLUID T.	TG- 2	TE 383	UPPER TIEPLATE A UP.2	FIG.5.116	273. - 0.125E+04 K	0.64%FS
384	FLUID T.	TG- 3	TE 384	UPPER TIEPLATE A UP.3	FIG.5.117	273. - 0.125E+04 K	0.64%FS
385	FLUID T.	TG- 4	TE 385	UPPER TIEPLATE A UP.4	FIG.5.118	273. - 0.125E+04 K	0.64%FS
386	FLUID T.	TG- 5	TE 386	UPPER TIEPLATE A UP.5	FIG.5.119	273. - 0.125E+04 K	0.64%FS
387	FLUID T.	TG- 6	TE 387	UPPER TIEPLATE A UP.6	FIG.5.120	273. - 0.125E+04 K	0.64%FS
388	FLUID T.	TG- 7	TE 388	UPPER TIEPLATE A UP.7	FIG.5.121	273. - 0.125E+04 K	0.64%FS
389	FLUID T.	TG- 8	TE 389	UPPER TIEPLATE A UP.8	FIG.5.122	273. - 0.125E+04 K	0.64%FS
390	FLUID T.	TG- 9	TE 390	UPPER TIEPLATE A UP.9	FIG.5.123	273. - 0.125E+04 K	0.64%FS
391	FLUID T.	TG-10	TE 391	UPPER TIEPLATE A UP.10	FIG.5.124	273. - 0.125E+04 K	0.64%FS
392	FLUID T.	TG-11	TE 392	UPPER TIEPLATE A LO.1	FIG.5.115	273. - 0.125E+04 K	0.64%FS
393	FLUID T.	TG-12	TE 393	UPPER TIEPLATE A LO.2	FIG.5.116	273. - 0.125E+04 K	0.64%FS
394	FLUID T.	TG-13	TE 394	UPPER TIEPLATE A LO.3	FIG.5.117	273. - 0.125E+04 K	0.64%FS
395	FLUID T.	TG-14	TE 395	UPPER TIEPLATE A LO.4	FIG.5.118	273. - 0.125E+04 K	0.64%FS
396	FLUID T.	TG-15	TE 396	UPPER TIEPLATE A LO.5	FIG.5.119	273. - 0.125E+04 K	0.64%FS
397	FLUID T.	TG-16	TE 397	UPPER TIEPLATE A LO.6	FIG.5.120	273. - 0.125E+04 K	0.64%FS
398	FLUID T.	TG-17	TE 398	UPPER TIEPLATE A LO.7	FIG.5.121	273. - 0.125E+04 K	0.64%FS
399	FLUID T.	TG-18	TE 399	UPPER TIEPLATE A LO.8	FIG.5.122	273. - 0.125E+04 K	0.64%FS
400	FLUID T.	TG-19	TE 400	UPPER TIEPLATE A LO.9	FIG.5.123	273. - 0.125E+04 K	0.64%FS

Table 3.1 (Continued)

** MEASUREMENT LIST **

401CH.- 450CH.

CH.	ITEM	SYMBOL	ID.	LOCATION	FIG.NO.	RANGE	ACCURACY
401	FLUID T.	TG-20	TE 401	UPPER TIEPLATE A LO.10	FIG.5.124	273. - 0.125E+04 K	0.64%FS
402	LEVEL	LB- 1	LM 402	C.B.LIQUID LEVEL A1-1	FIG.5.160		
403	LEVEL	LB- 2	LM 403	C.B.LIQUID LEVEL A1-2	FIG.5.160		
404	LEVEL	LB- 3	LM 404	C.B.LIQUID LEVEL A1-3	FIG.5.160		
405	LEVEL	LB- 4	LM 405	C.B.LIQUID LEVEL A1-4	FIG.5.160		
406	LEVEL	LB- 5	LM 406	C.B.LIQUID LEVEL A1-5	FIG.5.160		
407	LEVEL	LB- 6	LM 407	C.B.LIQUID LEVEL A1-6	FIG.5.160		
408	LEVEL	LB- 7	LM 408	C.B.LIQUID LEVEL A1-7	FIG.5.160		
409	LEVEL	LB- 8	LM 409	C.B.LIQUID LEVEL A2-1	FIG.5.161		
410	LEVEL	LB- 9	LM 410	C.B.LIQUID LEVEL A2-2	FIG.5.161		
411	LEVEL	LB-10	LM 411	C.B.LIQUID LEVEL A2-3	FIG.5.161		
412	LEVEL	LB-11	LM 412	C.B.LIQUID LEVEL A2-4	FIG.5.161		
413	LEVEL	LB-12	LM 413	C.B.LIQUID LEVEL A2-5	AMPLIFIER FAILED		
414	LEVEL	LB-13	LM 414	C.B.LIQUID LEVEL A2-6	FIG.5.161		
415	LEVEL	LB-14	LM 415	C.B.LIQUID LEVEL A2-7	FIG.5.161		
416	LEVEL	LB-15	LM 416	C.B.LIQUID LEVEL B-1	FIG.5.162		
417	LEVEL	LB-16	LM 417	C.B.LIQUID LEVEL B-2	FIG.5.162		
418	LEVEL	LB-17	LM 418	C.B.LIQUID LEVEL B-3	FIG.5.162		
419	LEVEL	LB-18	LM 419	C.B.LIQUID LEVEL B-4	FIG.5.162		
420	LEVEL	LB-19	LM 420	C.B.LIQUID LEVEL B-5	FIG.5.162		
421	LEVEL	LB-20	LM 421	C.B.LIQUID LEVEL B-6	AMPLIFIER FAILED		
422	LEVEL	LB-21	LM 422	C.B.LIQUID LEVEL B-7	FIG.5.162		
423	LEVEL	LB-22	LM 423	C.B.LIQUID LEVEL C-1	FIG.5.163		
424	LEVEL	LB-23	LM 424	C.B.LIQUID LEVEL C-2	FIG.5.163		
425	LEVEL	LB-24	LM 425	C.B.LIQUID LEVEL C-3	FIG.5.163		
426	LEVEL	LB-25	LM 426	C.B.LIQUID LEVEL C-4	FIG.5.163		
427	LEVEL	LB-26	LM 427	C.B.LIQUID LEVEL C-5	FIG.5.163		
428	LEVEL	LB-27	LM 428	C.B.LIQUID LEVEL C-6	FIG.5.163		
429	LEVEL	LB-28	LM 429	C.B.LIQUID LEVEL C-7	FIG.5.163		
430	LEVEL	LB-29	LM 430	C.B.LIQUID LEVEL D-1	FIG.5.164		
431	LEVEL	LB-30	LM 431	C.B.LIQUID LEVEL D-2	FIG.5.164		
432	LEVEL	LB-31	LM 432	C.B.LIQUID LEVEL D-3	FIG.5.164		
433	LEVEL	LB-32	LM 433	C.B.LIQUID LEVEL D-4	FIG.5.164		
434	LEVEL	LB-33	LM 434	C.B.LIQUID LEVEL D-5	AMPLIFIER FAILED		
435	LEVEL	LB-34	LM 435	C.B.LIQUID LEVEL D-6	FIG.5.164		
436	LEVEL	LB-35	LM 436	C.B.LIQUID LEVEL D-7	FIG.5.164		
437	LEVEL	L- 1	LM 437	DOWNCOMER D-SIDE 1	FIG.5.165		
438	LEVEL	L- 2	LM 438	DOWNCOMER D-SIDE 2	FIG.5.165		
439	LEVEL	L- 3	LM 439	DOWNCOMER D-SIDE 3	FIG.5.165		
440	LEVEL	L- 4	LM 440	DOWNCOMER D-SIDE 4	FIG.5.165		
441	LEVEL	L- 5	LM 441	DOWNCOMER D-SIDE 5	FIG.5.165		
442	LEVEL	L- 7	LM 442	DOWNCOMER B-SIDE 2	FIG.5.166		
443	LEVEL	L- 8	LM 443	DOWNCOMER B-SIDE 3	FIG.5.166		
444	LEVEL	L- 9	LM 444	DOWNCOMER B-SIDE 4	FIG.5.166		
445	LEVEL	L-10	LM 445	DOWNCOMER B-SIDE 5	FIG.5.166		
446	LEVEL	LL- 1	LM 446	L.P.CENTER HIGH	FIG.5.167		
447	LEVEL	LL- 2	LM 447	L.P.CENTER MIDDLE 1	FIG.5.167		
448	LEVEL	LL- 3	LM 448	L.P.CENTER MIDDLE 2	FIG.5.167		
449	LEVEL	LL- 4	LM 449	L.P.CENTER LOW	FIG.5.167		
450	LEVEL	LL- 5	LM 450	L.P.NORTH LOW	FIG.5.168		

Table 3.1 (Continued)

** MEASUREMENT LIST **

451CH.- 500CH.

CH.	ITEM	SYMBOL	ID.		LOCATION	FIG.NO.	RANGE			ACCURACY
451	LEVEL	LL- 6	LM	451	L.P.NORTH BOTTOM	FIG.5.168				
452	LEVEL	LL- 7	LM	452	L.P.SOUTH LOW	FIG.5.169				
453	LEVEL	LL- 8	LM	453	L.P.SOUTH BOTTOM	FIG.5.169				
454	VOID	VF- 1	VD	454	A55 TIE ROD POS.1	FIG.5.170	0.0	-	1.00	
455	VOID	VF- 2	VD	455	A55 TIE ROD POS.2	FIG.5.170	0.0	-	1.00	
456	VOID	VF- 3	VD	456	A55 TIE ROD POS.3	FIG.5.170	0.0	-	1.00	
457	VOID	VF- 4	VD	457	A55 TIE ROD POS.4	FIG.5.170	0.0	-	1.00	
458	VOID	VF- 5	VD	458	A55 TIE ROD POS.5	FIG.5.170	0.0	-	1.00	
459	VOID	VF- 6	VD	459	A55 TIE ROD POS.6	FIG.5.170	0.0	-	1.00	
460	VOID	VF- 7	VD	460	A55 TIE ROD POS.7	AMPLIFIER FAILED	0.0	-	1.00	
461	VOID	VF-15	VD	461	C55 TIE ROD POS.1	FIG.5.171	0.0	-	1.00	
462	VOID	VF-16	VD	462	C55 TIE ROD POS.2	FIG.5.171	0.0	-	1.00	
463	VOID	VF-17	VD	463	C55 TIE ROD POS.3	FIG.5.171	0.0	-	1.00	
464	VOID	VF-18	VD	464	C55 TIE ROD POS.4	FIG.5.171	0.0	-	1.00	
465	VOID	VF-19	VD	465	C55 TIE ROD POS.5	FIG.5.171	0.0	-	1.00	
466	VOID	VF-20	VD	466	C55 TIE ROD POS.6	FIG.5.171	0.0	-	1.00	
467	VOID	VF-21	VD	467	C55 TIE ROD POS.7	FIG.5.171	0.0	-	1.00	
468	VOID	VE- 1	VD	468	LOWER PL. NORTH	NOT MEASURED	0.0	-	1.00	
469	VOID	VE- 2	VD	469	LOWER PL. CENTER	NOT MEASURED	0.0	-	1.00	
470	VOID	VE- 3	VD	470	LOWER PL. SOUTH	NOT MEASURED	0.0	-	1.00	
471	VOID	VE- 4	VD	471	CHANNEL A OUTLET	NOT MEASURED	0.0	-	1.00	
472	VOID	VE- 5	VD	472	CHANNEL A OUTLET	NOT MEASURED	0.0	-	1.00	
473	VOID	VE- 6	VD	473	CHANNEL A OUTLET	NOT MEASURED	0.0	-	1.00	
474	VOID	VE- 7	VD	474	CHANNEL B OUTLET	NOT MEASURED	0.0	-	1.00	
475	VOID	VE- 8	VD	475	CHANNEL B OUTLET	NOT MEASURED	0.0	-	1.00	
476	VOID	VE- 9	VD	476	CHANNEL B OUTLET	NOT MEASURED	0.0	-	1.00	
477	VOID	VE-10	VD	477	CHANNEL C OUTLET	NOT MEASURED	0.0	-	1.00	
478	VOID	VE-11	VD	478	CHANNEL C OUTLET	NOT MEASURED	0.0	-	1.00	
479	VOID	VE-12	VD	479	CHANNEL C OUTLET	NOT MEASURED	0.0	-	1.00	
480	VOID	VE-13	VD	480	CHANNEL D OUTLET	NOT MEASURED	0.0	-	1.00	
481	VOID	VE-14	VD	481	CHANNEL D OUTLET	NOT MEASURED	0.0	-	1.00	
482	VOID	VE-15	VD	482	CHANNEL D OUTLET	NOT MEASURED	0.0	-	1.00	
483	VOID	VP- 1	VD	483	LOWER PLENUM 1-1	NOT MEASURED	0.0	-	1.00	
484	VOID	VP- 2	VD	484	LOWER PLENUM 1-2	NOT MEASURED	0.0	-	1.00	
485	VOID	VP- 3	VD	485	LOWER PLENUM 2-1	NOT MEASURED	0.0	-	1.00	
486	VOID	VP- 4	VD	486	LOWER PLENUM 2-2	NOT MEASURED	0.0	-	1.00	
487	DENSITY	DF- 1	DE	487	JP-1,2 OUTLET BEAM A	FIG.5.172	0.0	-	0.100E+04 KG/M3	1.00%FS
488	DENSITY	DF- 2	DE	488	JP-1,2 OUTLET BEAM B	FIG.5.173	0.0	-	0.100E+04 KG/M3	1.00%FS
489	DENSITY	DF- 3	DE	489	JP-1,2 OUTLET BEAM C	FIG.5.174	0.0	-	0.100E+04 KG/M3	1.00%FS
490	DENSITY	DF- 4	DE	490	JP-3,4 OUTLET BEAM A	FIG.5.175	0.0	-	0.100E+04 KG/M3	1.00%FS
491	DENSITY	DF- 5	DE	491	JP-3,4 OUTLET BEAM B	FIG.5.176	0.0	-	0.100E+04 KG/M3	1.00%FS
492	DENSITY	DF- 6	DE	492	JP-3,4 OUTLET BEAM C	FIG.5.177	0.0	-	0.100E+04 KG/M3	1.00%FS
493	DENSITY	DF- 7	DE	493	BREAK A BEAM A	FIG.5.178	0.0	-	0.100E+04 KG/M3	1.00%FS
494	DENSITY	DF- 8	DE	494	BREAK A BEAM B	FIG.5.179	0.0	-	0.100E+04 KG/M3	1.00%FS
495	DENSITY	DF- 9	DE	495	BREAK B BEAM A	FIG.5.180	0.0	-	0.100E+04 KG/M3	1.00%FS
496	DENSITY	DF-10	DE	496	BREAK B BEAM B	FIG.5.181	0.0	-	0.100E+04 KG/M3	1.00%FS
497	MO.FLUX	M- 1	MF	497	JP-1,2 OUTLET SPOOL	NOT MEASURED	0.0	-	0.150E+06 KG/MS2	1.00%FS
498	MO.FLUX	M- 2	MF	498	JP-3,4 OUTLET SPOOL	NOT MEASURED	0.0	-	0.150E+06 KG/MS2	1.00%FS
499	MO.FLUX	M- 3	MF	499	BREAK A SPOOL PIECE	NOT MEASURED	0.0	-	0.150E+06 KG/MS2	1.00%FS
500	MO.FLUX	M- 4	MF	500	BREAK B SPOOL PIECE	NOT MEASURED	0.0	-	0.150E+06 KG/MS2	1.00%FS

Table 3.2 Core Instrumentation List

Item	Pos. / DL / Rod NO.	Core Outlet	Pos.1	Pos.2	Pos.3	Pos.4	Pos.5	Pos.6	Pos.7	Core Inlet
		3660	3417	3114.5	2879.5	2527	2174.5	1939.5	1637	1454
Surface Temp.	A11		TF 1	TF 2	TF 3	TF 4	TF 5	TF 6	TF 7	
	A12		TF 8	TF 9	TF 10	TF 11	TF 12	TF 13	TF 14	
	A13		TF 15	TF 16	TF 17	TF 18	TF 19	TF 20	TF 21	
	A14		TF 22	TF 23	TF 24	TF 25	TF 26	TF 27	TF 28	
	A15		TF 29			TF 30				
	A17		TF 31			TF 32				
	A22		TF 33	TF 34	TF 35	TF 36	TF 37	TF 38	TF 39	
	A23		TF 40	TF 41	TF 42	TF 43	TF 44	TF 45	TF 46	
	A24		TF 47	TF 48	TF 49	TF 50	TF 51	TF 52	TF 53	
	A26		TF 54			TF 55				
	A28		TF 56			TF 57				
	A31		TF 58			TF 59				
	A33		TF 60	TF 61	TF 62	TF 63	TF 64	TF 65	TF 66	
	A34		TF 67	TF 68	TF 69	TF 70	TF 71	TF 72	TF 73	
	A35		TF 74			TF 75				
	A37		TF 76			TF 77				
	A42		TF 78			TF 79				
Fluid Temp.	A44	TC 1	TF180	TF181	TF182	TF183	TF184	TF185	TF186	TC 2
Surface Temp.	A45		TF 80			TF 81				
	A46		TF 82			TF 83				
	A48		TF 84			TF 85				
	A51		TF 86			TF 87				
	A53		TF 88			TF 89				
	A54		TF 90							
	A57		TF 91			TF 92				
	A62		TF 93			TF 94				
	A64		TF 95			TF 96				
	A66		TF 97			TF 98				
	A68		TF 99			TF100				
	A71		TF101			TF102				
	A73		TF103			TF104				
	A75		TF105			TF106				
	A77		TF107			TF108				

Table 3.2 (Continued)

Item	Pos. / Rod NO. / DL	Core Outlet	Pos.1	Pos.2	Pos.3	Pos.4	Pos.5	Pos.6	Pos.7	Core Inlet
		3660	3417	3114.5	2879.5	2527	2174.5	1939.5	1637	1454
Surface Temp.	A82		TF109			TF110				
	A84		TF111			TF112				
	A86		TF113			TF114				
	A88		TF115			TF116				
	B11					TF117				
	B13					TF118				
	B15		TF119	TF120	TF121	TF122	TF123	TF124	TF125	
	B31					TF126				
	B33					TF127				
	B35					TF128				
Fluid Temp.	B44	TC 3	TF187	TF188	TF189	TF190	TF191	TF192	TF193	TC 4
Surface Temp.	B51					TF129				
	B53					TF130				
	B85		TF131	TF132	TF133	TF134	TF135	TF136	TF137	
	C11					TF138				
	C13					TF139				
	C15					TF140				
	C31					TF141				
	C33		TF142	TF143	TF144	TF145	TF146	TF147	TF148	
	C35					TF149				
Fluid Temp.	C44	TC 5	TF194	TF195	TF196	TF197	TF198	TF199	TF200	TC 6
Surface Temp.	C51					TF150				
	C53					TF151				
	C77		TF152	TF153	TF154	TF155	TF156	TF157	TF158	
	D11					TF159				
	D13					TF160				
	D27		TF161	TF162	TF163	TF164	TF165	TF166	TF167	
	D31					TF168				
	D33					TF169				
	D35					TF170				
Fluid Temp.	D44	TC 7	TF201	TF202	TF203	TF204	TF205	TF206	TF207	TC 8
Surface Temp.	D51					TF171				
	D53					TF172				
	D88		TF173	TF174	TF175	TF176	TF177	TF178	TF179	

Table 3.2 (Continued)

Item	Pos. / Rod NO. / DL	Core Outlet	Pos.1	Pos.2	Pos.3	Pos.4	Pos.5	Pos.6	Pos.7	Core Inlet
		3660	3417	3114.5	2879.5	2527	2174.5	1939.5	1673	1454
Void	A55		VF 1	VF 2	VF 3	VF 4	VF 5	VF 6	VF 7	
	B55		VF 8	VF 9	VF 10	VF 11	VF 12	VF 13	VF 14	
	C55		VF 15	VF 16	VF 17	VF 18	VF 19	VF 20	VF 21	
	D55		VF 22	VF 23	VF 24	VF 25	VF 26	VF 27	VF 28	
Channel Box Surface Temp.	A1*		TB 1	TB 2	TB 3	TB 4	TB 5	TB 6	TB 7	
	A2*		TB 8	TB 9	TB 10	TB 11	TB 12	TB 13	TB 14	
	B*		TB 15	TB 16	TB 17	TB 18	TB 19	TB 20	TB 21	
	C*		TB 22	TB 23	TB 24	TB 25	TB 26	TB 27	TB 28	
	D*		TB 29	TB 30	TB 31	TB 32	TB 33	TB 34	TB 35	
Liquid Level in the Channel Box	A1*		LB 1	LB 2	LB 3	LB 4	LB 5	LB 6	LB 7	
	A2*		LB 8	LB 9	LB 10	LB 11	LB 12	LB 13	LB 14	
	B*		LB 15	LB 16	LB 17	LB 18	LB 19	LB 20	LB 21	
	C*		LB 22	LB 23	LB 24	LB 25	LB 26	LB 27	LB 28	
	D*		LB 29	LB 30	LB 31	LB 32	LB 33	LB 34	LB 35	

Table 4.1 Test Conditions of Run 7341

Parameter	Specified Value	Measured Value
Break Conditions		
Location	MRP Suction	MRP Suction
Type	Double-ended	Double-ended
Break Nozzle Diameter (mm)	26.2 / 26.2	26.2 / 26.2
Initial System Conditions		
Steam Dome Pressure (MPa)	7.35	7.28
Lower Plenum Temperature (K)	---	551.0
Lower Plenum Subcooling (K)	---	11.0
Core Inlet Flow Rate (kg/s)	15.3	15.3
Core Outlet Quality (%)	---	13.6**
Power Level (kW)	500+1131+1923	500+1132+1923
Maximum Liniar Heat Rate (kW/m)		
Channel A	13.6	13.6
Channel B,C and D	9.7	9.7
Water Level in PV * (m)	4.62	4.64
Feedwater Conditions		
Temperature (K)	489	490
Flow Rate (kg/s)	keep steady value	1.86
Initiation of Line Closure (s)	2.0	2.0
Steam Discharge Conditions		
Steady state Flow Rate (kg/s)		1.75
Transient Flow Rate (kg/s)	Keep Steady Value	Fig. 5.41
Orifice Diameter (mm)	20.0	20.0
Initiation of Line Closure (s)	3.0	5.0

Note ; * L3 Level for Scram

** not include core bypass flow.
bypass flow is assumed to be 10% of core flow.

Table 4.1 (Continued)

Parameter	Specified Value	Measured Value
ECCS Conditions		
HPCS		
Injection Location	Upper Plenum	Upper Plenum
Initiation Condition	27.0 (s)	27.0 (s)
	---	5.4 (MPa)
Coolant Temperation (K)	313	313
Injection Flow Rate (m^3/s)	2.28×10^{-4}	Fig. 5.42
LPCS		
Injection Location	Upper Plenum	Upper Plenum
Initiation Condition	---	63.5 (s)
	2.156 (MPa)	2.26 (MPa)
Coolant Temperature (K)	313	313
Injection Flow Rate (m^3/s)	9.67×10^{-4}	Fig. 5.42
LPCI		
Injection Location	Top of Core Bypass	Top of Core Bypass
Initiation Condition	13 (s) after LPCS activation	76.5 (s)
		2.0 (MPa)
Coolant Temperature (K)	313	314
Injection Flow Rate (m^3/s)	3.83×10^{-3}	Fig. 5.42
ADS Conditions		
Initiation (s)	120.0	120.0
Flow Rate	---	---
Orifice Diameter (mm)	6.0	6.0

Table 4.2 Valve Chracteristics of Steam Discharge Line

Valve	Close to Open (s)	Open to Close (s)
AV-168	---	0.1
AV-169	0.3	2.0

Orifice	Diameter (mm)	Area (mm^2)
OR-4	15.5	188.7
OR-3	18.0	324.0

Table 5.1 Sequence of Events in Run 7341

Time (s)	Event
0.0	Break
	Initiate core power control
	Terminate recirculation pump power
3.2	Closure of feedwater line
6.5	Closure of steam discharge line
8.4	Jet pump suction nozzle uncovery
12.9	Initiation of power reduction
14.0	Recirculation pump suction nozzle uncovery
16.3	Initiation of lower plenum flashing
27.0	HPCS initiation (at system pressure 5.4 MPa)
54.0	Whole core uncovery
61.5	Initiation of feedwater line flashing
63.5	LPCS initiation (at system pressure 2.26 MPa)
76.5	LPCI initiation (at system pressure 2.0 MPa)
115.0	Completion of core reflooding
120.0	ADS valve opening
160	All heater rod quenched

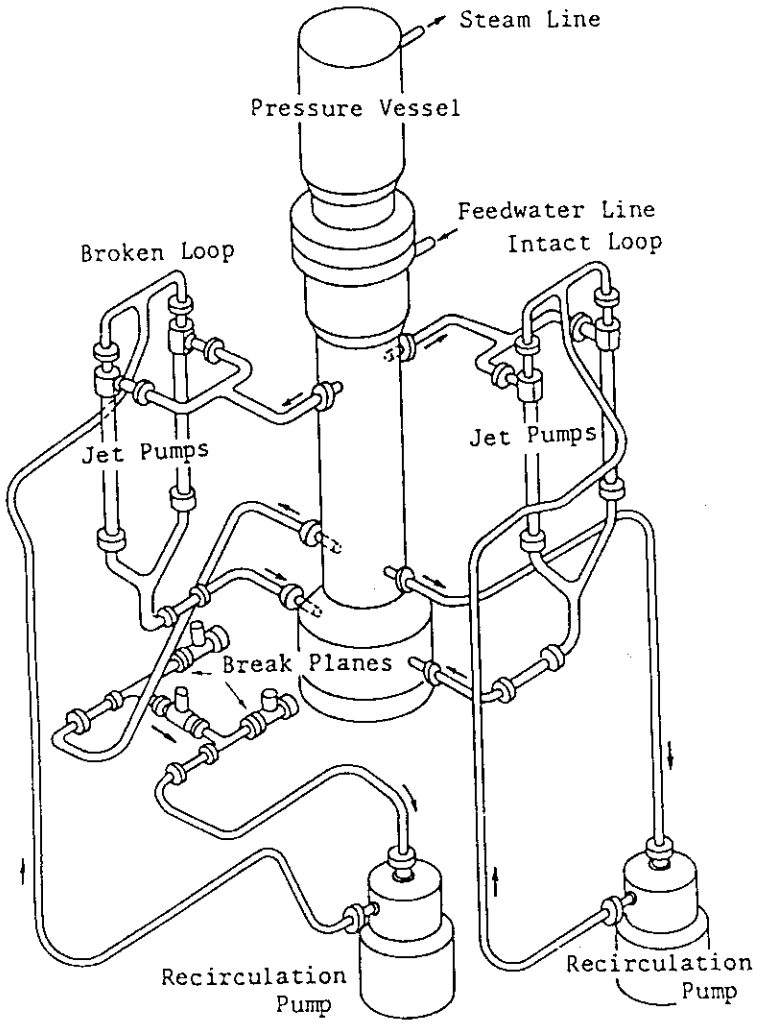

Fig. 2.1 Schematic Diagram of ROSA-III Test Facility

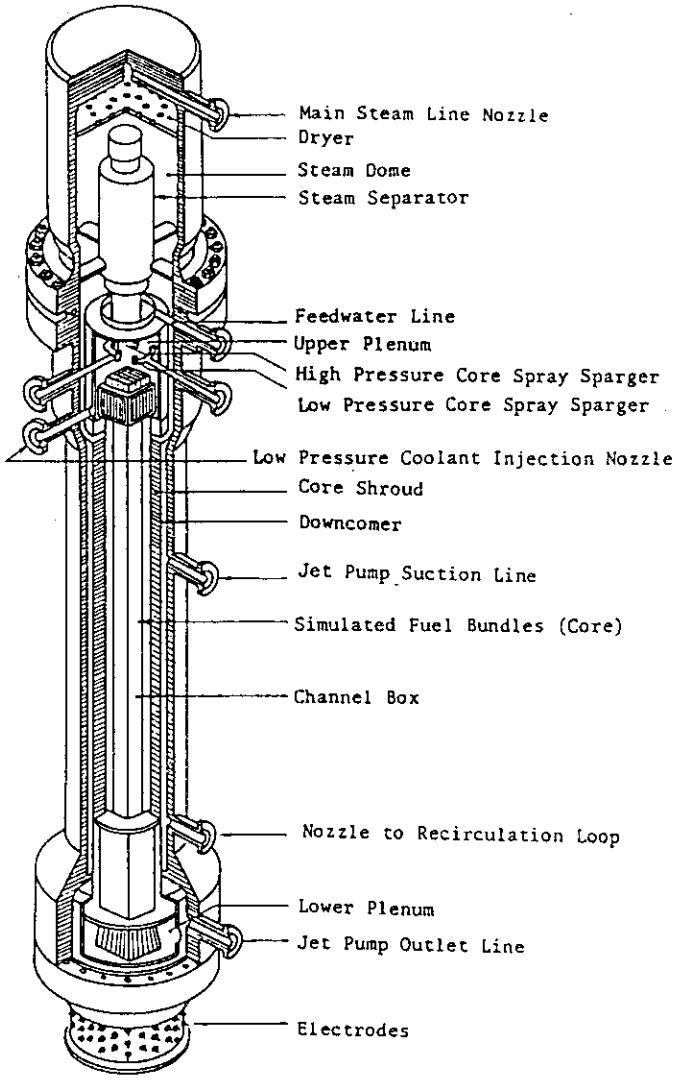

Fig. 2.2 Internal Structure of Pressure Vessel of ROSA-III

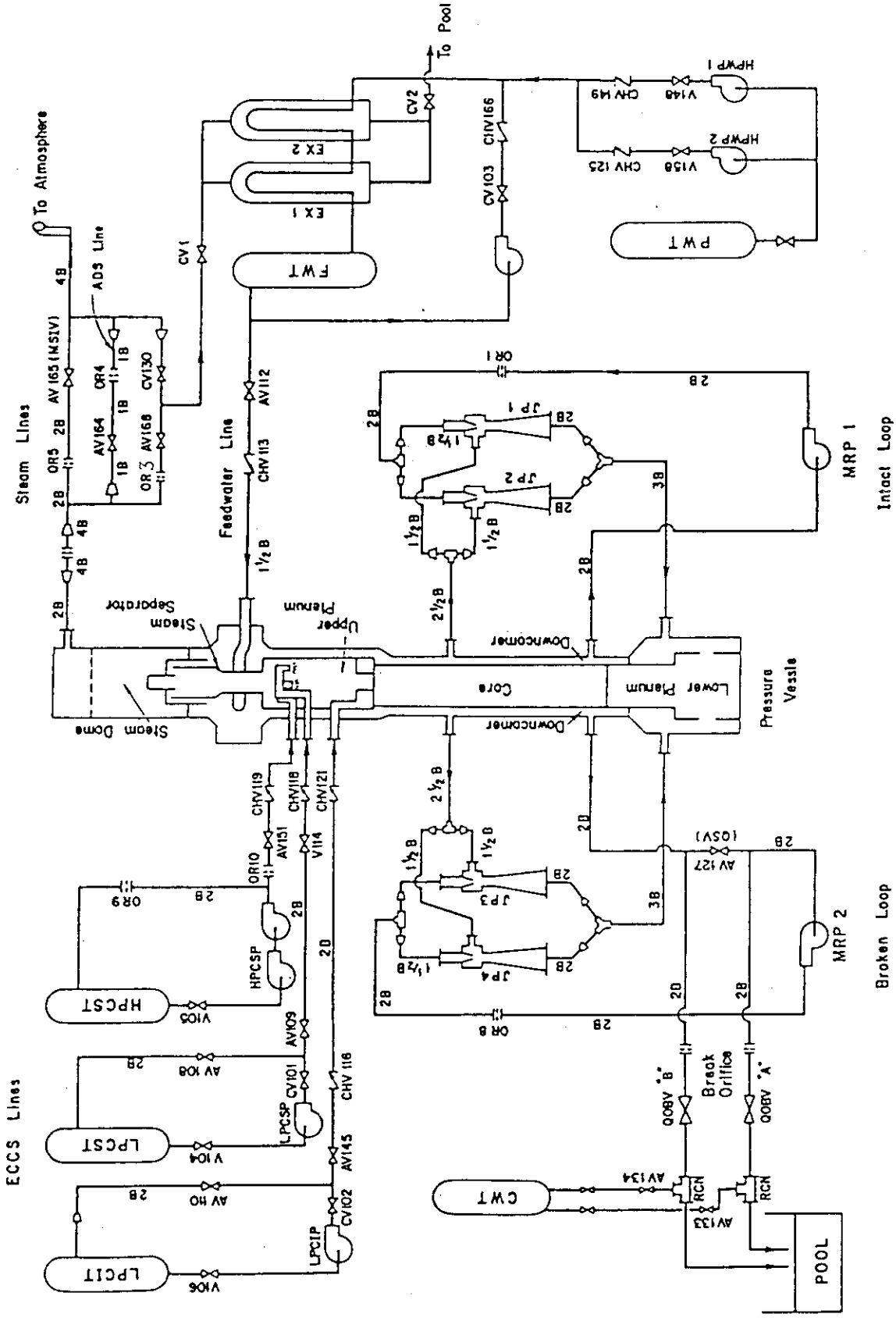

Fig. 2.3 ROSA-III Piping Schematic

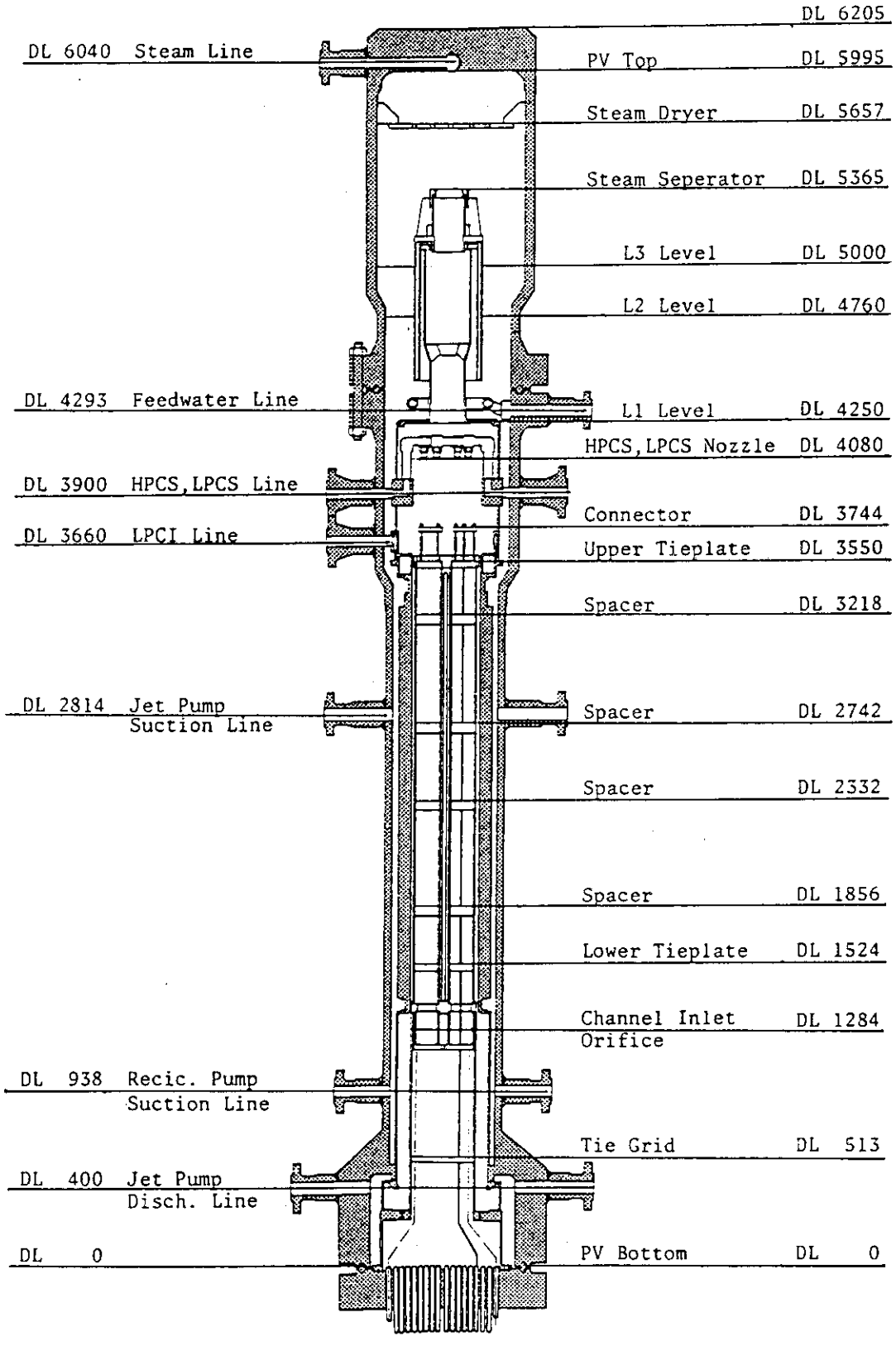

Fig.2.4 Pressure Vessel Internals Arrangement

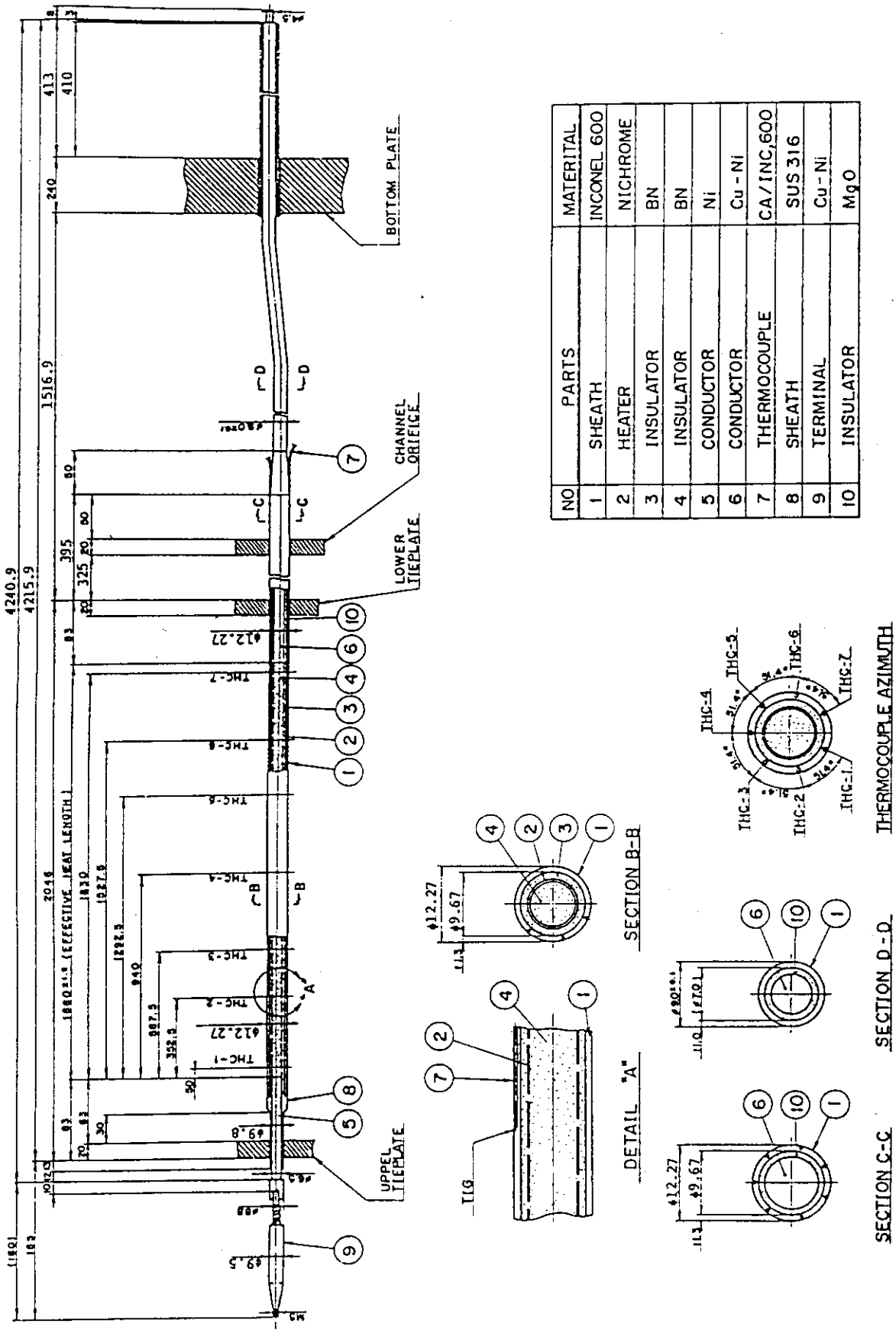

NO	PARTS	MATERITAL
1	SHEATH	INCONEL 600
2	HEATER	NICHROME
3	INSULATOR	BN
4	INSULATOR	BN
5	CONDUCTOR	Ni
6	CONDUCTOR	Cu - Ni
7	THERMOCOUPLE	CA/INC,600
8	SHEATH	SUS 316
9	TERMINAL	Cu - Ni
10	INSULATOR	MgO

Fig. 2.5 Simulated Fuel Rod of ROSA-III

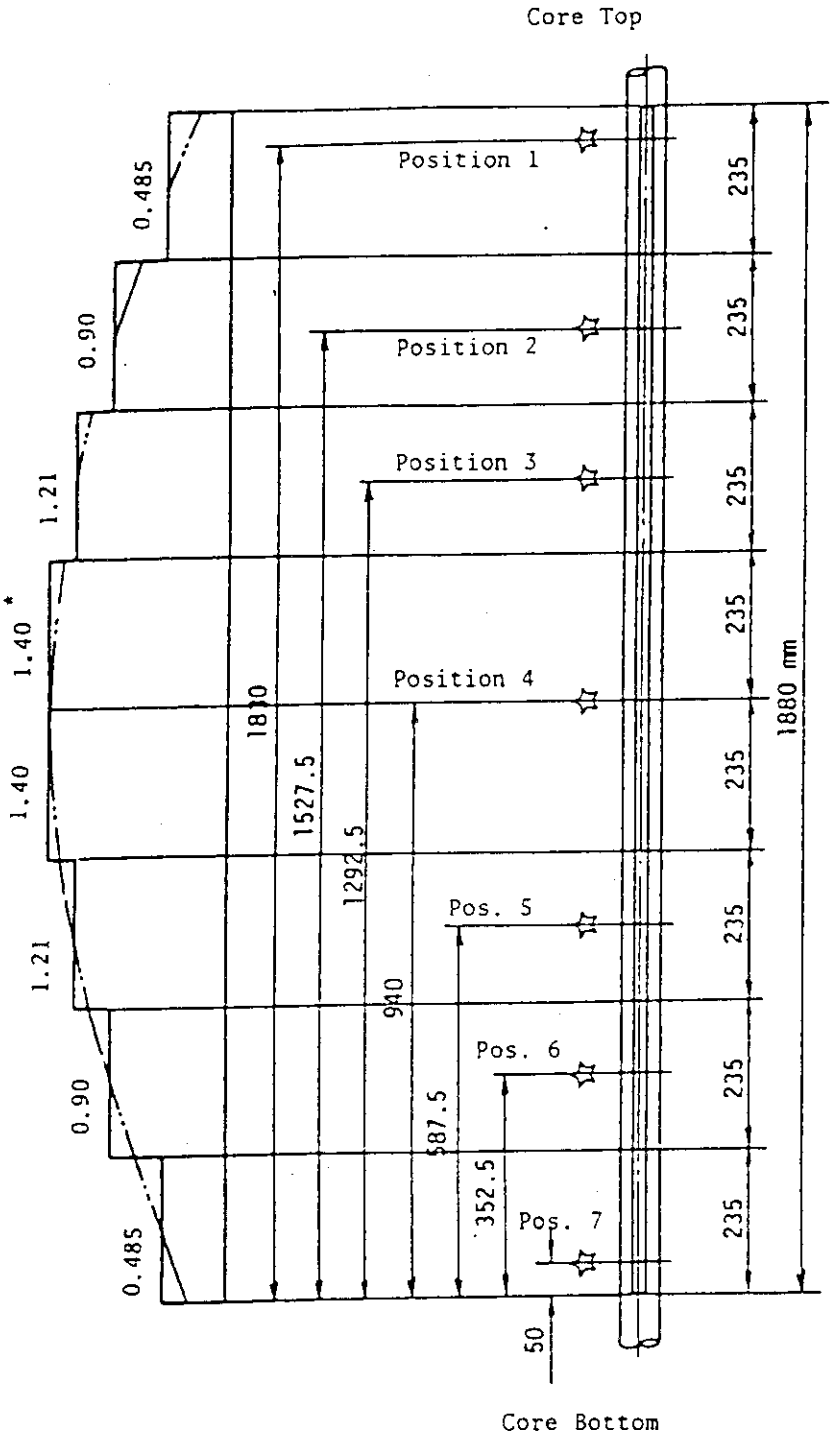

Fig.2.6 Axial Power Distribution of Heater Rod

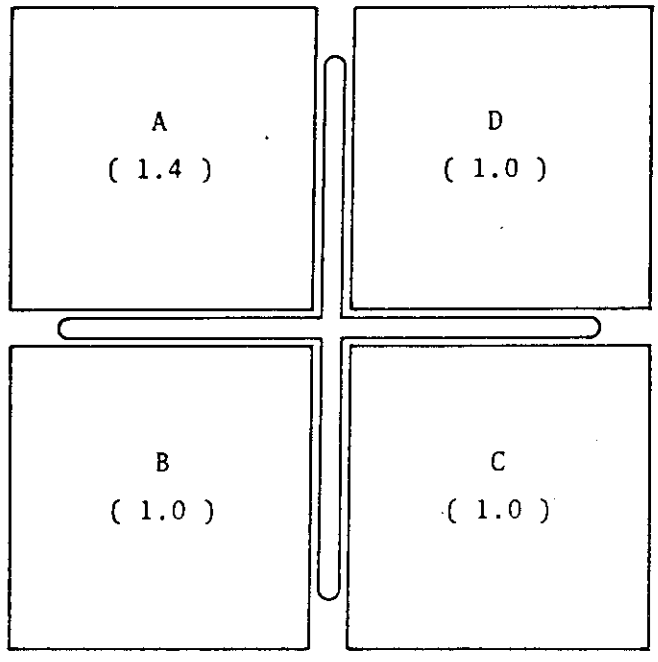

Fig. 2.7 Radial Power Distribution in the Core

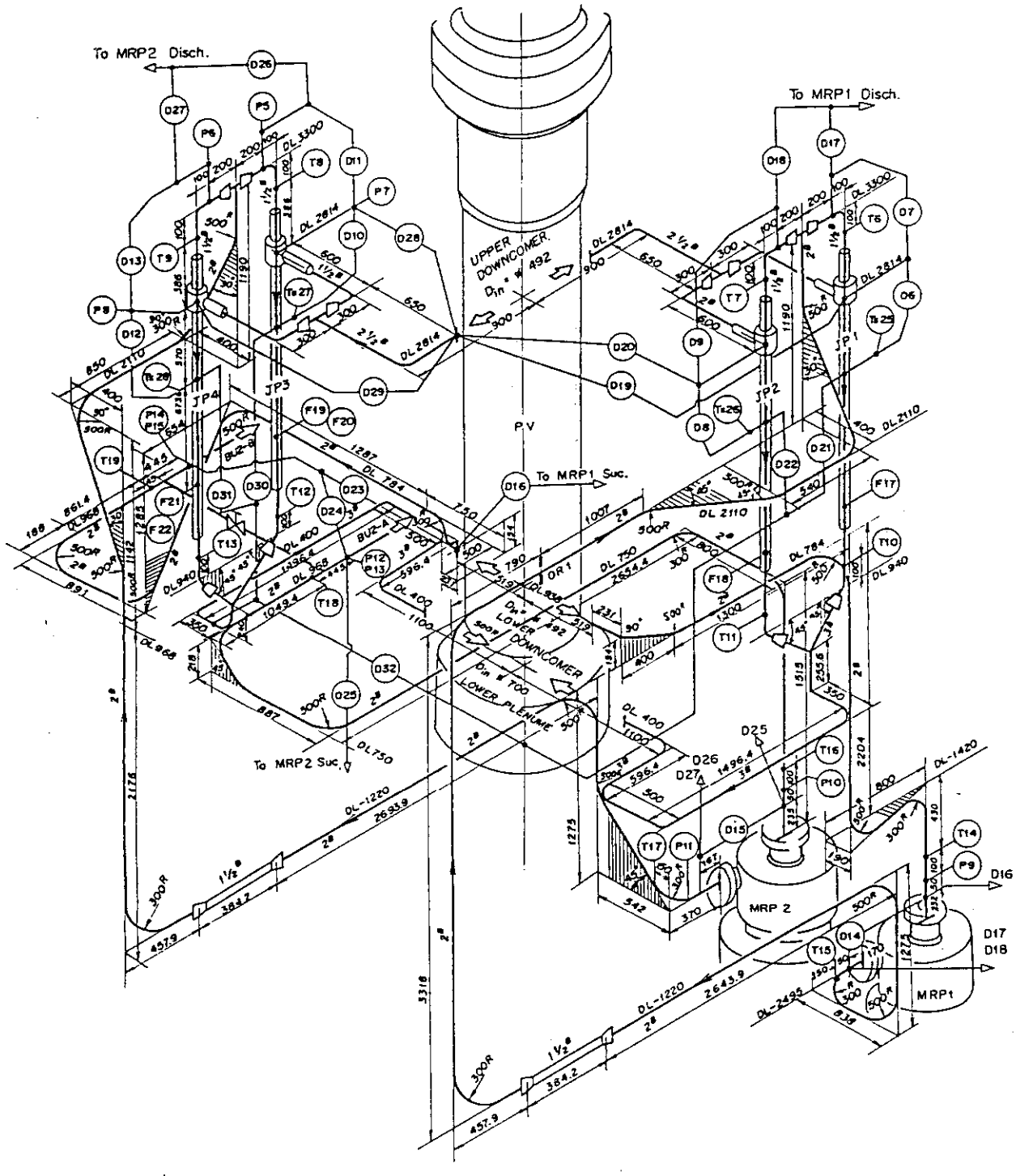

Fig. 2.8 Piping Layout of Recirculation Loops and Jet Pumps

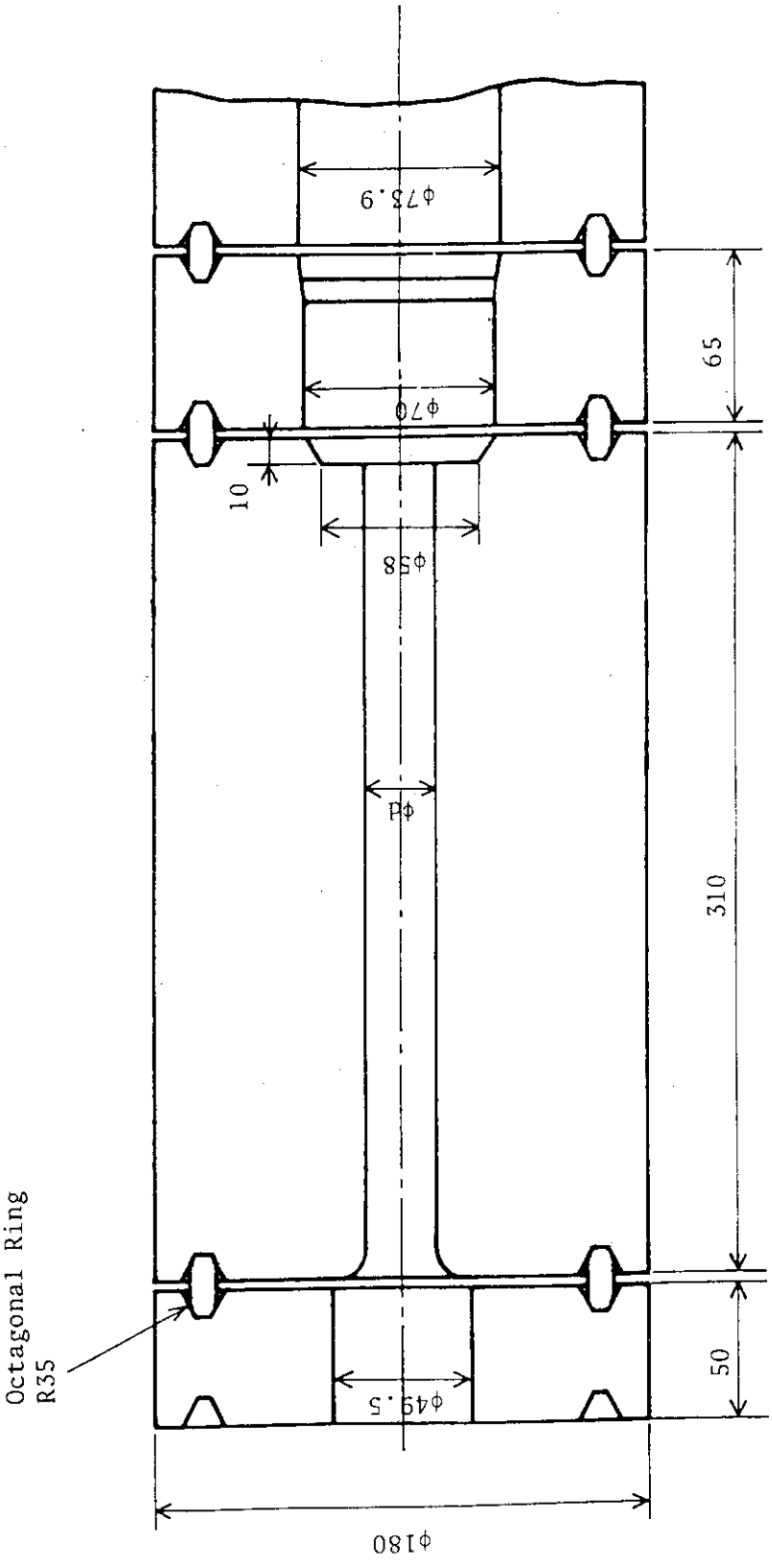

Break area ratio (%)	d (mm)
100	26.2
15	10.1

Material SUS304
Dimension in mm

Fig. 2.9 Break Nozzle Detailes

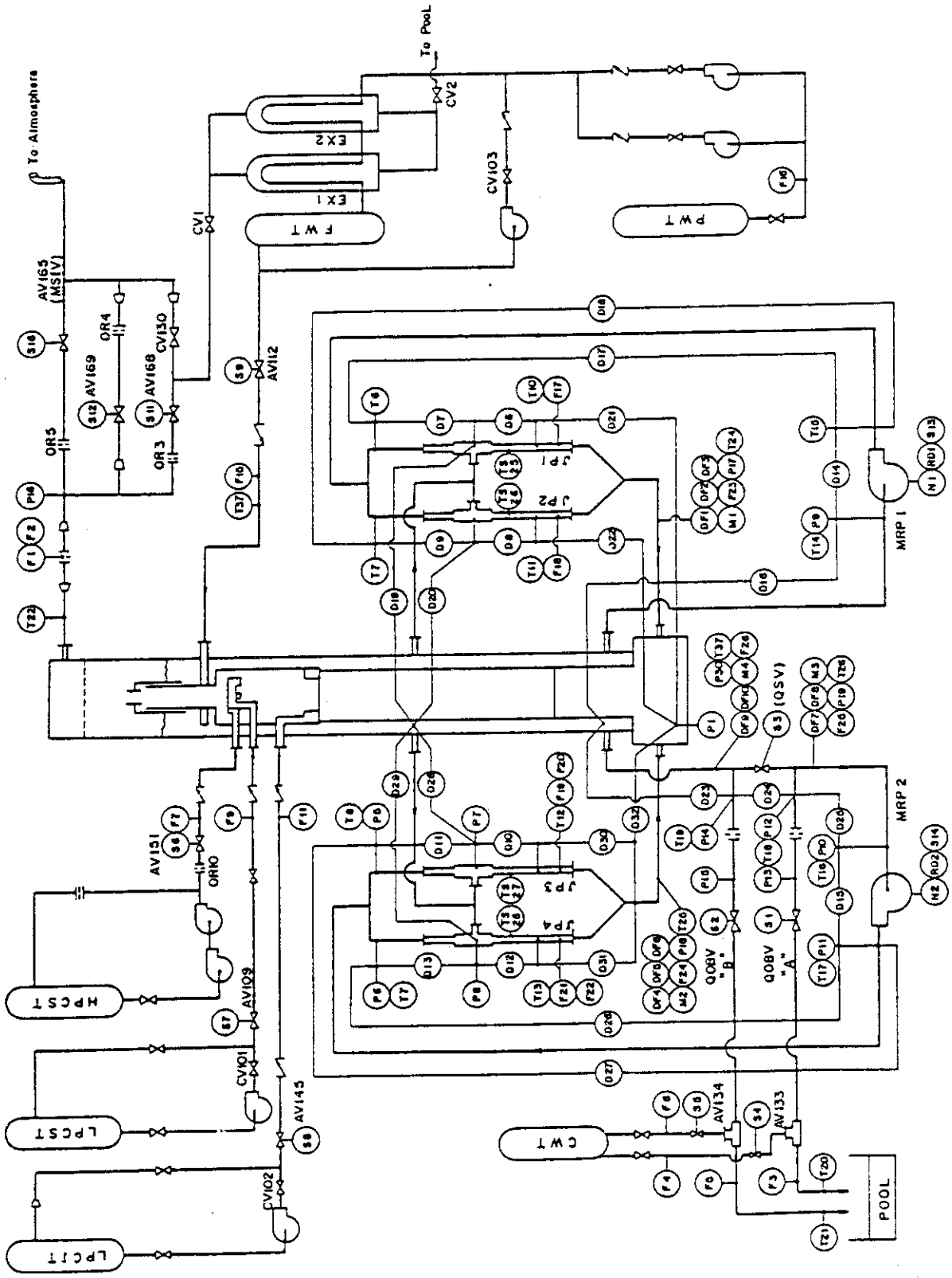

Fig. 3.1 Instrumentation Location of ROSA-III Test Facility

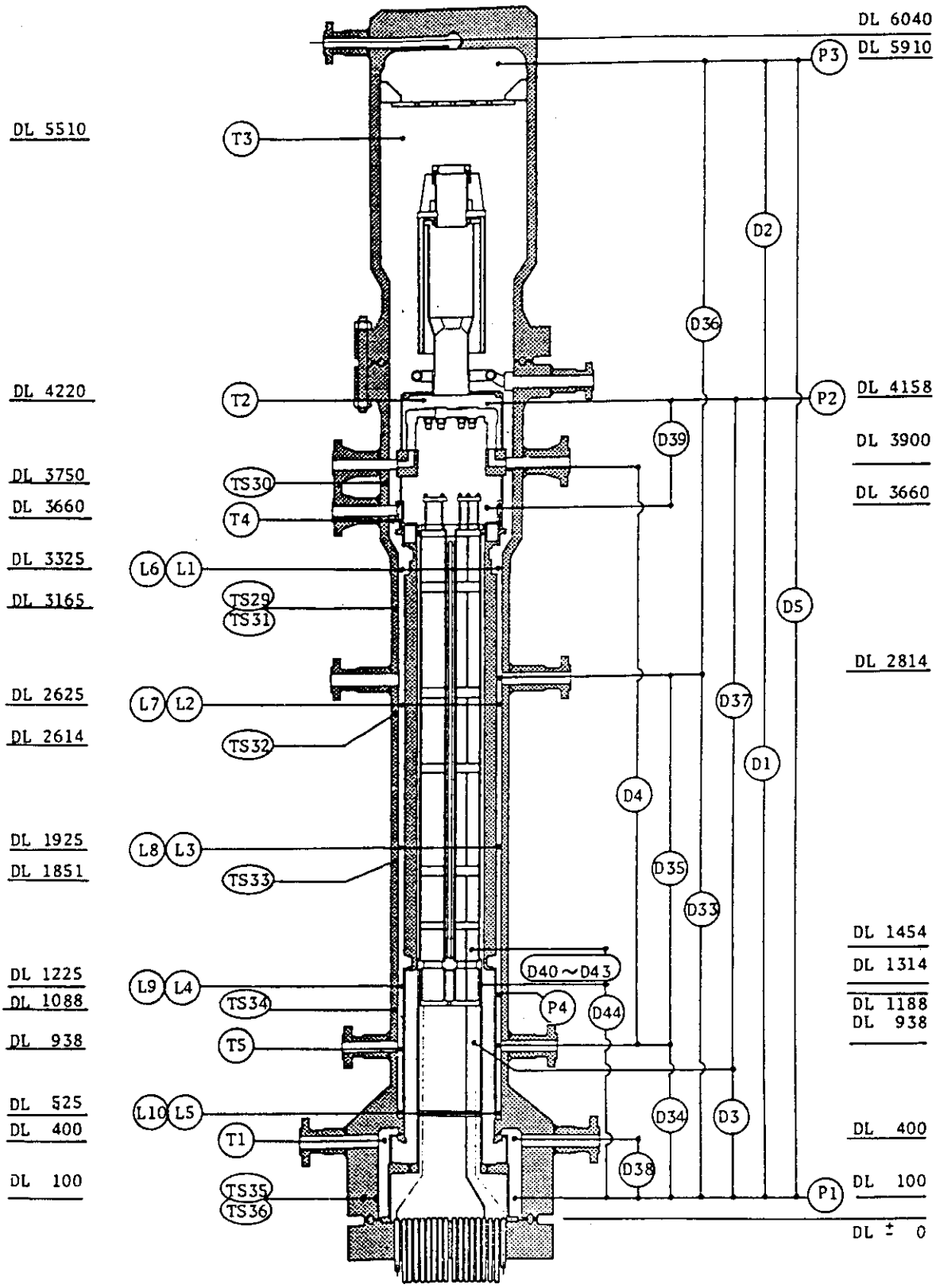

Fig. 3.2 Instrumentation Location in Pressure Vessel

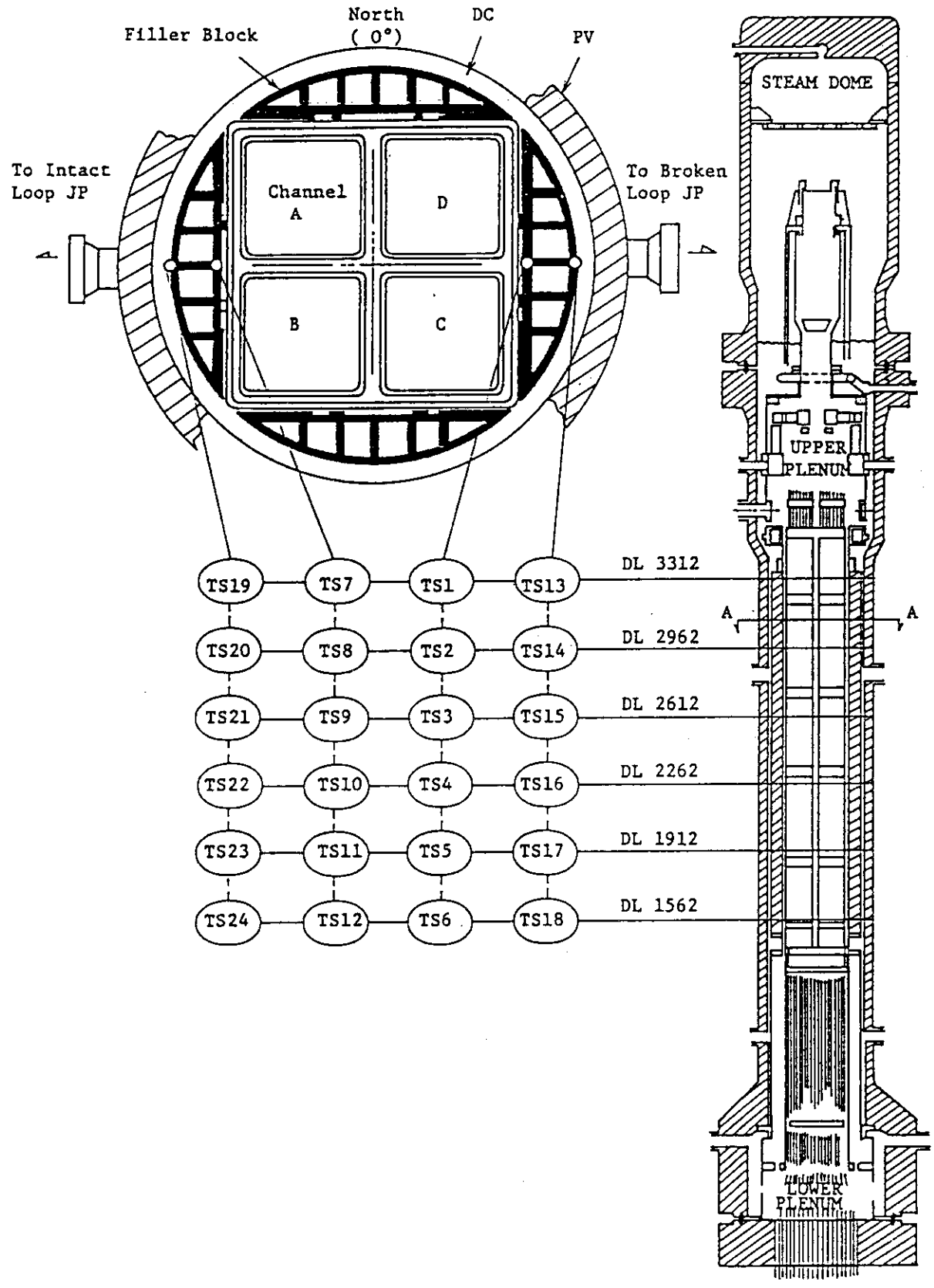

Fig. 3.3 Location of Thermocouples in Filler Blocks

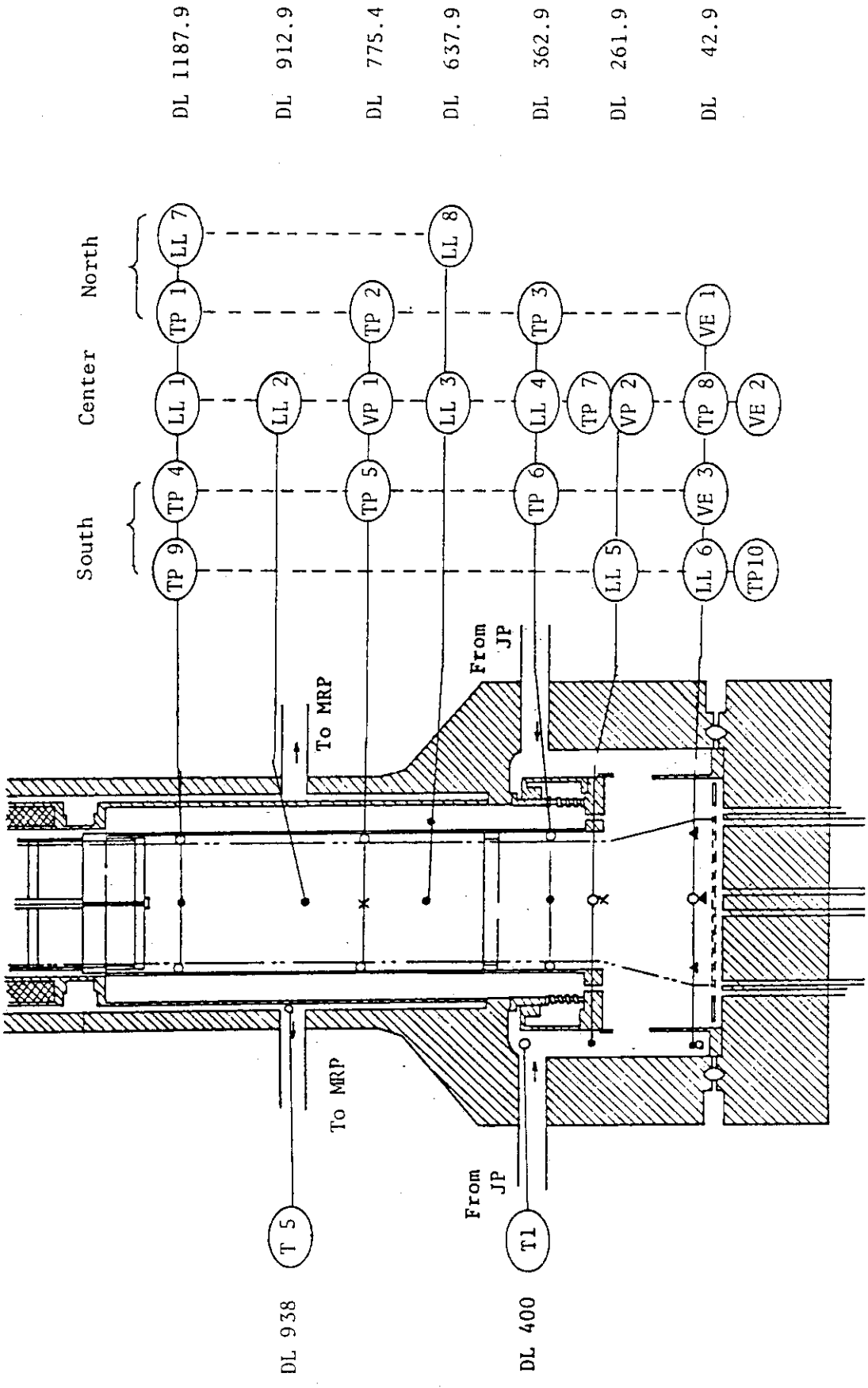

Fig. 3.4 Lower Plenum Instrumentation

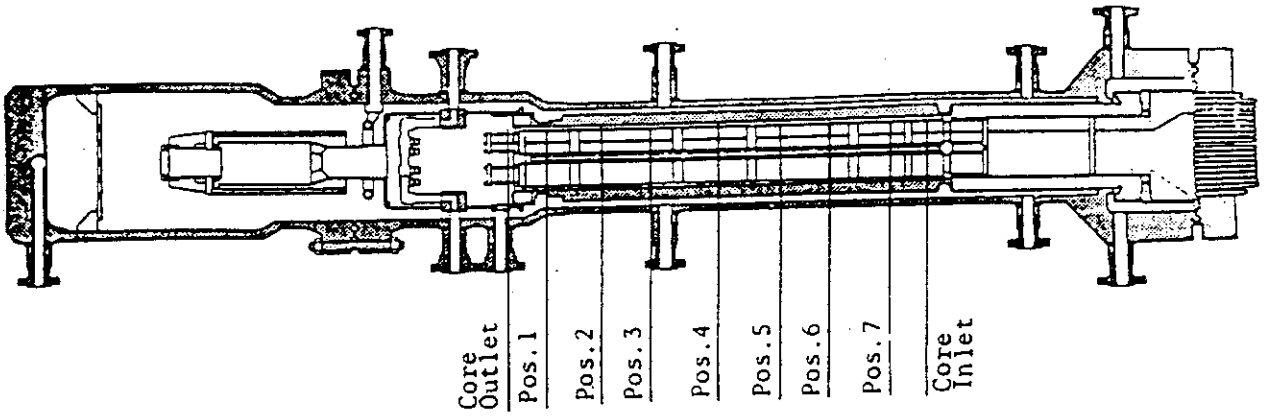

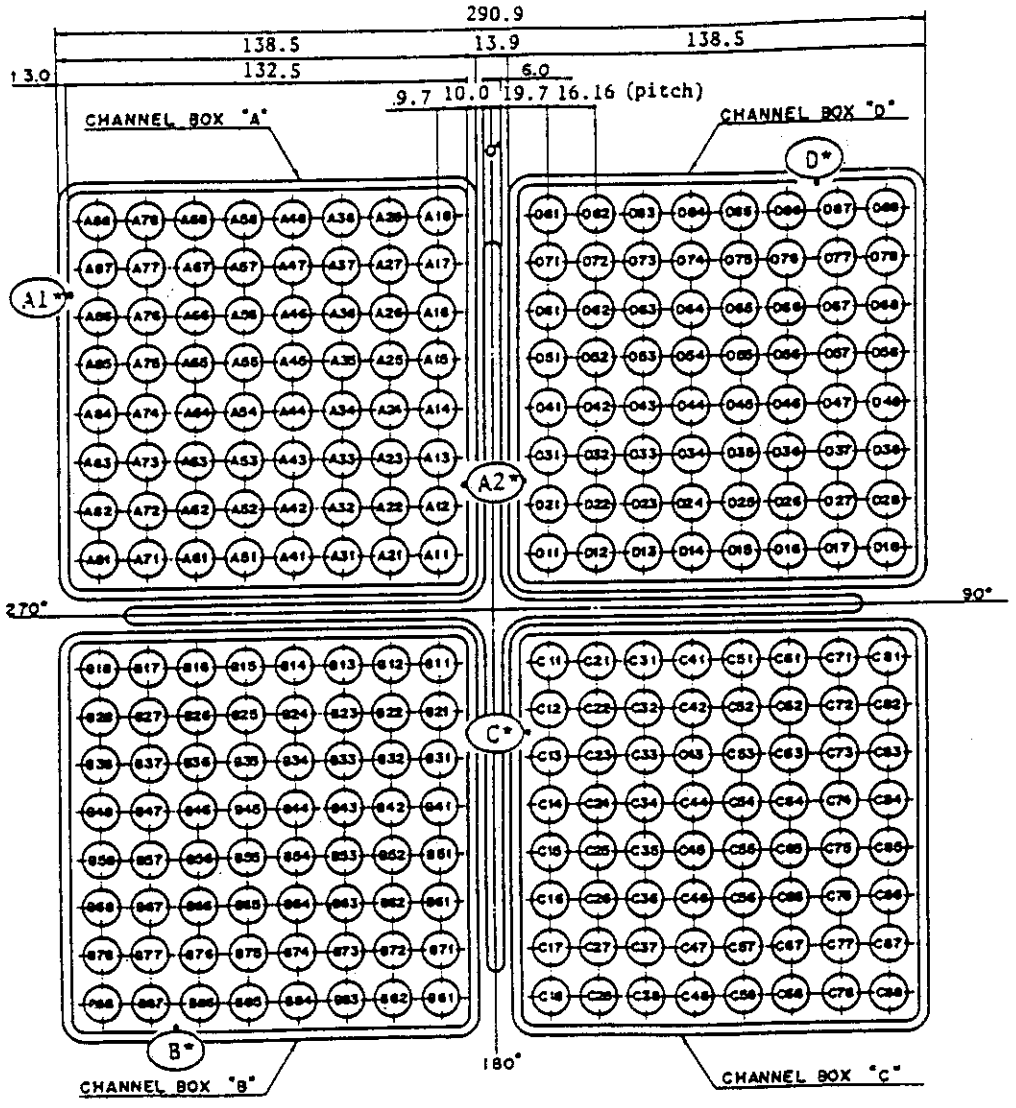

Peaking Factor ; A = 1.4, B = 1.0, C = 1.0, D = 1.0
Heater rod O.D. is 12.27 mm.
A44,A55,B44,B55,C44,C55,D44 and D55 are water rod simulators.
The O.D. is 15.01 mm.

Fig. 3.5 Core Instrumentation (cf. Table 3.2)

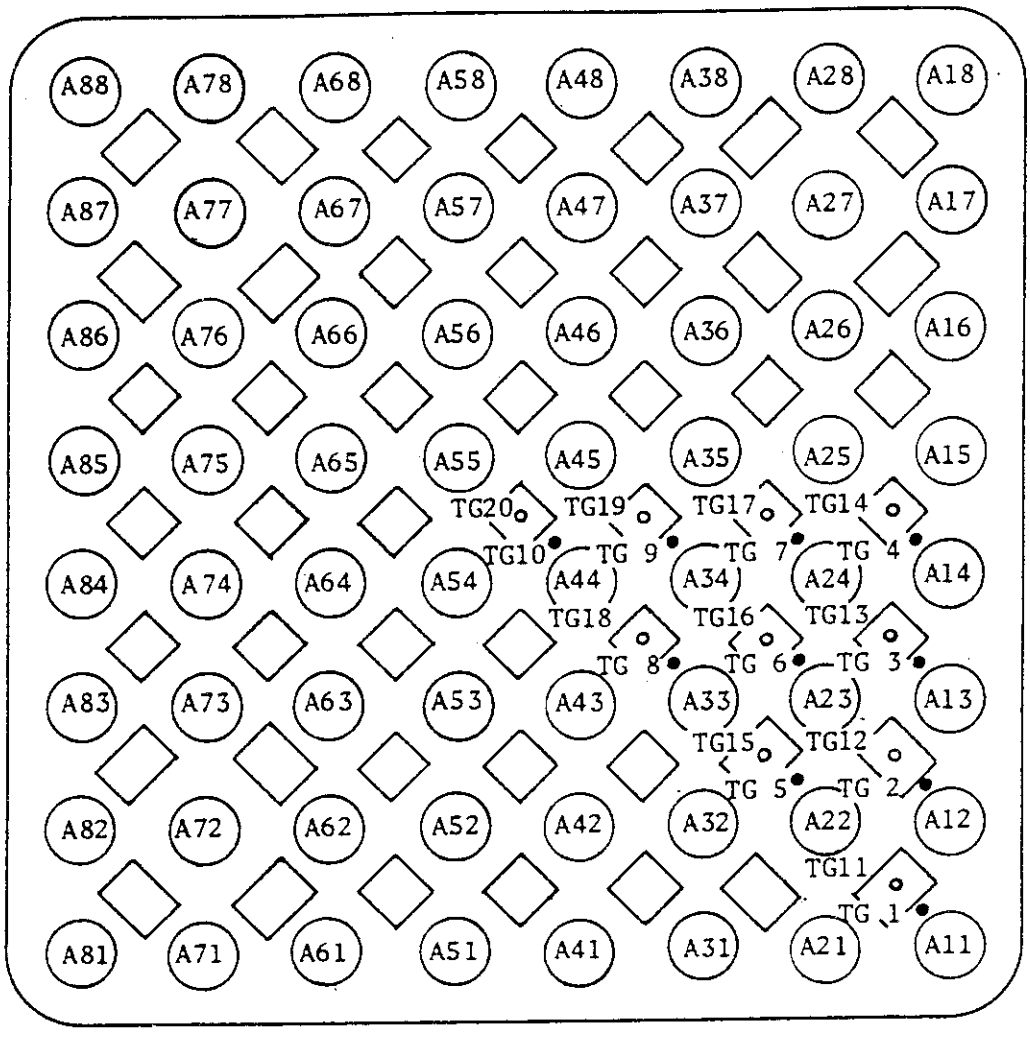

Thermocouples ;

- ● TG 1～TG10 : 3 mm above the UTP* upper surface
- ○ TG11～TG20 : In the holes at the same level as the UTP* lower surface

* UTP : Upper Tieplate

Fig. 3.6 Upper Tieplate Instrumentation

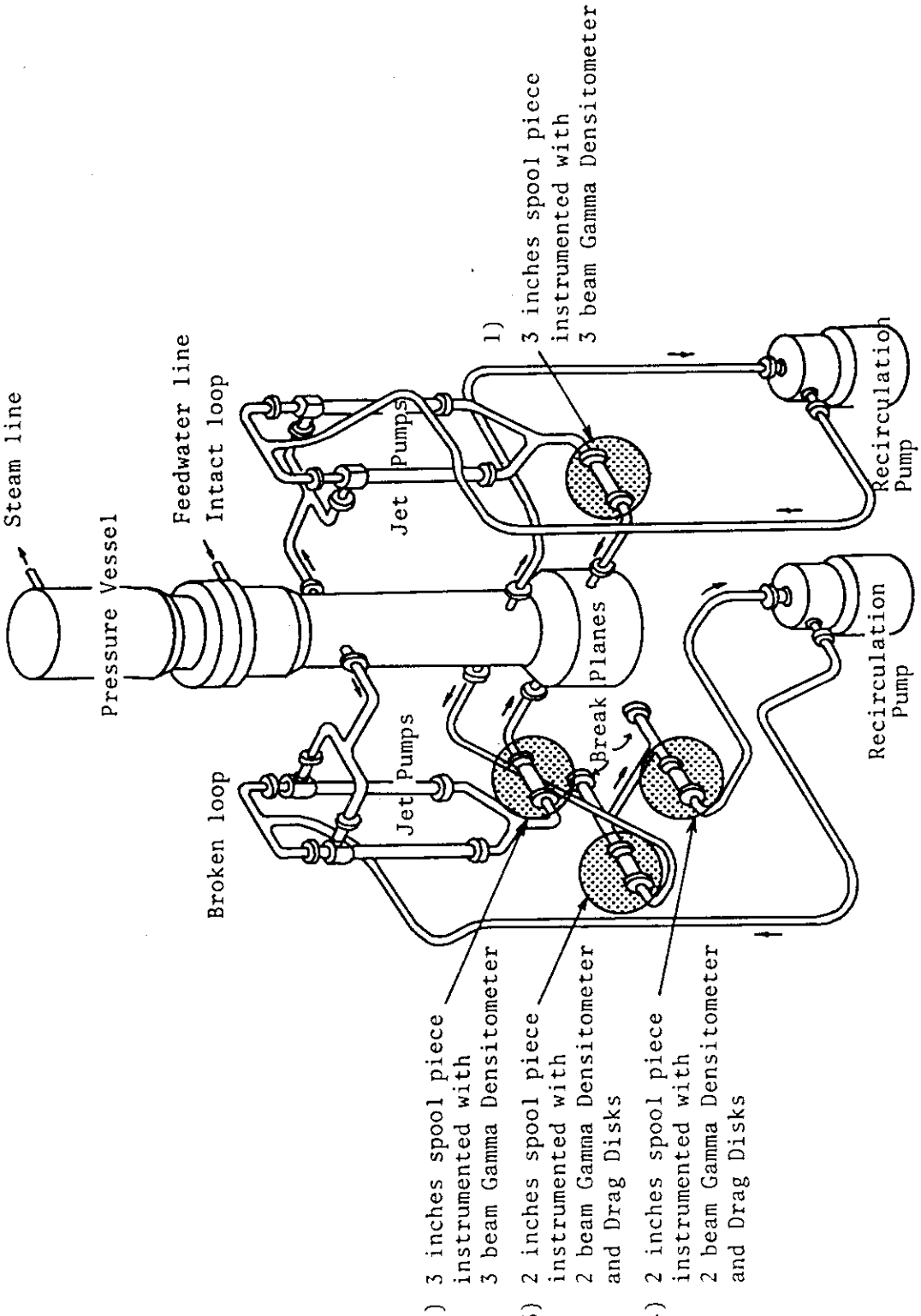

Fig. 3.7 Location of Two-phase Flow Measurement Spool Pieces

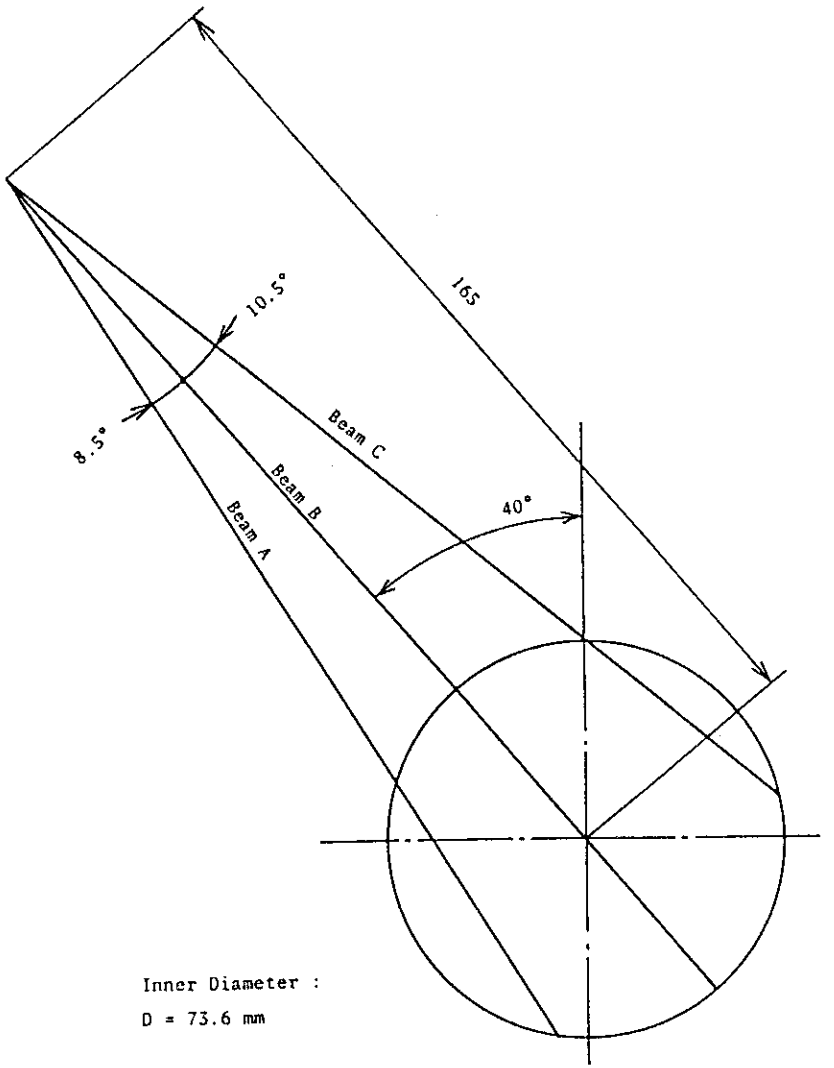

Fig. 3.8 Beam Configuration of Three-Beam Gamma Densitometer

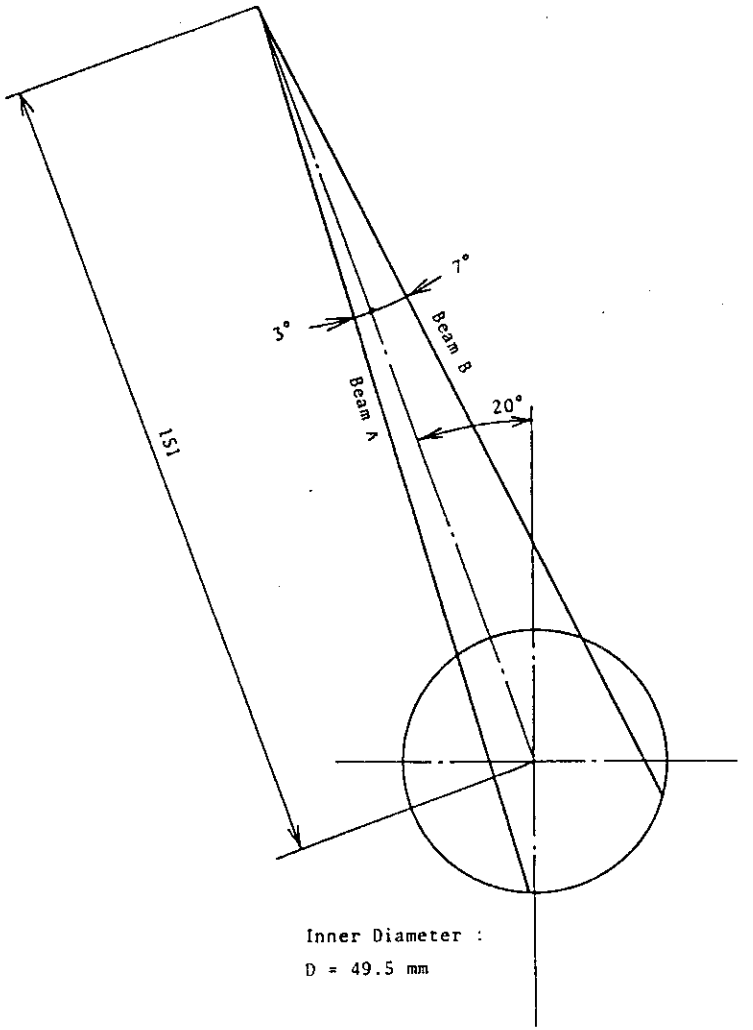

Fig. 3.9 Beam Configuration of Two-Beam Gamma Densitometer

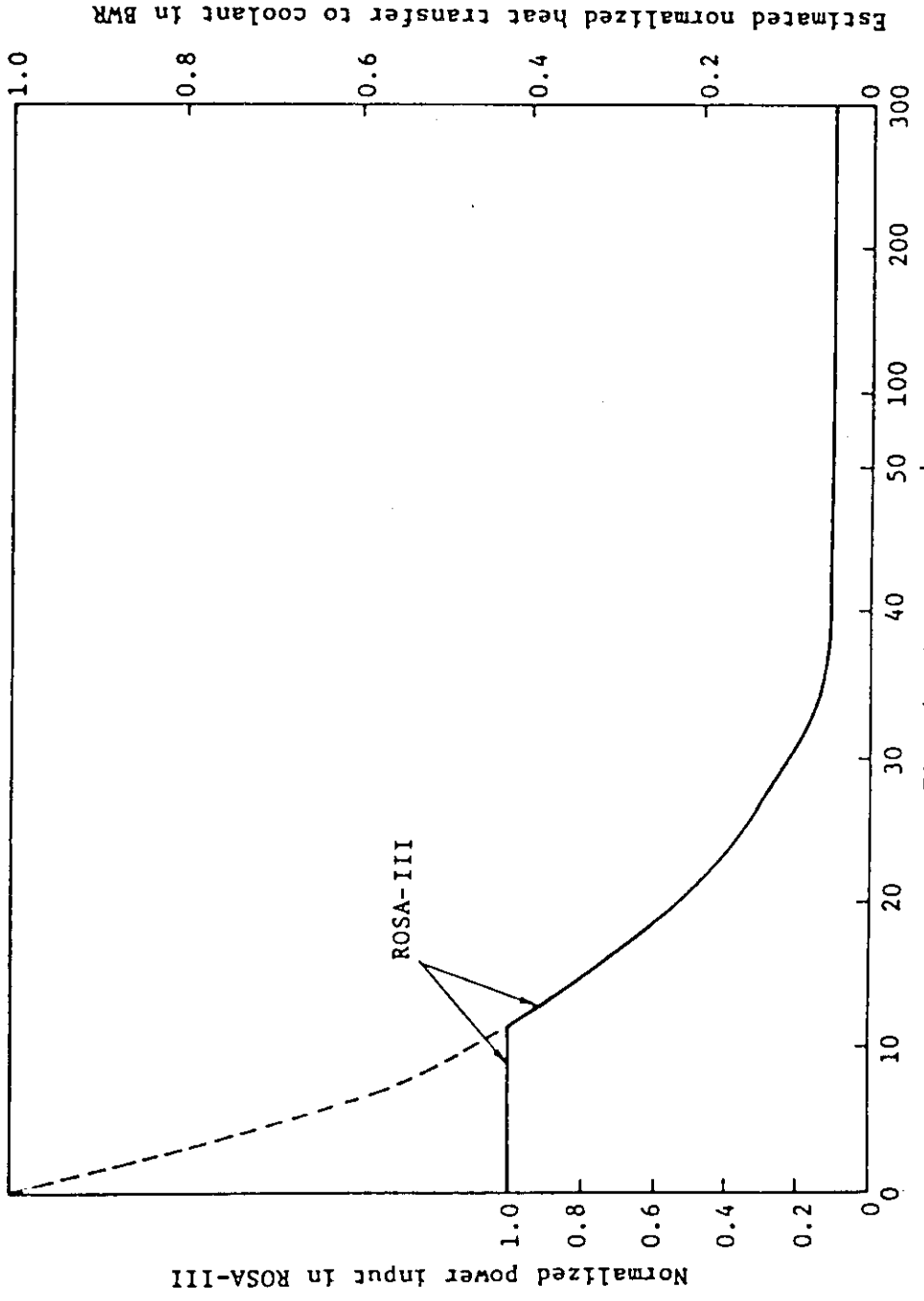

Fig. 4.1 Normalized Power Transient in BWR and ROSA-III

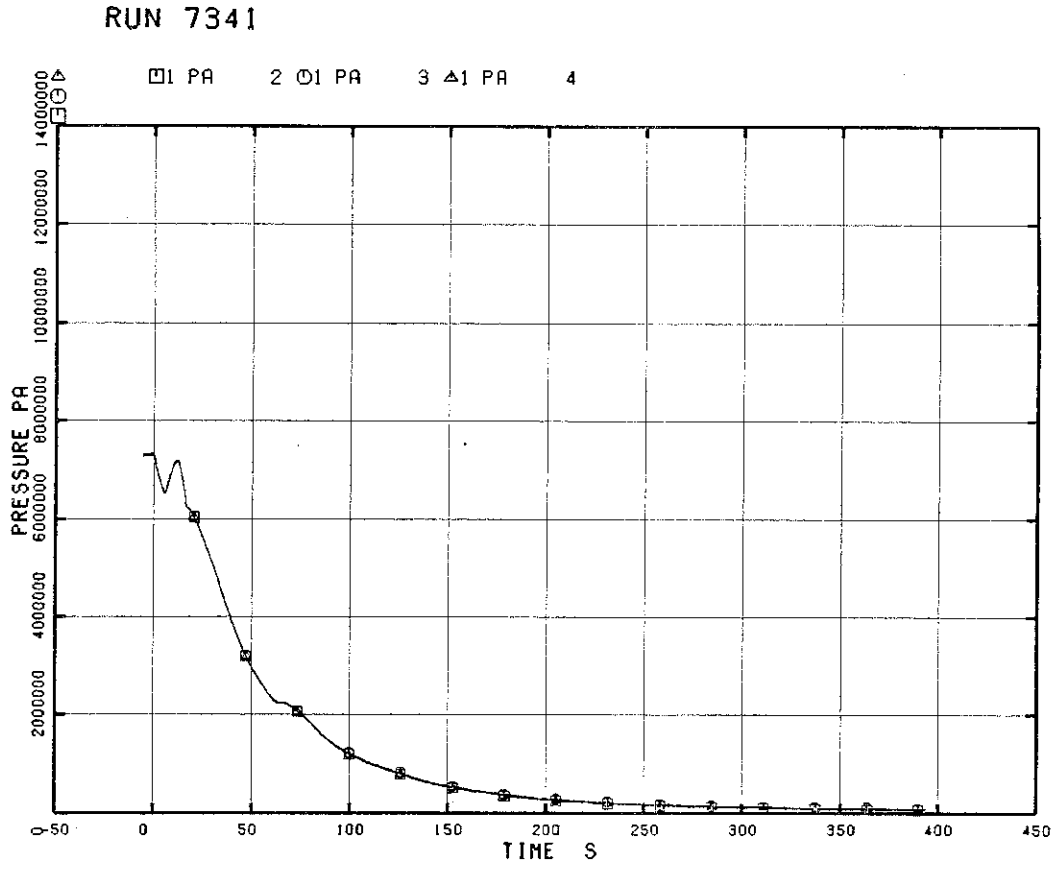

Fig. 5.1 Pressures in Pressure Vessel

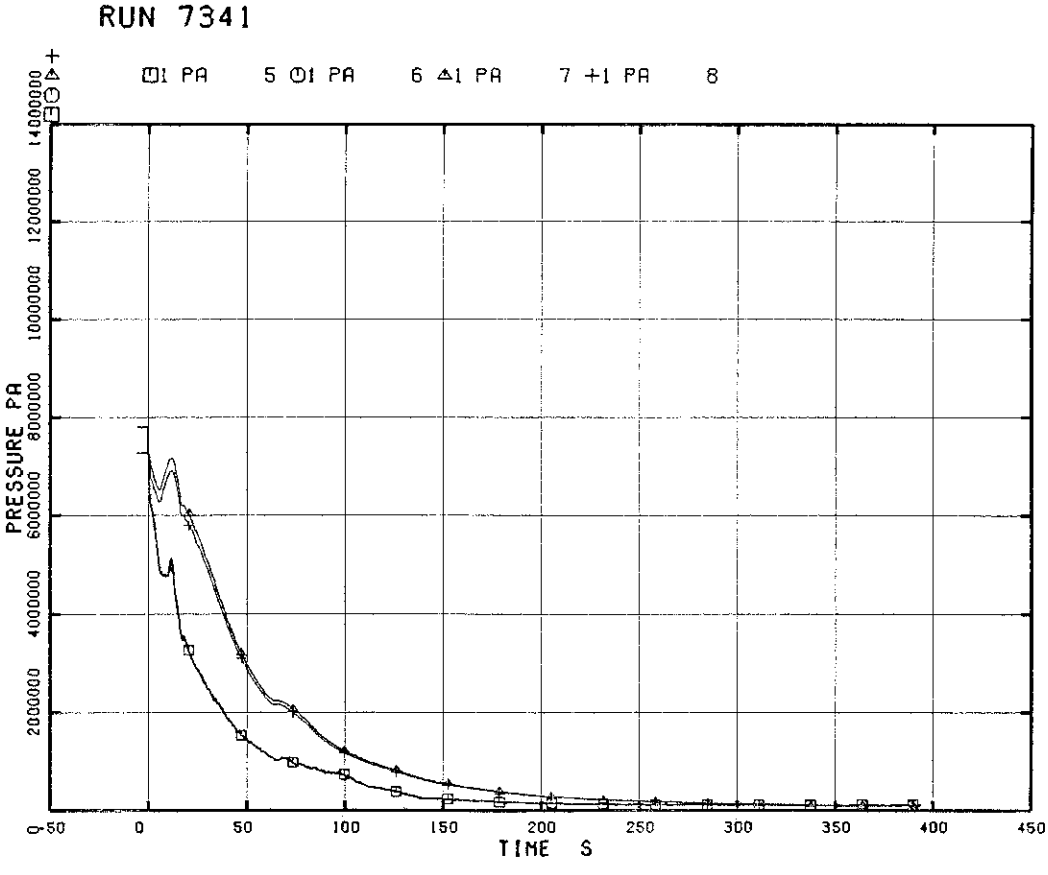

Fig. 5.2 Pressures in Broken Loop Jet Pump

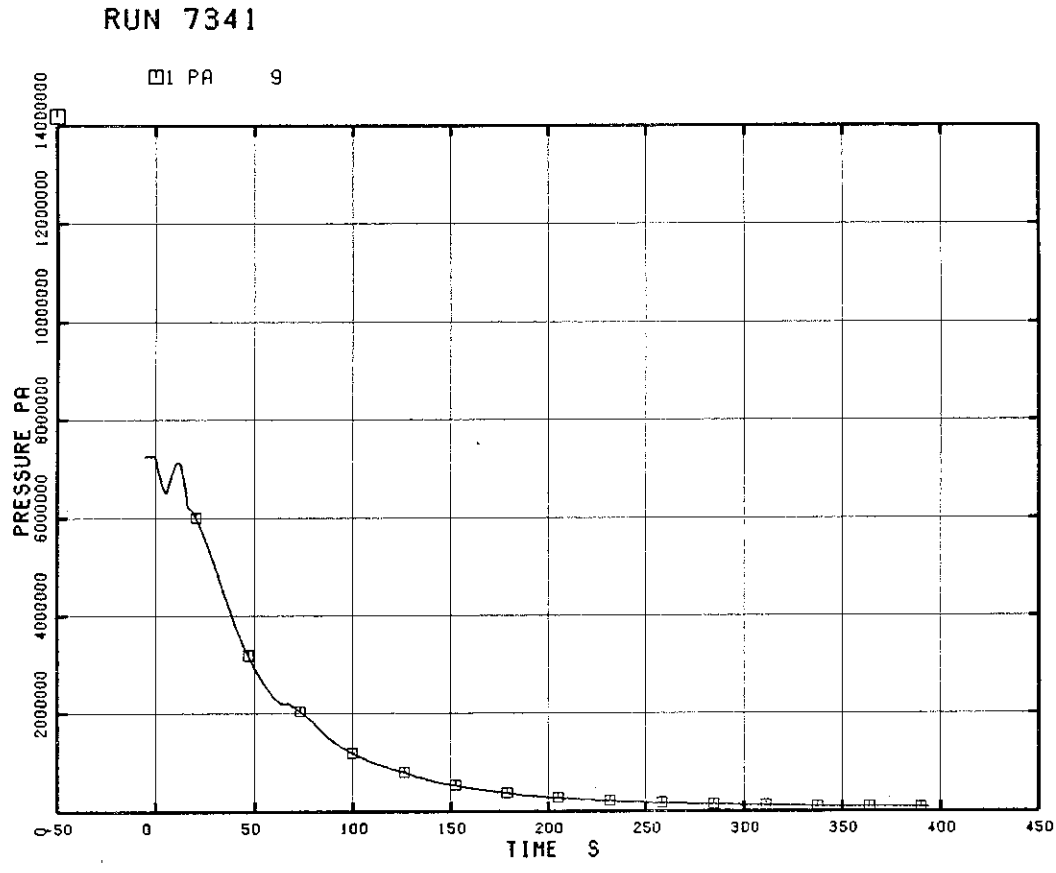

Fig. 5.3 Pressure in Intact Loop

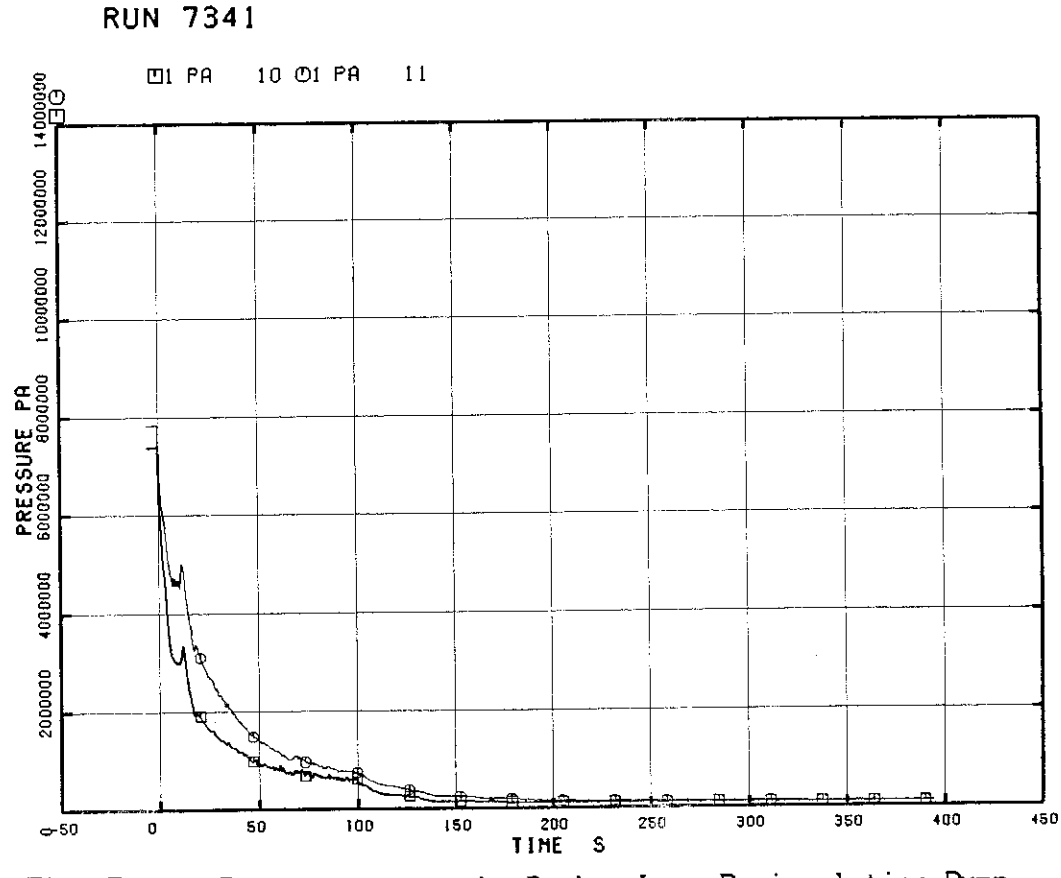

Fig. 5.4 Pressures near the Broken Loop Recirculation Pump

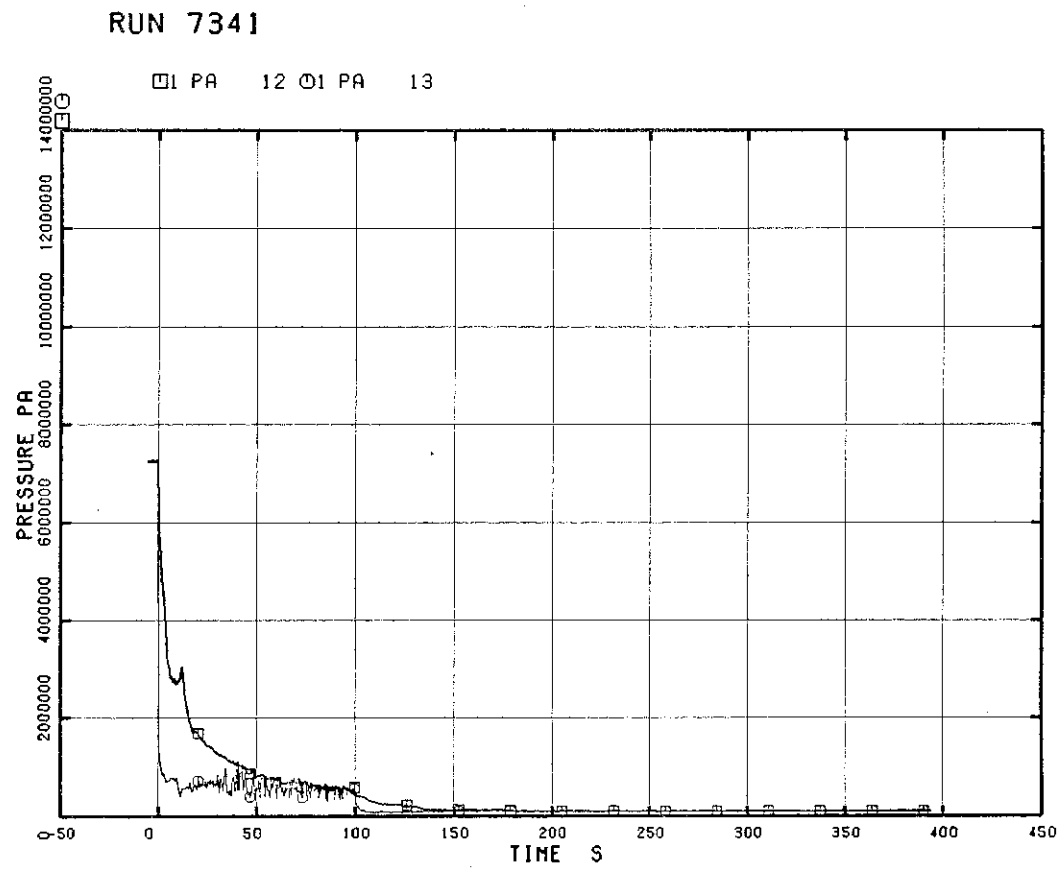

Fig. 5.5 Pressures at the Pump Side of the Break

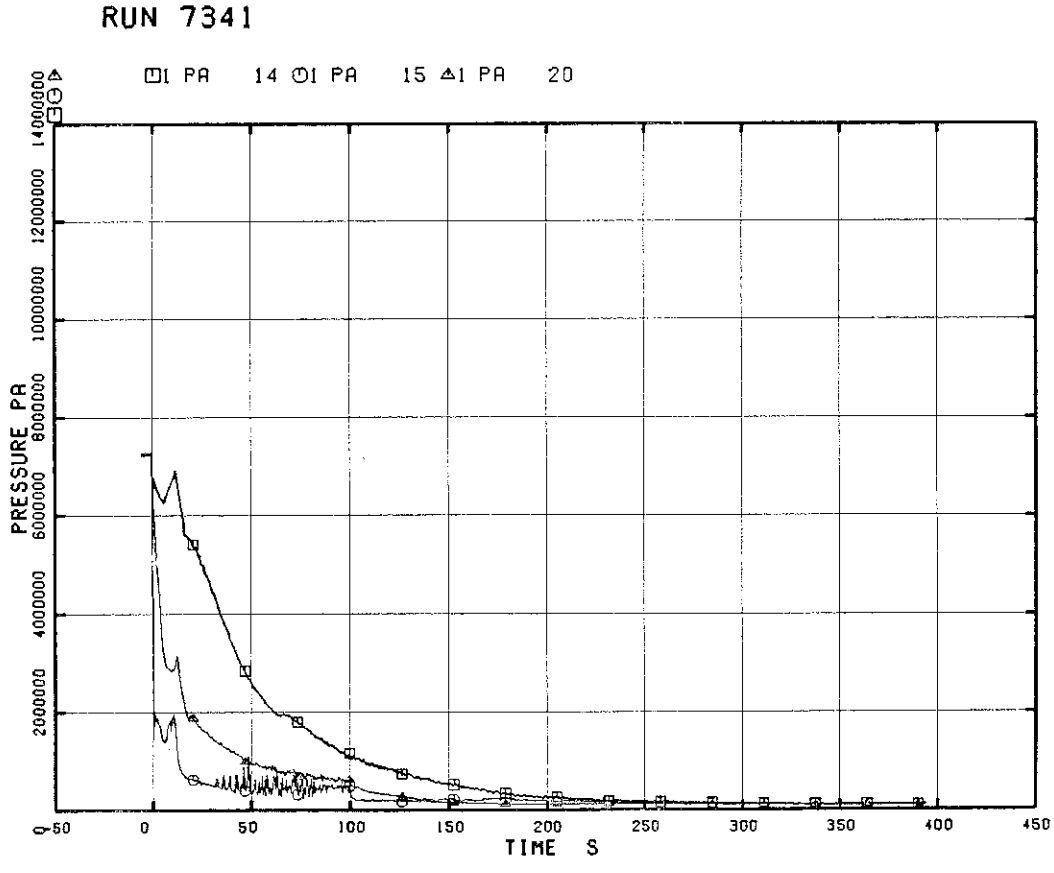

Fig. 5.6 Pressures at the Vessel Side of the Break

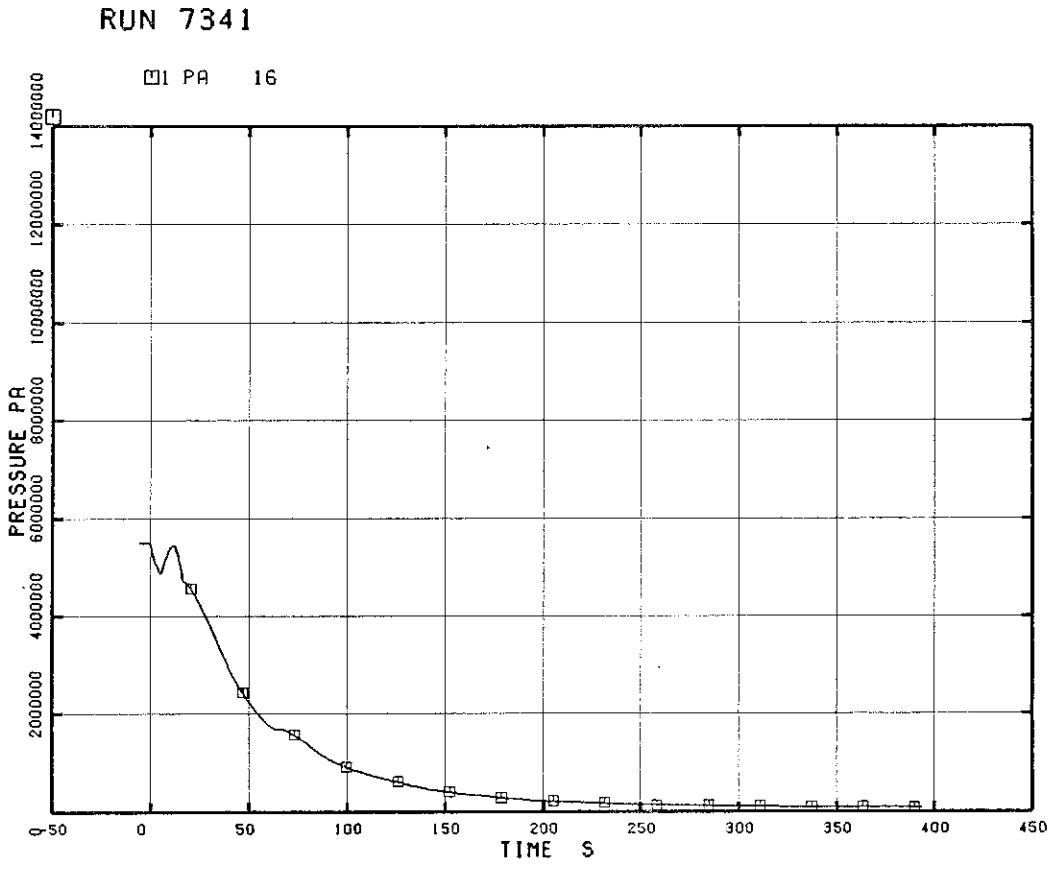

Fig. 5.7 Pressure in Steam Line

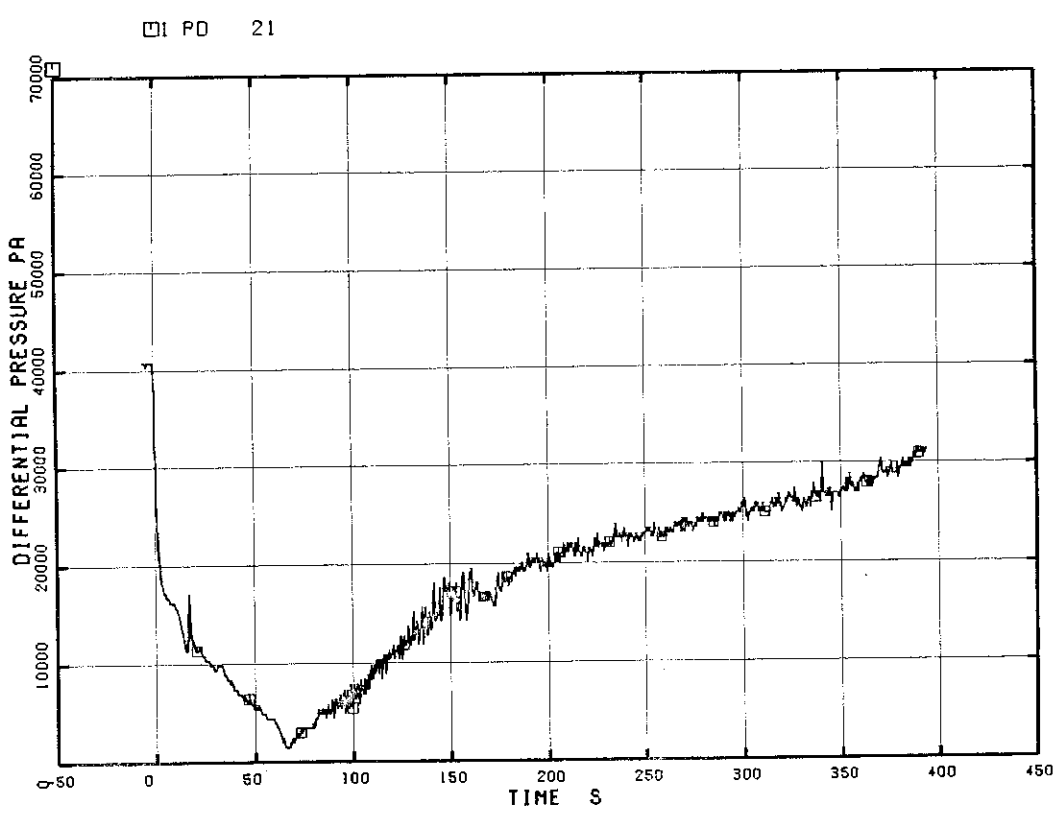

Fig. 5.8 Differential Pressure between Lower Plenum and Upper Plenum

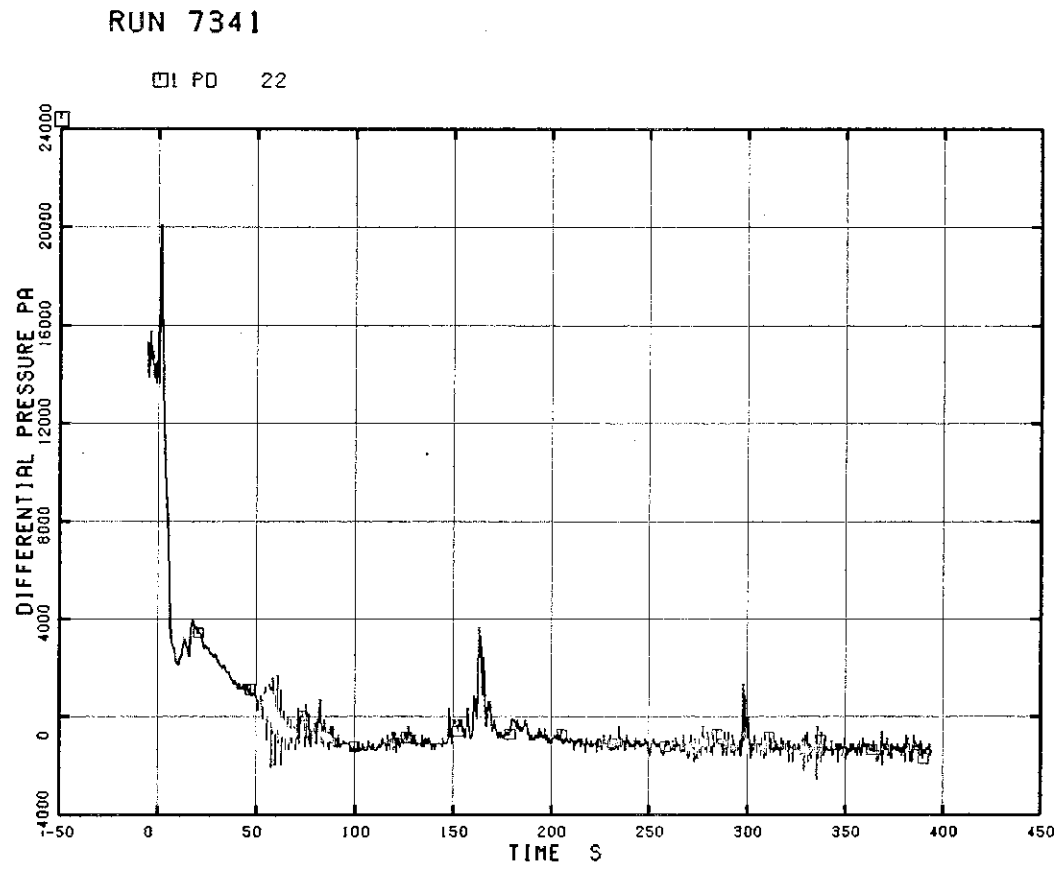

Fig. 5.9 Differential Pressure between Upper Plenum and Steam Dome

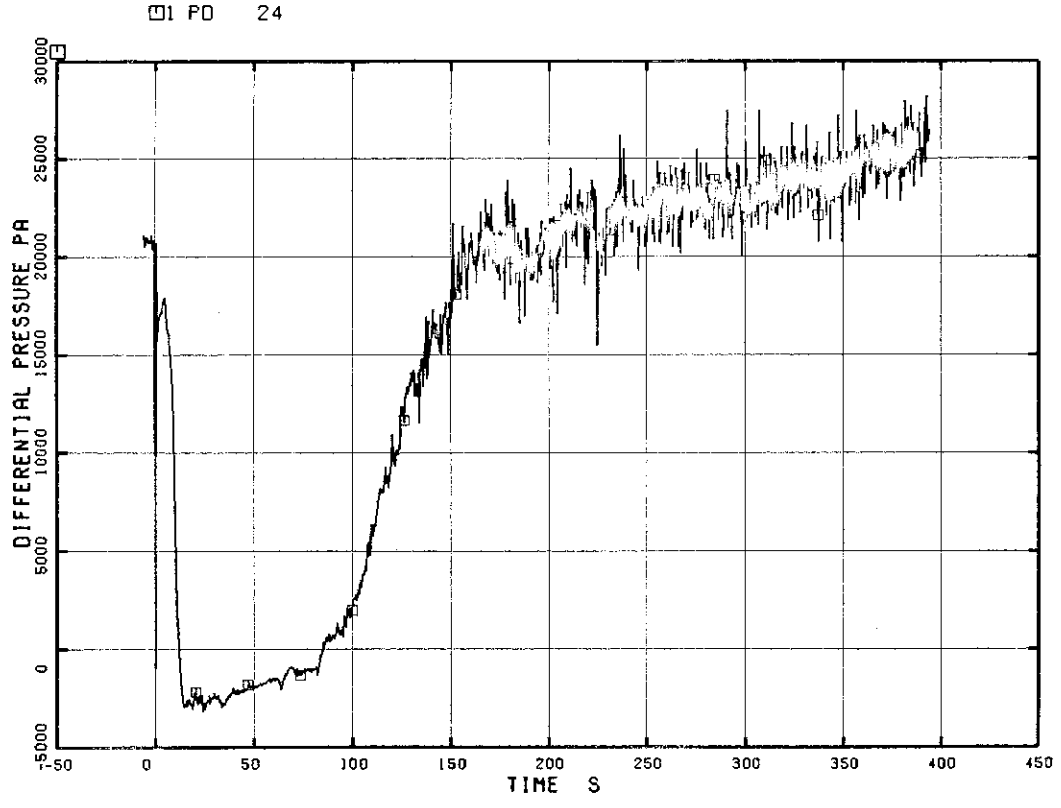

Fig. 5.10 Differential Pressure in Downcomer

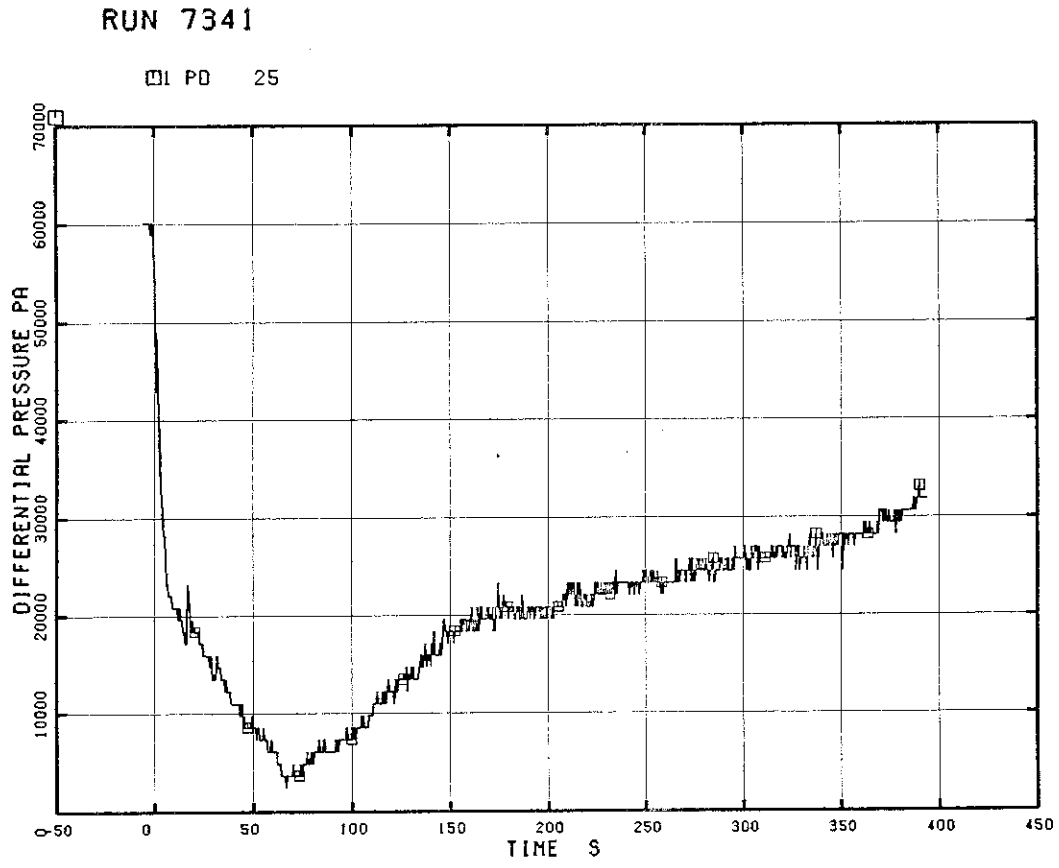

Fig. 5.11 Differential Pressure between Vessel Bottom and Top

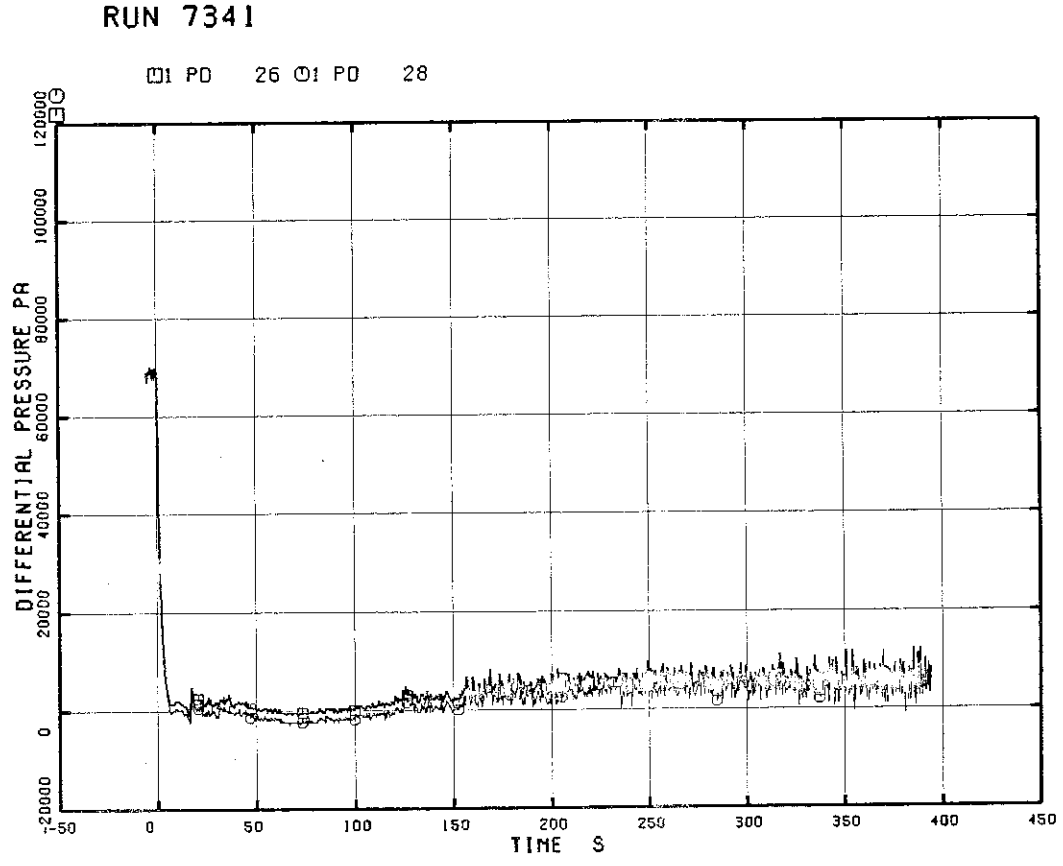

Fig. 5.12 Differential Pressure between Intact Loop Jet Pump Discharge and Suction

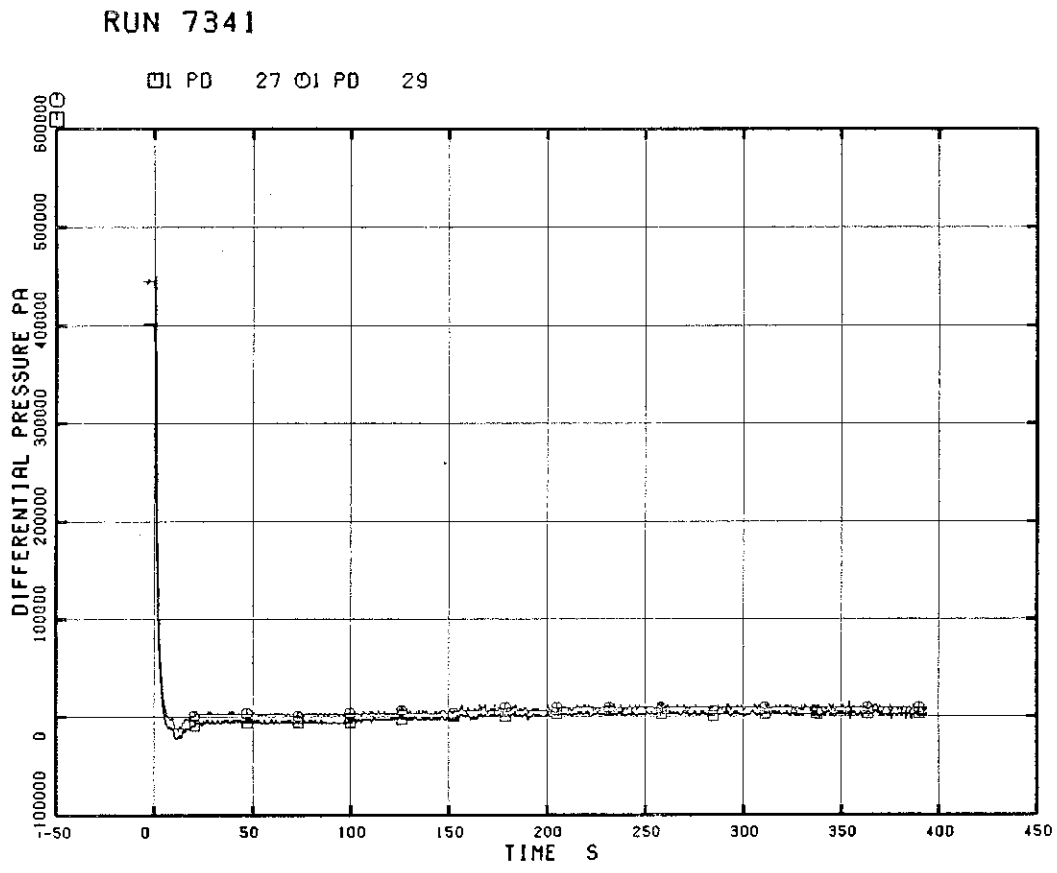

Fig. 5.13 Differential Pressure between Intact Loop Jet Pump Drive and Suction

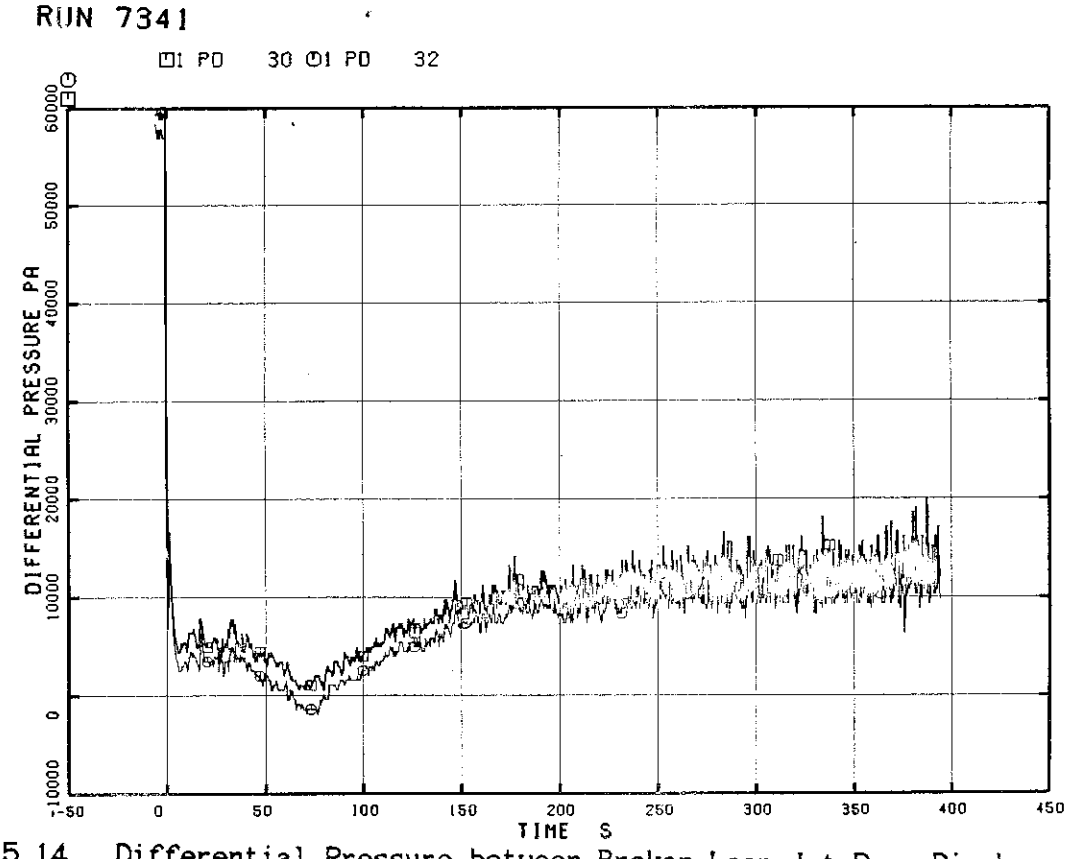

Fig. 5.14 Differential Pressure between Broken Loop Jet Pump Discharge and Suction

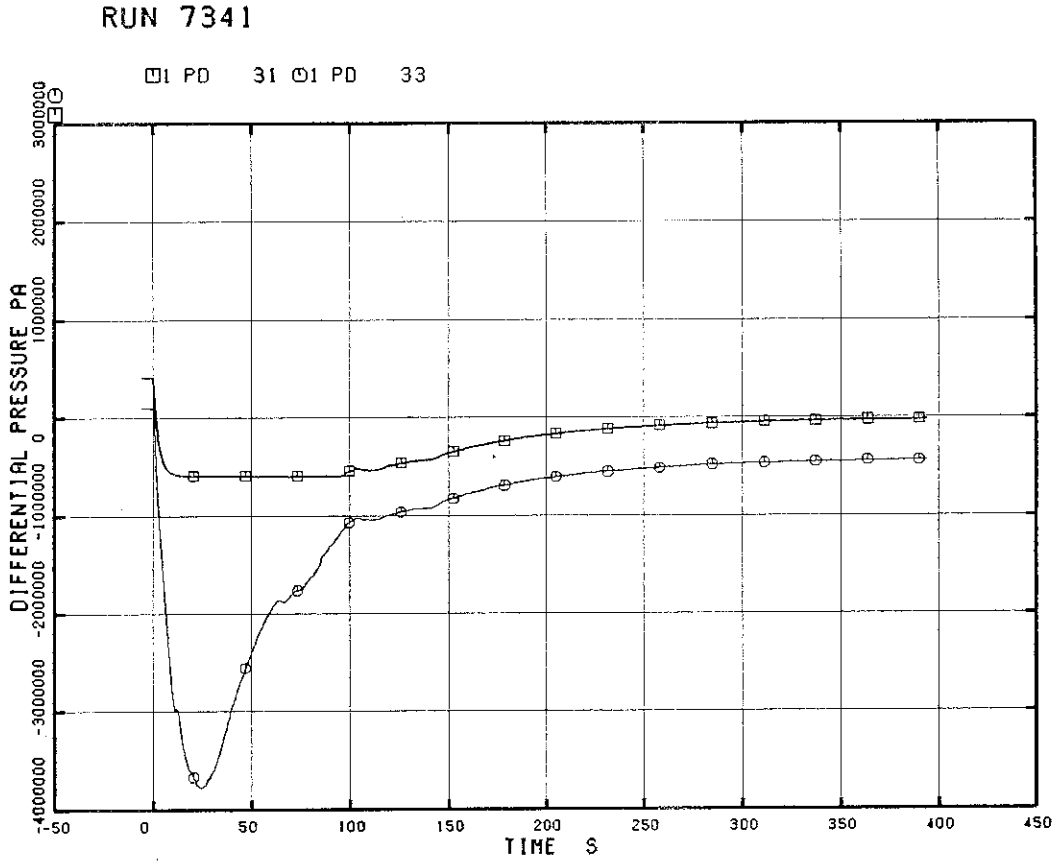

Fig. 5.15 Differential Pressure between Broken Loop Jet Pump Drive and Suction

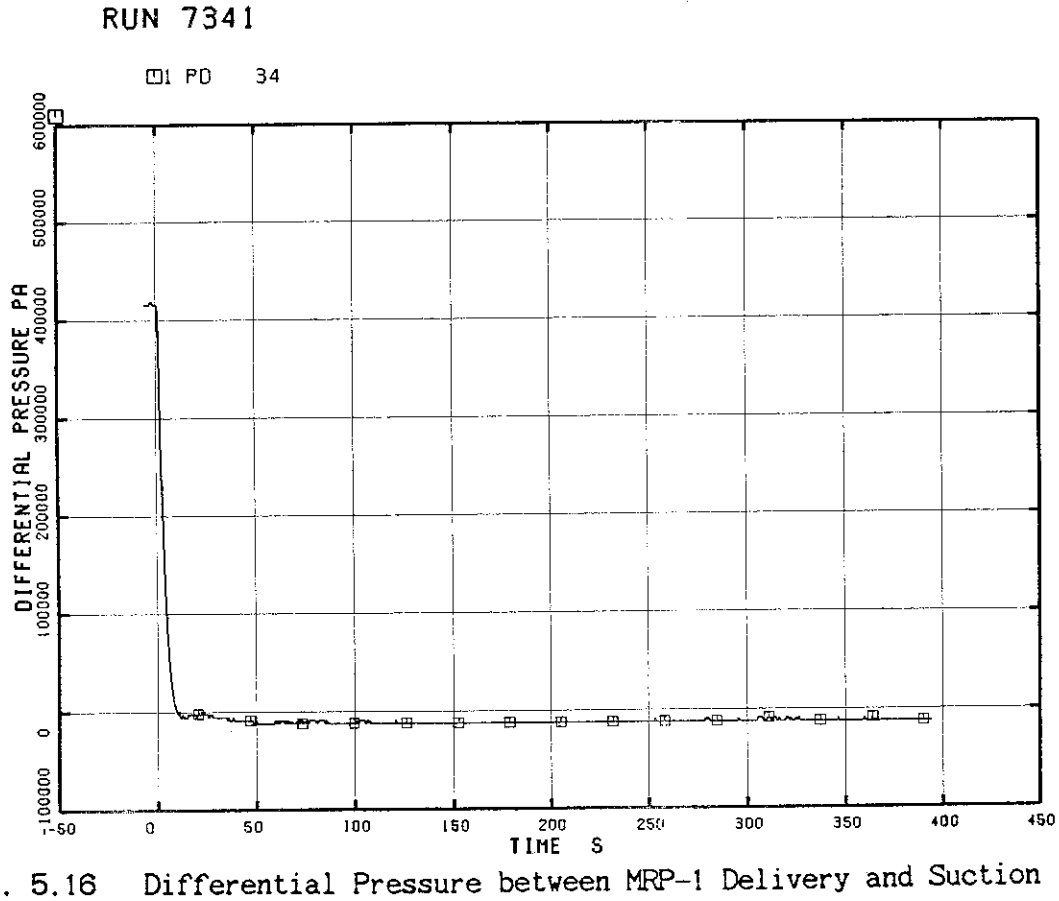

Fig. 5.16 Differential Pressure between MRP-1 Delivery and Suction

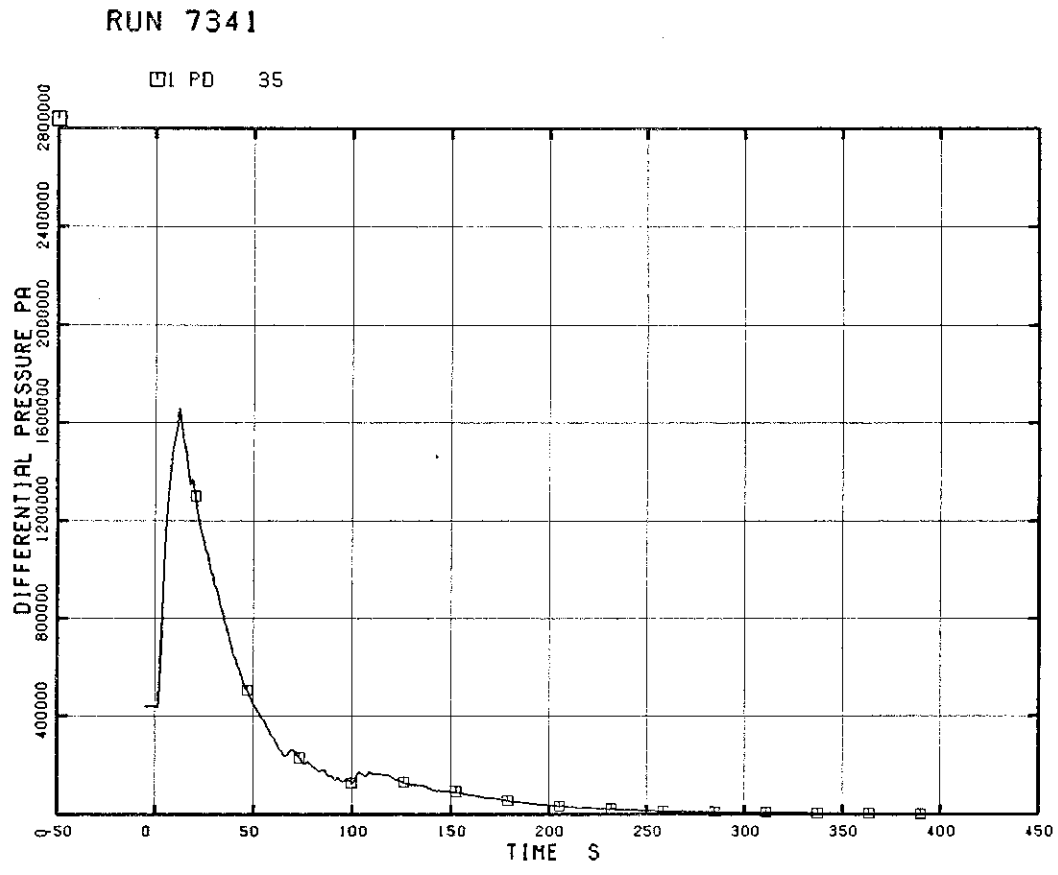

Fig. 5.17 Differential Pressure between MRP-2 Delivery and Suction

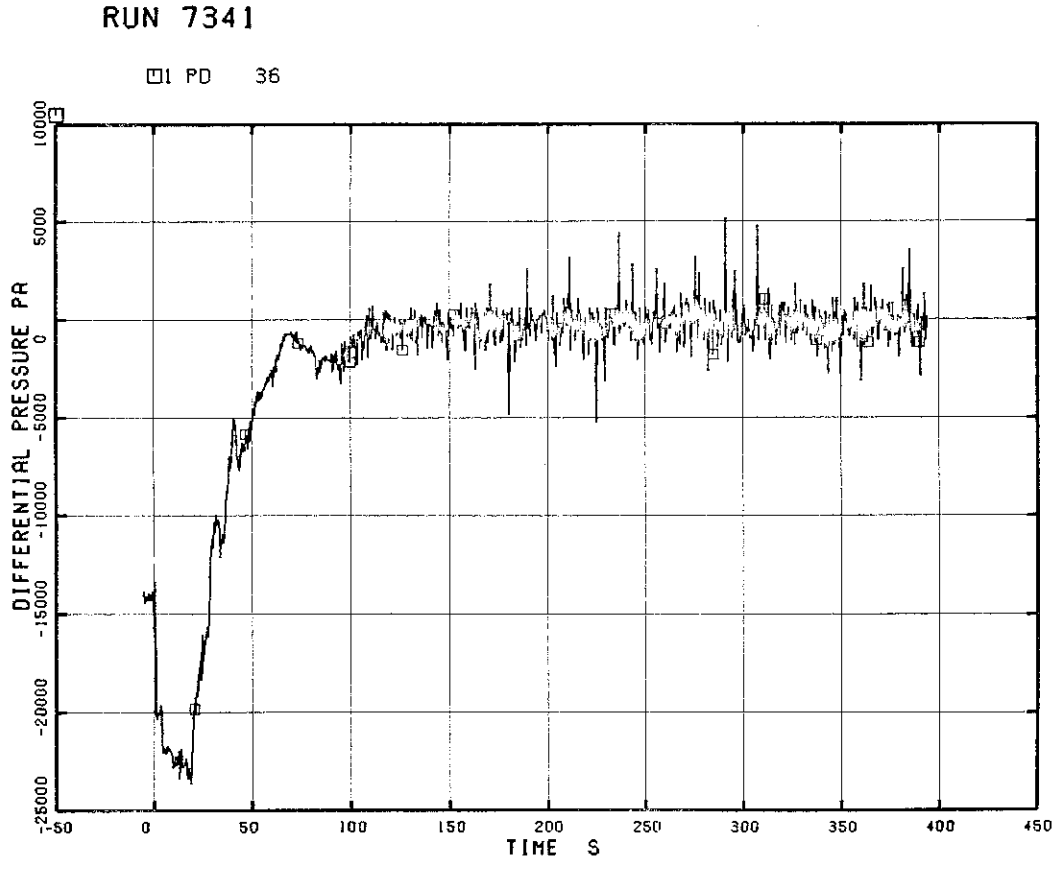

Fig. 5.18 Differential Pressure between Downcomer Bottom and MRP-1 Suction

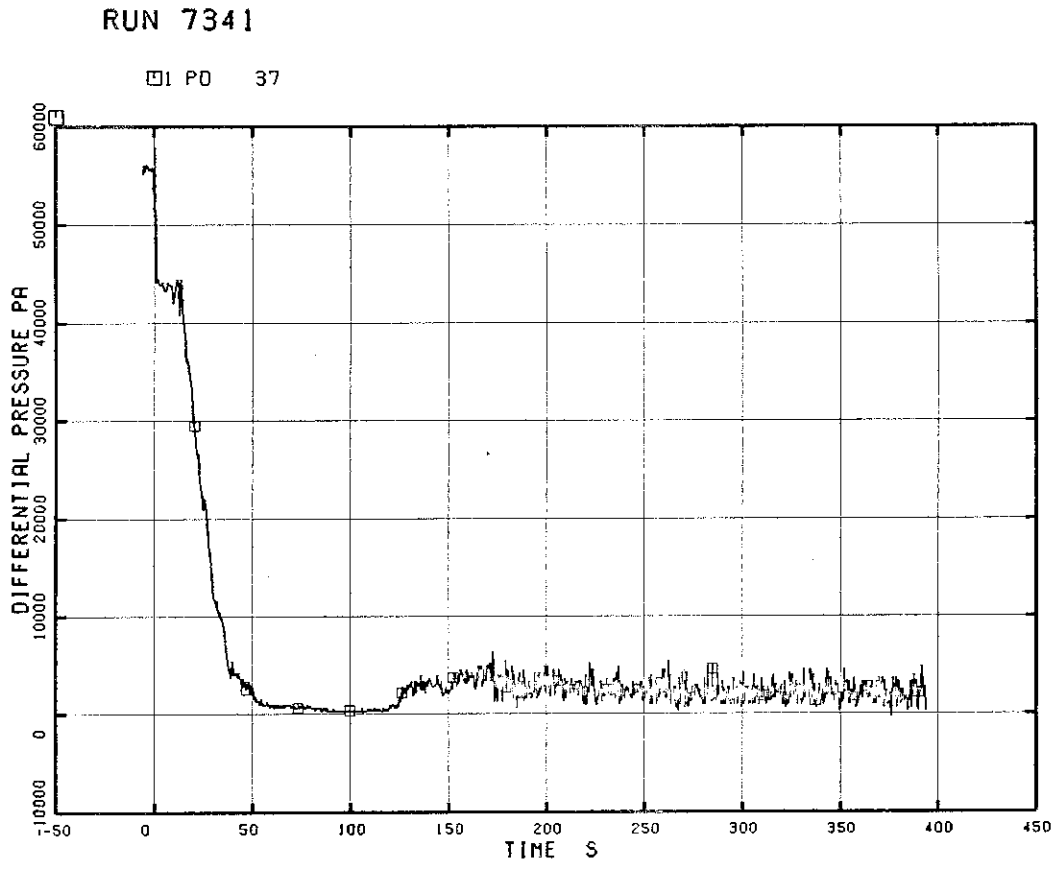

Fig. 5.19 Differential Pressure between MRP-1 Delivery and JP-1 Drive

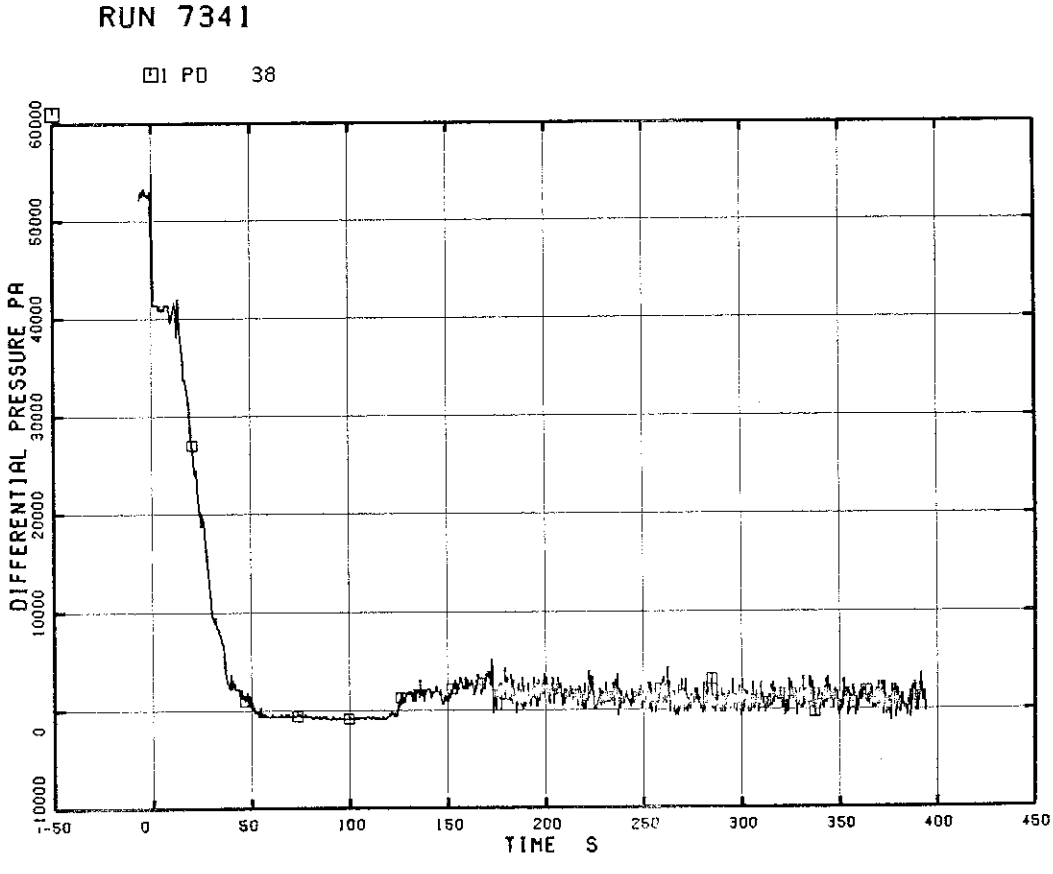

Fig. 5.20 Differential Pressure between MRP-1 Delivery and JP-2 Drive

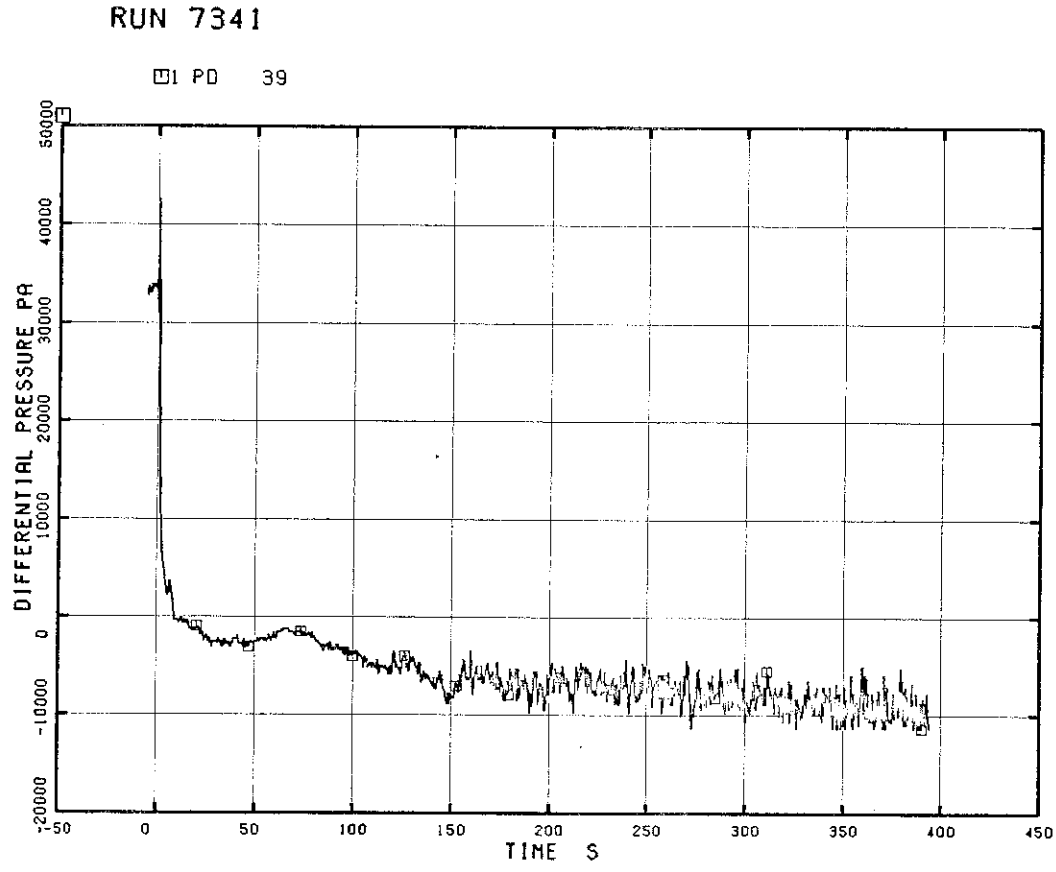

Fig. 5.21 Differential Pressure between Downcomer Middle and JP-1 Suction

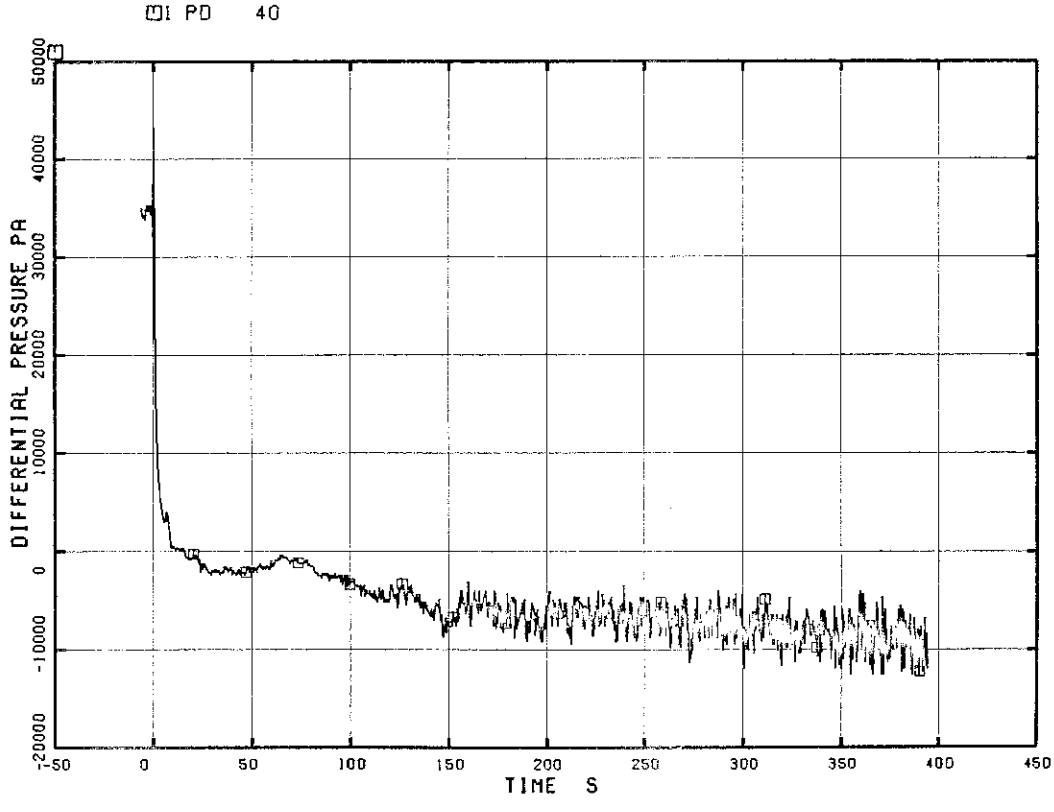

Fig. 5.22 Differential Pressure between Downcomer Middle and JP-2 Suction

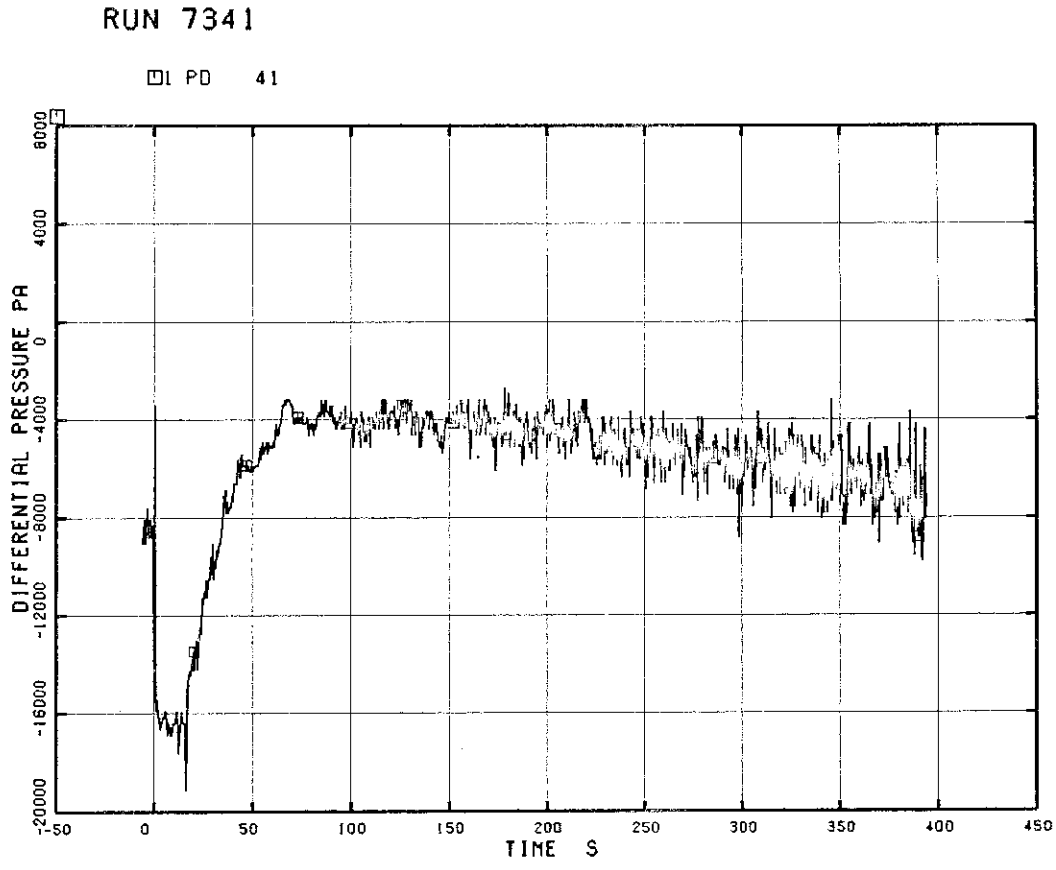

Fig. 5.23 Differential Pressure between JP-1 Discharge and Lower Plenum

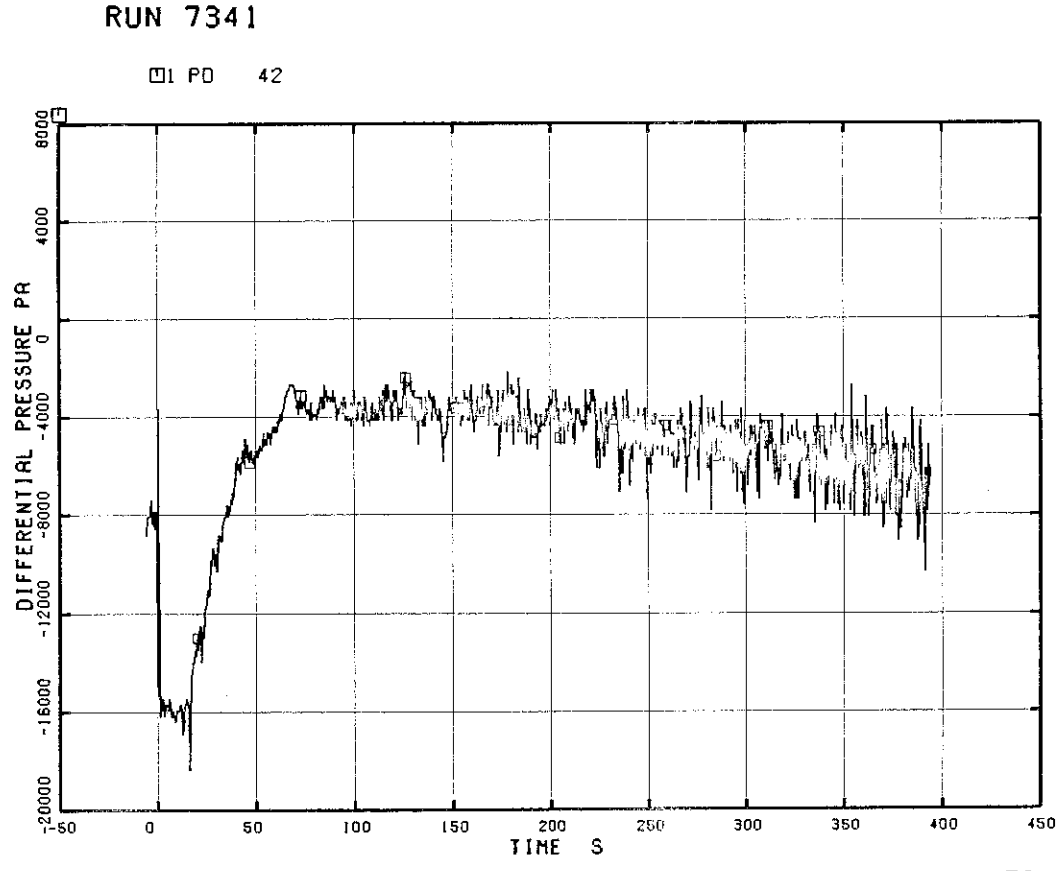

Fig. 5.24 Differential Pressure between JP-2 Discharge and Lower Plenum

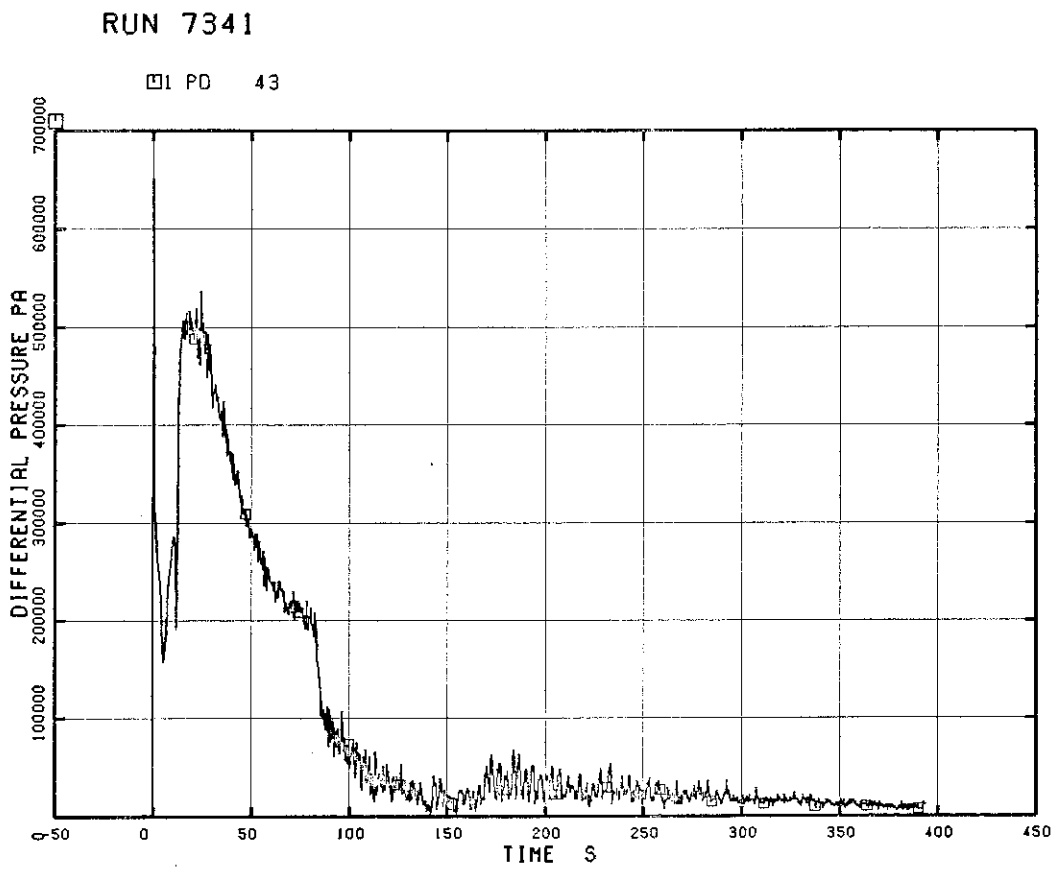

Fig. 5.25 Differential Pressure between Downcomer Bottom and Break B

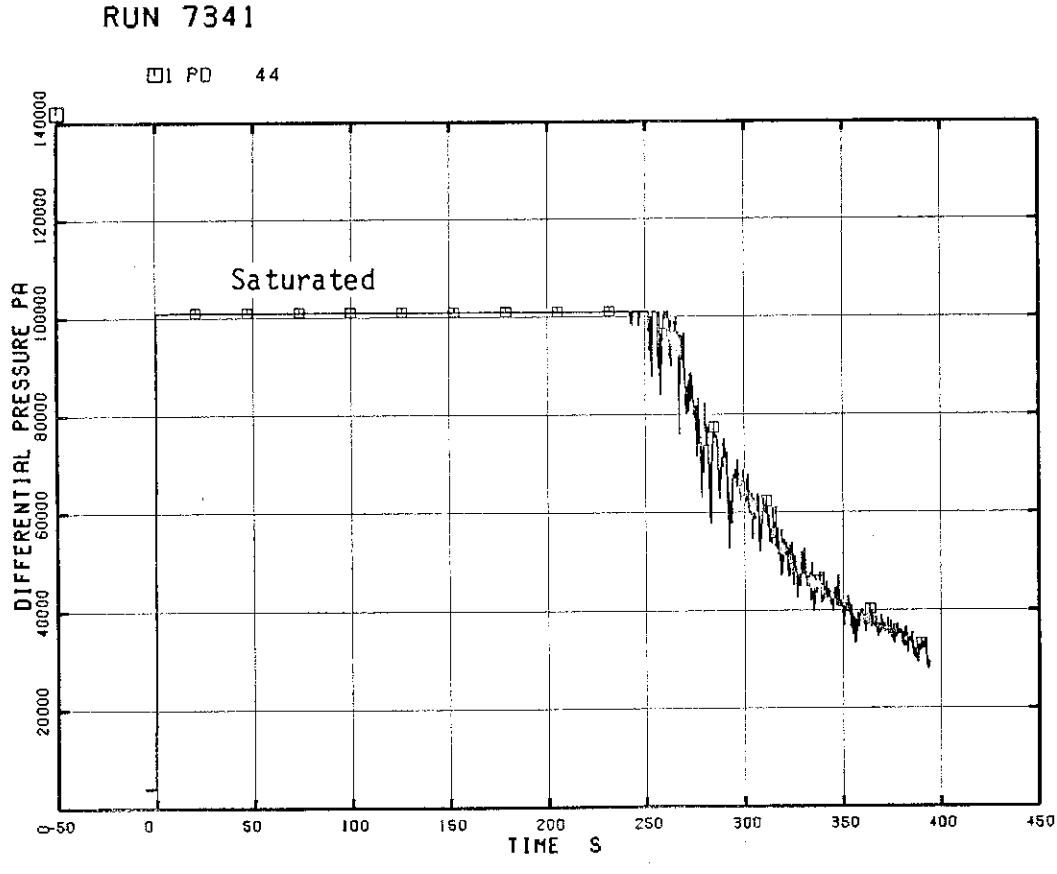

Fig. 5.26 Differential Pressure between Break B and Break A

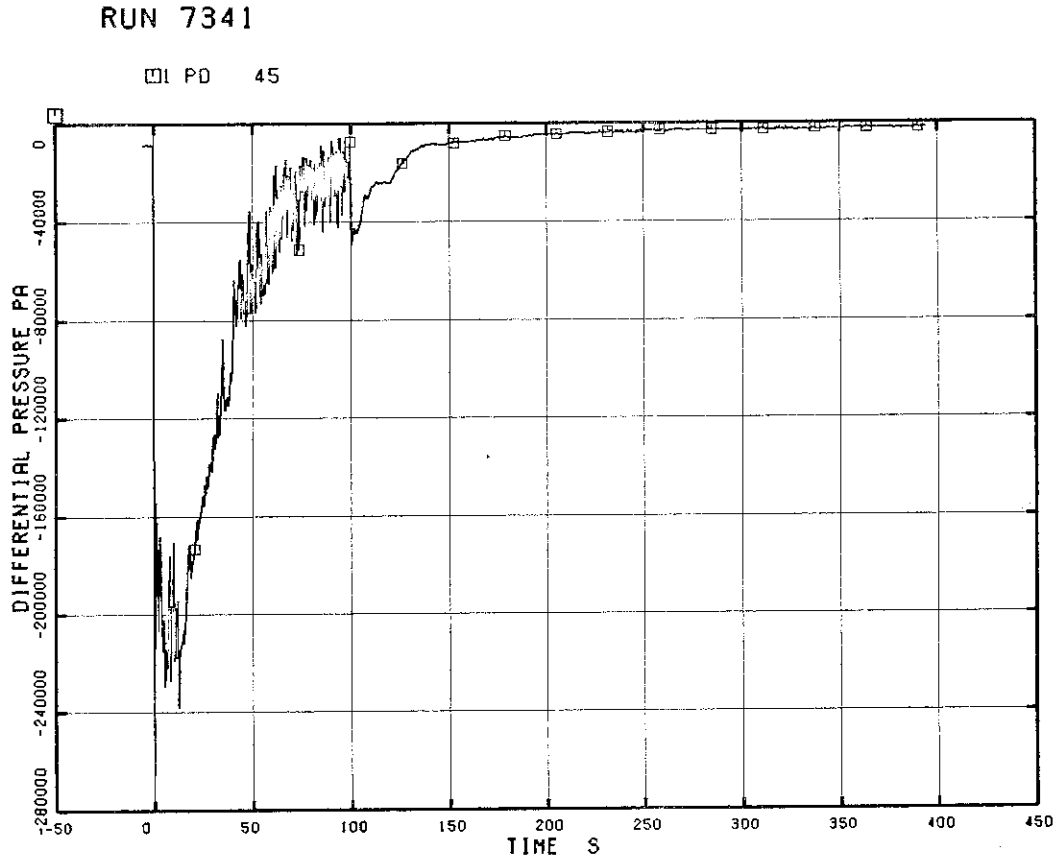

Fig. 5.27 Differential Pressure between Break A and MRP-2 Suction

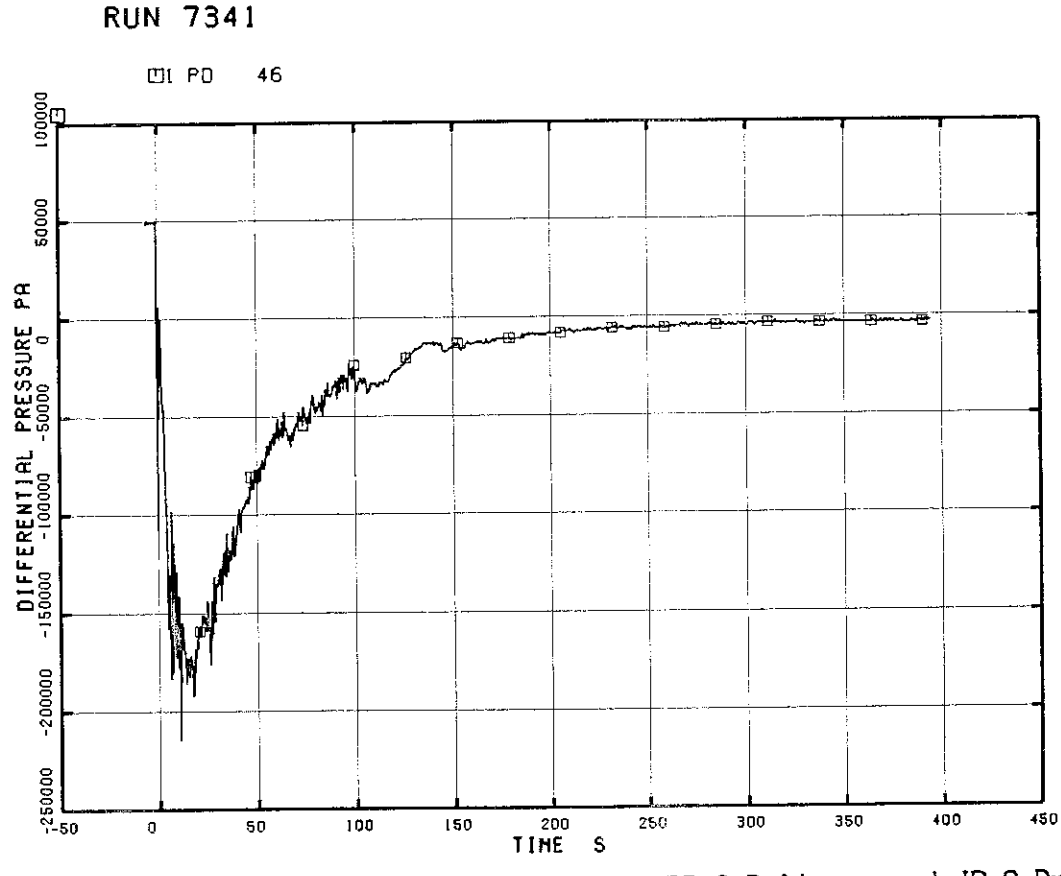

Fig. 5.28 Differential Pressure between MRP-2 Delivery and JP-3 Drive

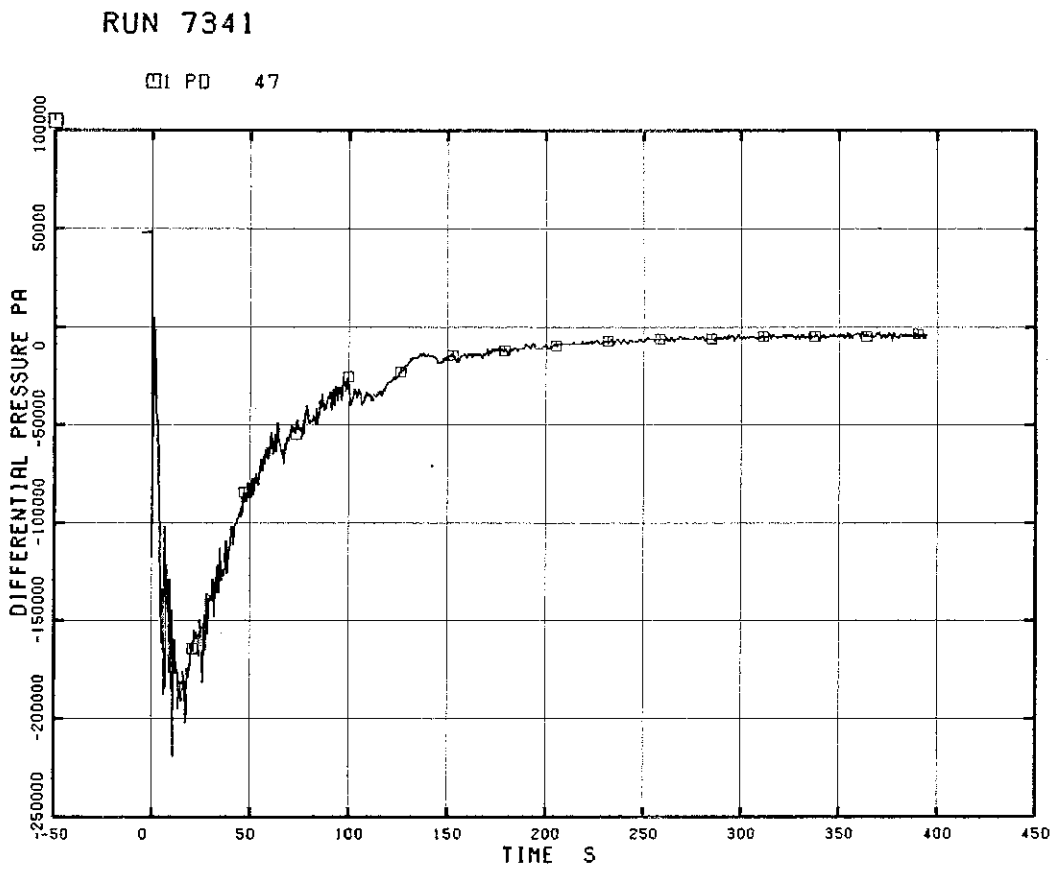

Fig. 5.29 Differential Pressure between MRP-2 Delivery and JP-4 Drive

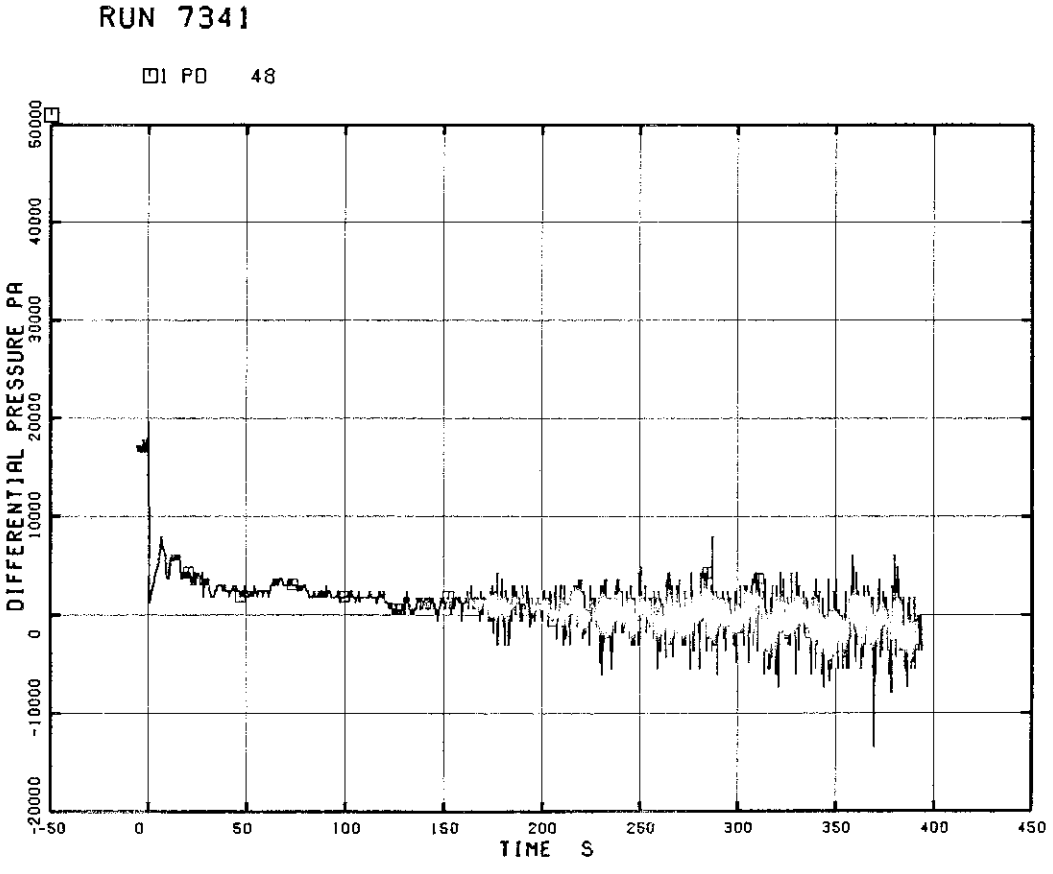

Fig. 5.30 Differential Pressure between Downcomer Middle and JP-3 Suction

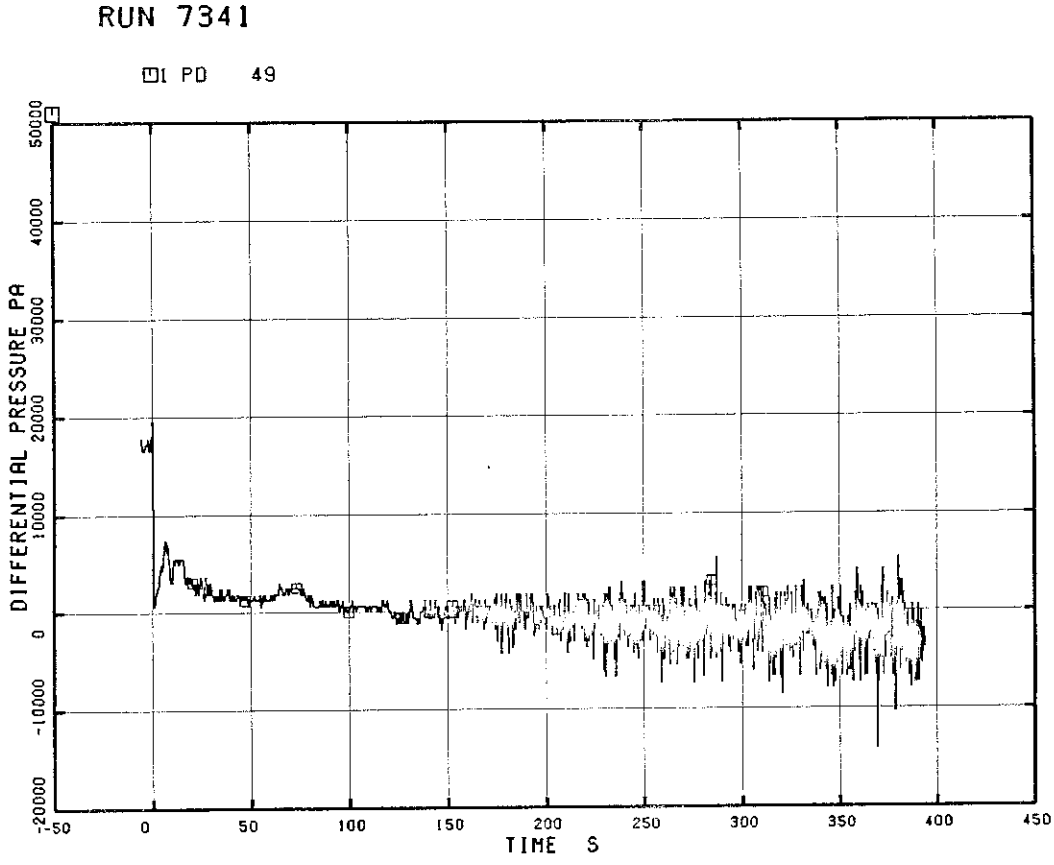

Fig. 5.31 Differential Pressure between Downcomer Middle and JP-4 Suction

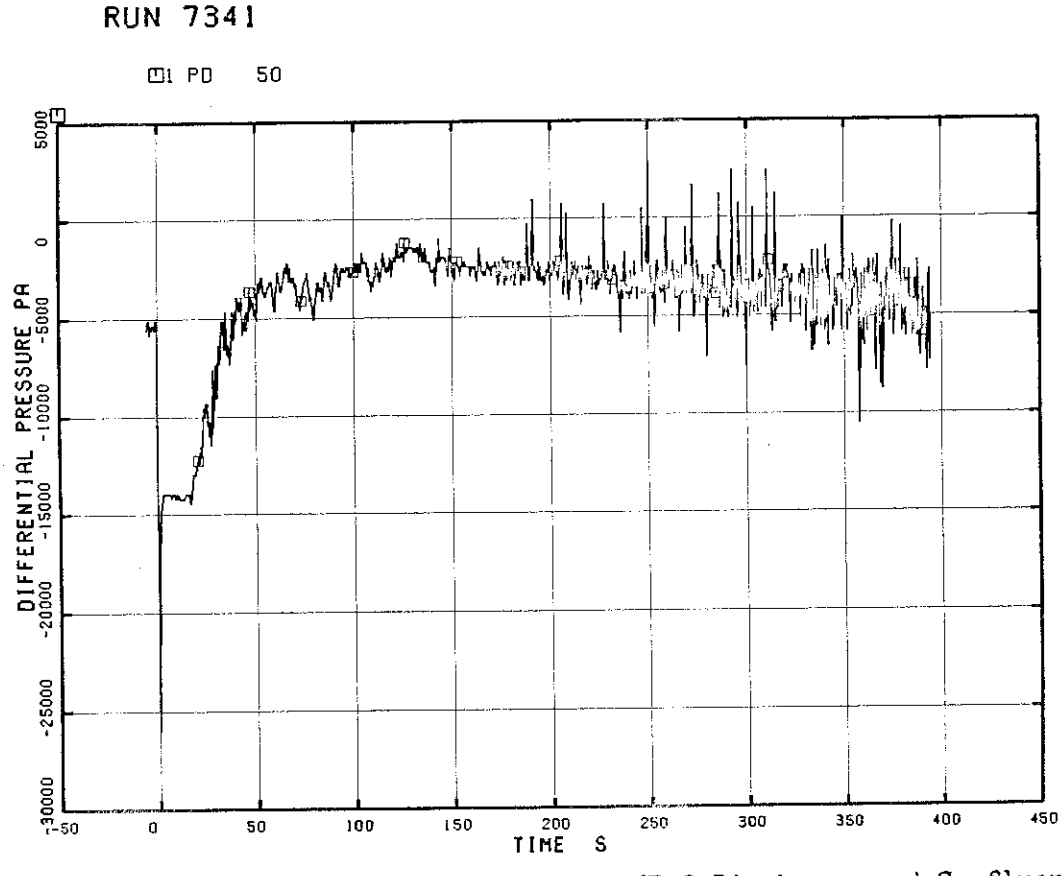

Fig. 5.32 Differential Pressure between JP-3 Discharge and Confluence

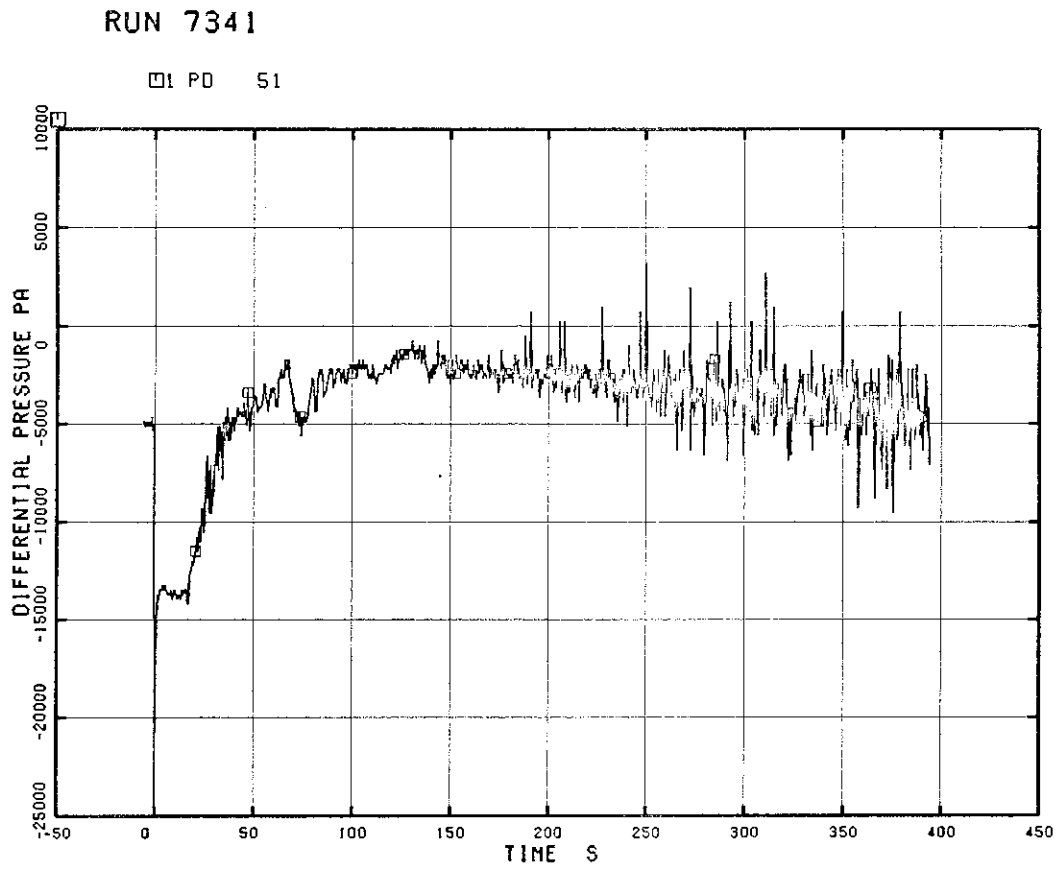

Fig. 5.33 Differential Pressure between JP-4 Discharge and Confluence

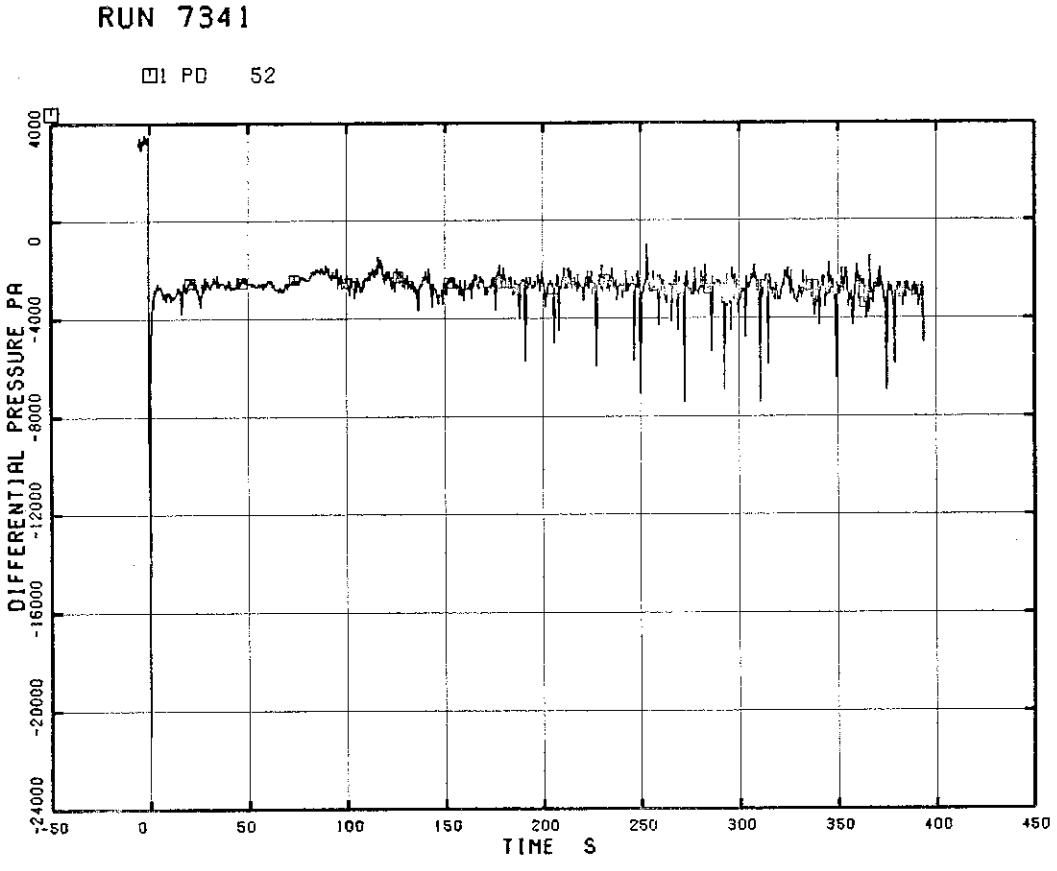

Fig. 5.34 Differential Pressure between Confluence and Lower Plenum

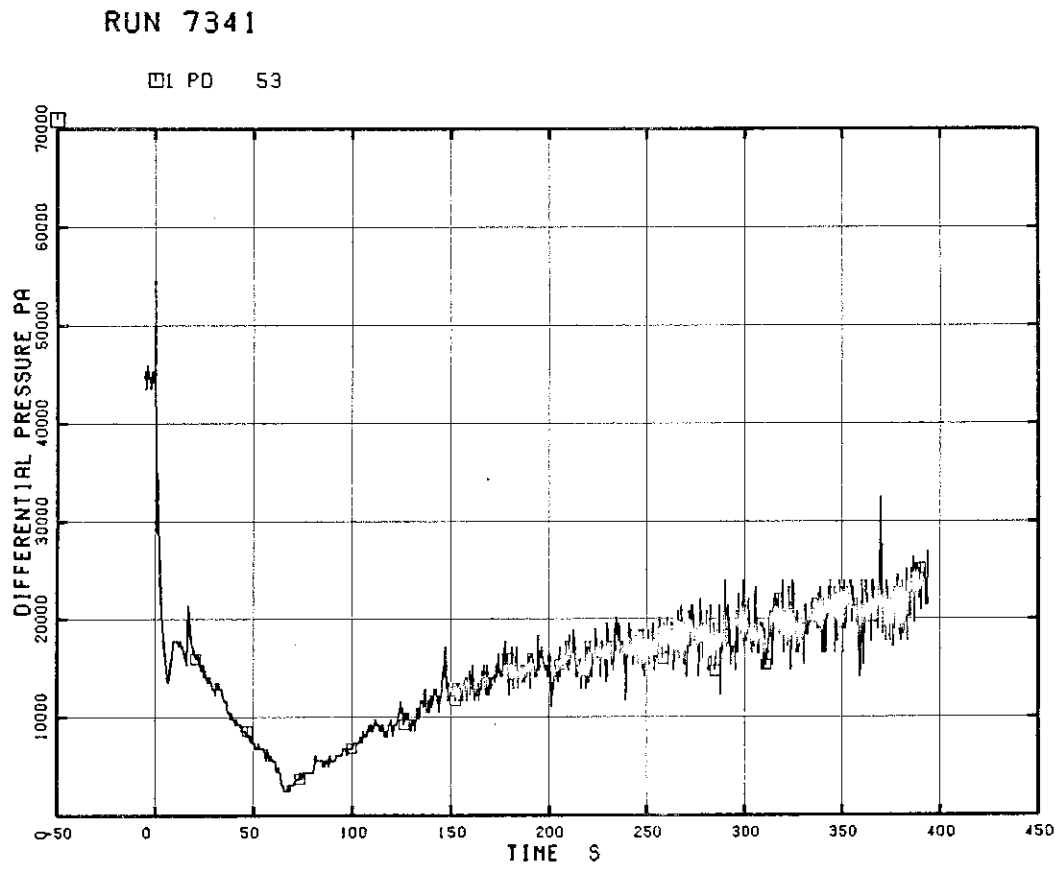

Fig. 5.35 Differential Pressure between Lower Plenum and Downcomer Middle

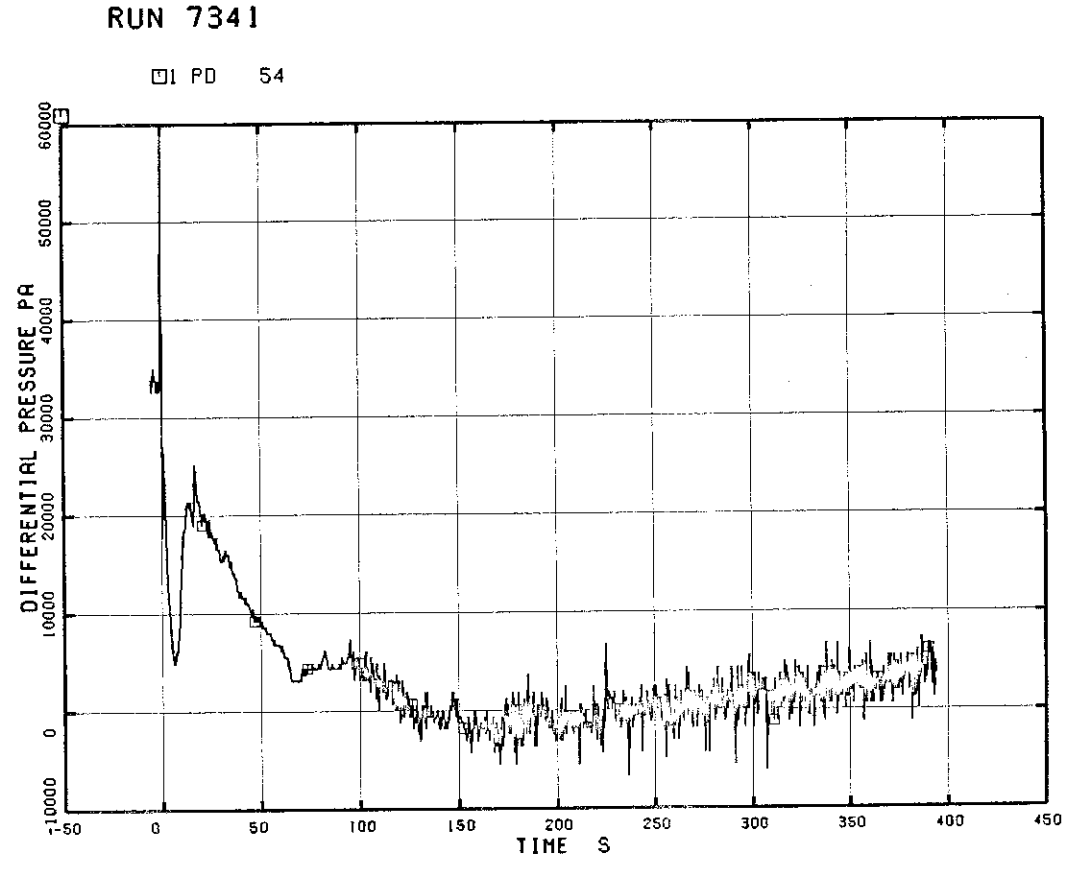

Fig. 5.36 Differential Pressure between Lower Plenum and Downcomer Bottom

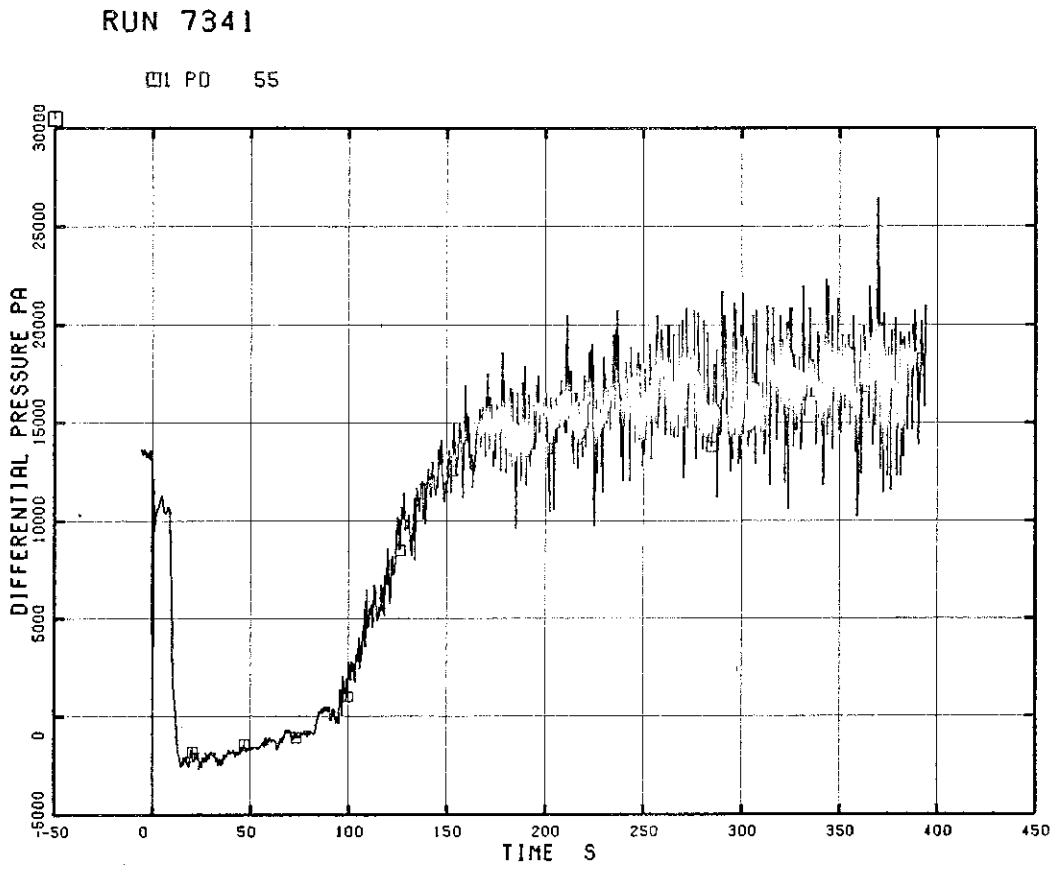

Fig. 5.37 Differential Pressure between Downcomer Bottom and Downcomer Middle

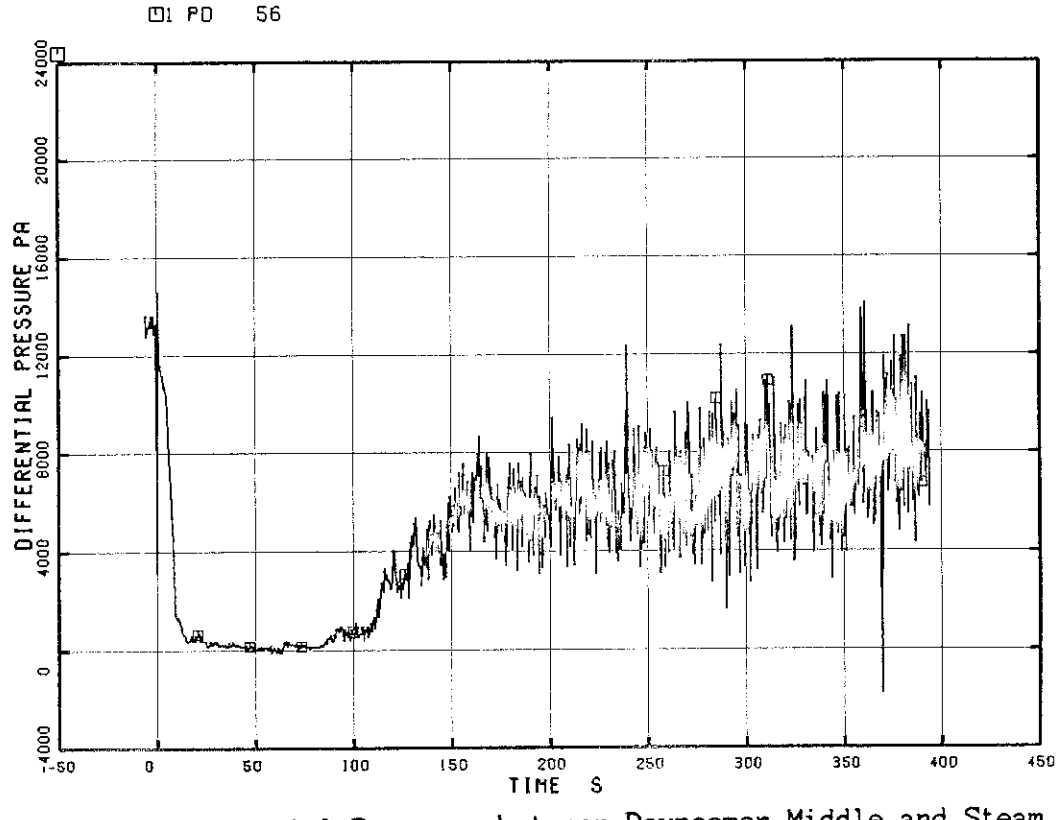

Fig. 5.38 Differential Pressure between Downcomer Middle and Steam Dome

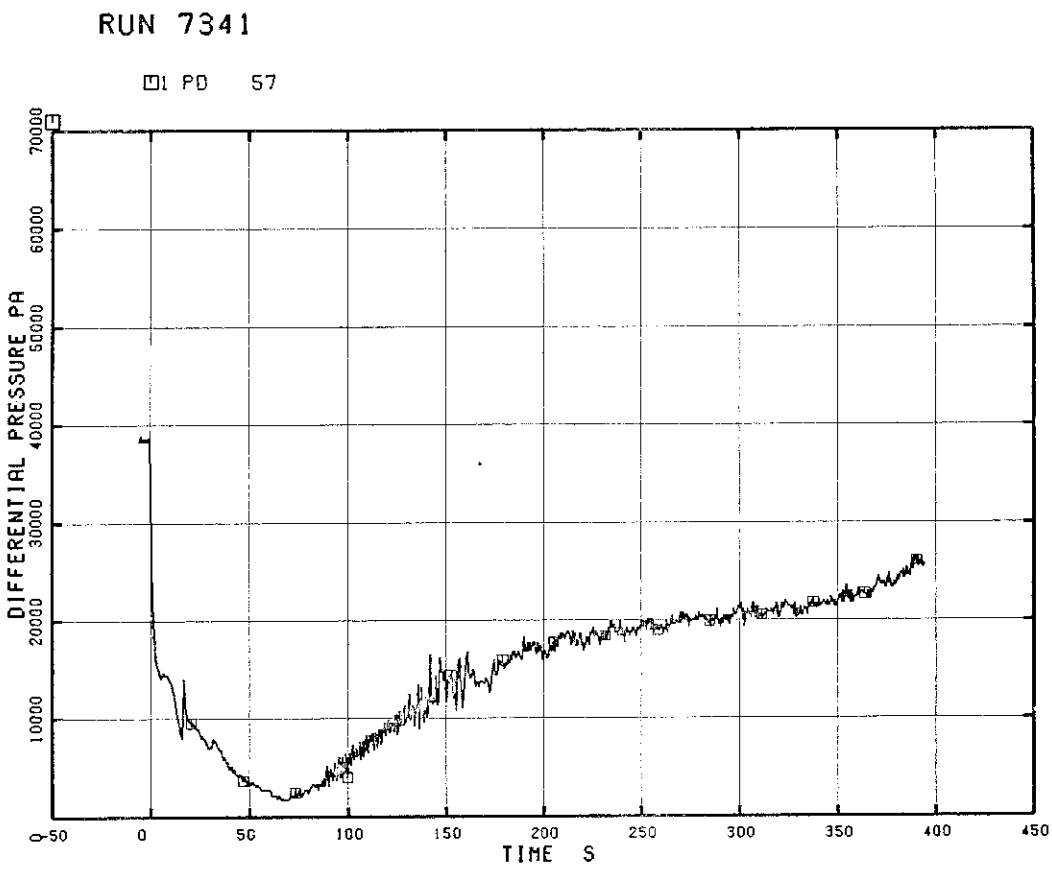

Fig. 5.39 Differential Pressure between Lower Plenum Middle and Upper Plenum

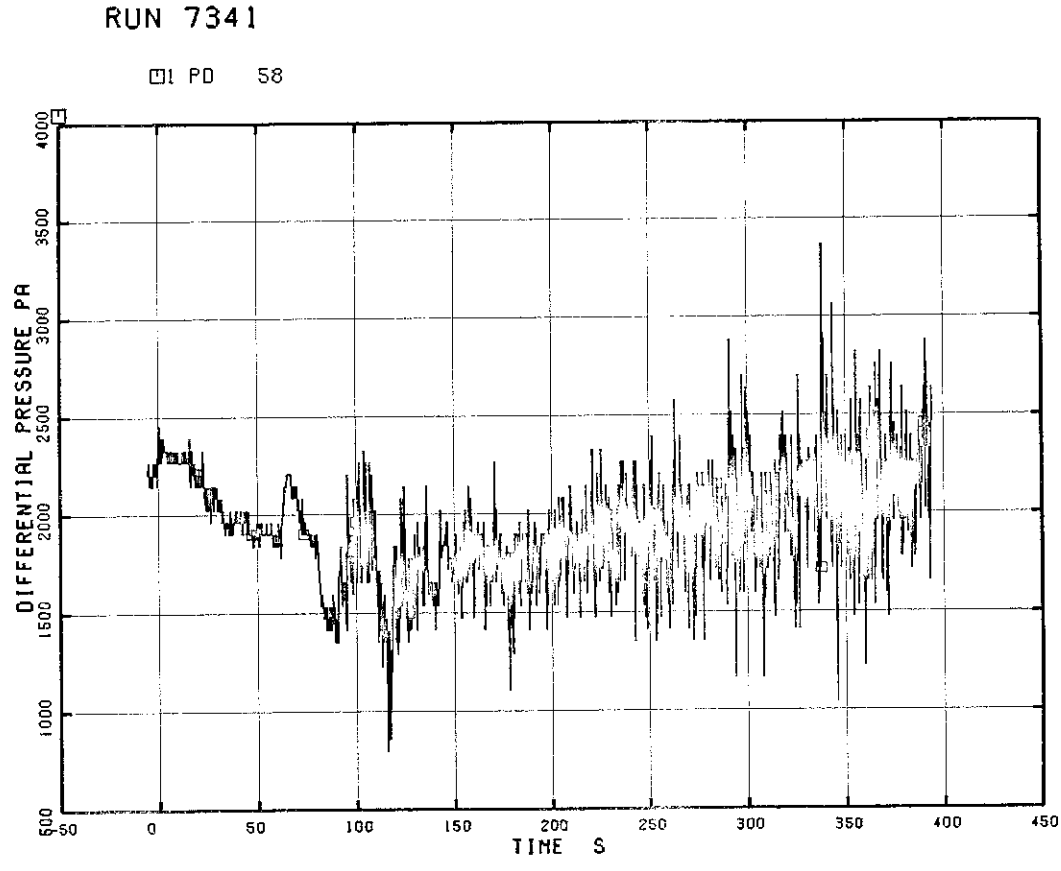

Fig. 5.40 Differential Pressure between Lower Plenum Bottom and Middle

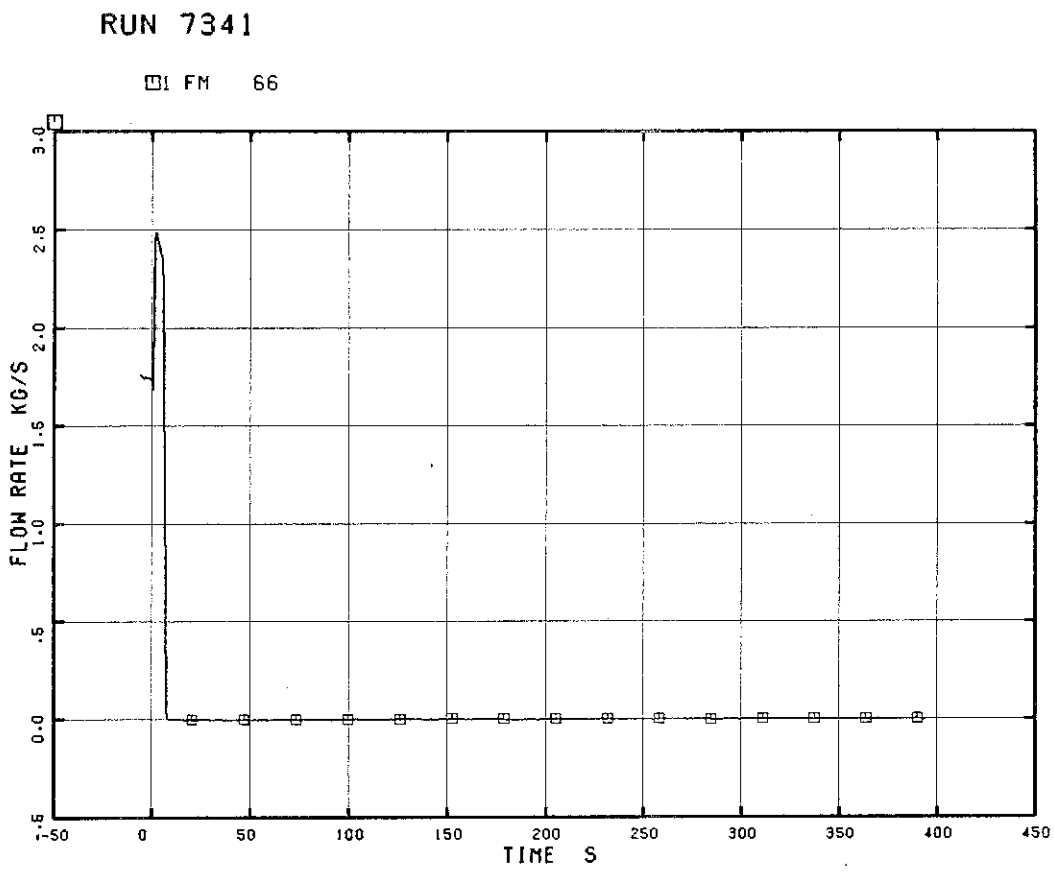

Fig. 5.41 Mass Flow Rate in the Steam Discharge Line

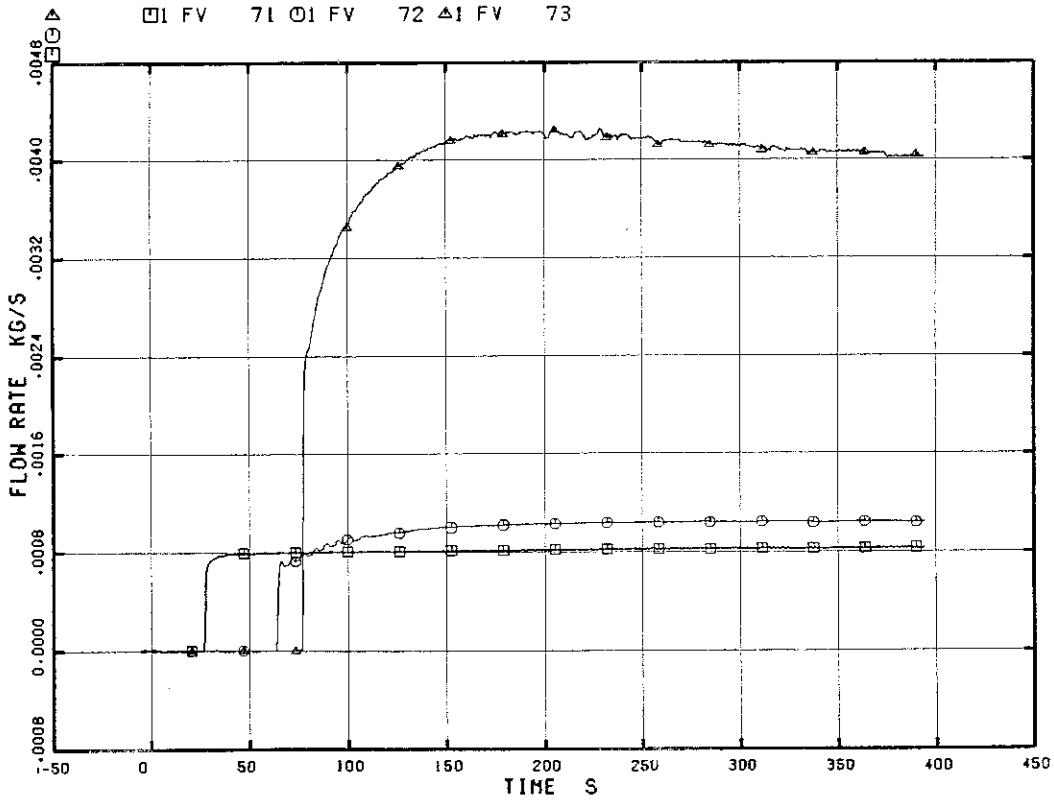

Fig. 5.42 ECCS Injection Flow Rate

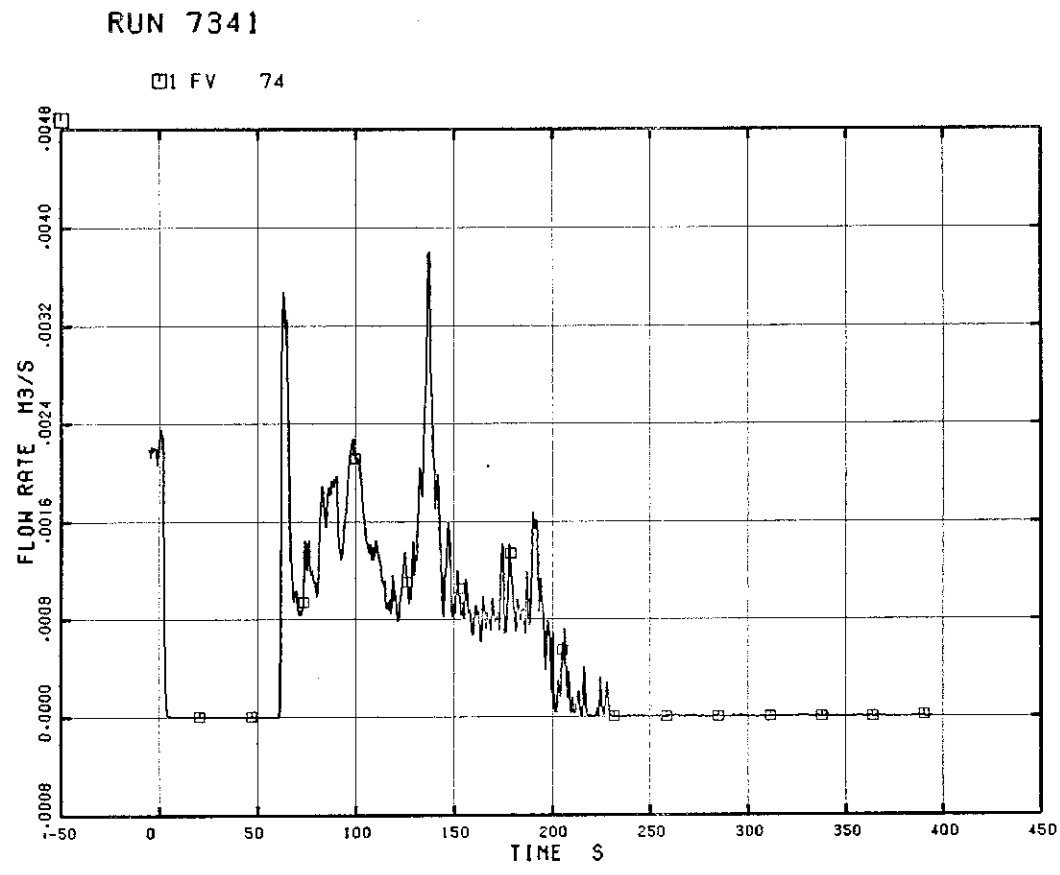

Fig. 5.43 Feedwater Flow Rate

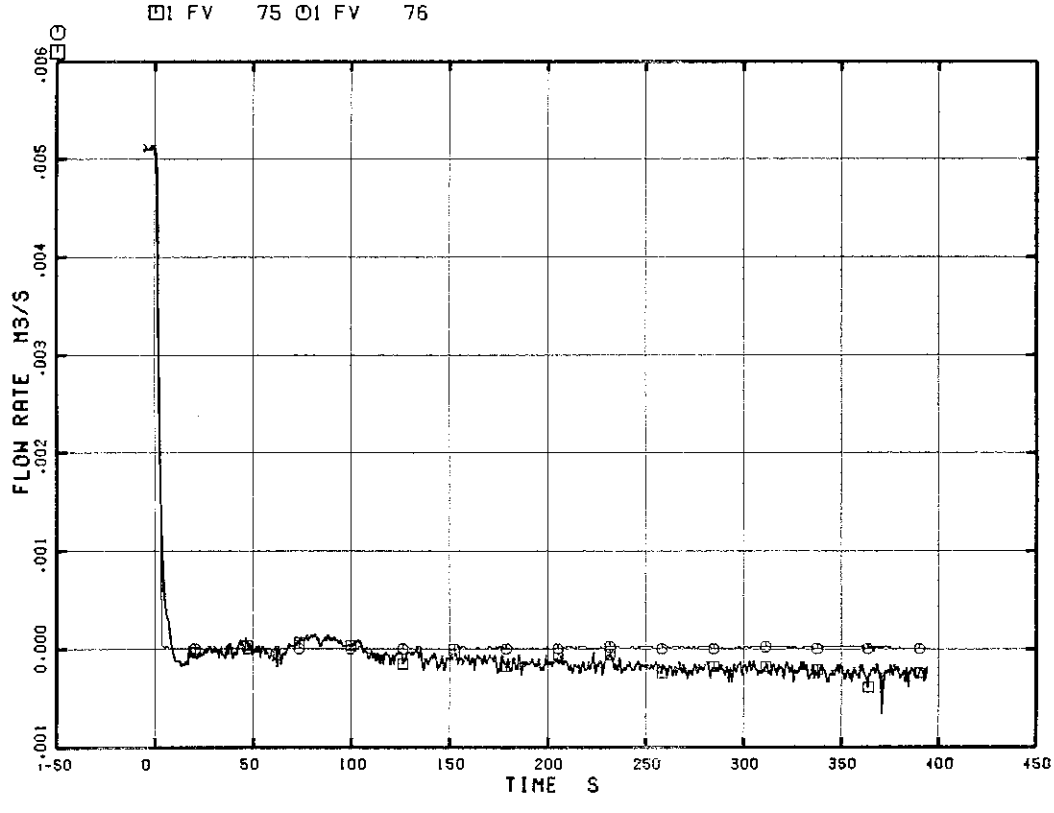

Fig. 5.44 Intact Loop Jet Pump Discharge Flow Rate

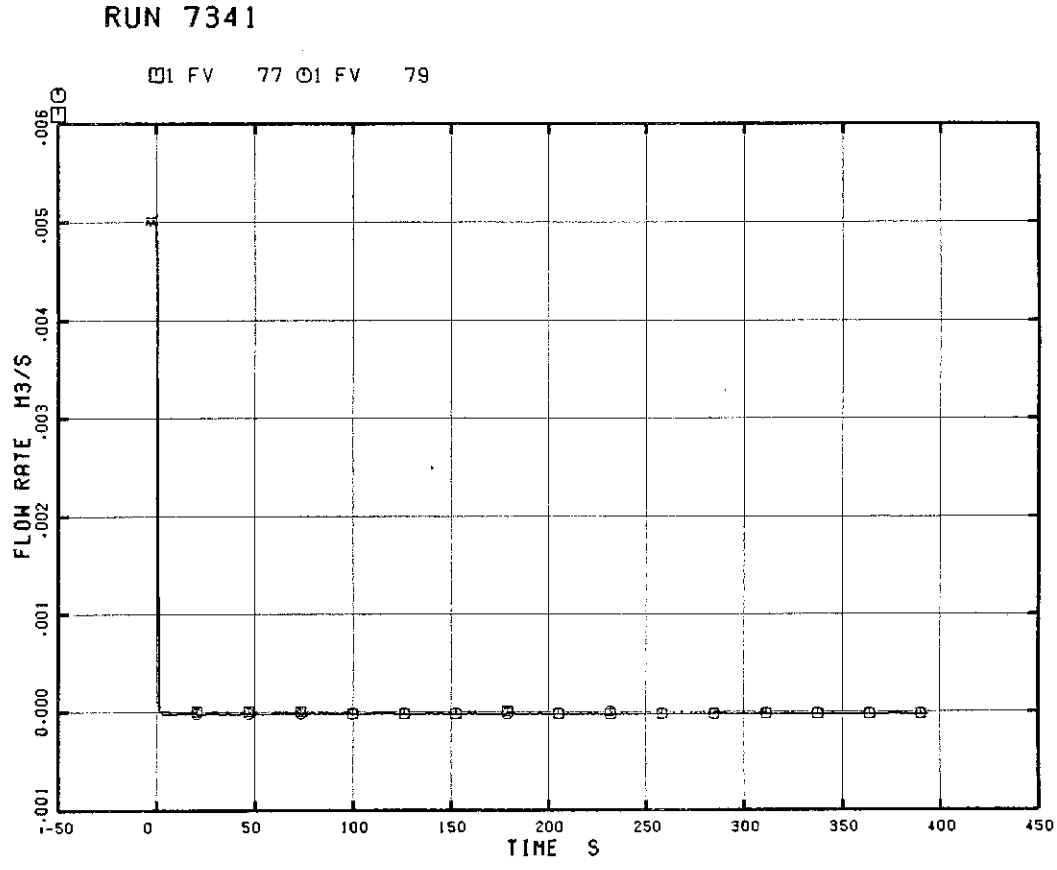

Fig. 5.45 Broken Loop Jet Pump Discharge Flow Rate

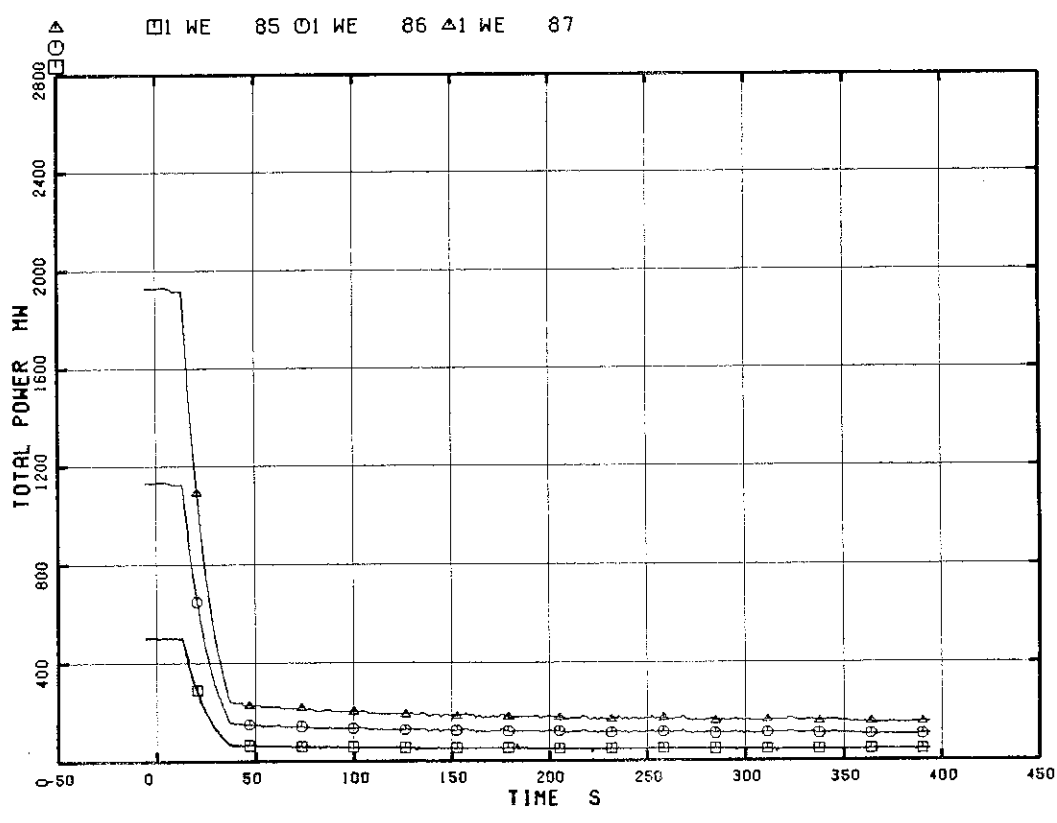

Fig. 5.46 Core Power

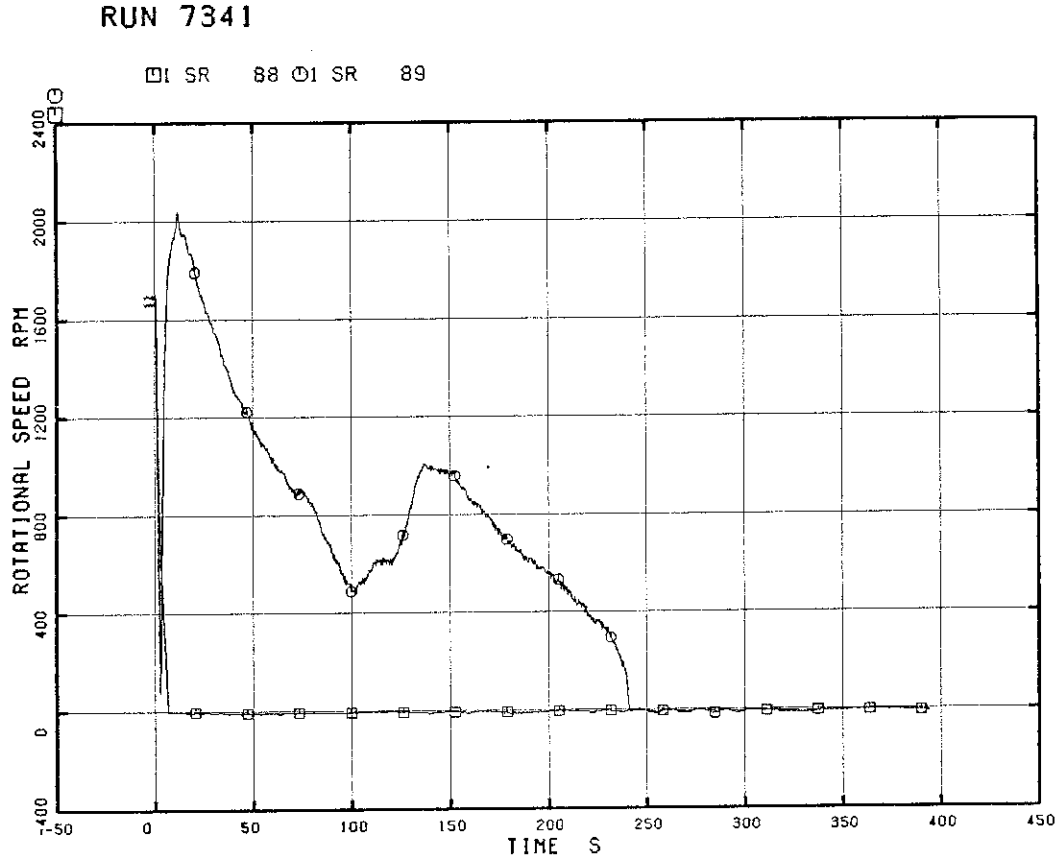

Fig. 5.47 Pump Speed

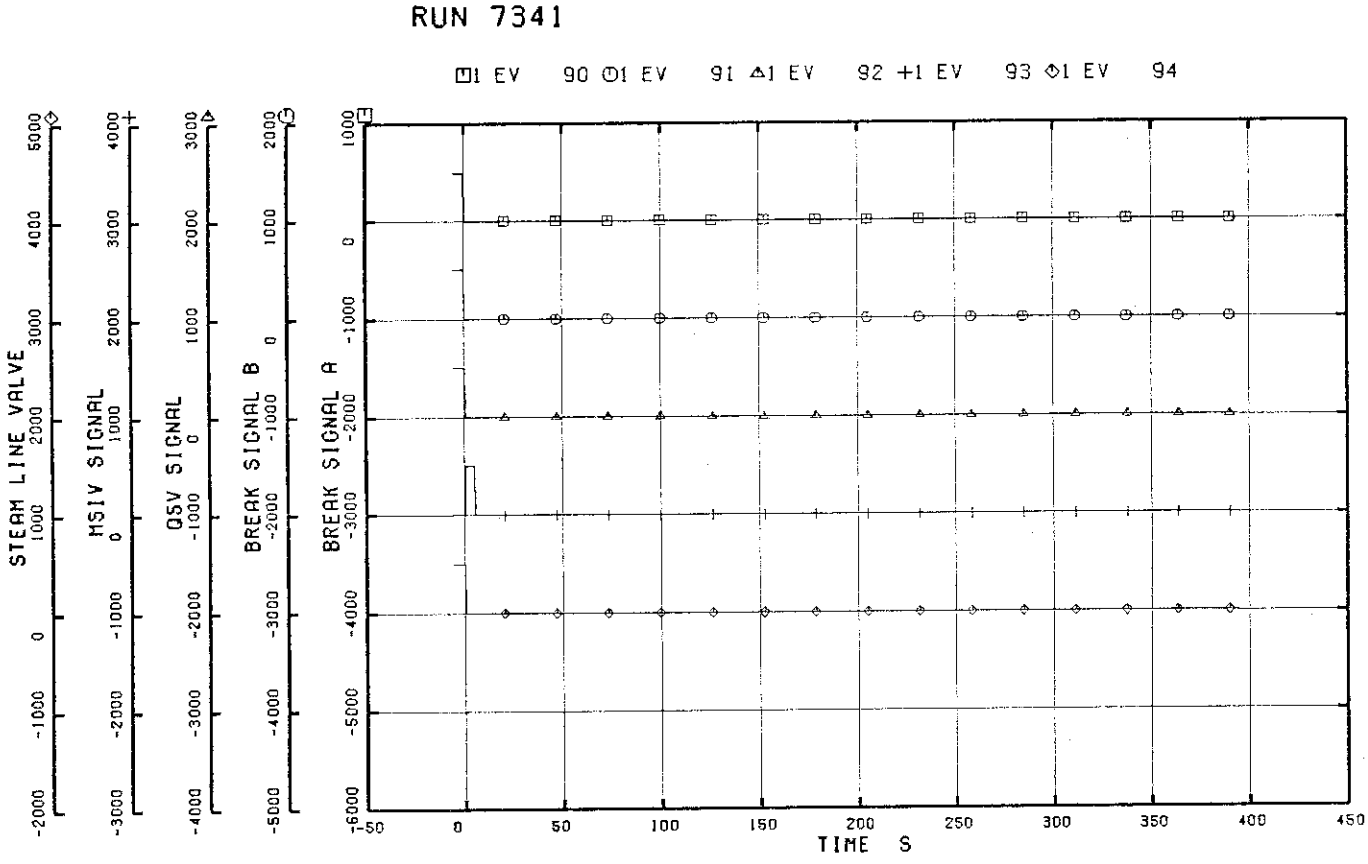

Fig. 5.48 Valve Operation Signals

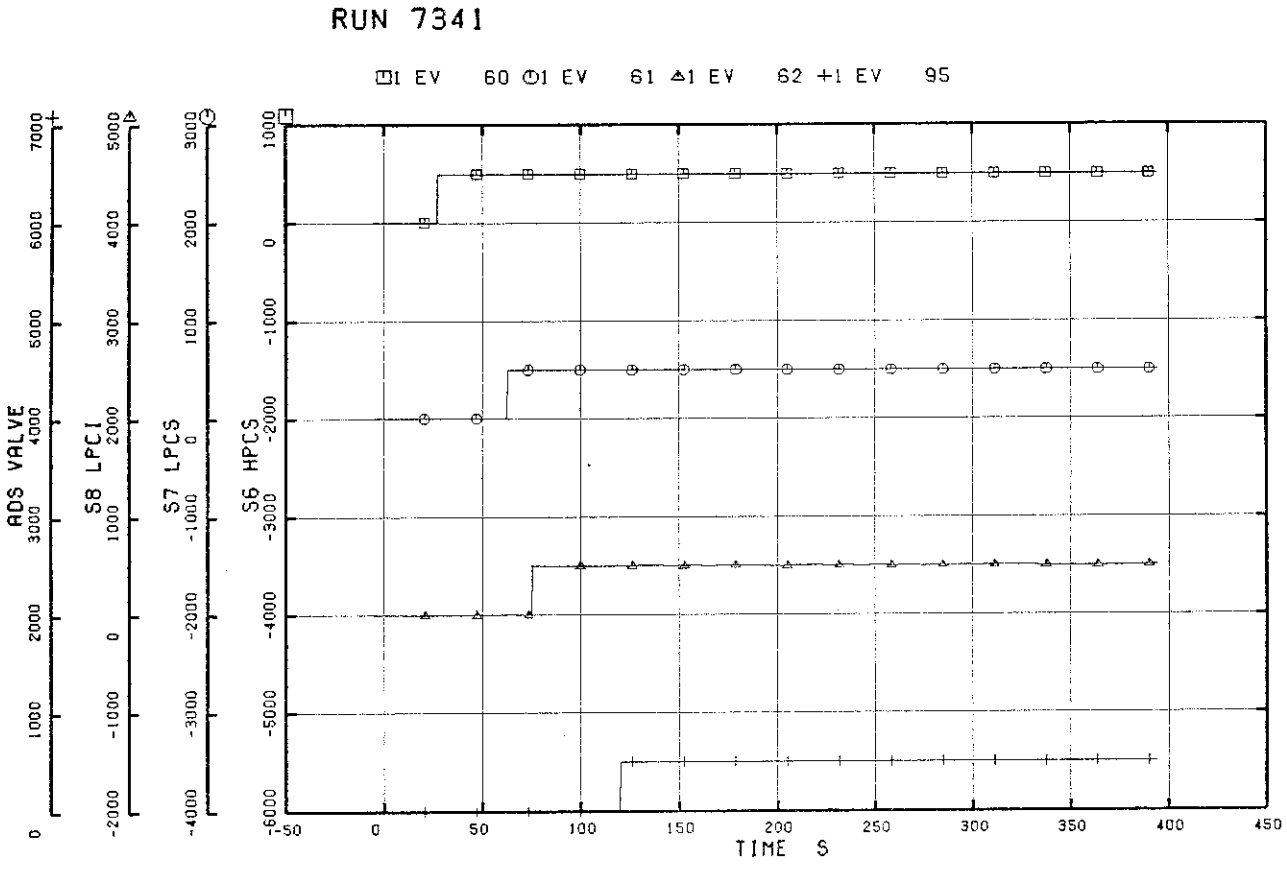

Fig. 5.49 ECCS Operation Signals

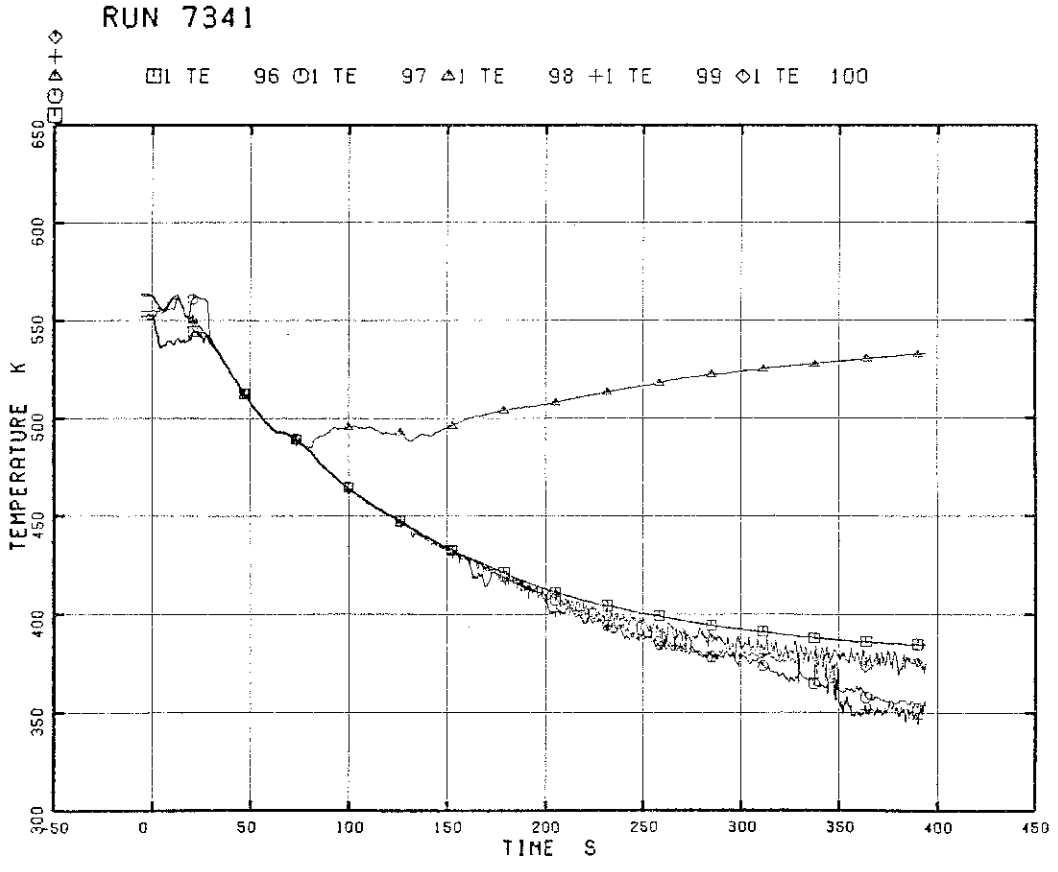

Fig. 5.50 Fluid Temperature in Pressure Vessel

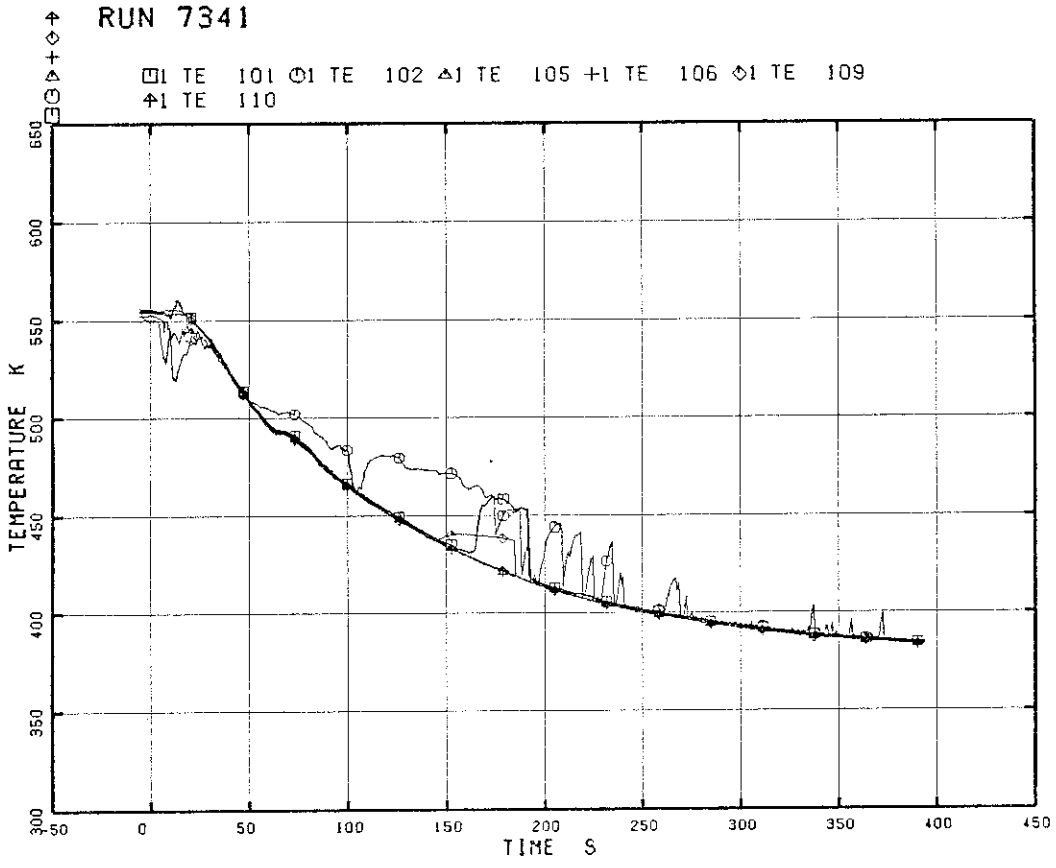

Fig. 5.51 Fluid Temperature in Intact Loop

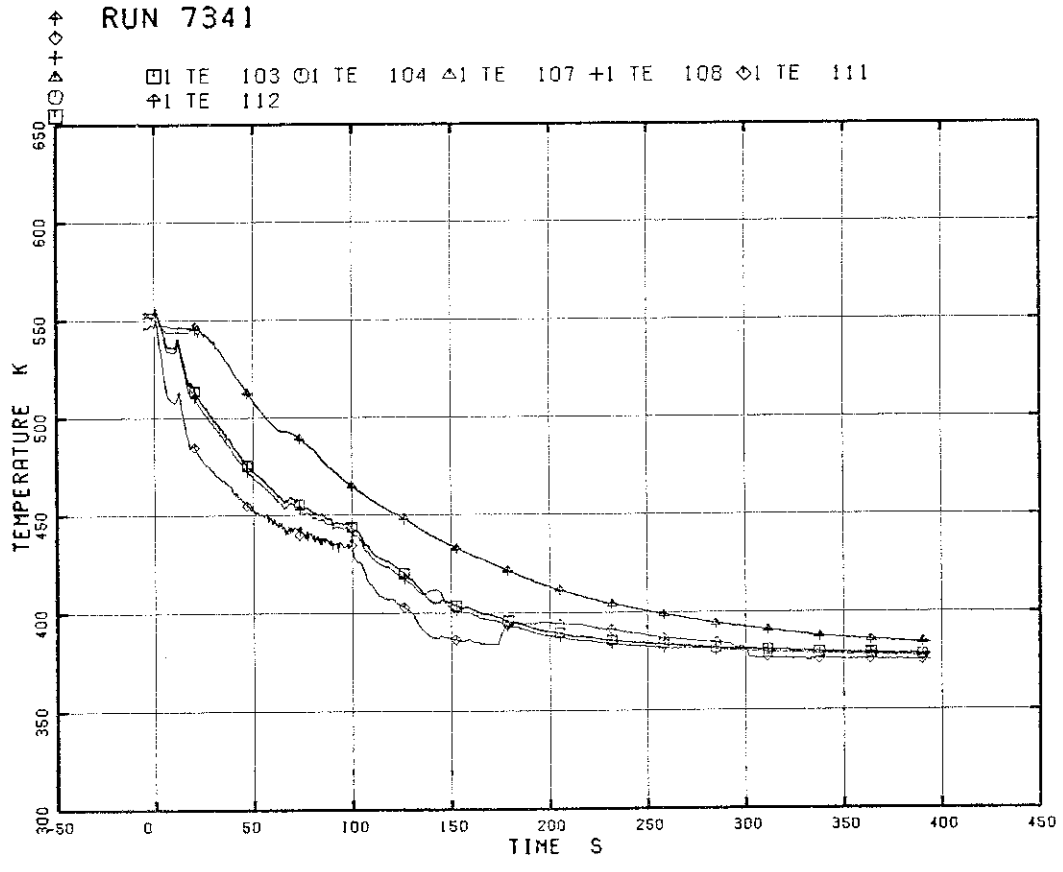

Fig. 5.52 Fluid Temperature in Broken Loop

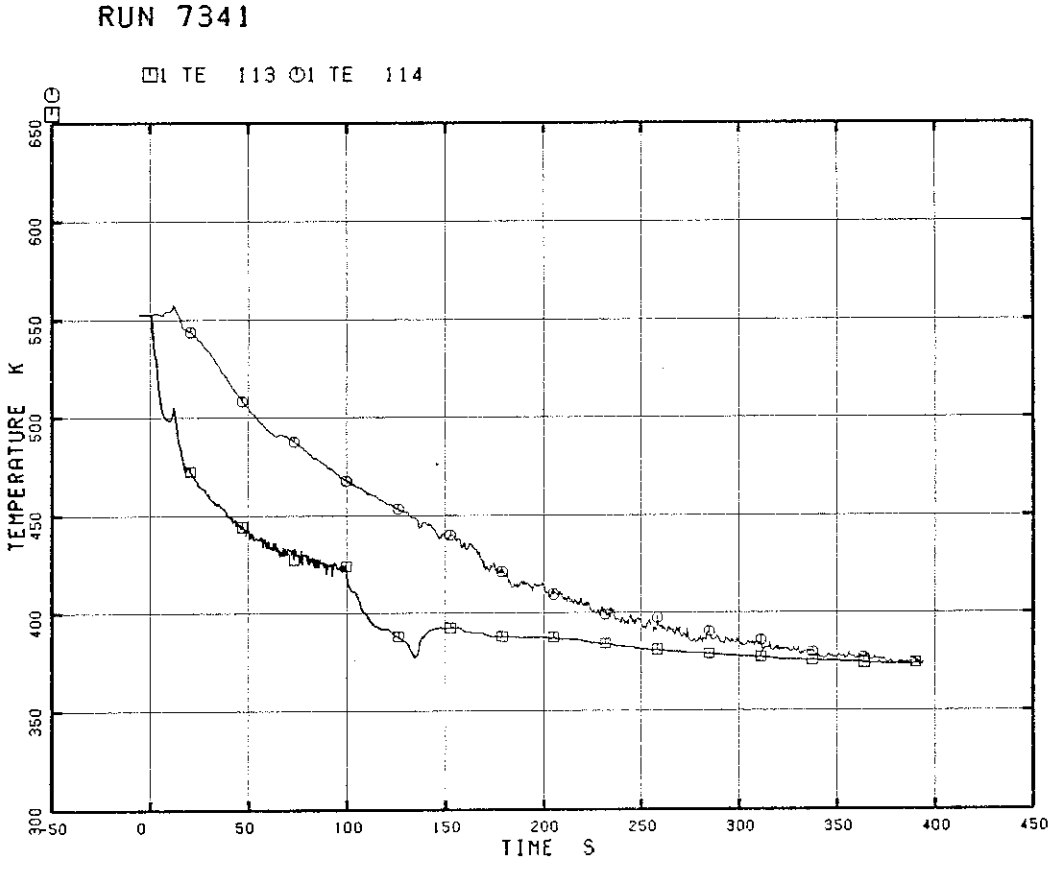

Fig. 5.53 Fluid Temperature in Break A and B

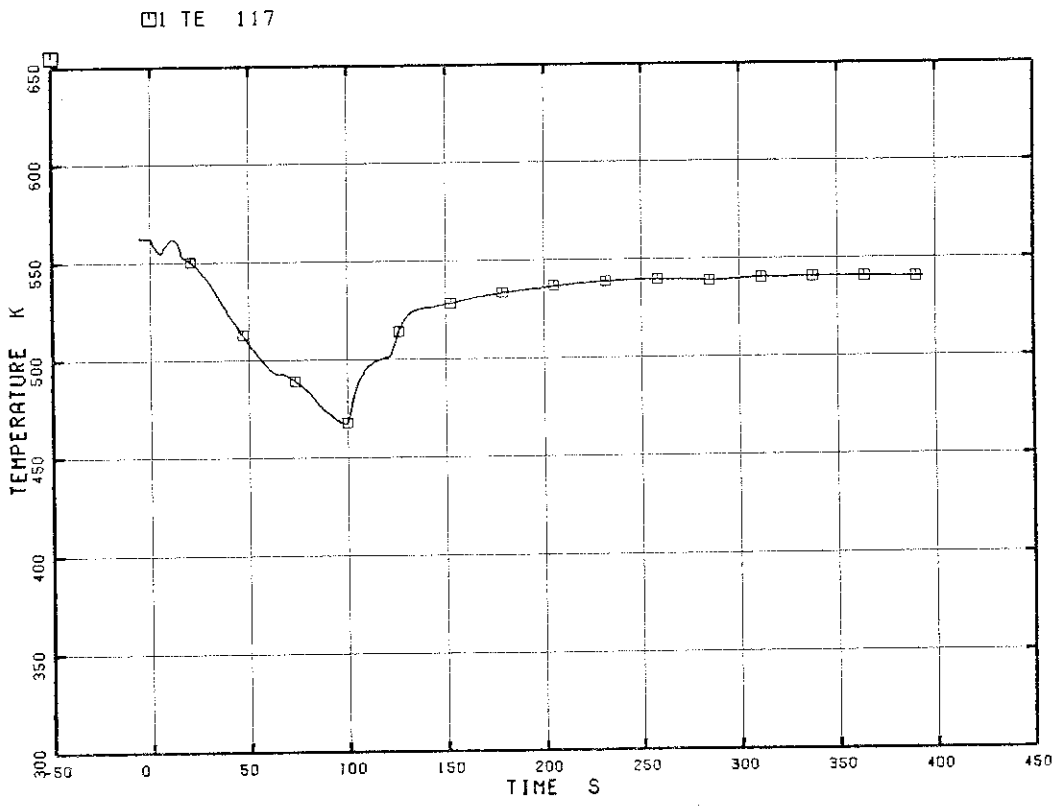

Fig. 5.54 Fluid Temperature in the Steam Discharge Line

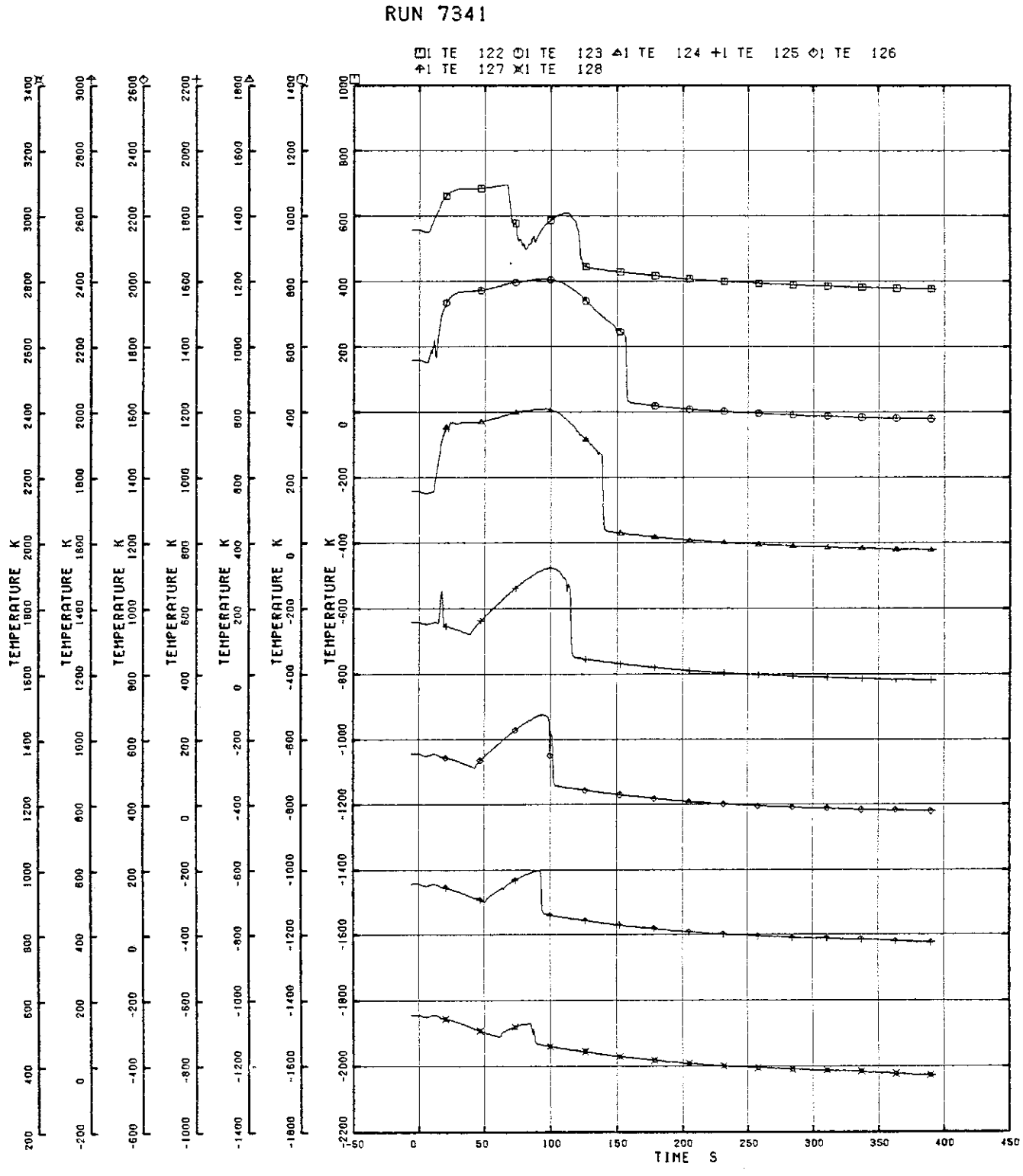

Fig. 5.55 Heater Rod Surface Temperature of A11 Rod

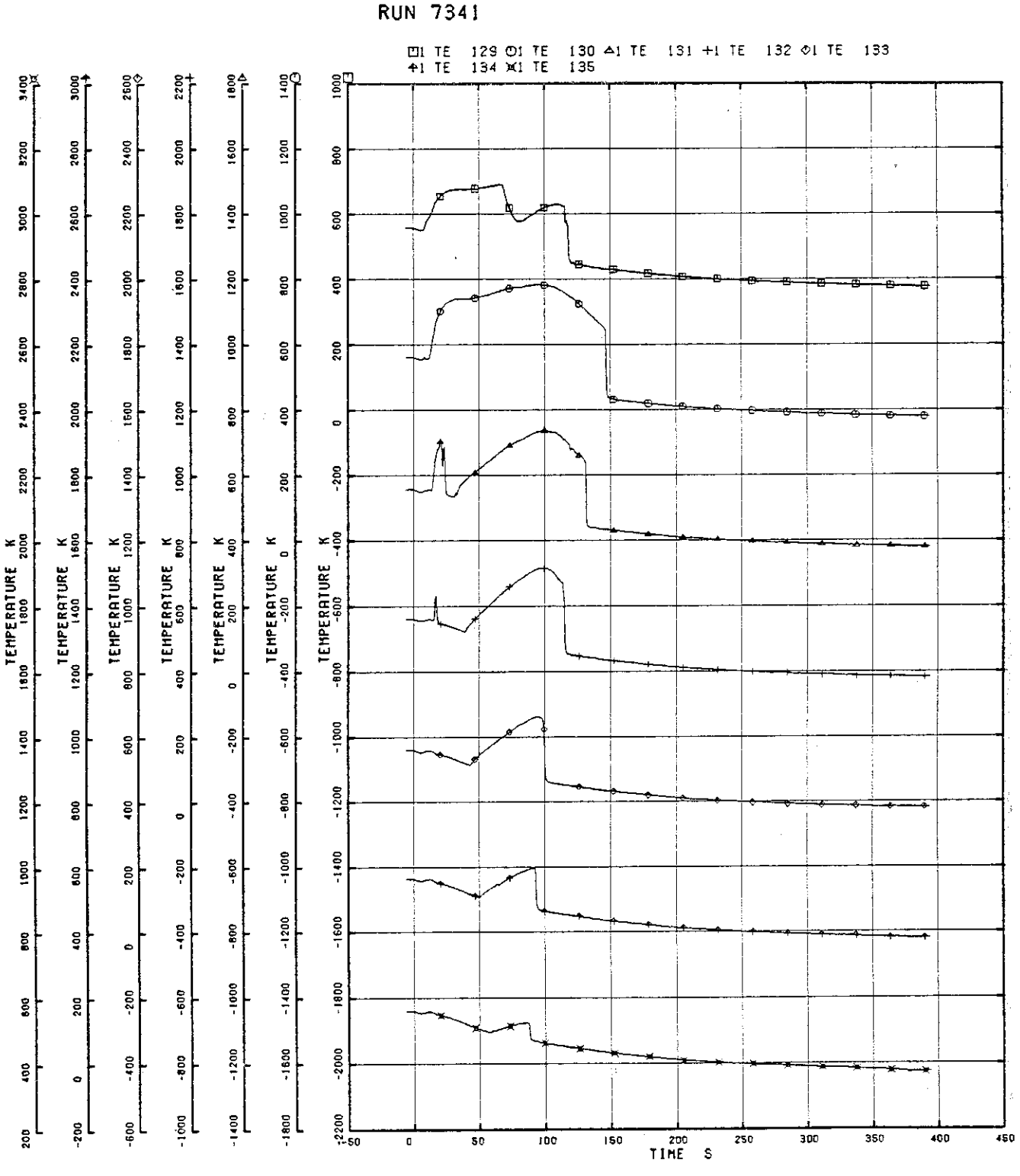

Fig. 5.56 Heater Rod Surface Temperature of A12 Rod

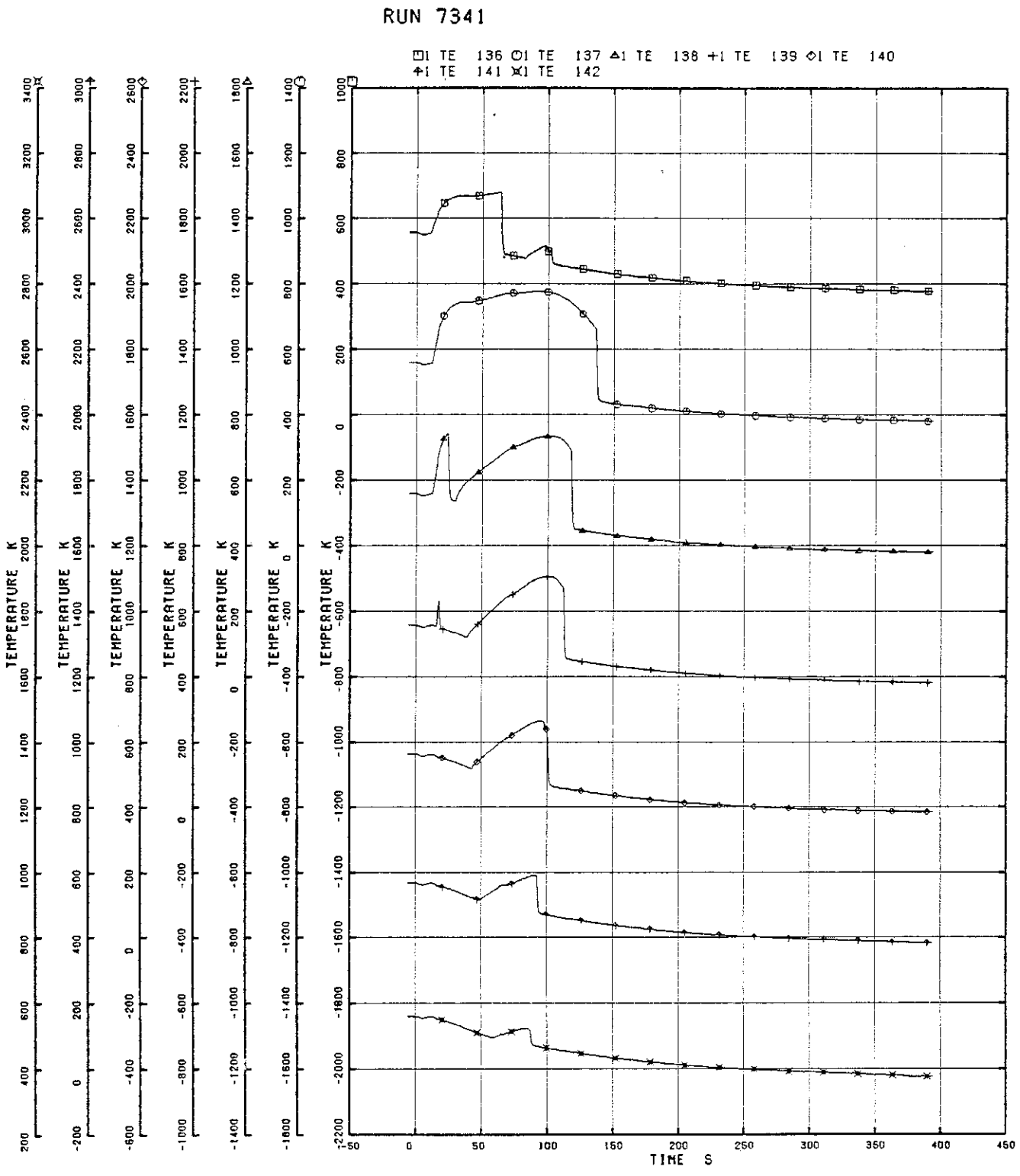

Fig. 5.57 Heater Rod Surface Temperature of A13 Rod

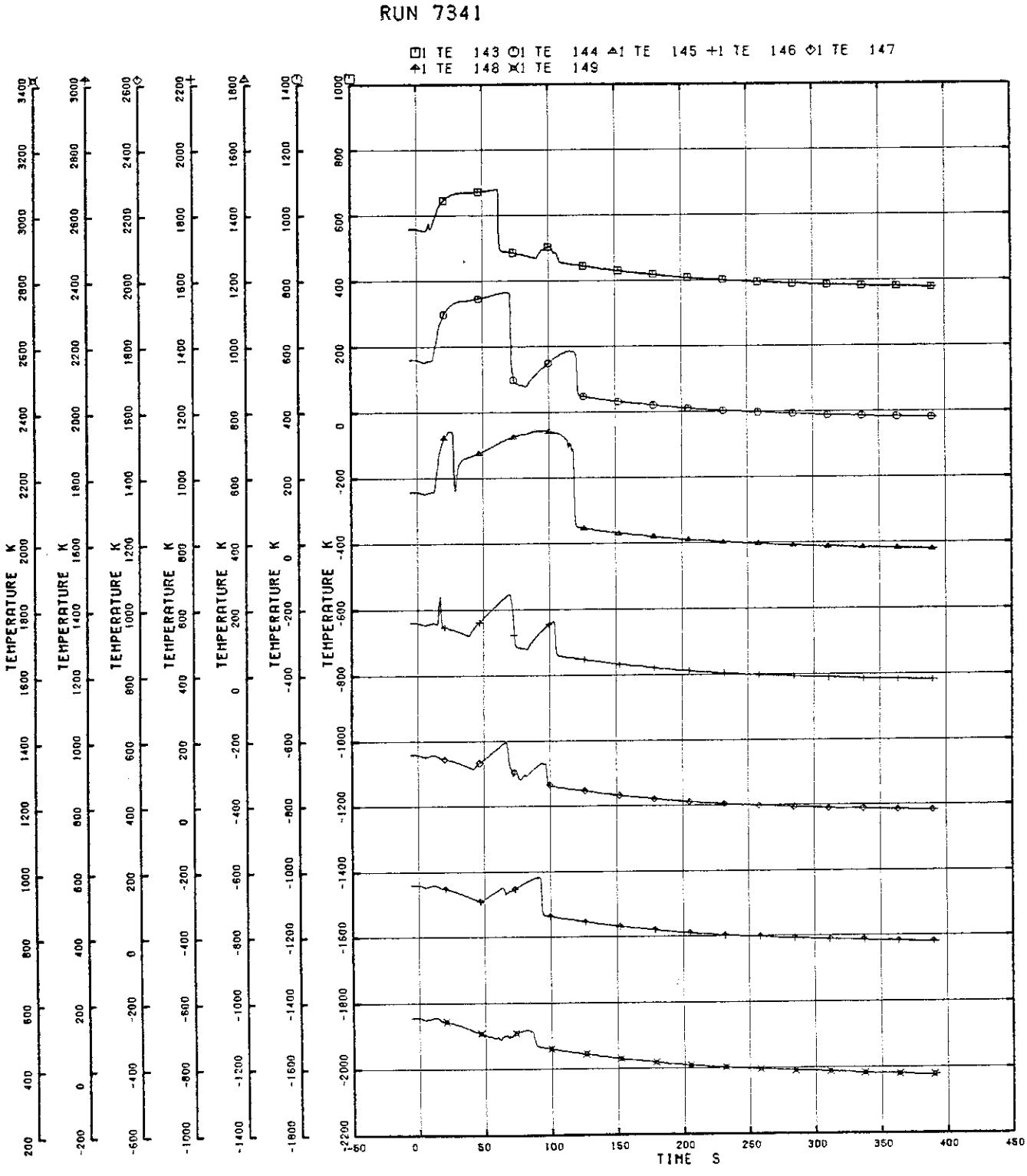

Fig. 5.58 Heater Rod Surface Temperature of A14 Rod

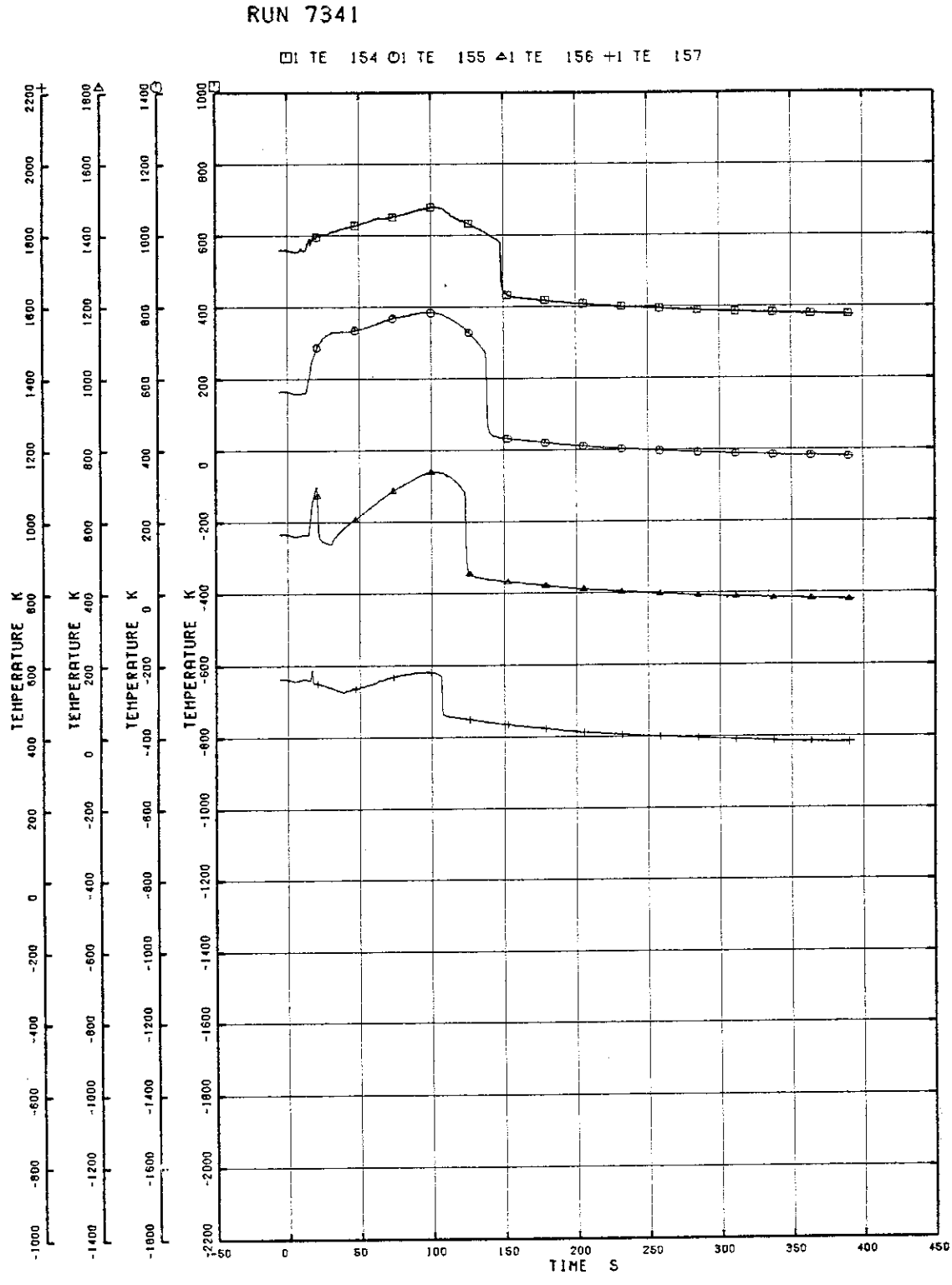

Fig. 5.59 Heater Rod Surface Temperature of A22 Rod

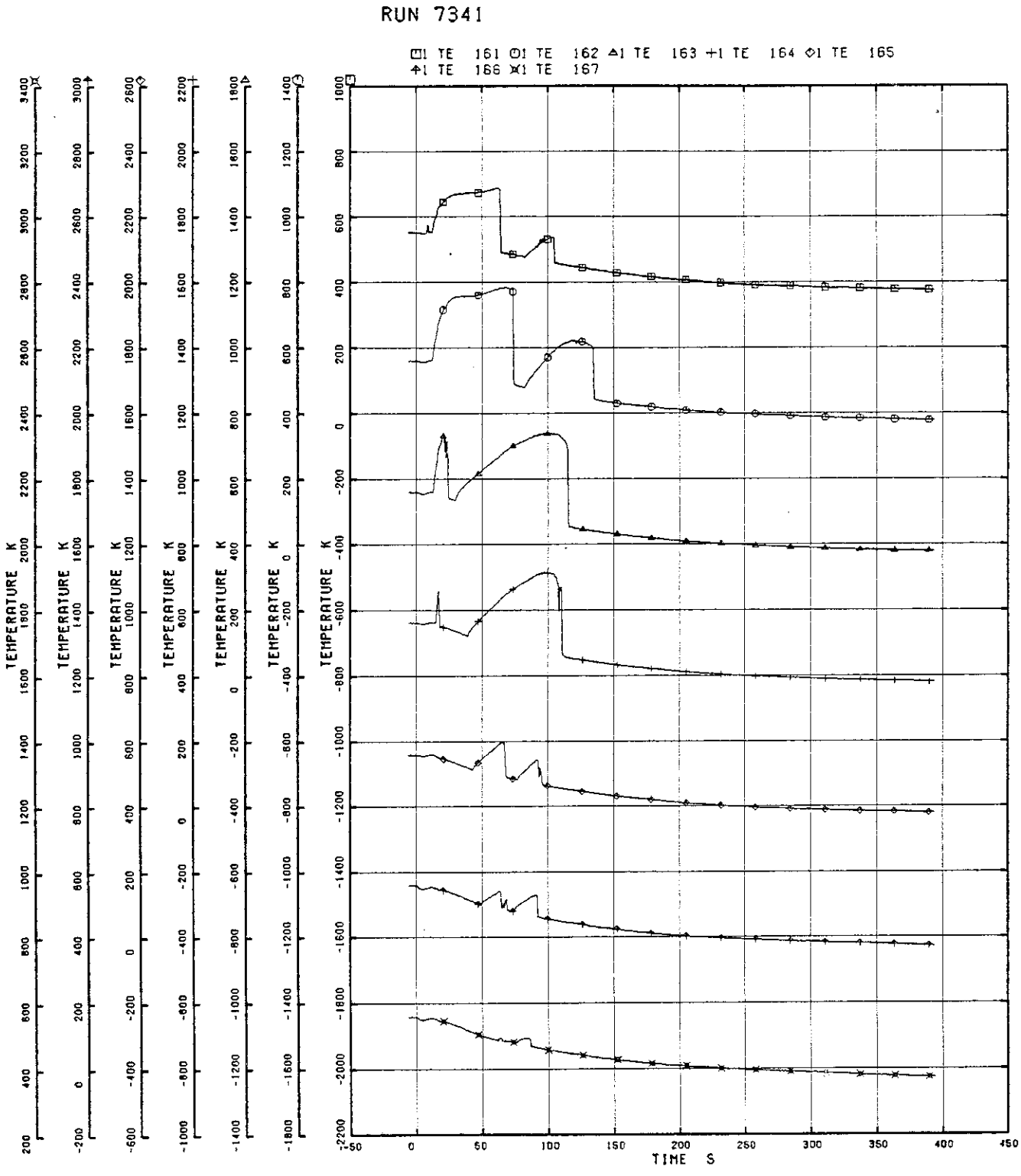

Fig. 5.60 Heater Rod Surface Temperature of A23 Rod

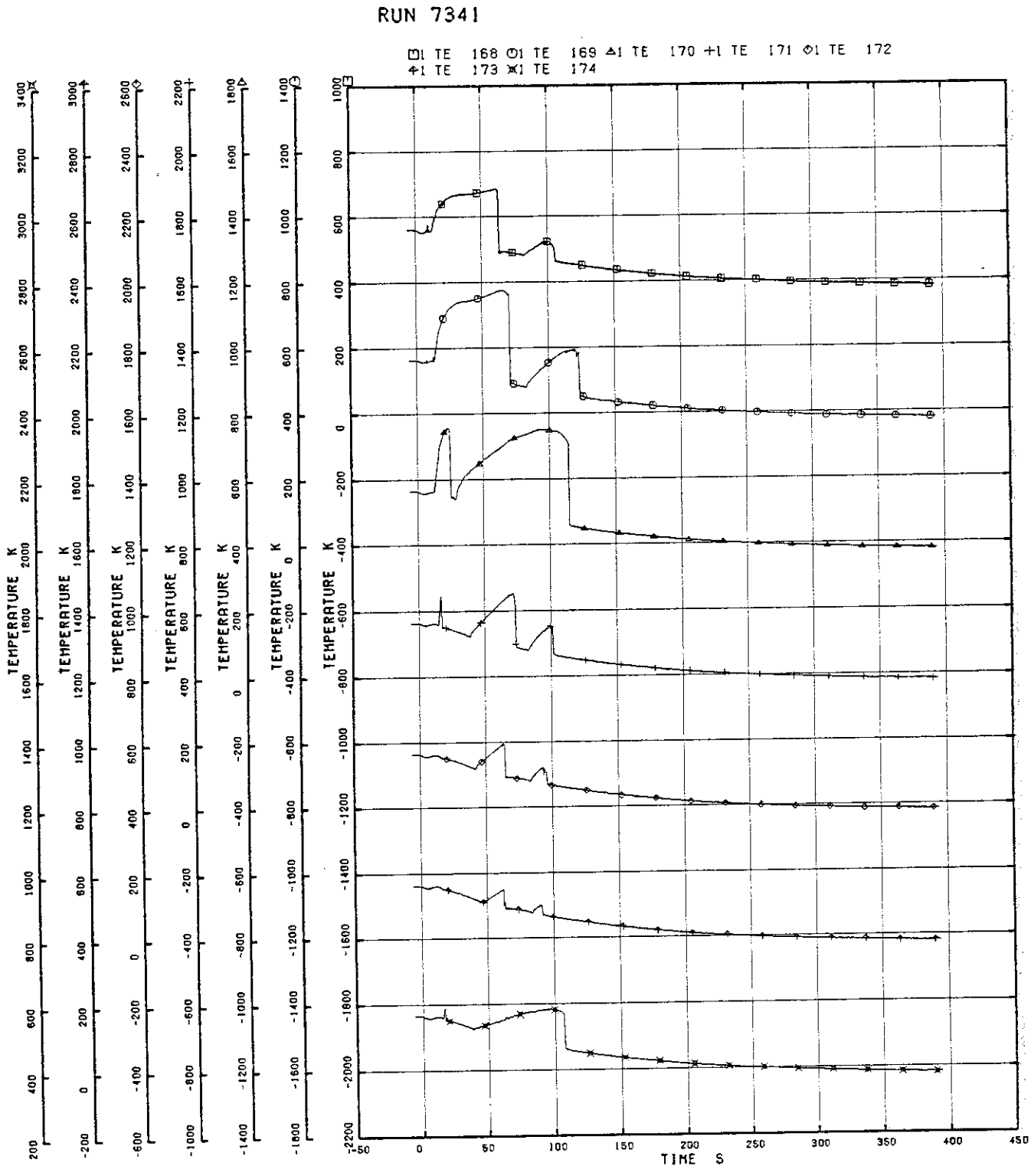

Fig. 5.61 Heater Rod Surface Temperature of A24 Rod

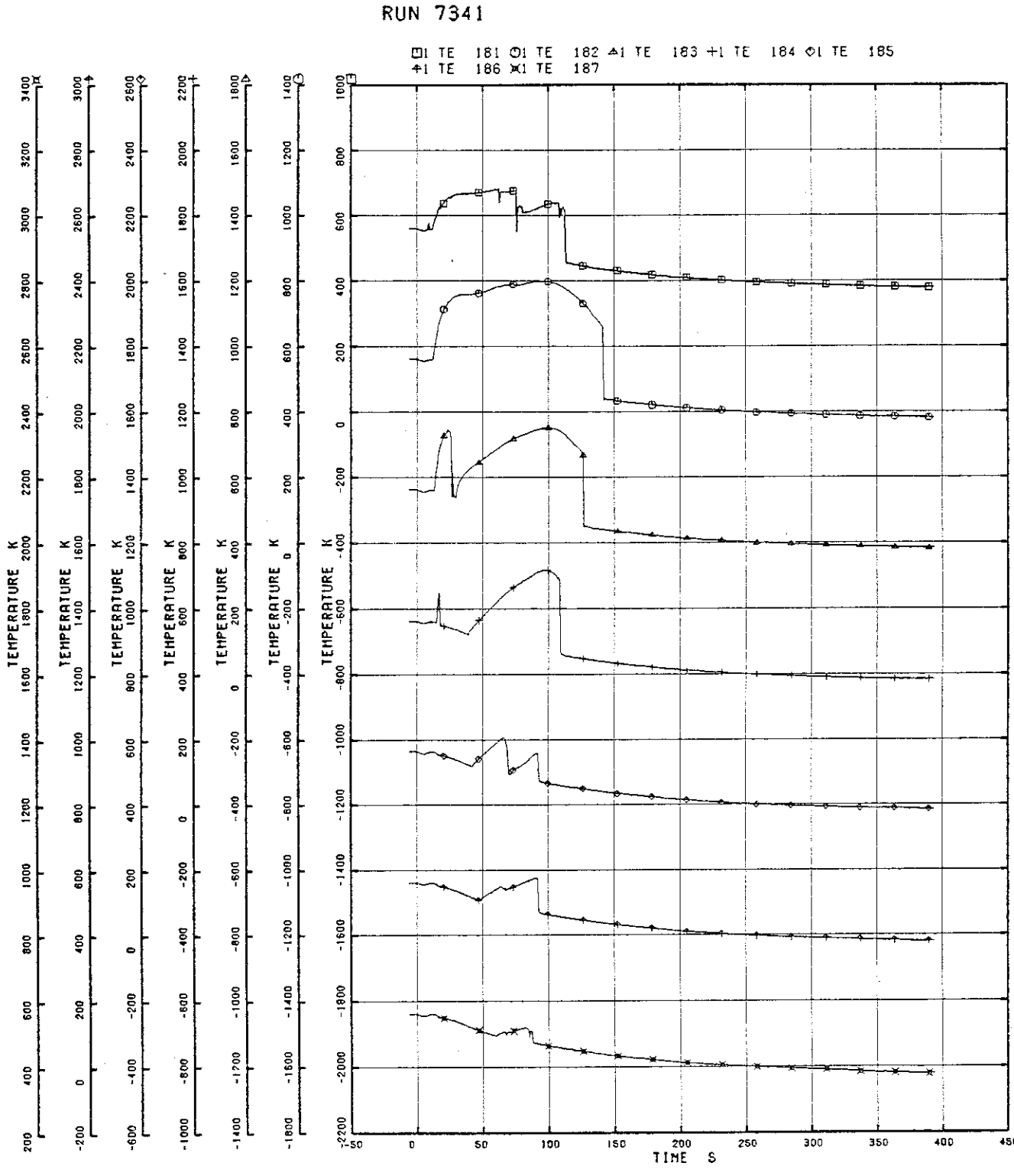

Fig. 5.62 Heater Rod Surface Temperature of A33 Rod

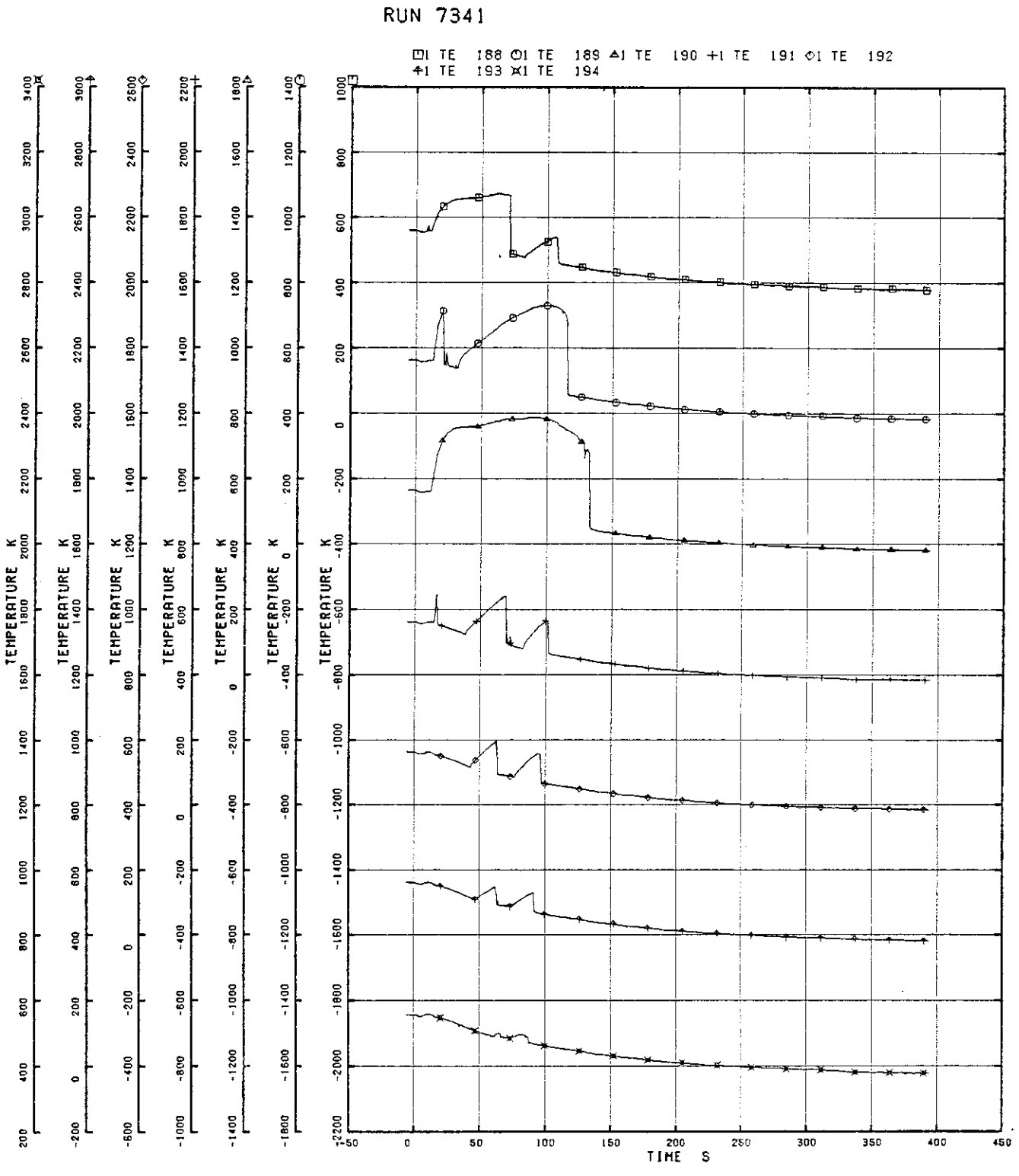

Fig. 5.63 Heater Rod Surface Temperature of A34 Rod

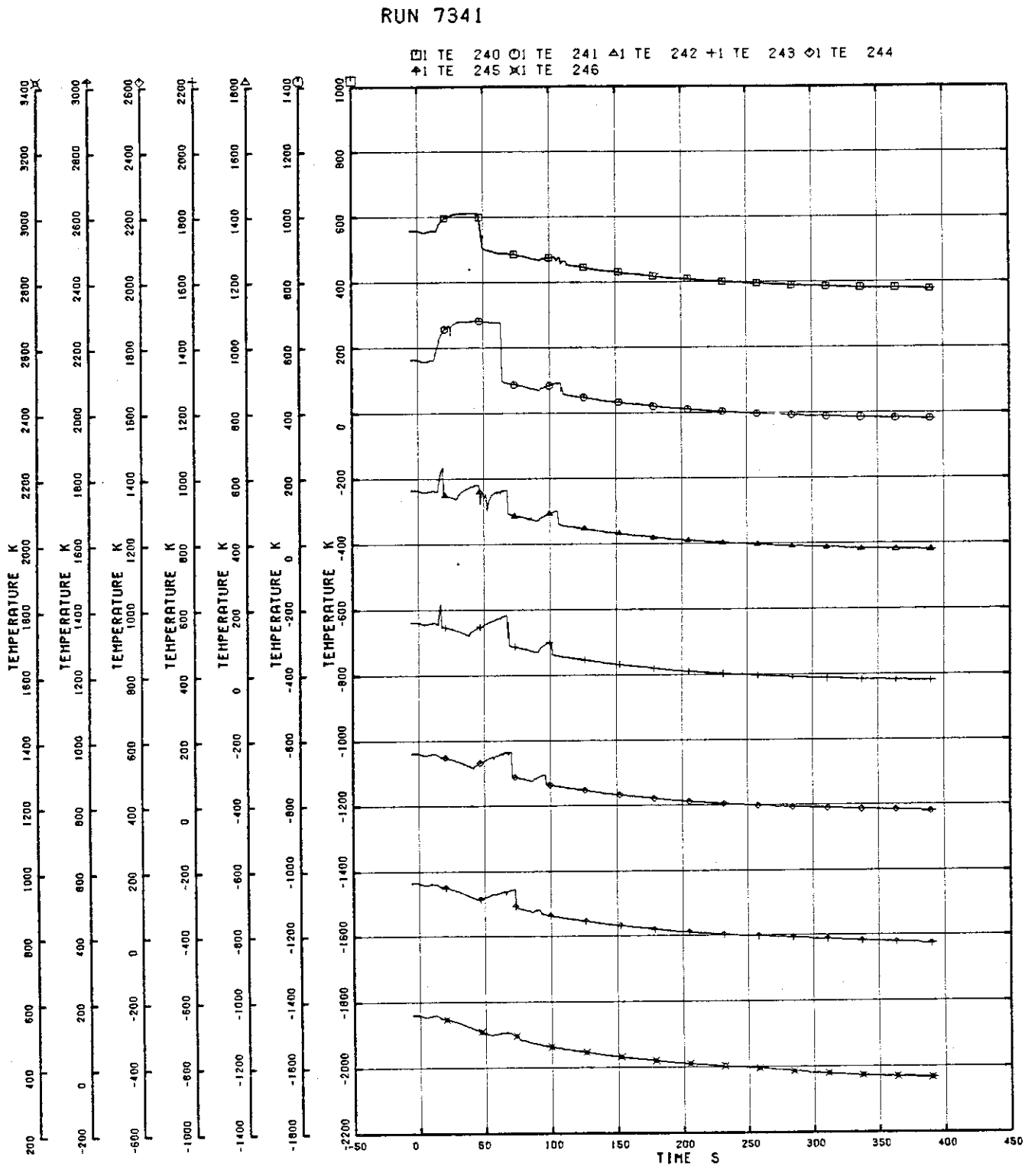

Fig. 5.64 Heater Rod Surface Temperature of B15 Rod

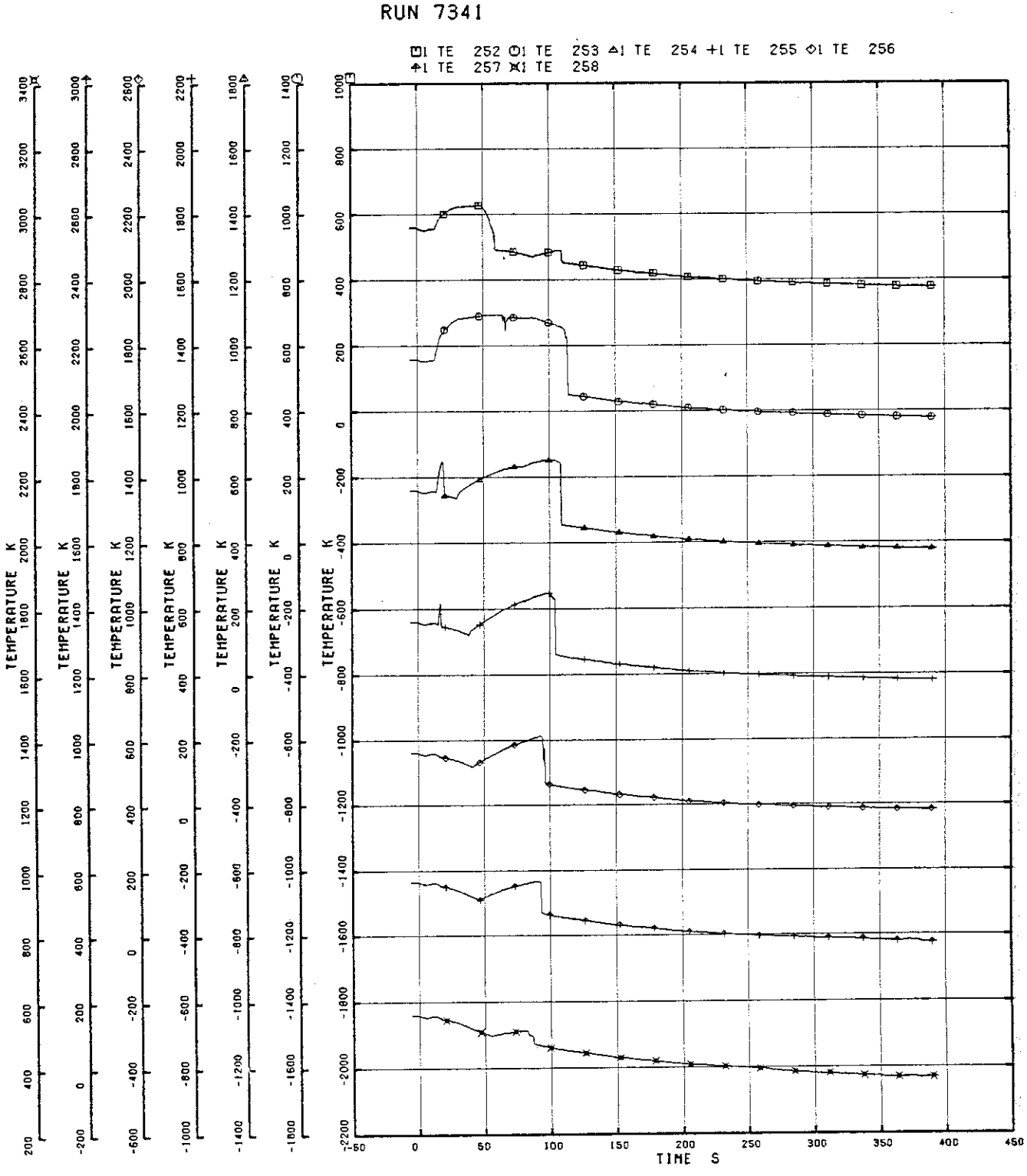

Fig. 5.65 Heater Rod Surface Temperature of B85 Rod

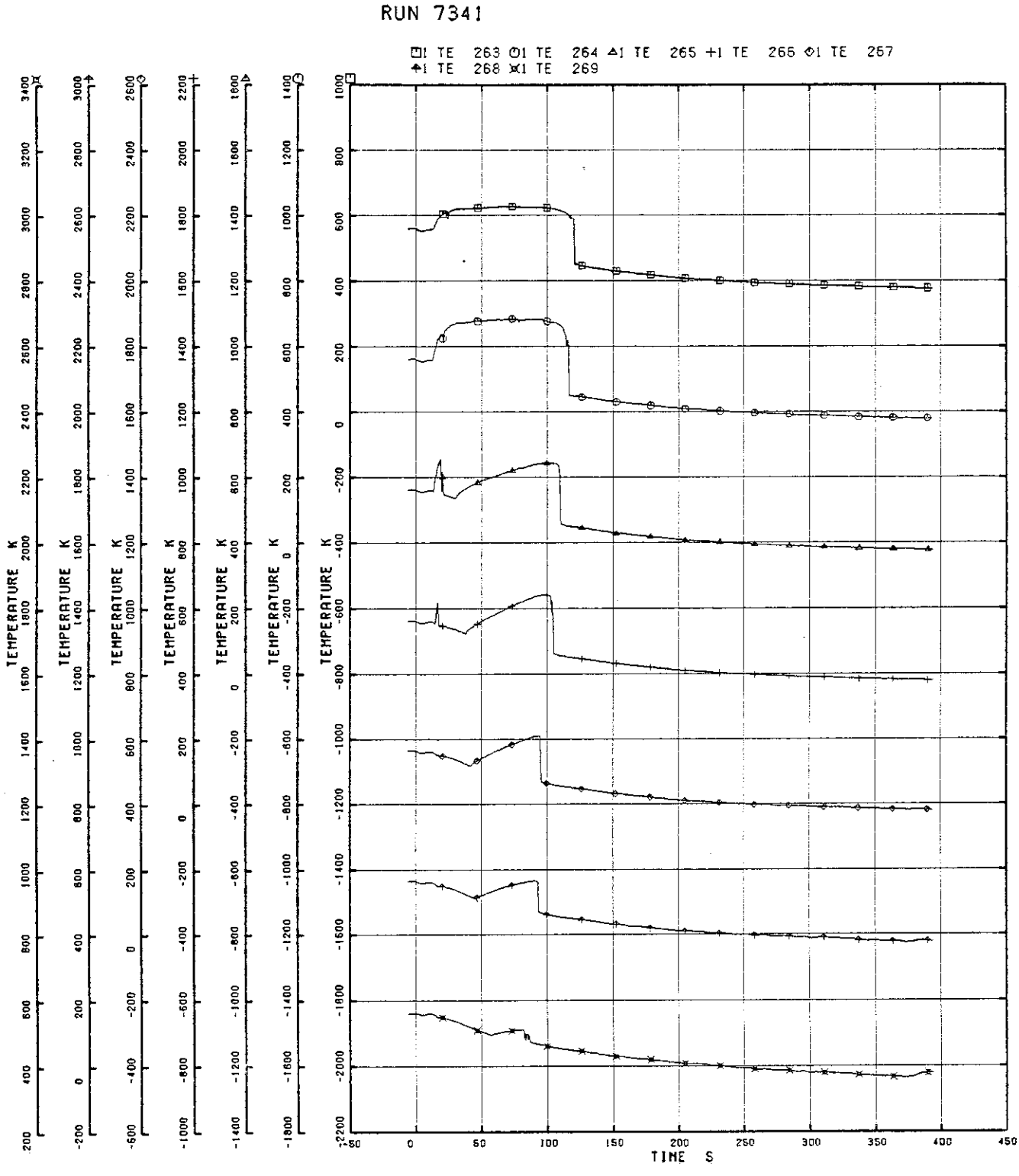

Fig. 5.66 Heater Rod Surface Temperature of C33 Rod

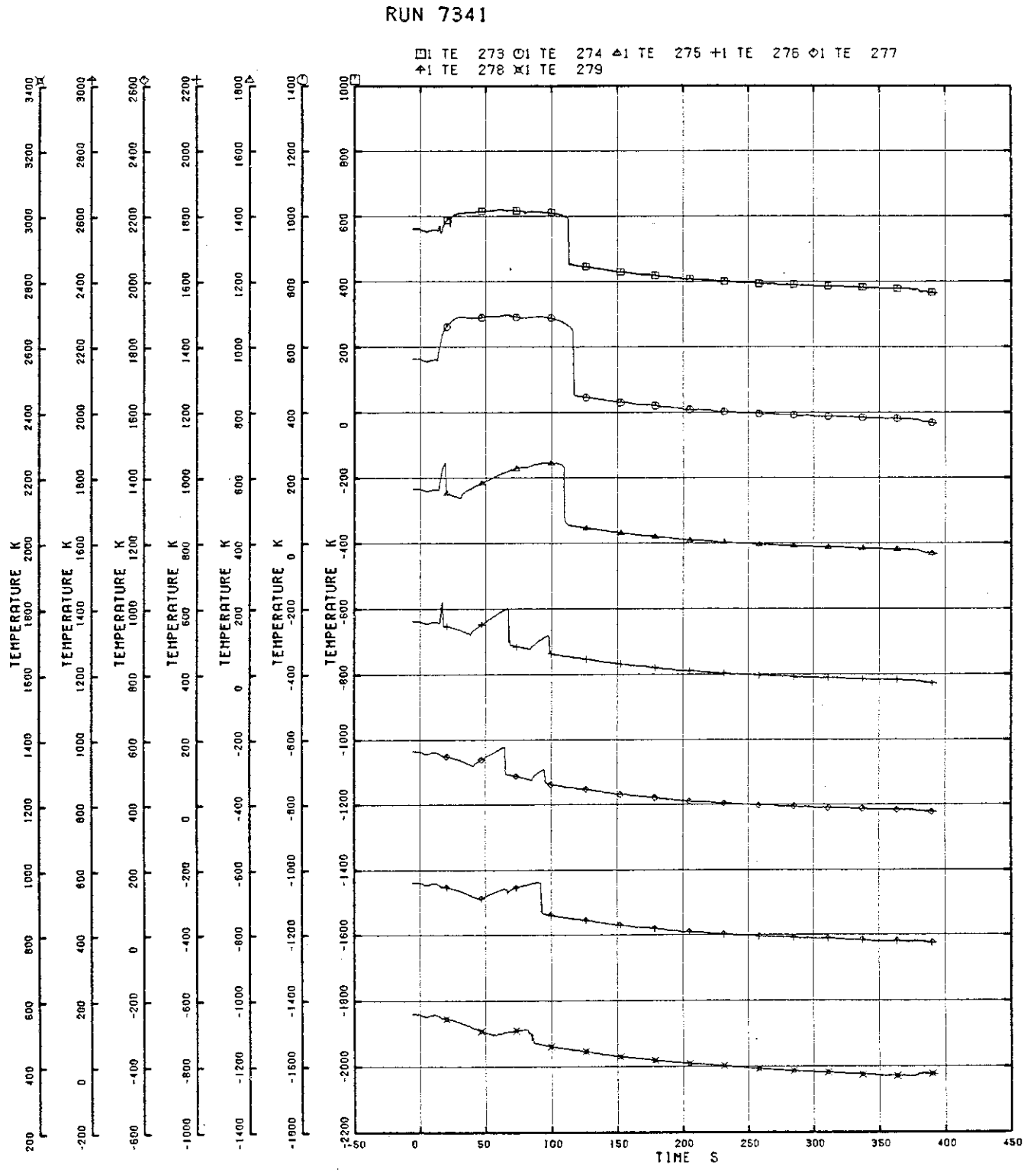

Fig. 5.67 Heater Rod Surface Temperature of C77 Rod

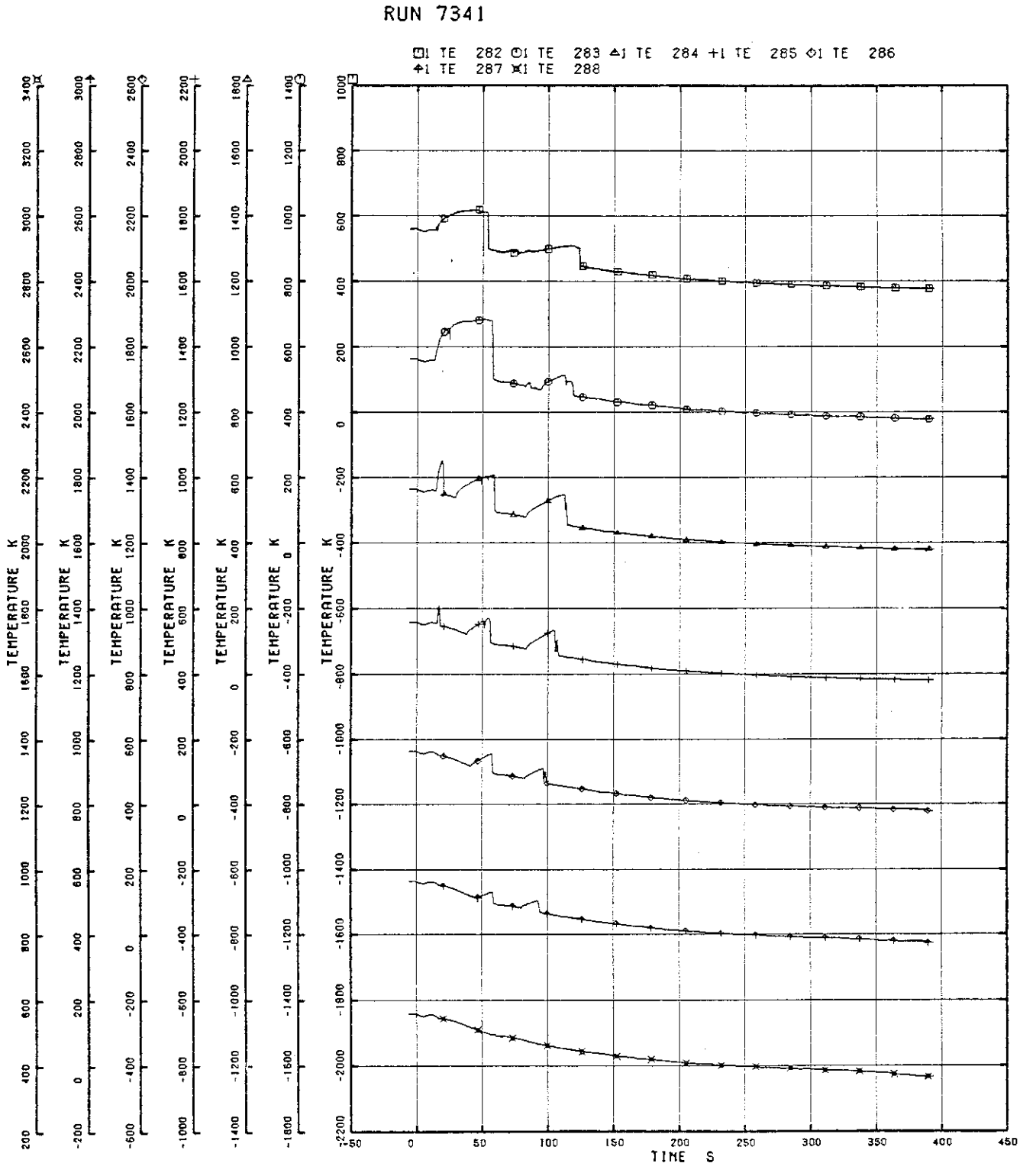

Fig. 5.68 Heater Rod Surface Temperature of D27 Rod

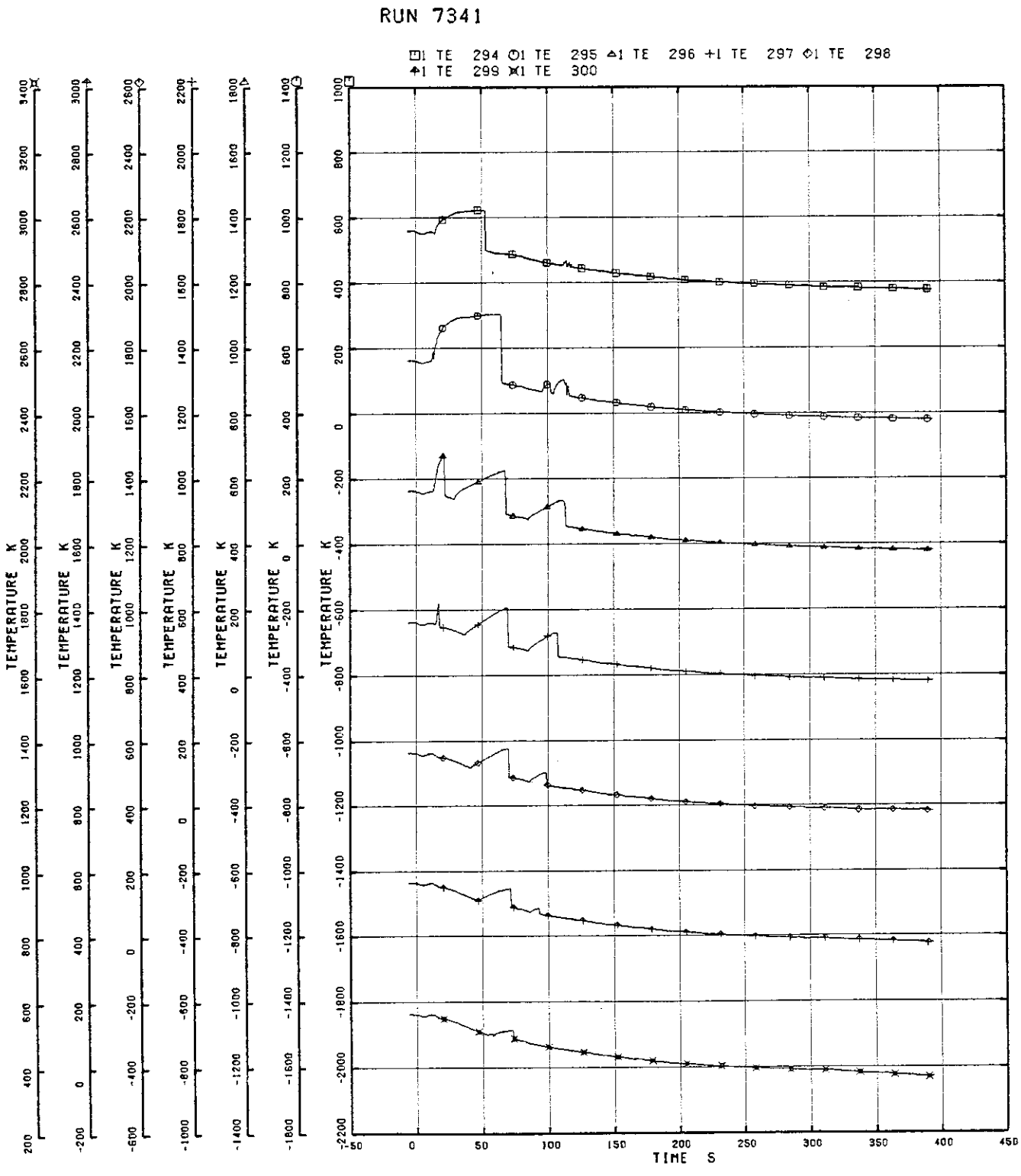

Fig. 5.69 Heater Rod Surface Temperature of D88 Rod

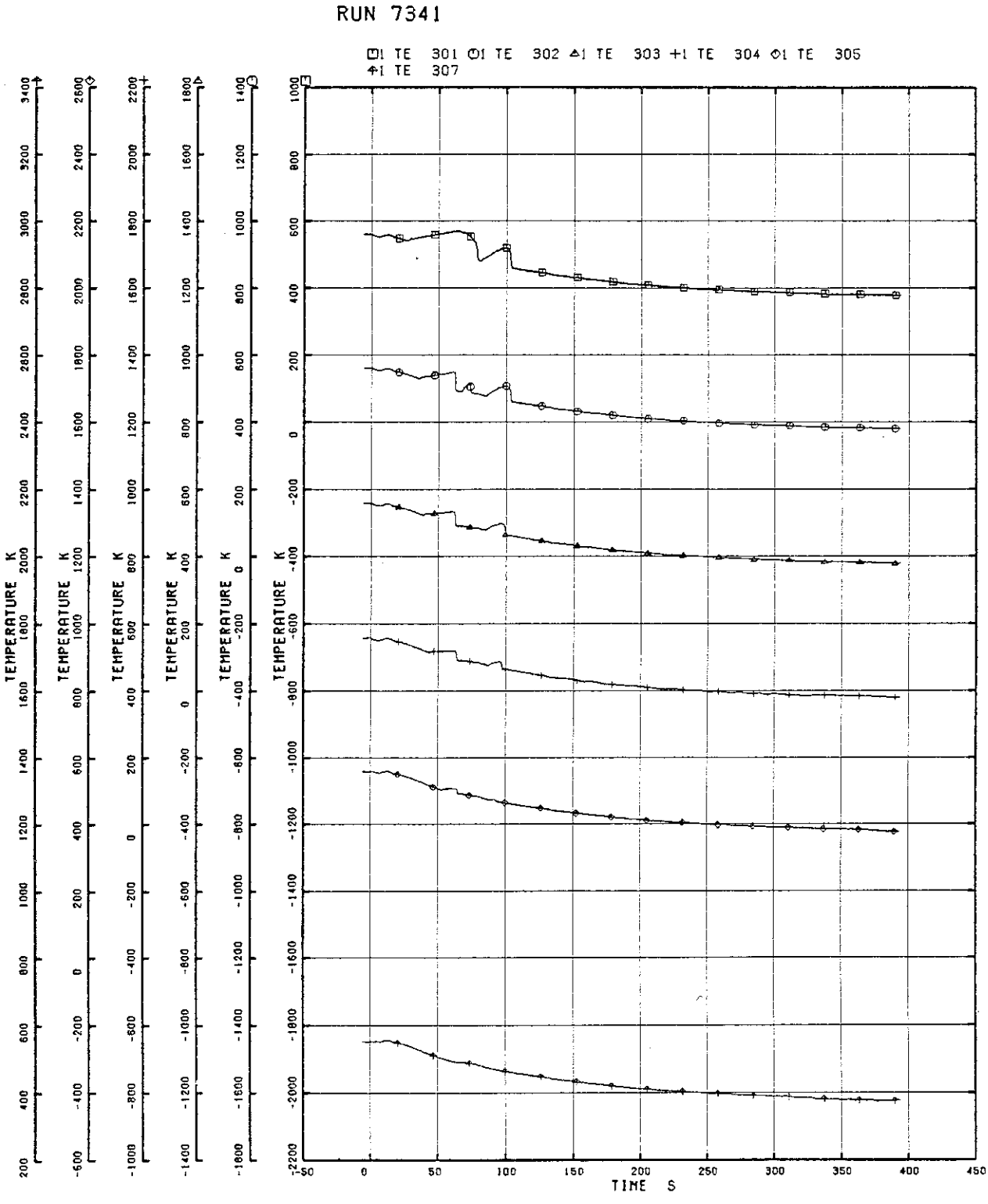

Fig. 5.70 Surface Temperture of Tie Rod A44

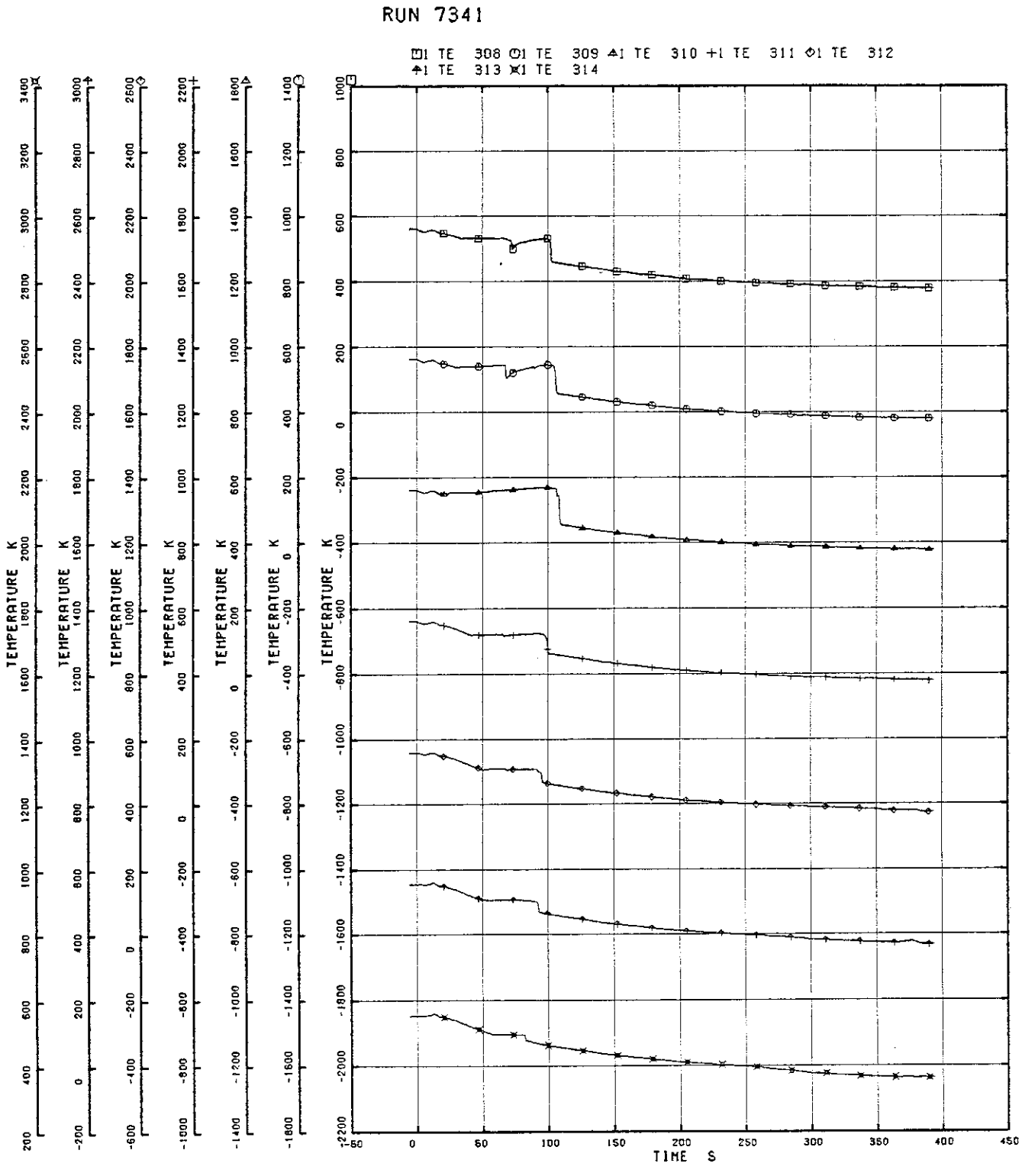

Fig. 5.71 Surface Temperture of Tie Rod B44

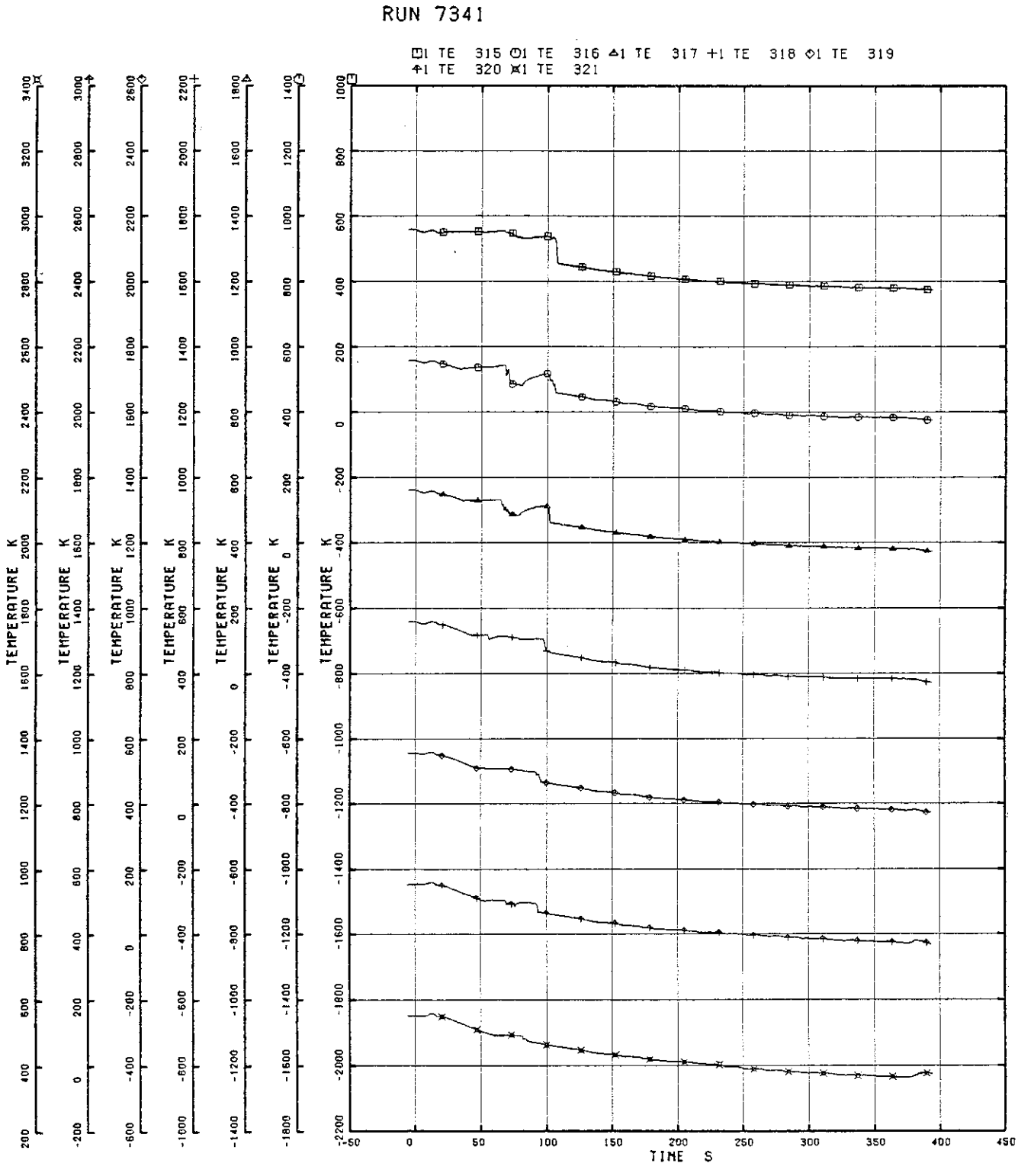

Fig. 5.72 Surface Temperture of Tie Rod C44

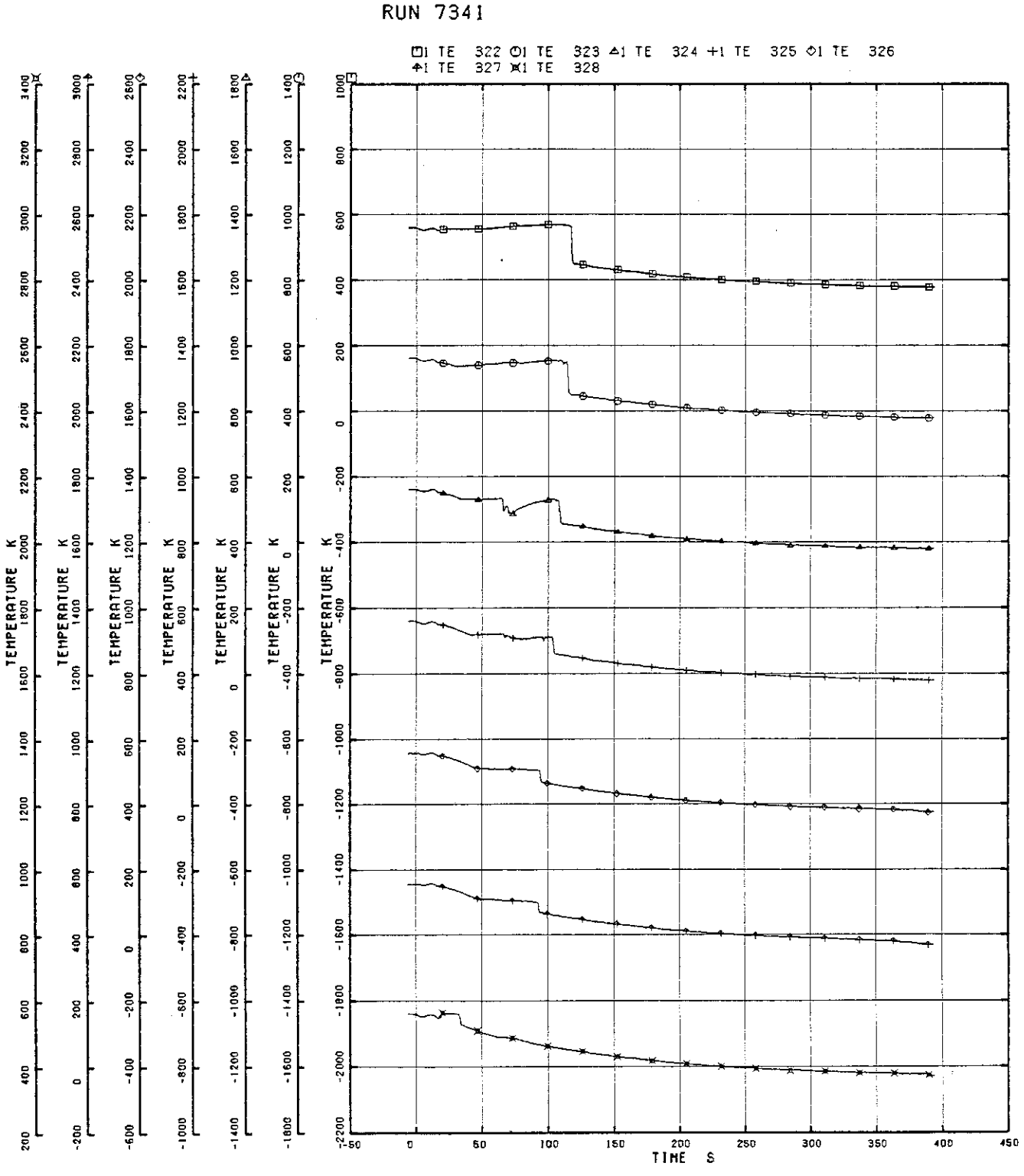

Fig. 5.73 Surface Temperture of Tie Rod D44

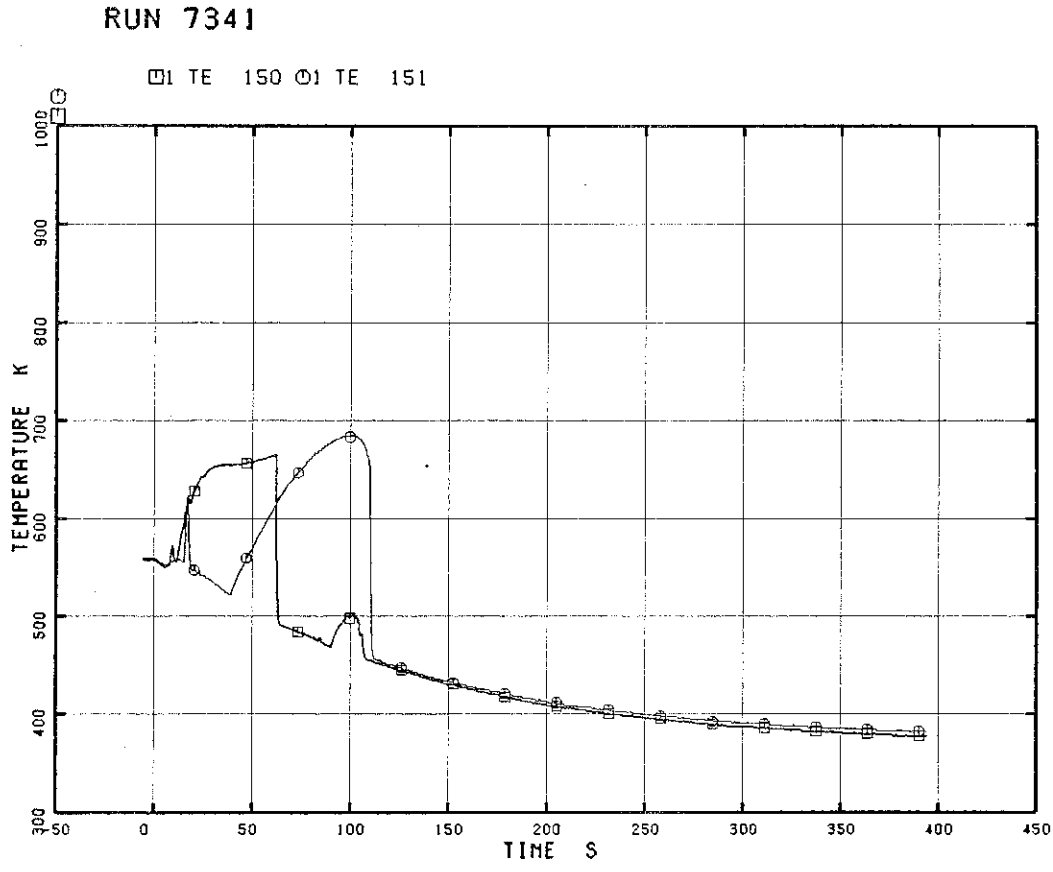

Fig. 5.74 Heater Rod Surface Temperature of A15 Rod

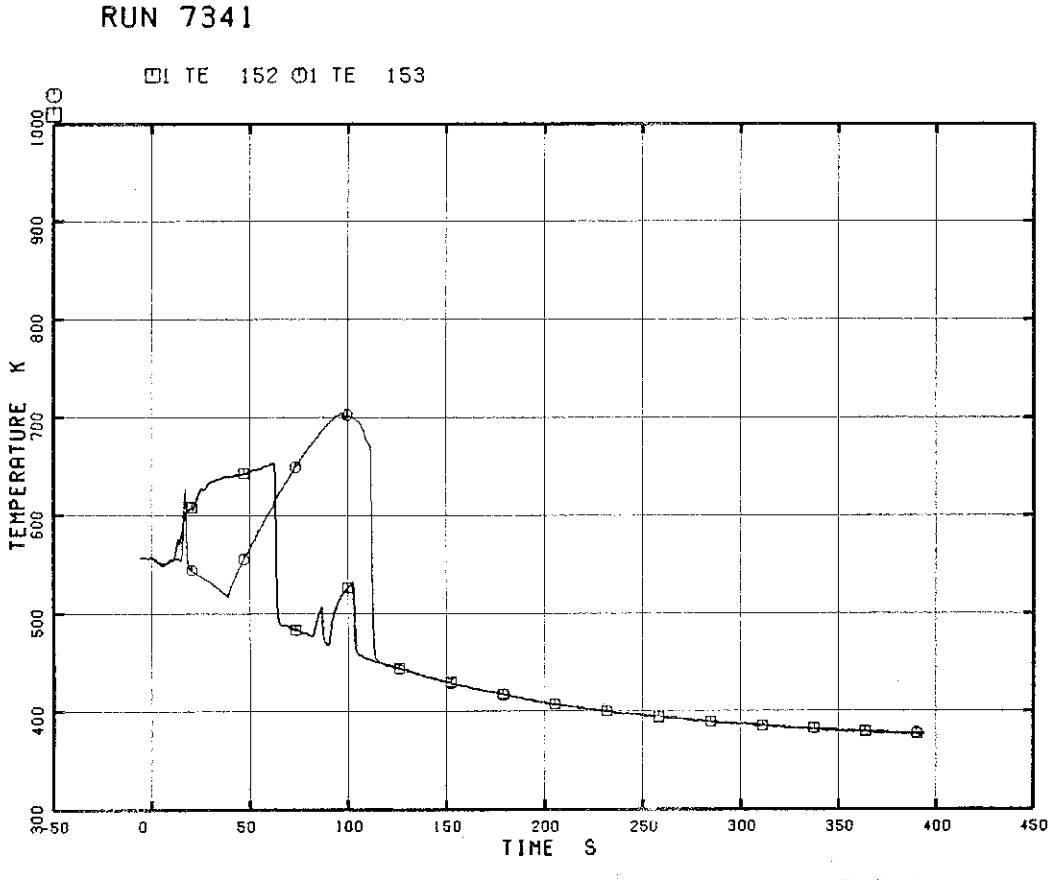

Fig. 5.75 Heater Rod Surface Temperature of A17 Rod

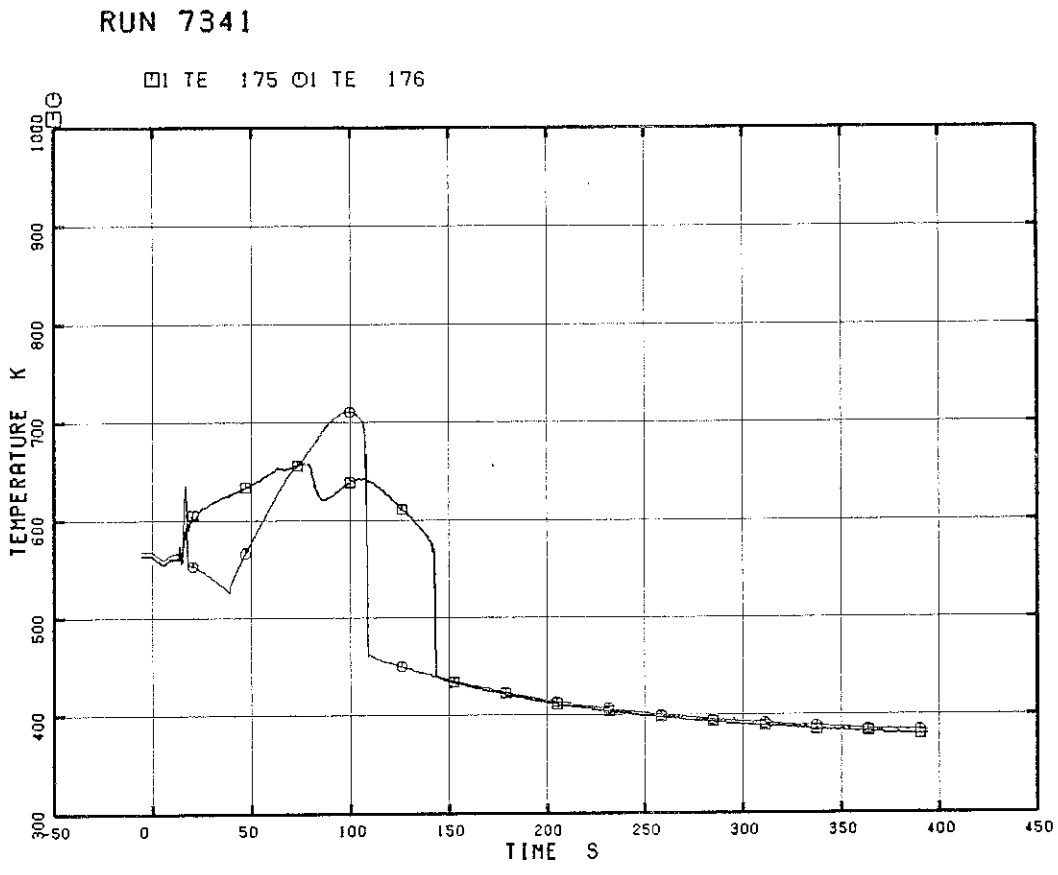

Fig. 5.76 Heater Rod Surface Temperature of A26 Rod

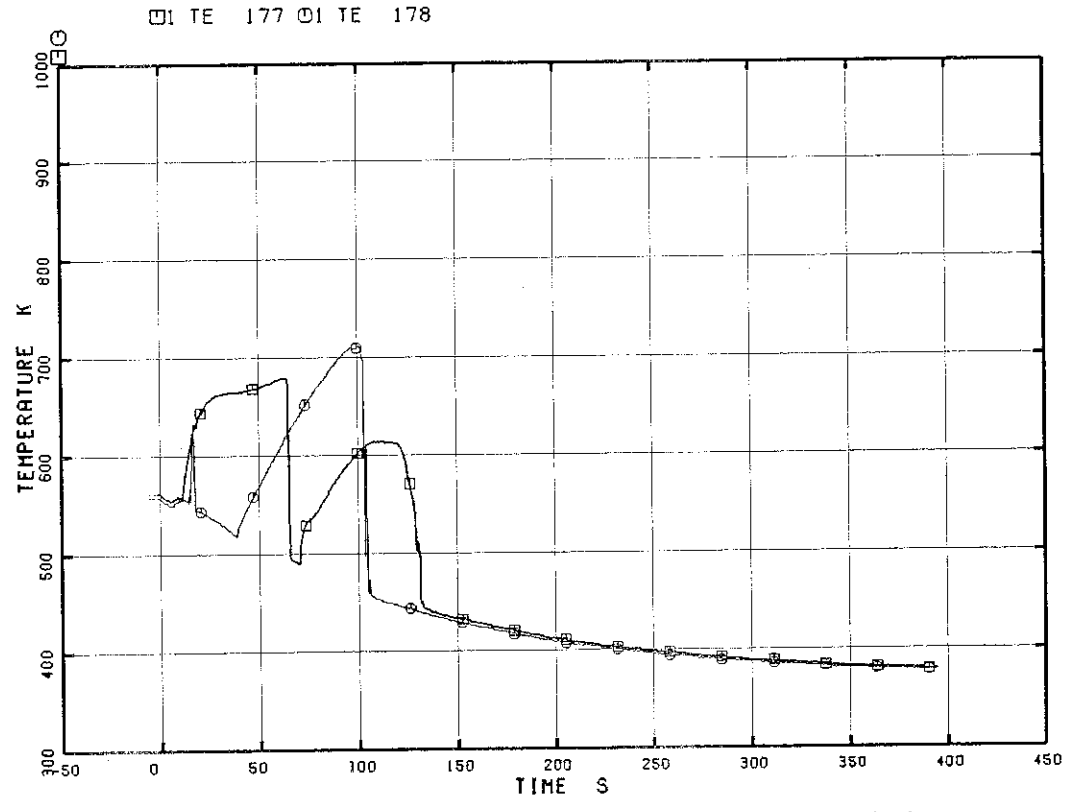

Fig. 5.77 Heater Rod Surface Temperature of A28 Rod

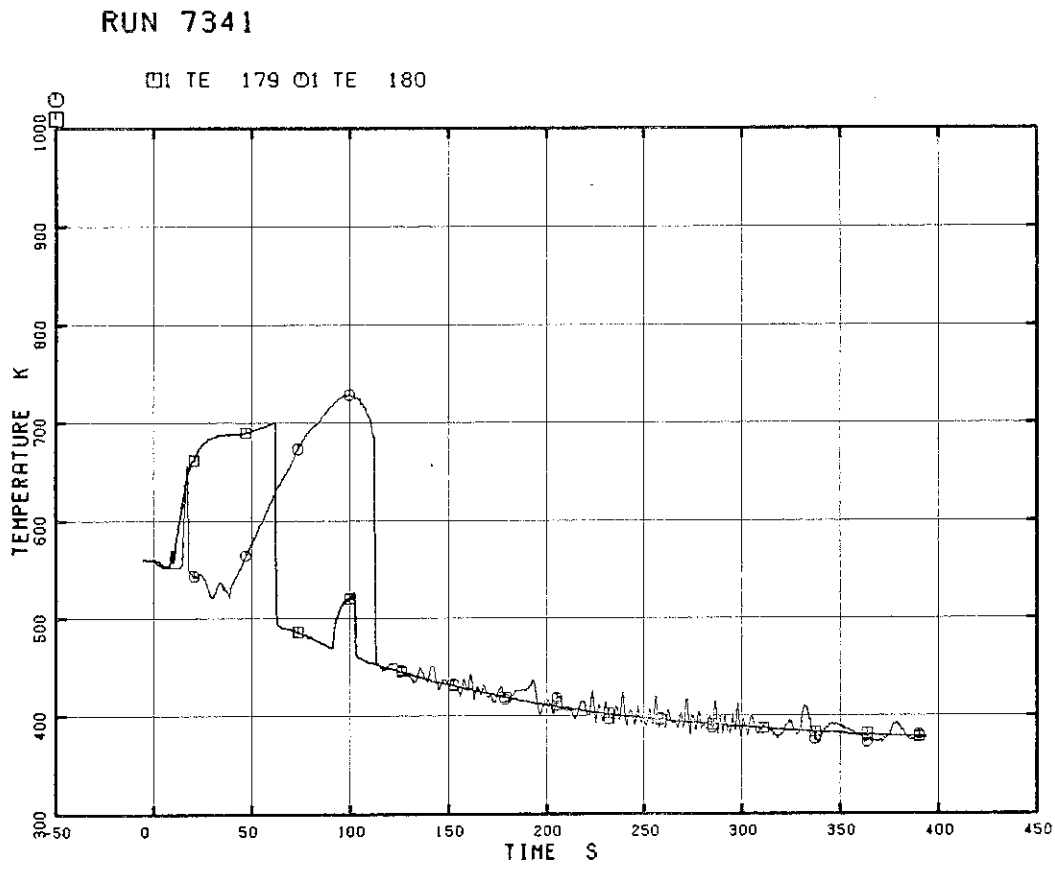

Fig. 5.78 Heater Rod Surface Temperature of A31 Rod

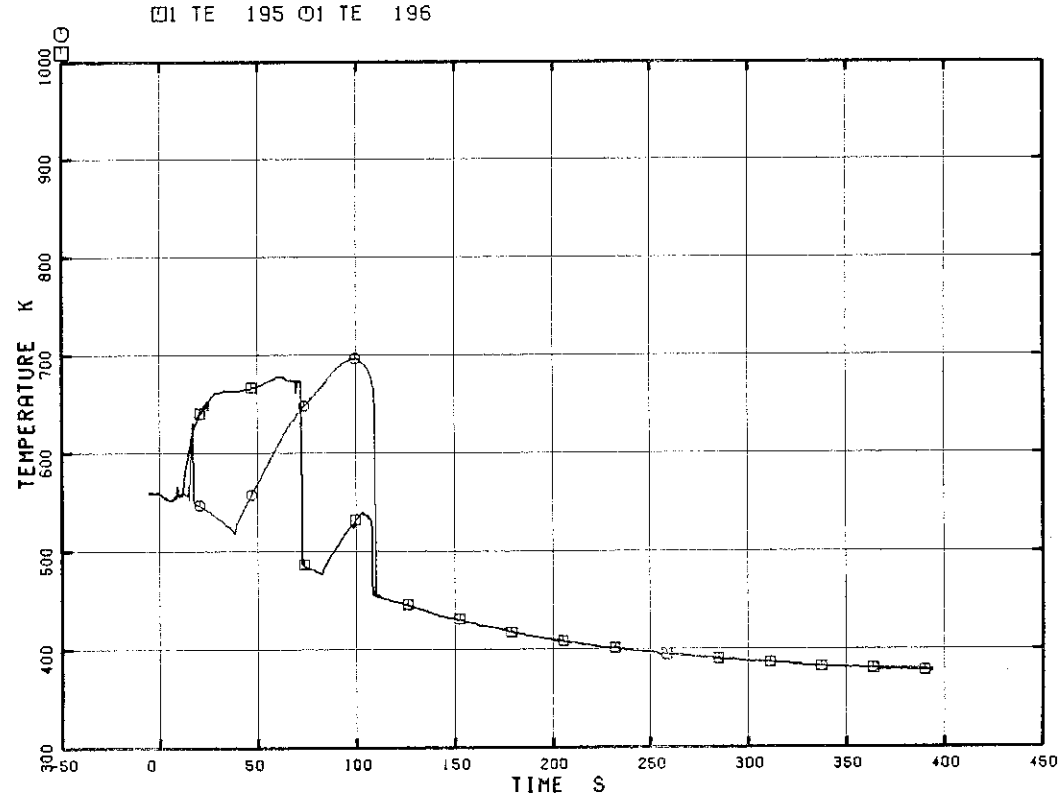

Fig. 5.79 Heater Rod Surface Temperature of A35 Rod

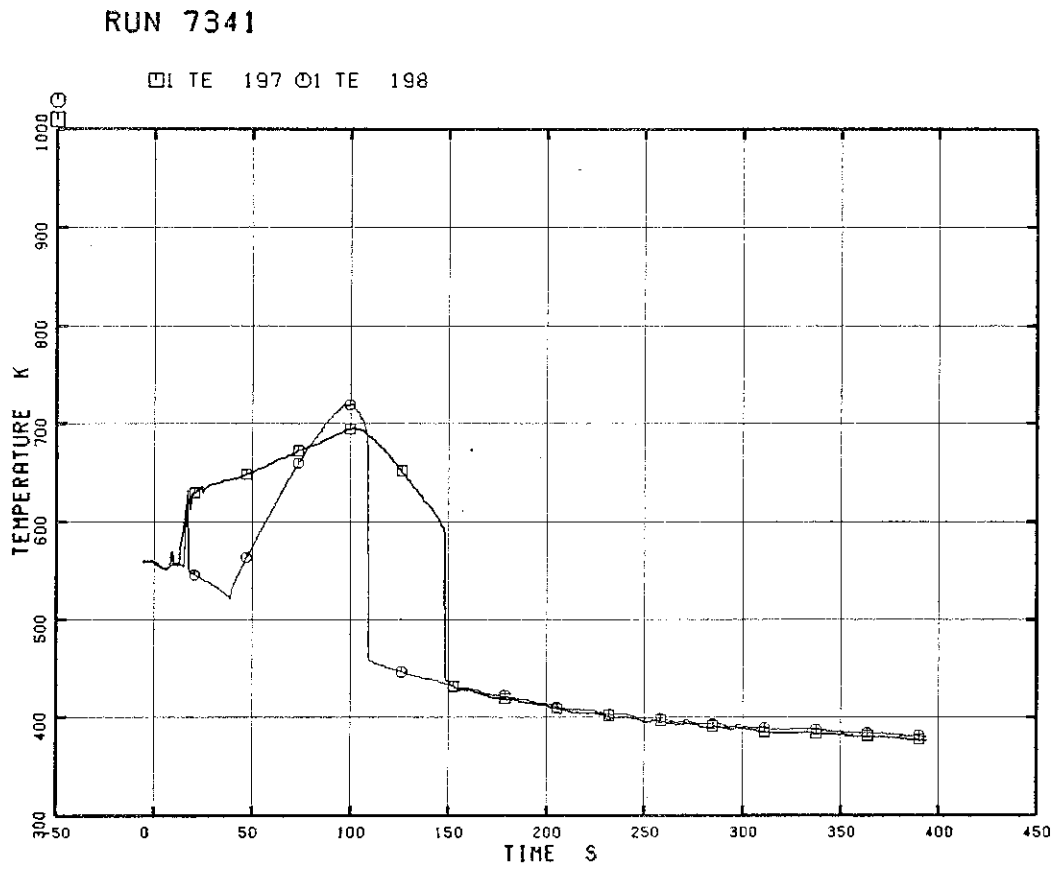

Fig. 5.80 Heater Rod Surface Temperature of A37 Rod

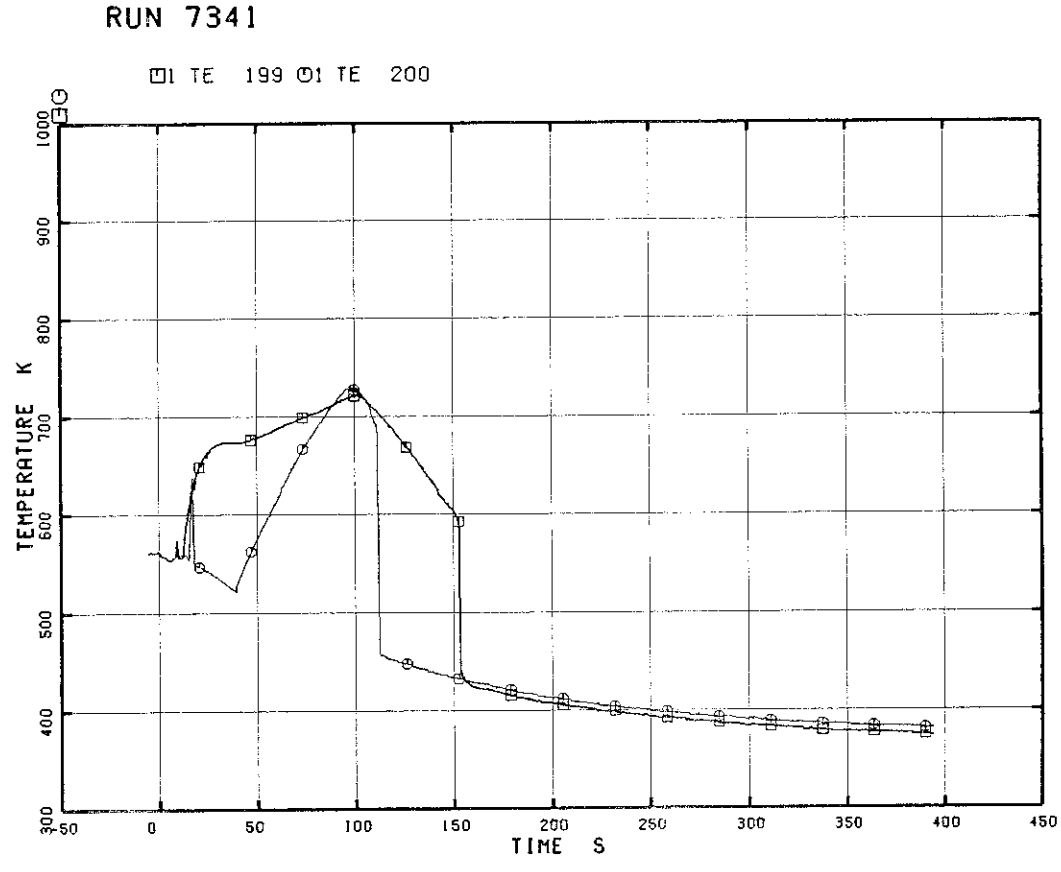

Fig. 5.81 Heater Rod Surface Temperature of A42 Rod

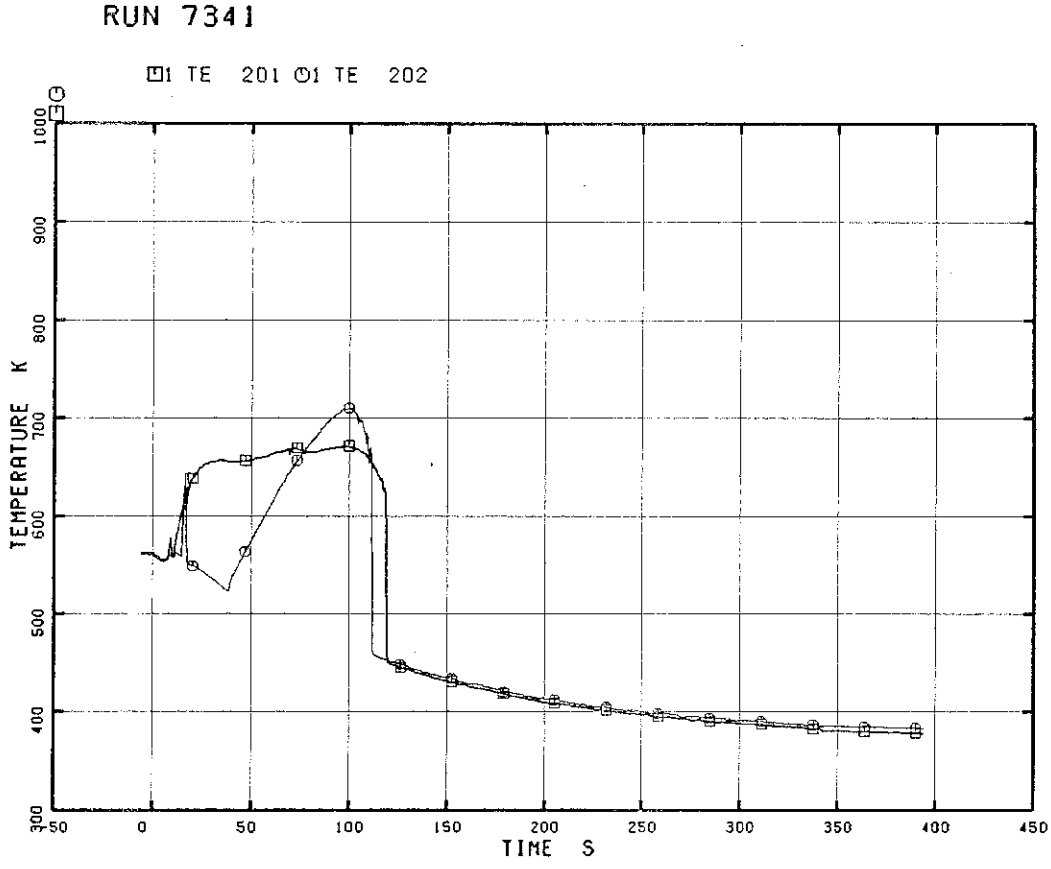

Fig. 5.82 Heater Rod Surface Temperature of A45 Rod

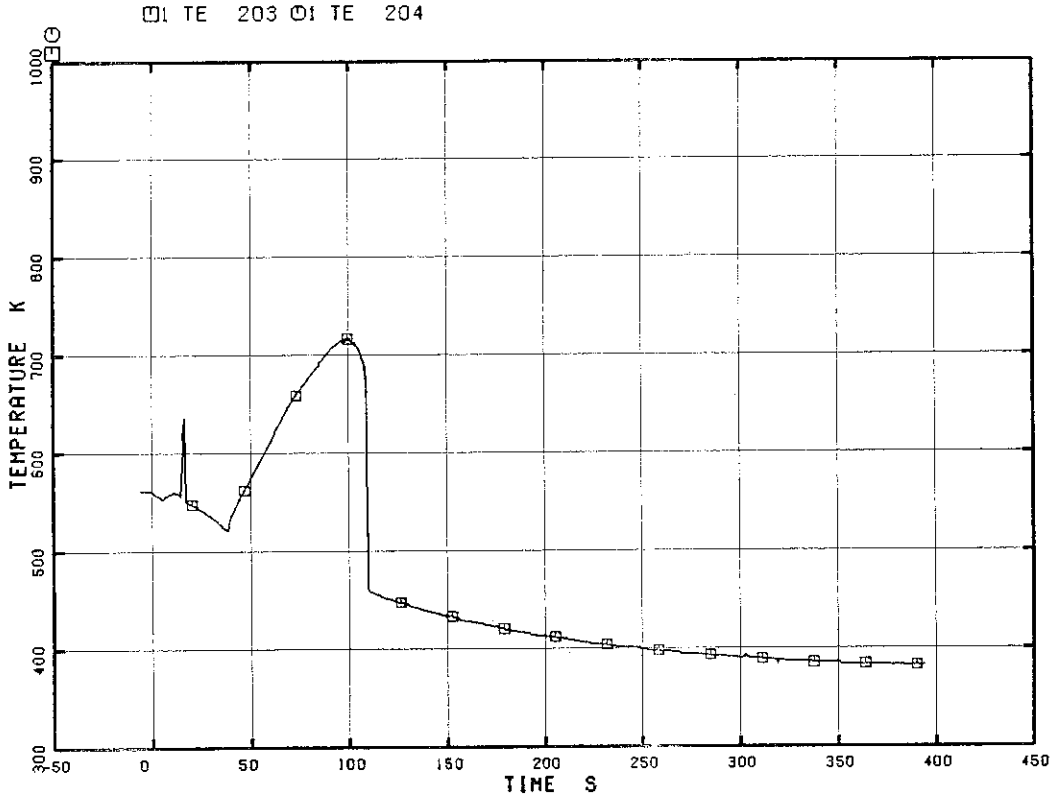

Fig. 5.83 Heater Rod Surface Temperature of A46 Rod

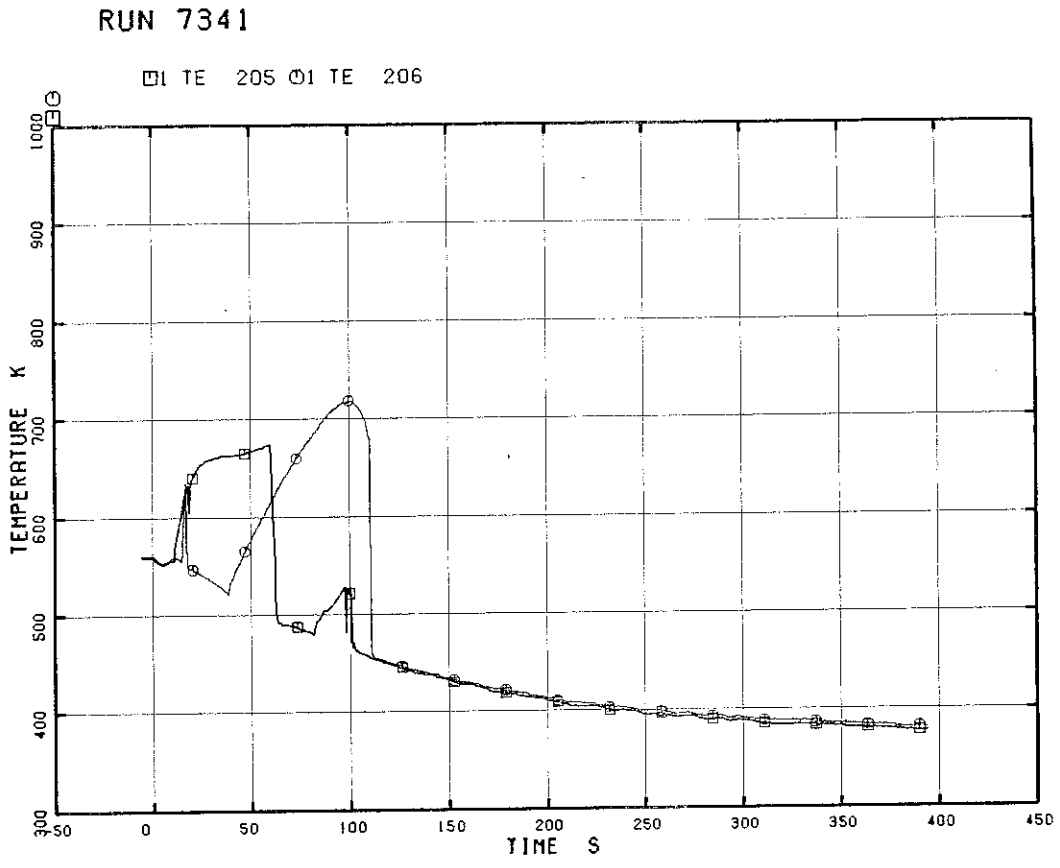

Fig. 5.84 Heater Rod Surface Temperature of A48 Rod

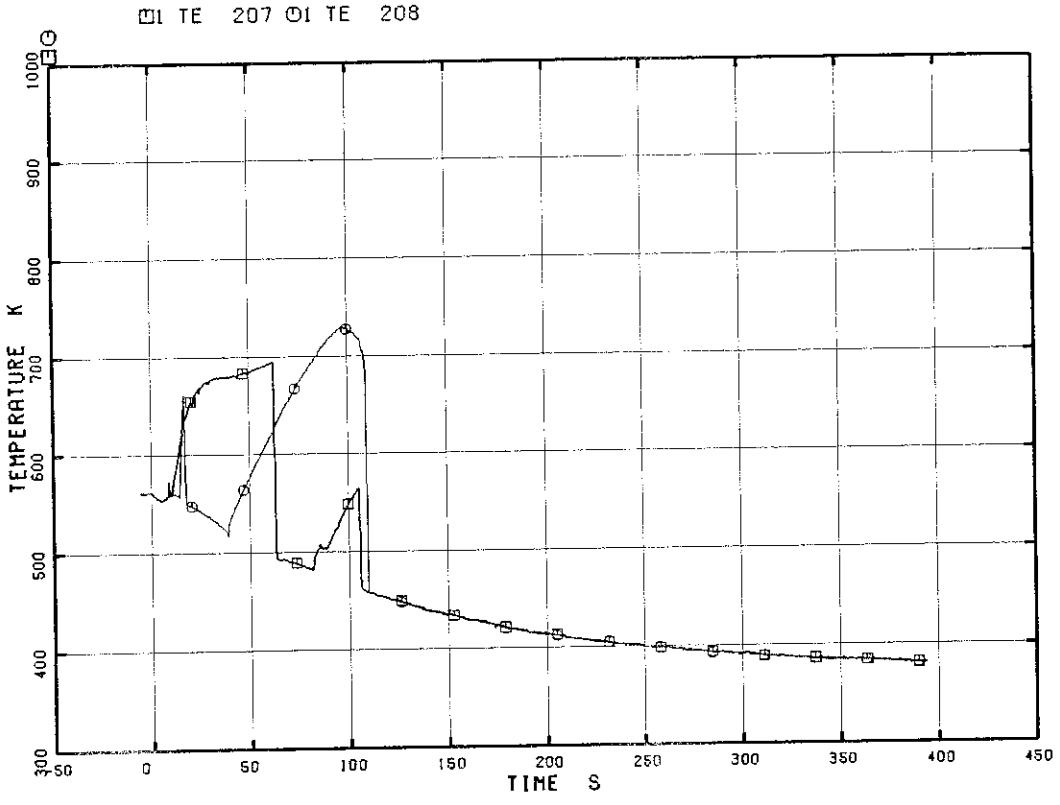

Fig. 5.85 Heater Rod Surface Temperature of A51 Rod

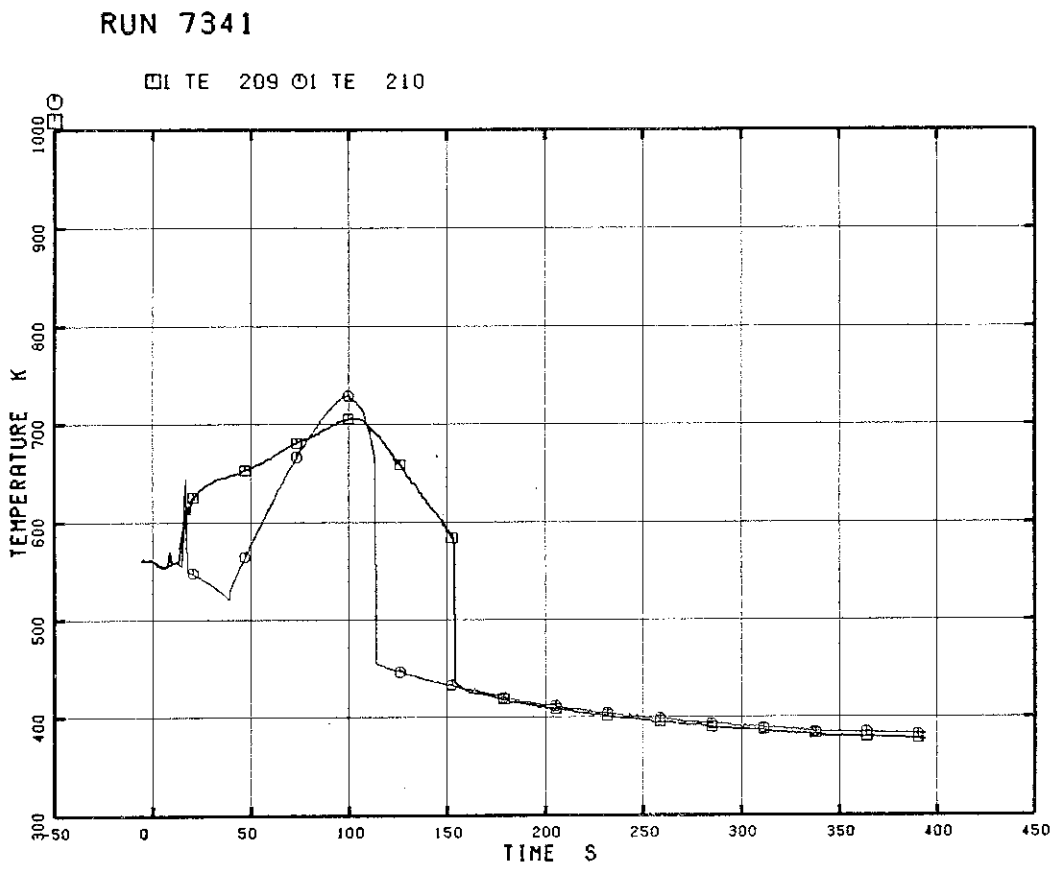

Fig. 5.86 Heater Rod Surface Temperature of A53 Rod

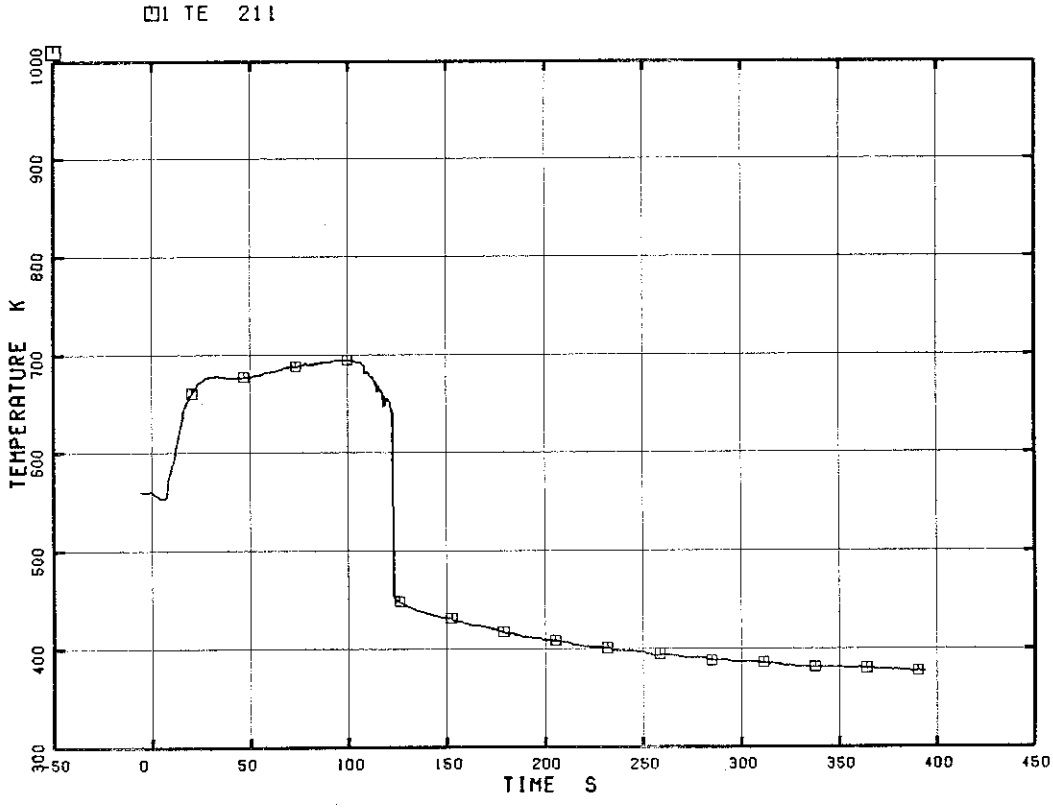

Fig. 5.87 Heater Rod Surface Temperature of A54 Rod

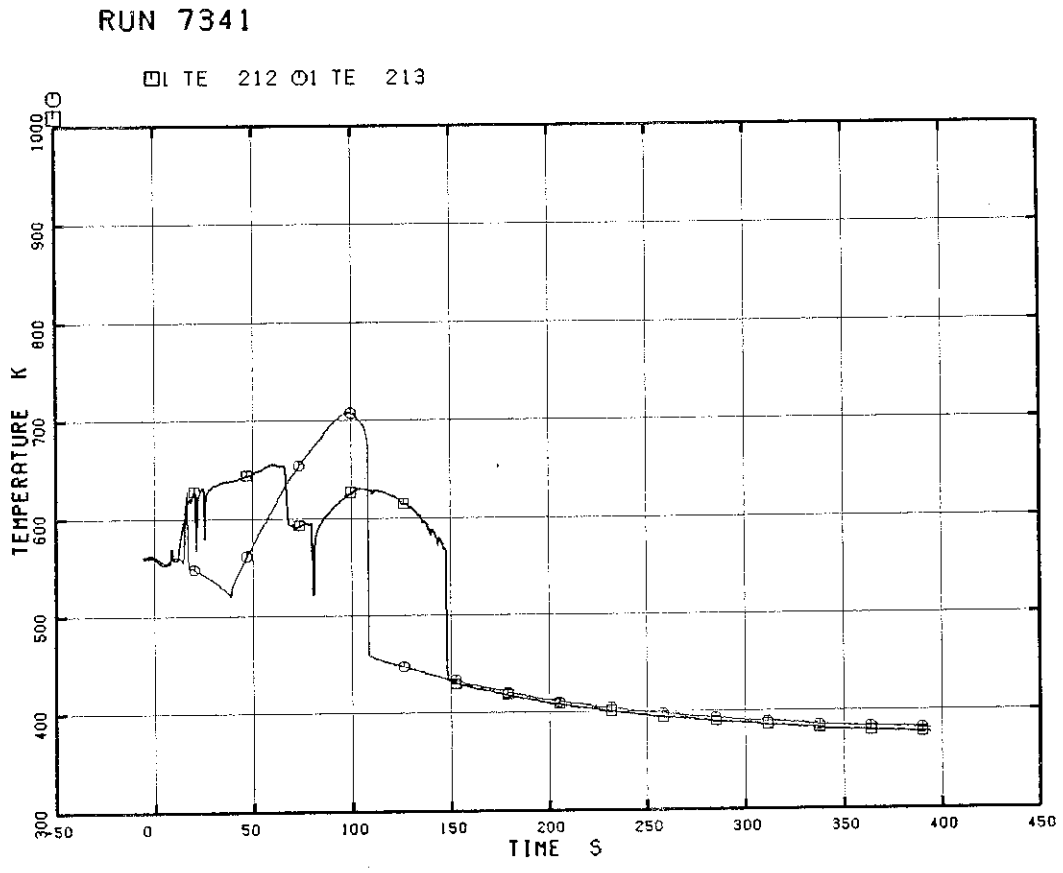

Fig. 5.88 Heater Rod Surface Temperature of A57 Rod

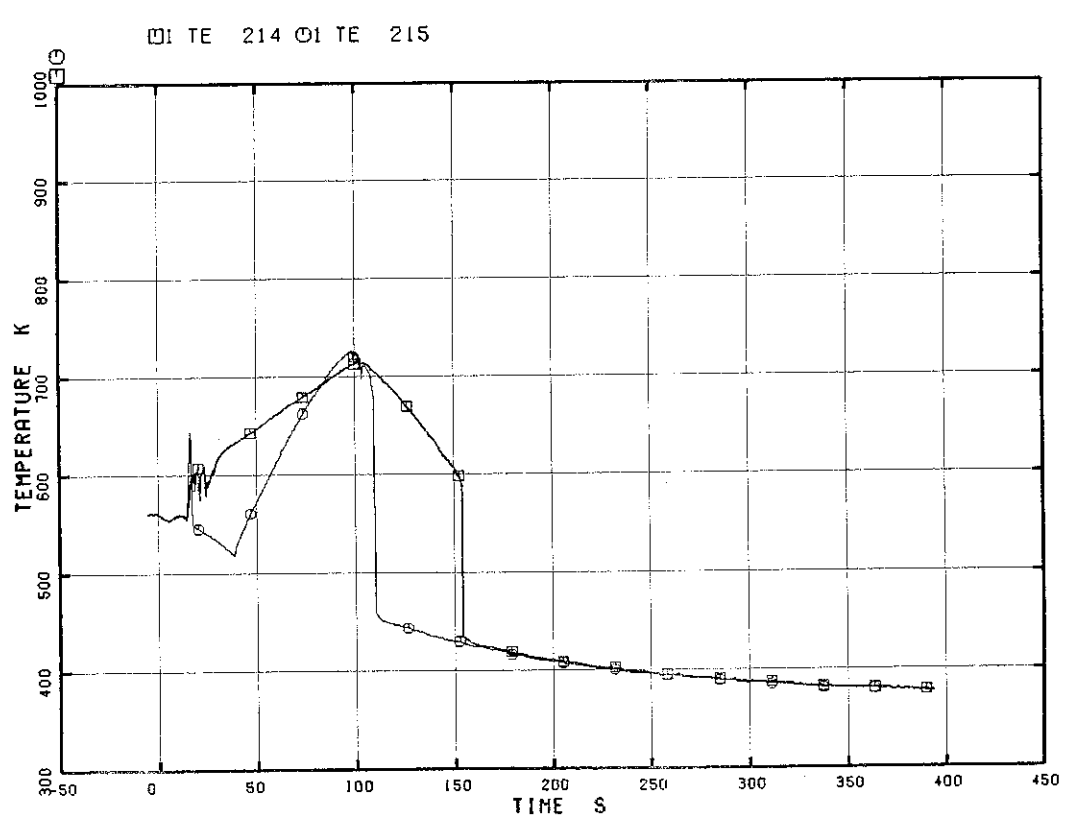

Fig. 5.89 Heater Rod Surface Temperature of A62 Rod

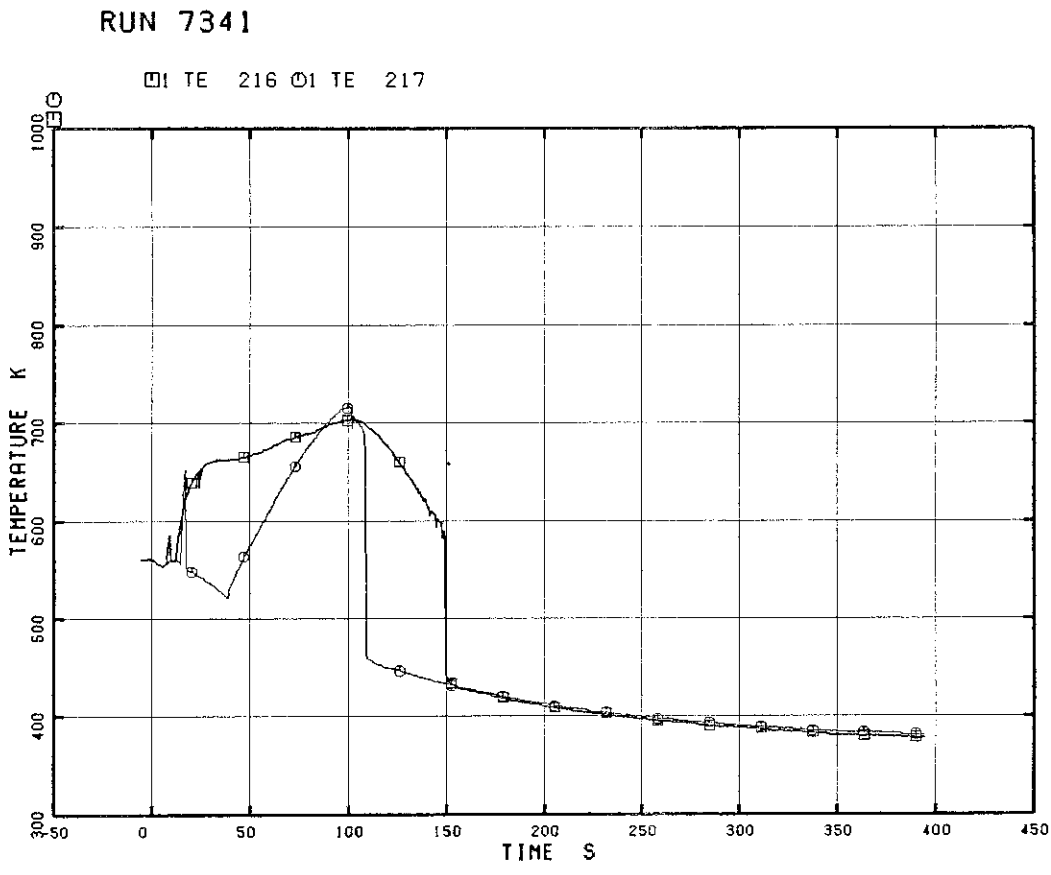

Fig. 5.90 Heater Rod Surface Temperature of A64 Rod

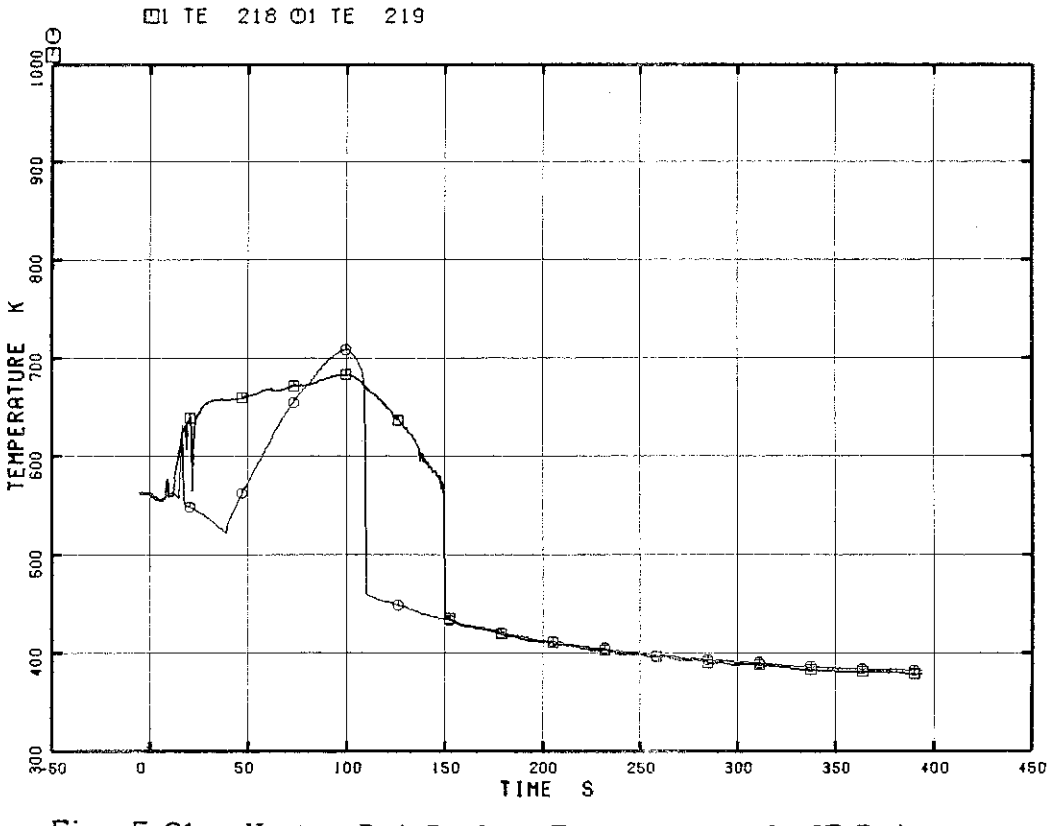

Fig. 5.91 Heater Rod Surface Temperature of A67 Rod

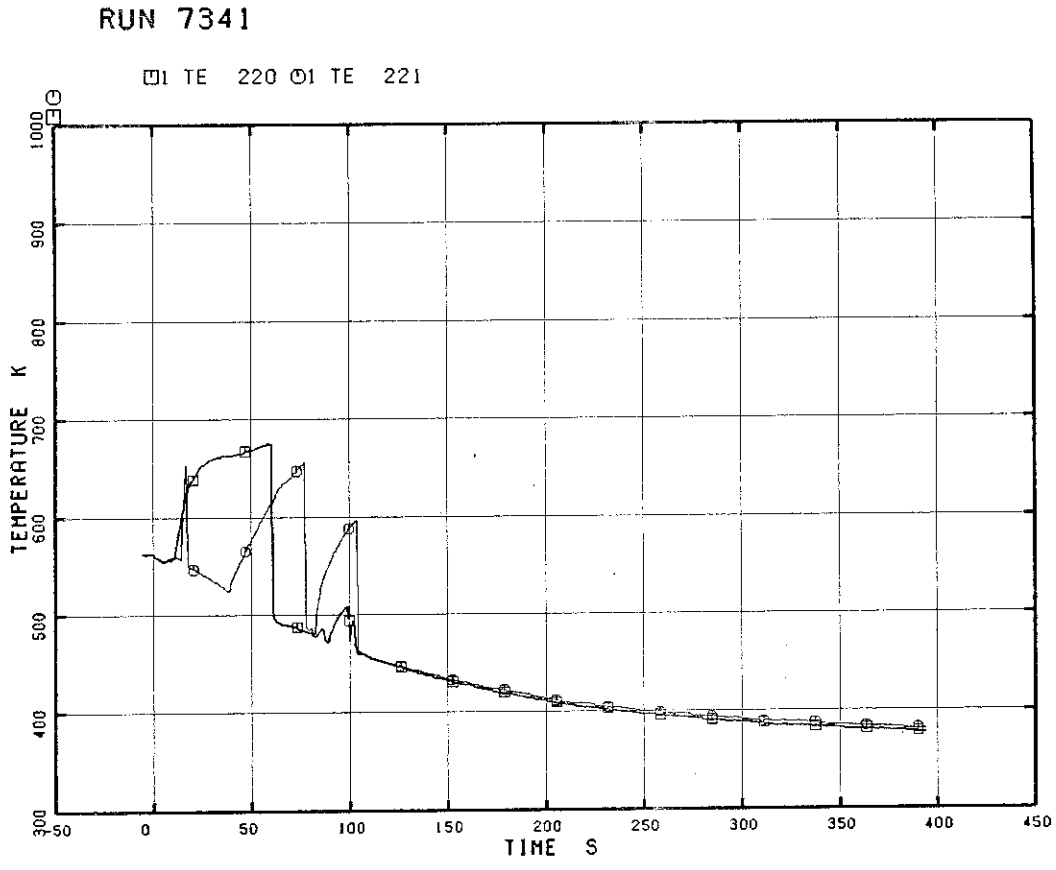

Fig. 5.92 Heater Rod Surface Temperature of A68 Rod

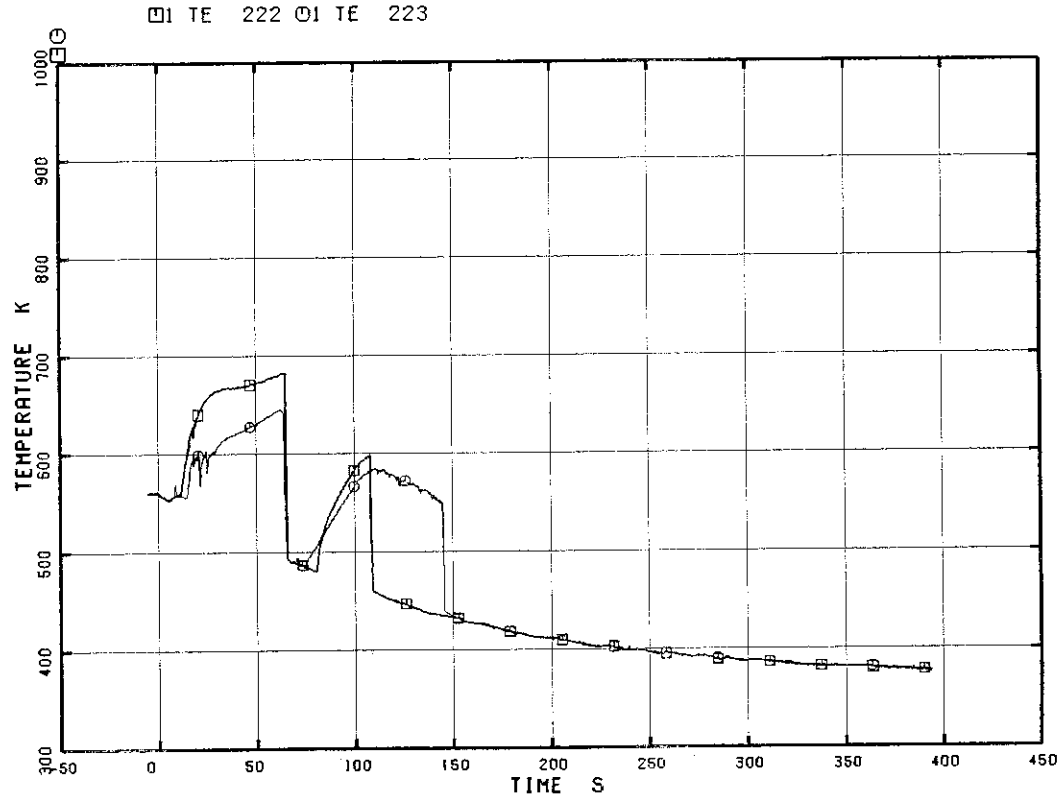

Fig. 5.93 Heater Rod Surface Temperature of A71 Rod

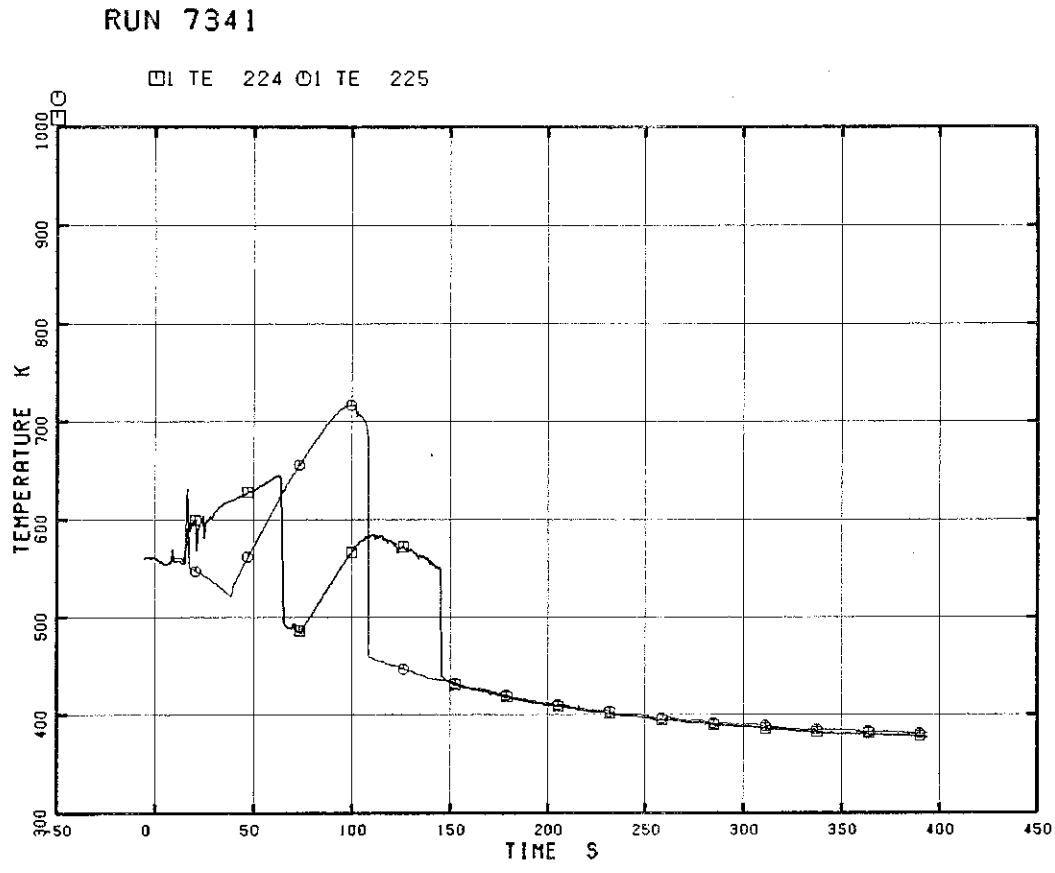

Fig. 5.94 Heater Rod Surface Temperature of A73 Rod

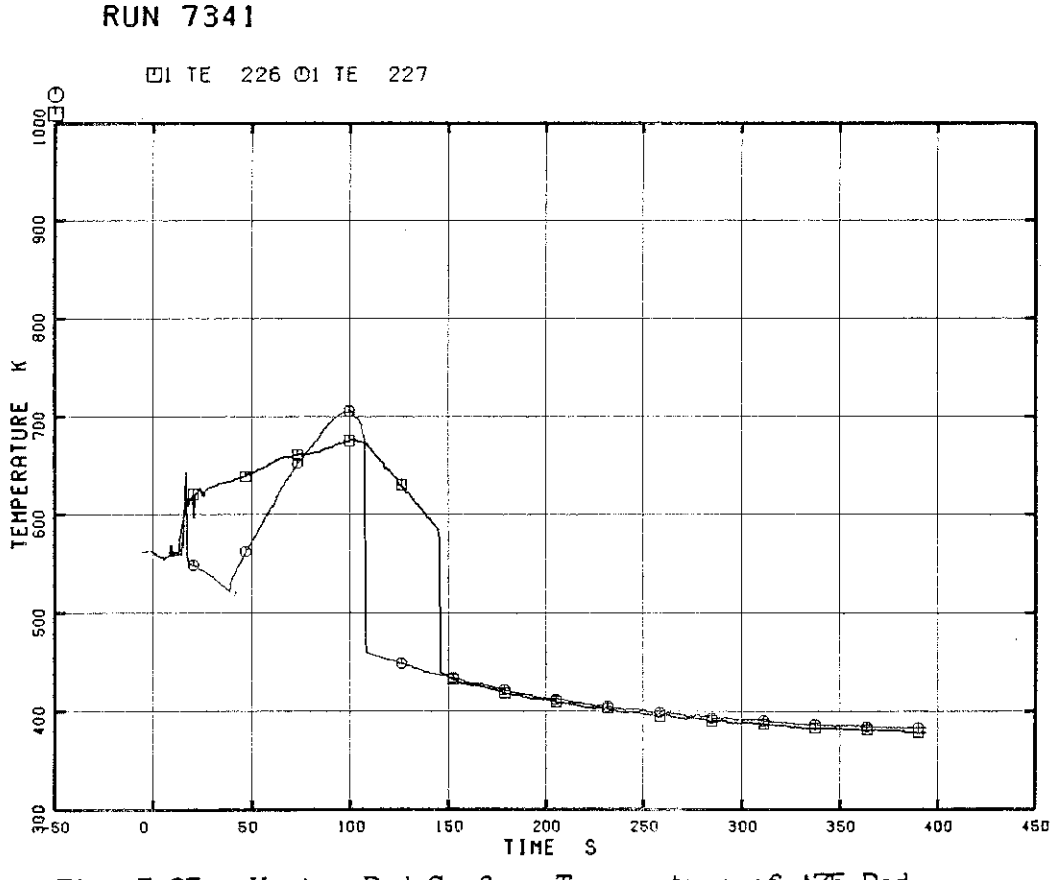

Fig. 5.95 Heater Rod Surface Temperature of A75 Rod

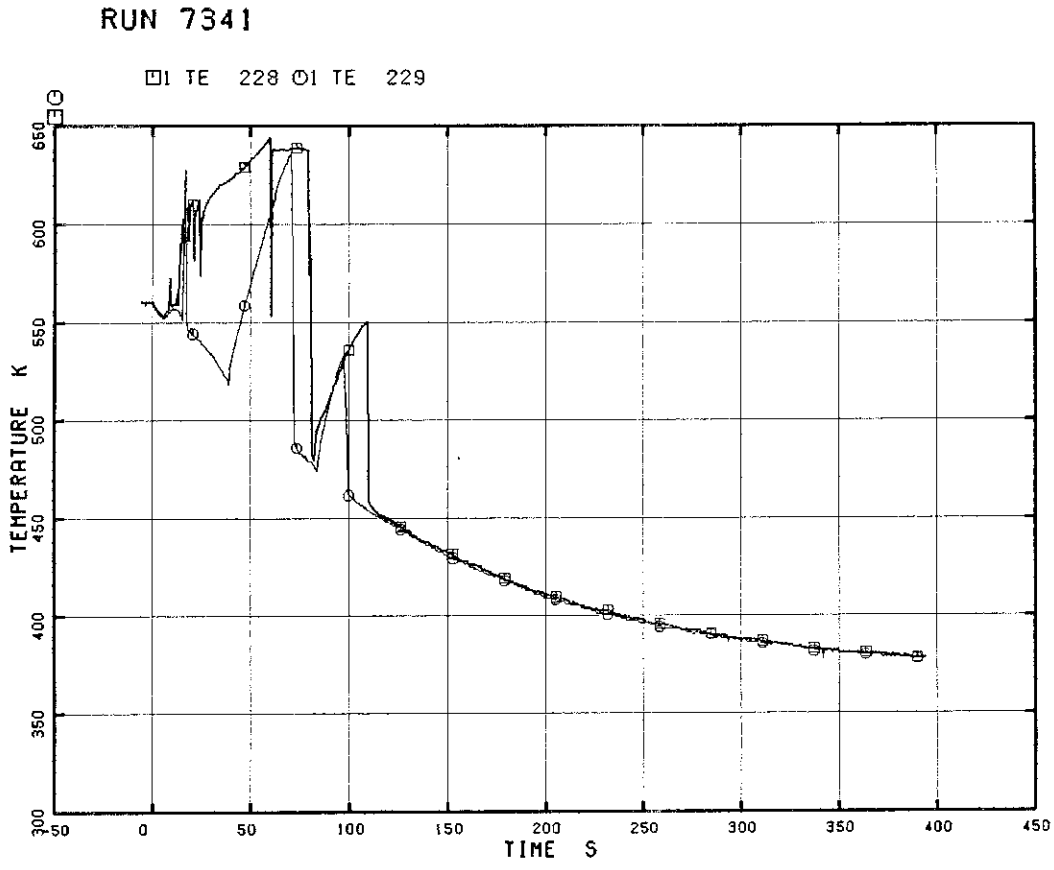

Fig. 5.96 Heater Rod Surface Temperature of A77 Rod

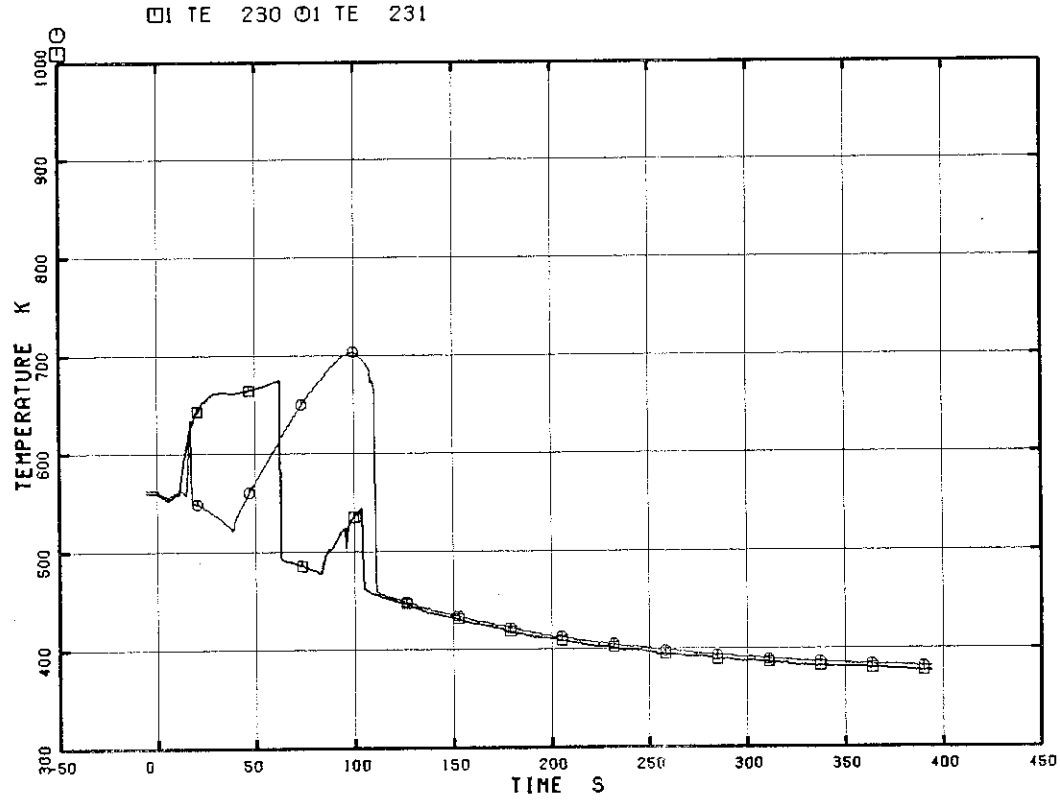

Fig. 5.97 Heater Rod Surface Temperature of A82 Rod

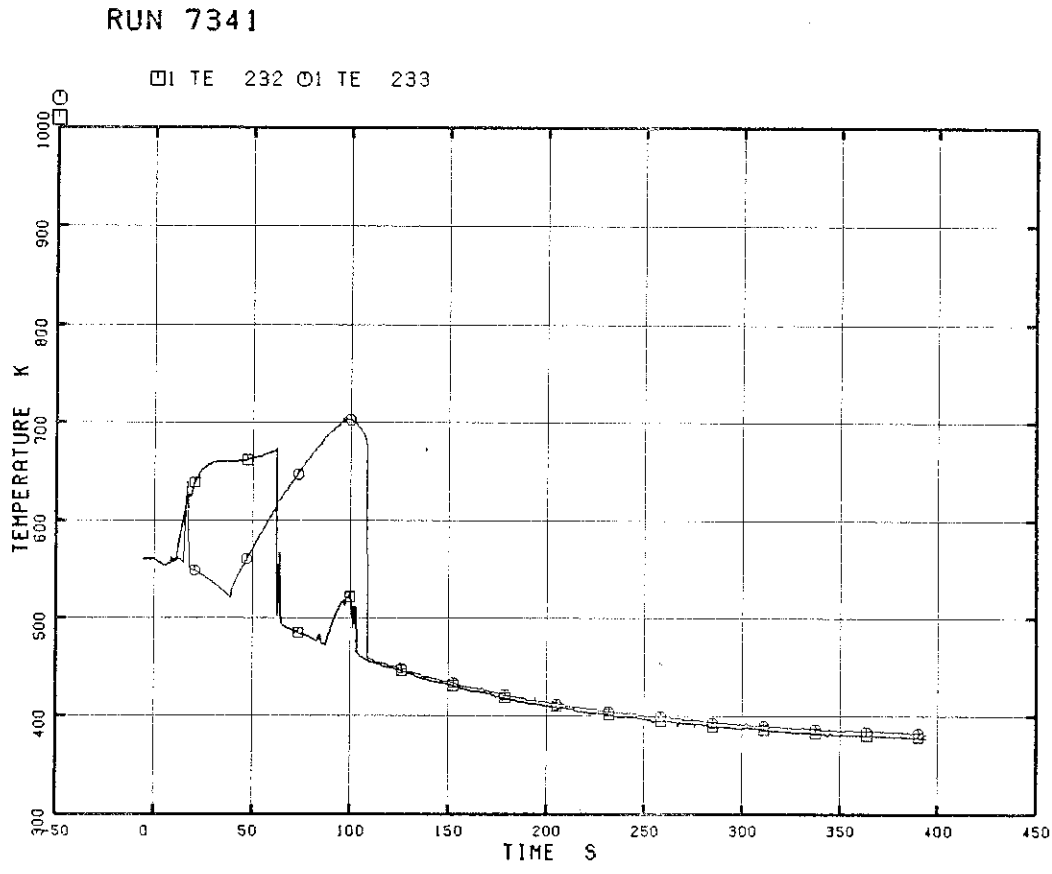

Fig. 5.98 Heater Rod Surface Temperature of A84 Rod

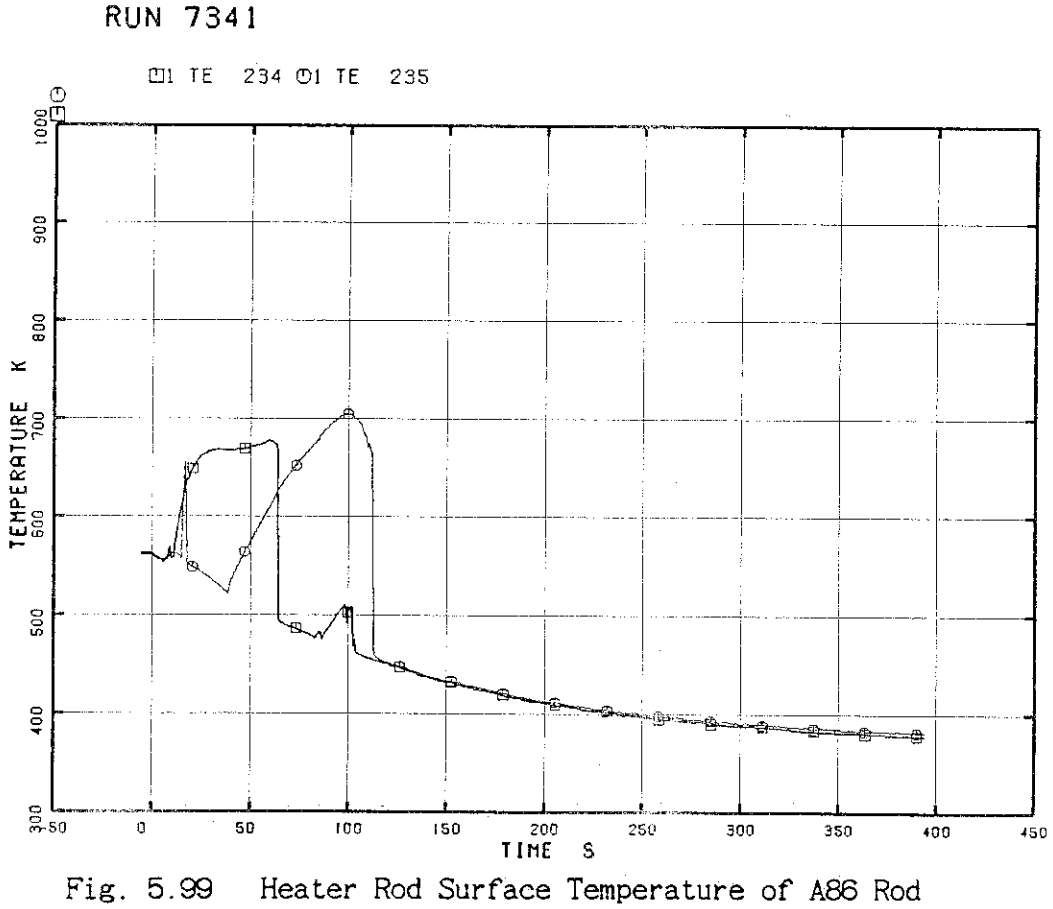

Fig. 5.99 Heater Rod Surface Temperature of A86 Rod

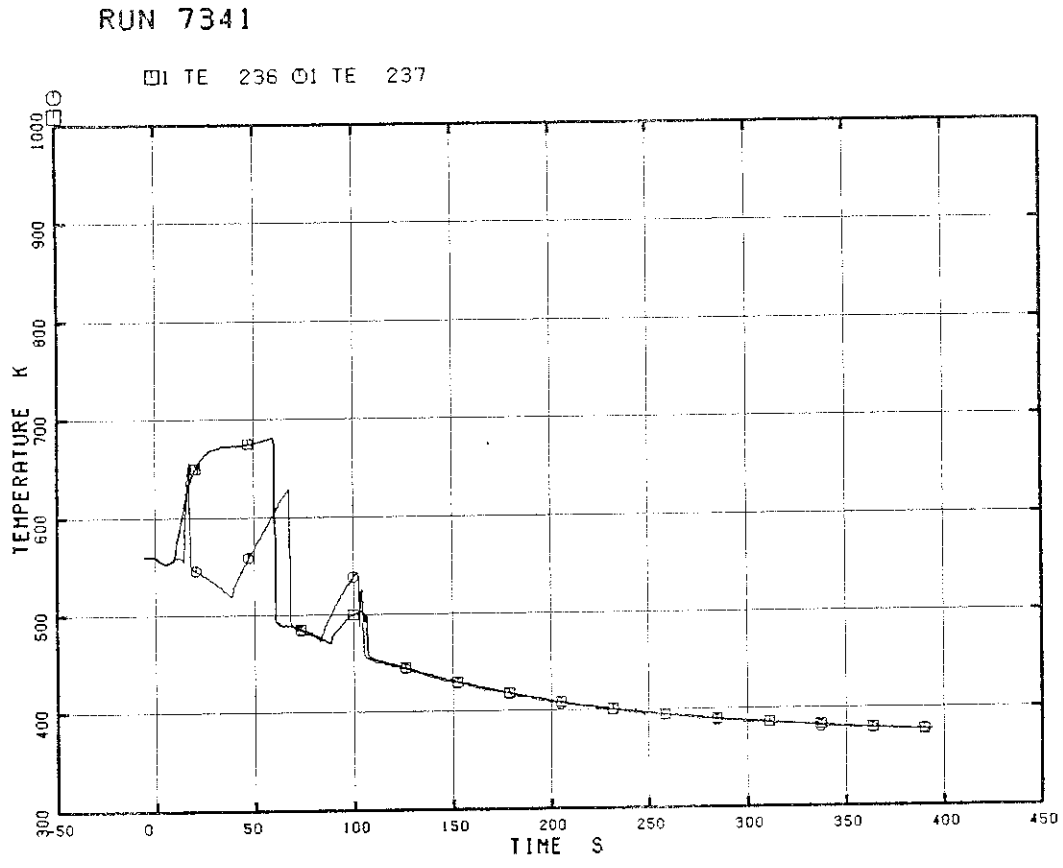

Fig. 5.100 Heater Rod Surface Temperature of A88 Rod

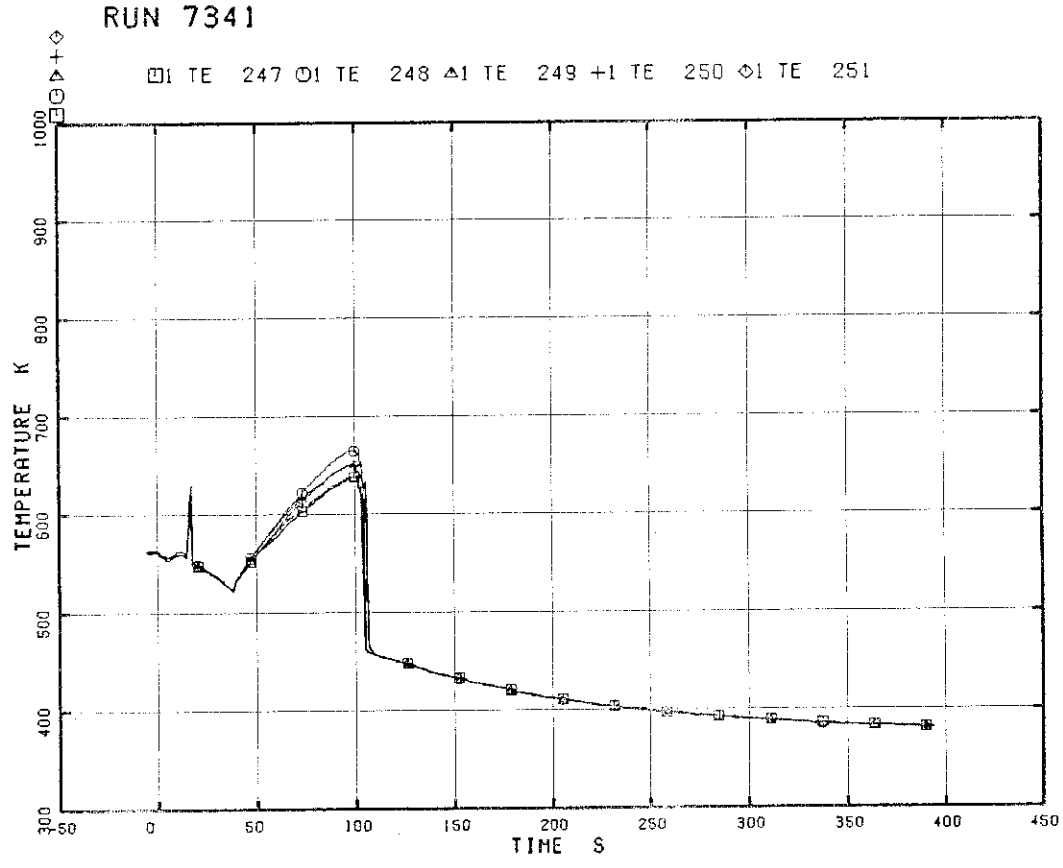

Fig. 5.101 Heater Rod Surface Temperature at Position 4 of Rods B31, B33, B35, B51, B53

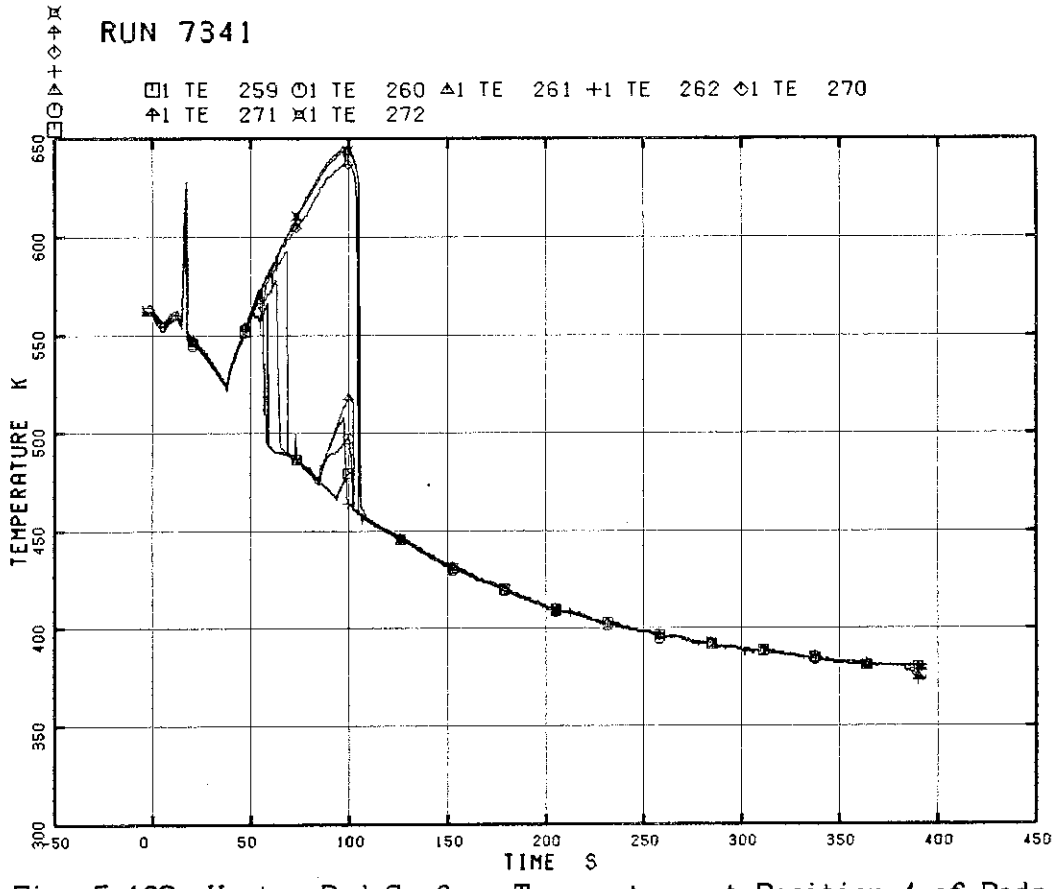

Fig. 5.102 Heater Rod Surface Temperature at Position 4 of Rods C11,C13,C15,C31,C35,C51,C53

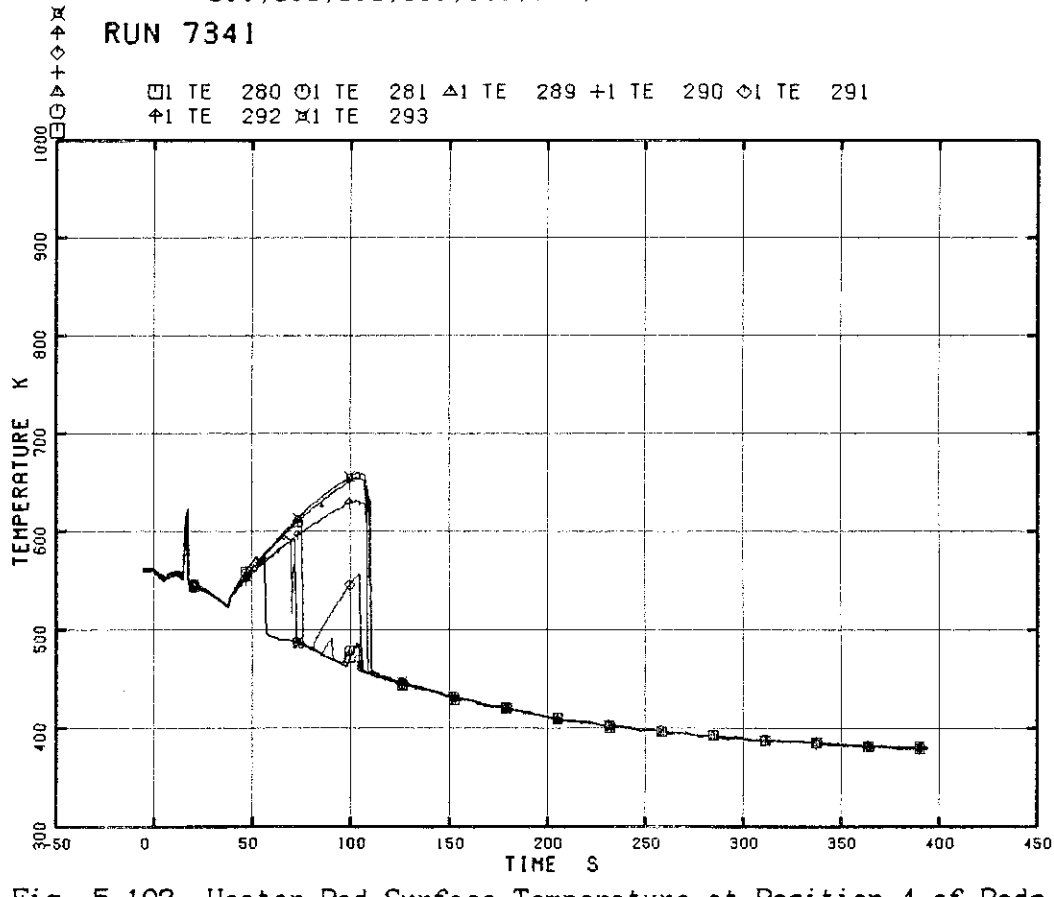

Fig. 5.103 Heater Rod Surface Temperature at Position 4 of Rods D11,D13,D31,D33,D35,D51,D53

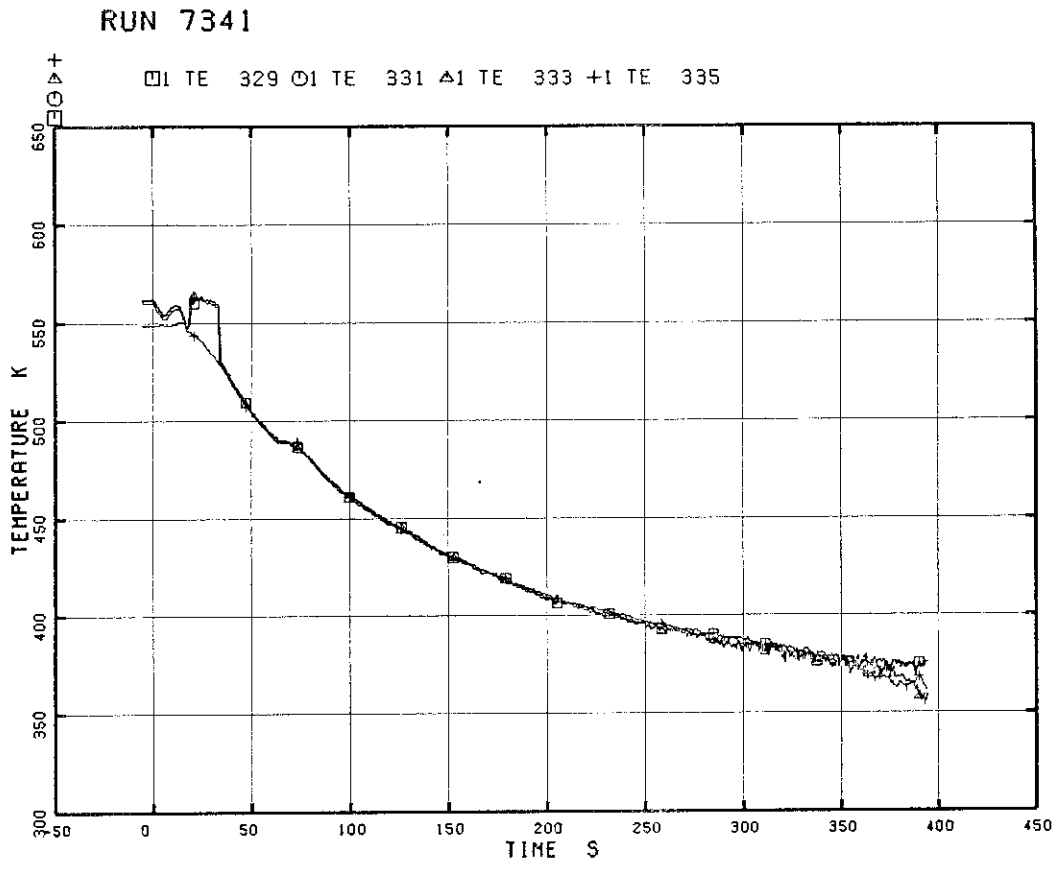

Fig. 5.104 Fluid Temperature at Channel Box Outlet

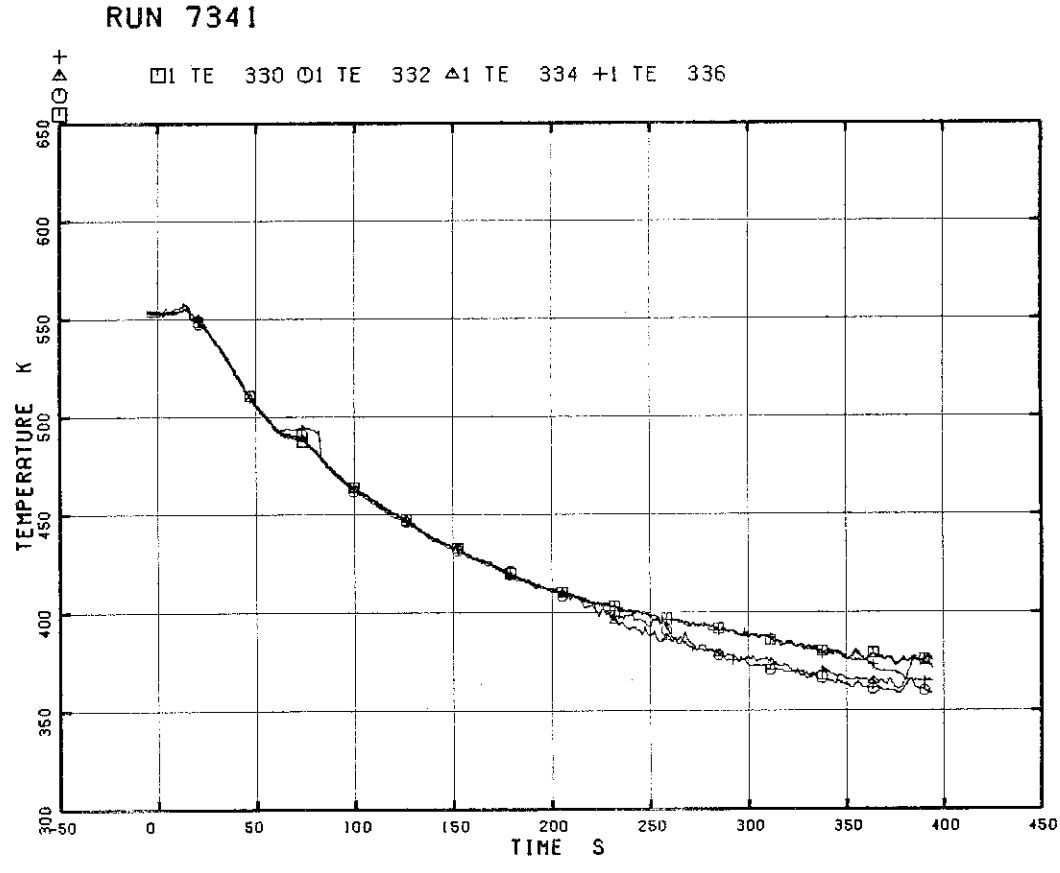

Fig. 5.105 Fluid Temperature at Channel Box Inlet

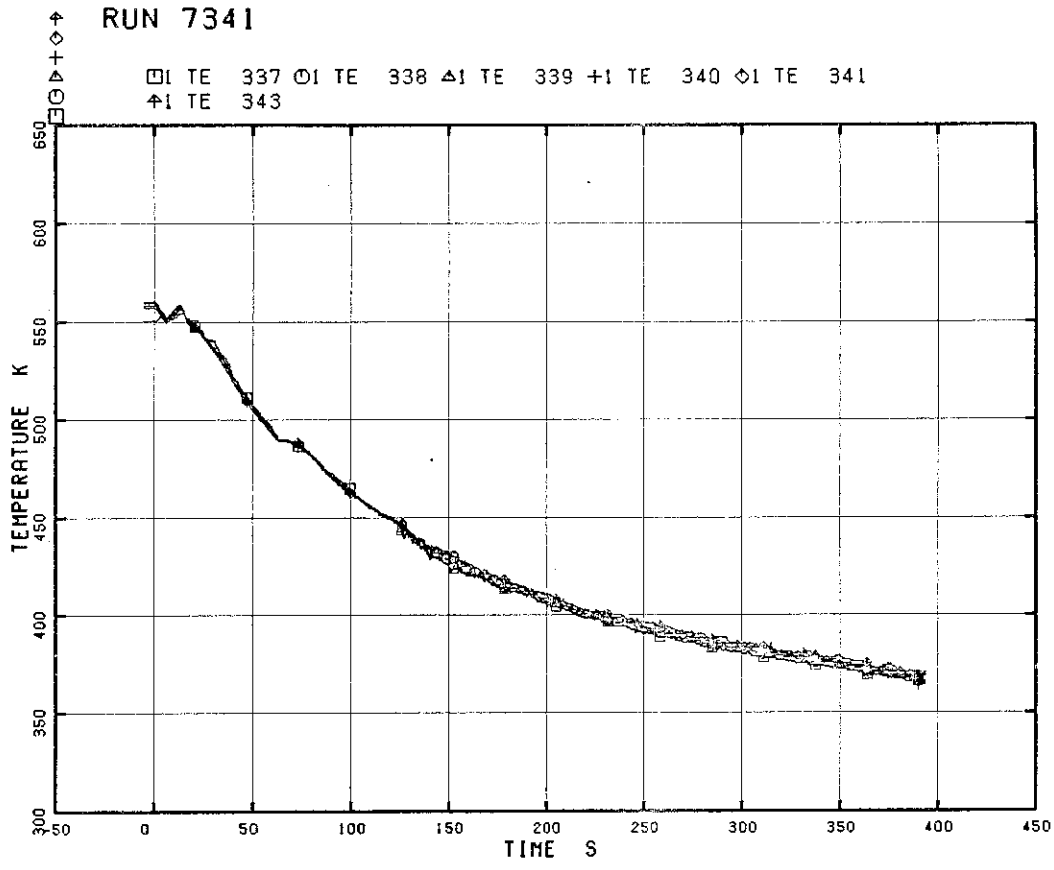

Fig. 5.106 Inner Surface Temperature of Channel Box A, A1 Location

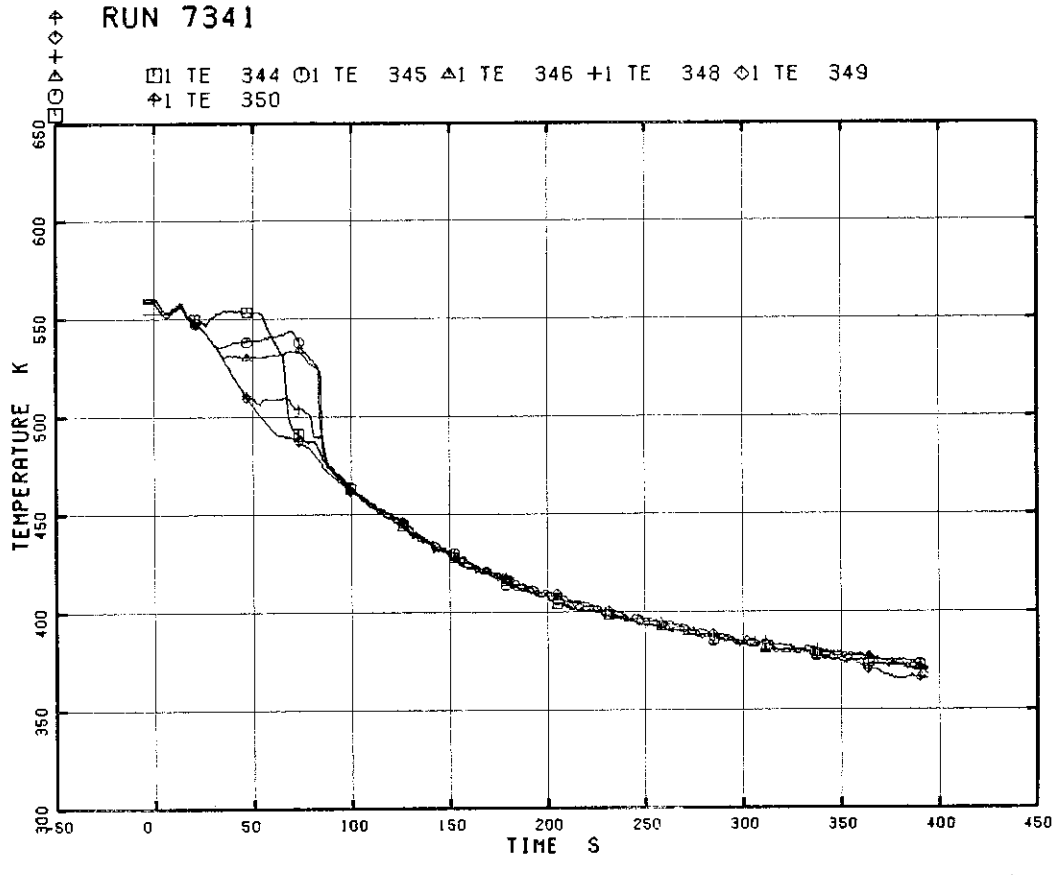

Fig. 5.107 Inner Surface Temperature of Channel Box A, A2 Location

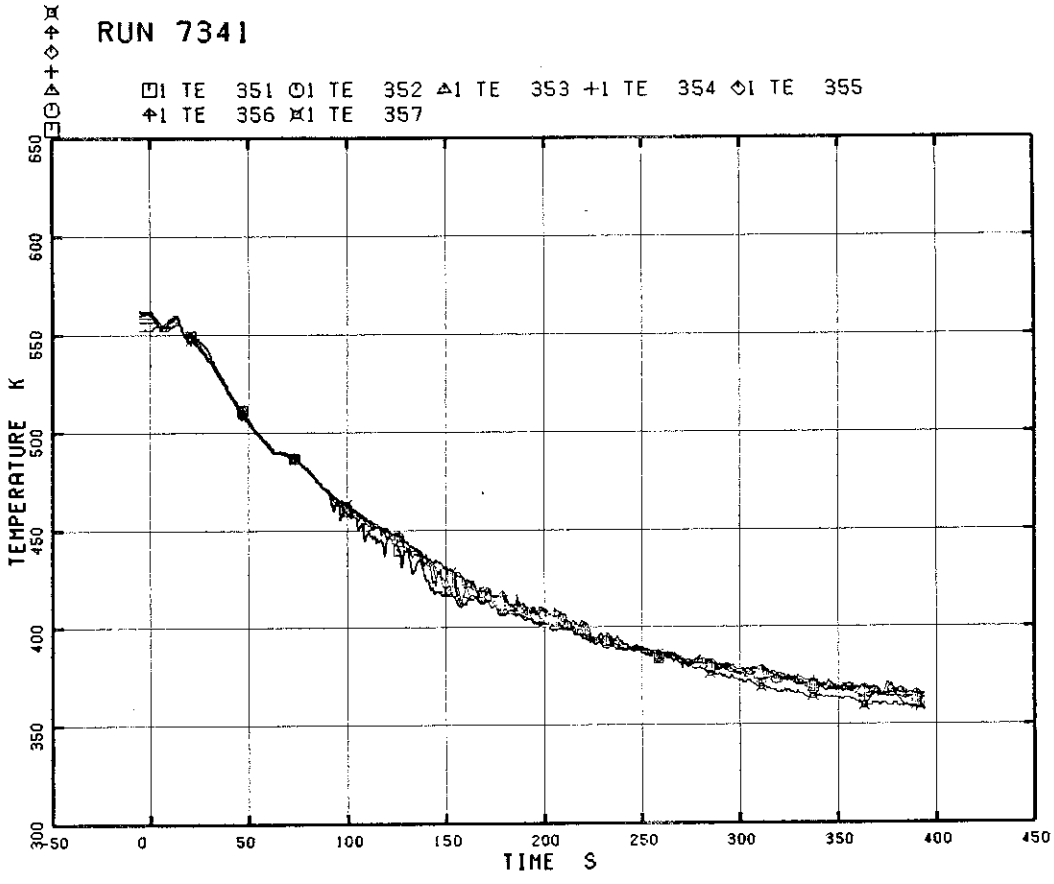

Fig. 5.108 Inner Surface Temperature of Channel Box B

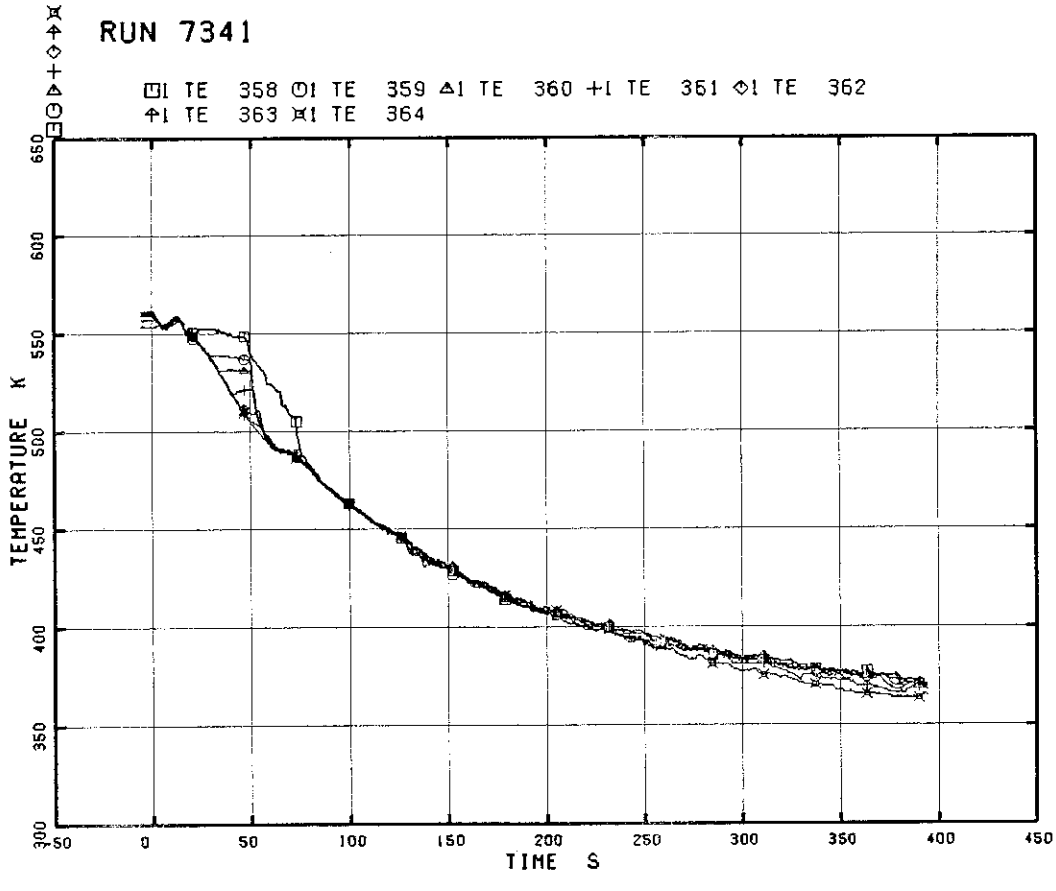

Fig. 5.109 Inner Surface Temperature of Channel Box C

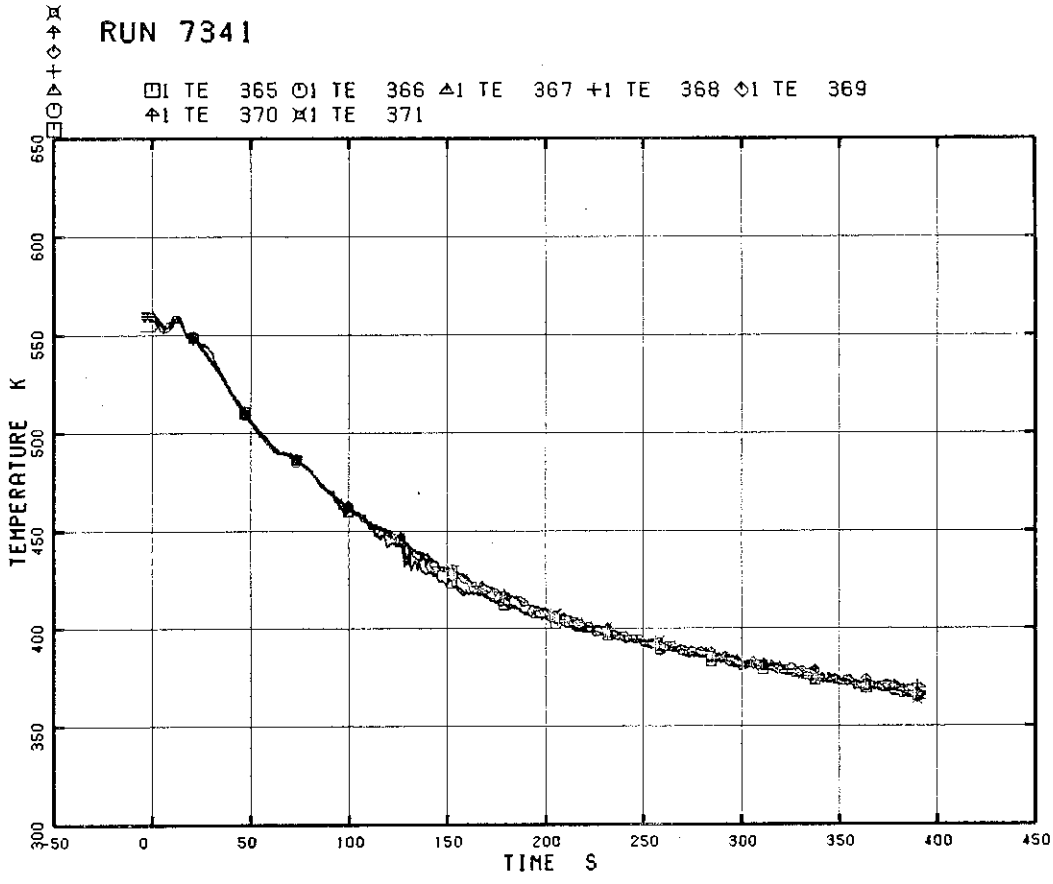

Fig. 5.110 Inner Surface Temperature of Channel Box D

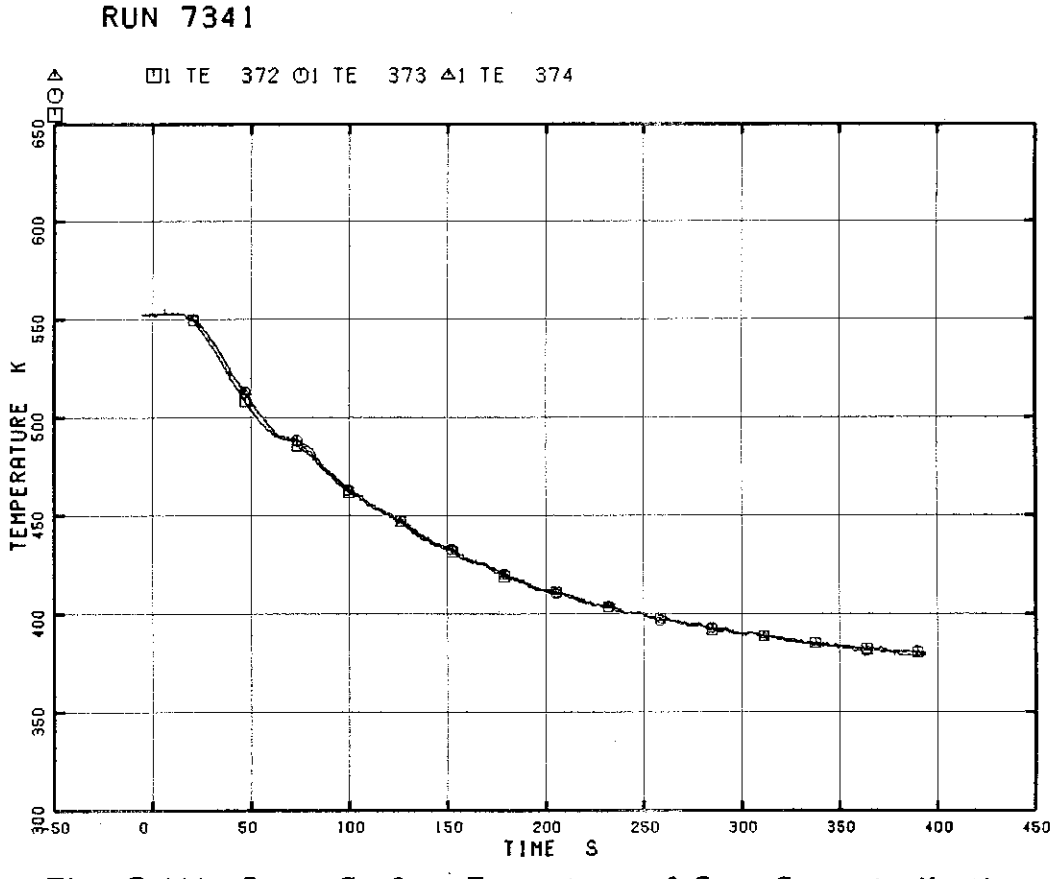

Fig. 5.111 Inner Surface Temprature of Core Support, North

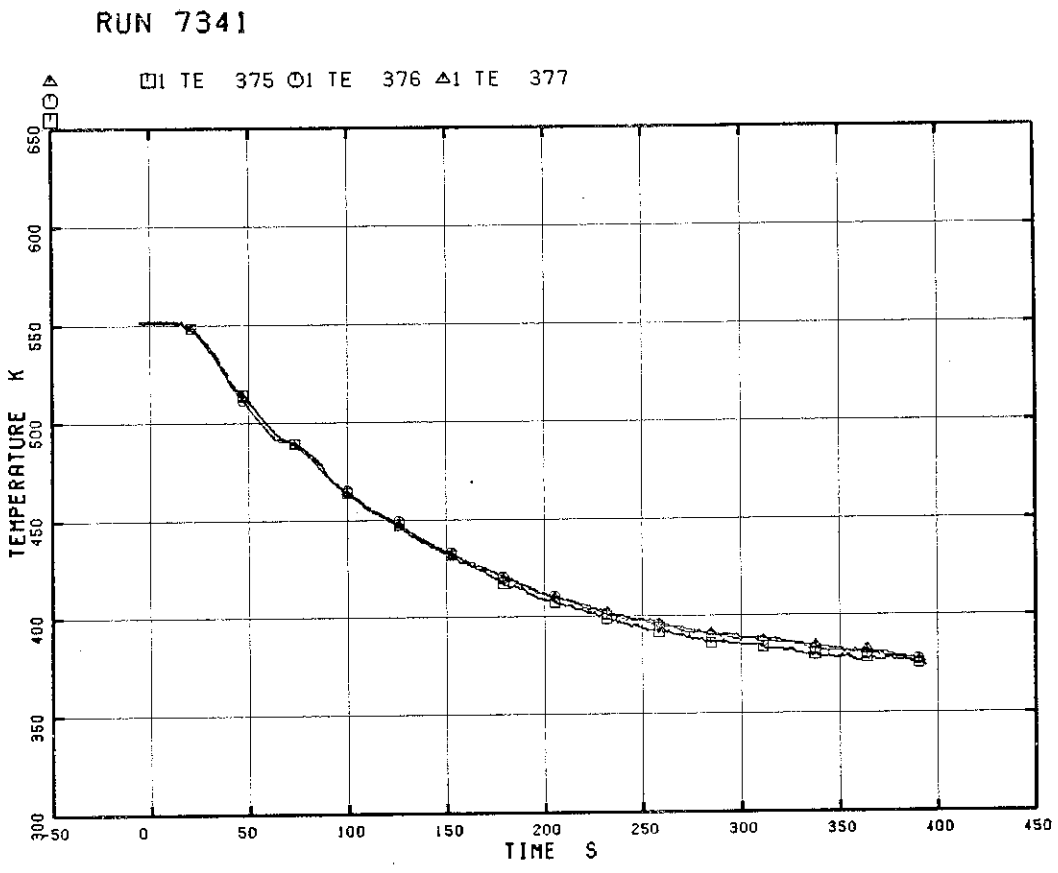

Fig. 5.112 Inner Surface Temprature of Core Support, South

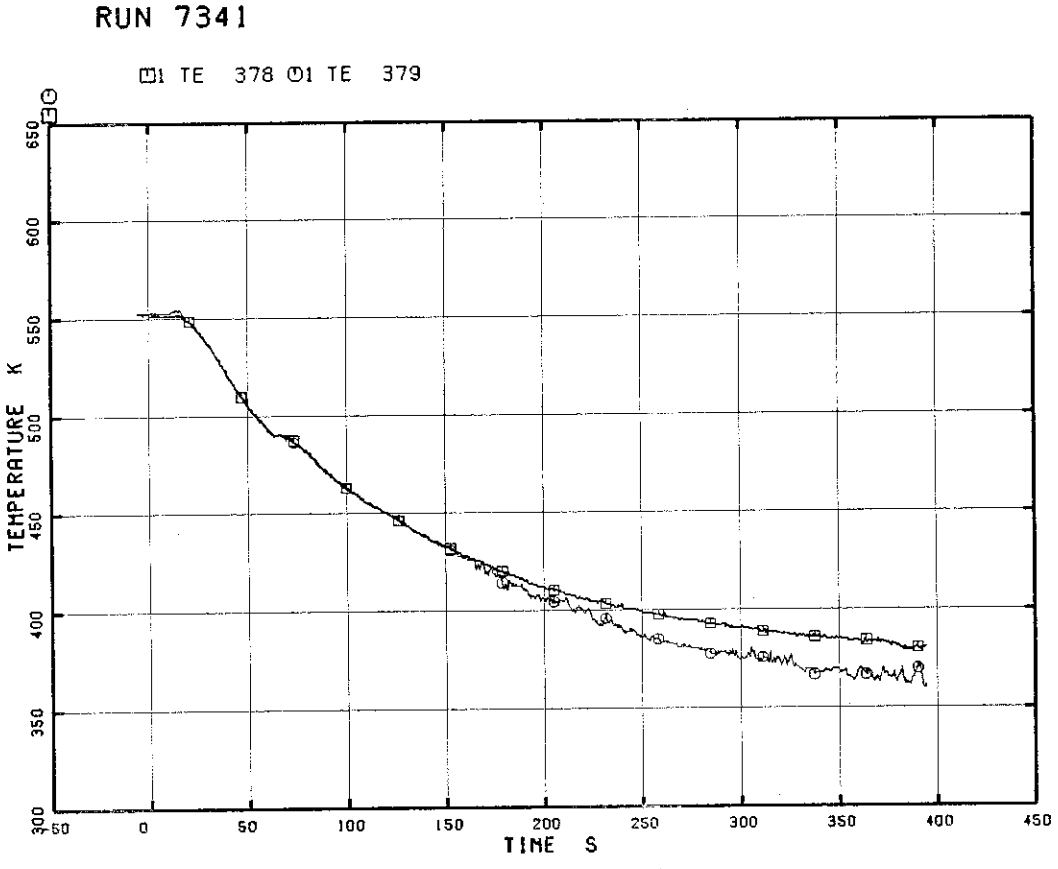

Fig. 5.113 Fluid Temperature in Lower Plenum

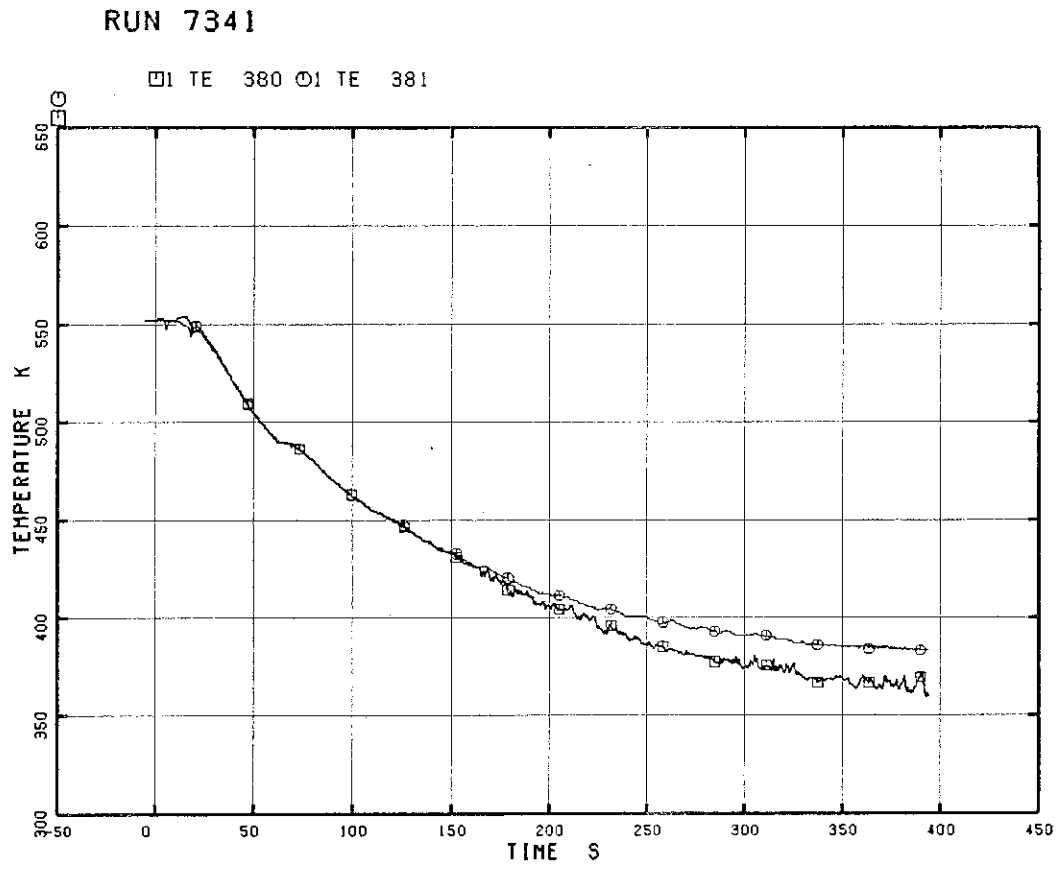

Fig. 5.114 Fluid Temperature in Guide Tube

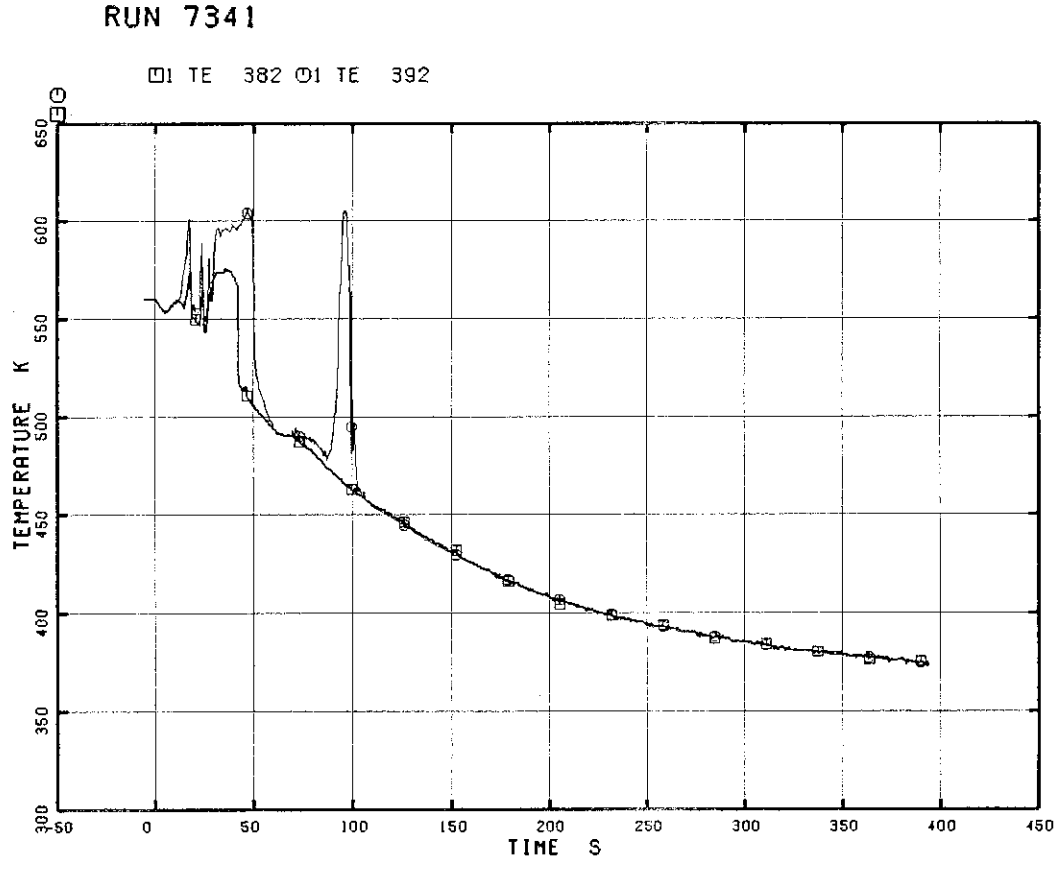

Fig. 5.115 Fluid Temperature in the Upper Tieplate A, Opening 1

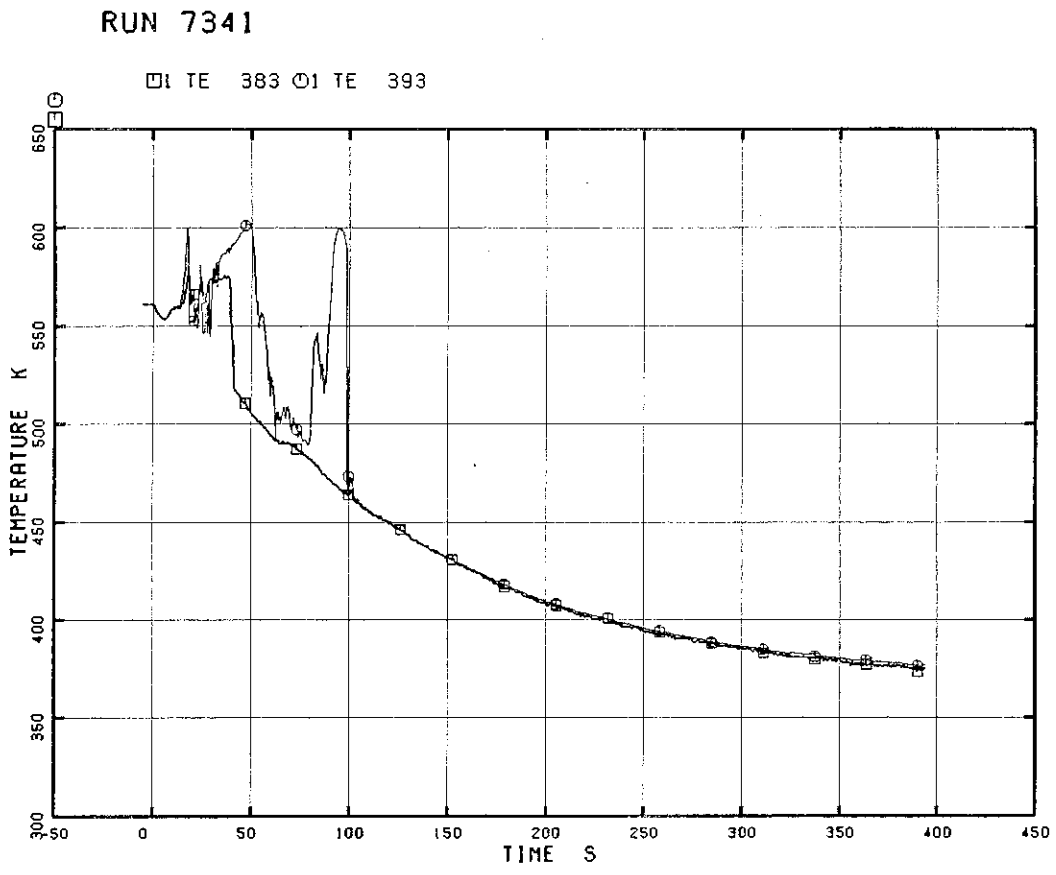

Fig. 5.116 Fluid Temperature in the Upper Tieplate A, Opening 2

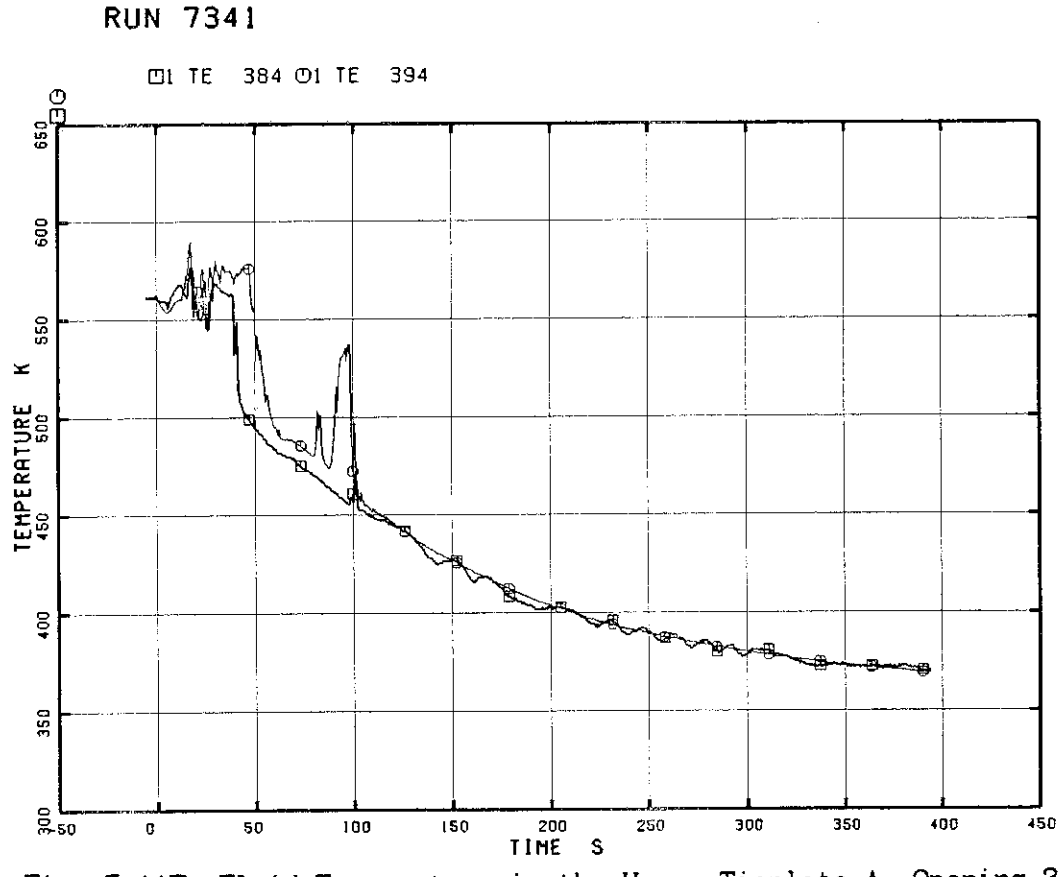

Fig. 5.117 Fluid Temperature in the Upper Tieplate A, Opening 3

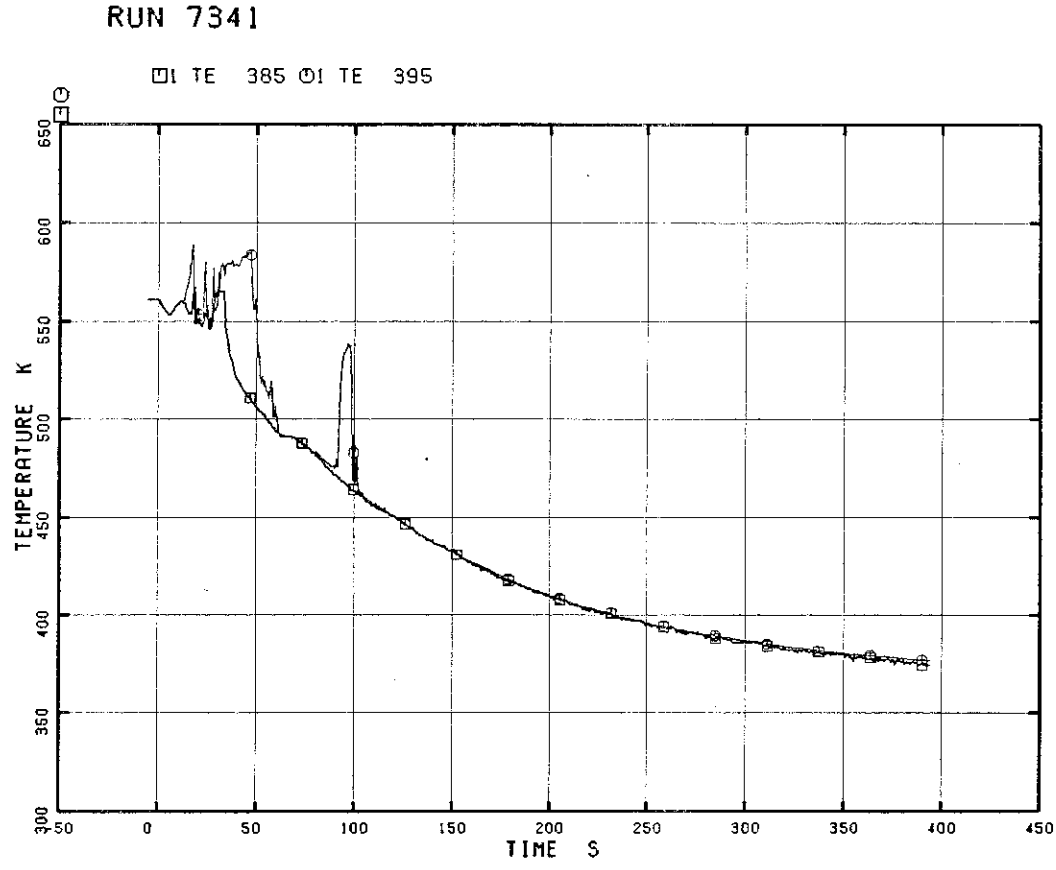

Fig. 5.118 Fluid Temperature in the Upper Tieplate A, Opening 4

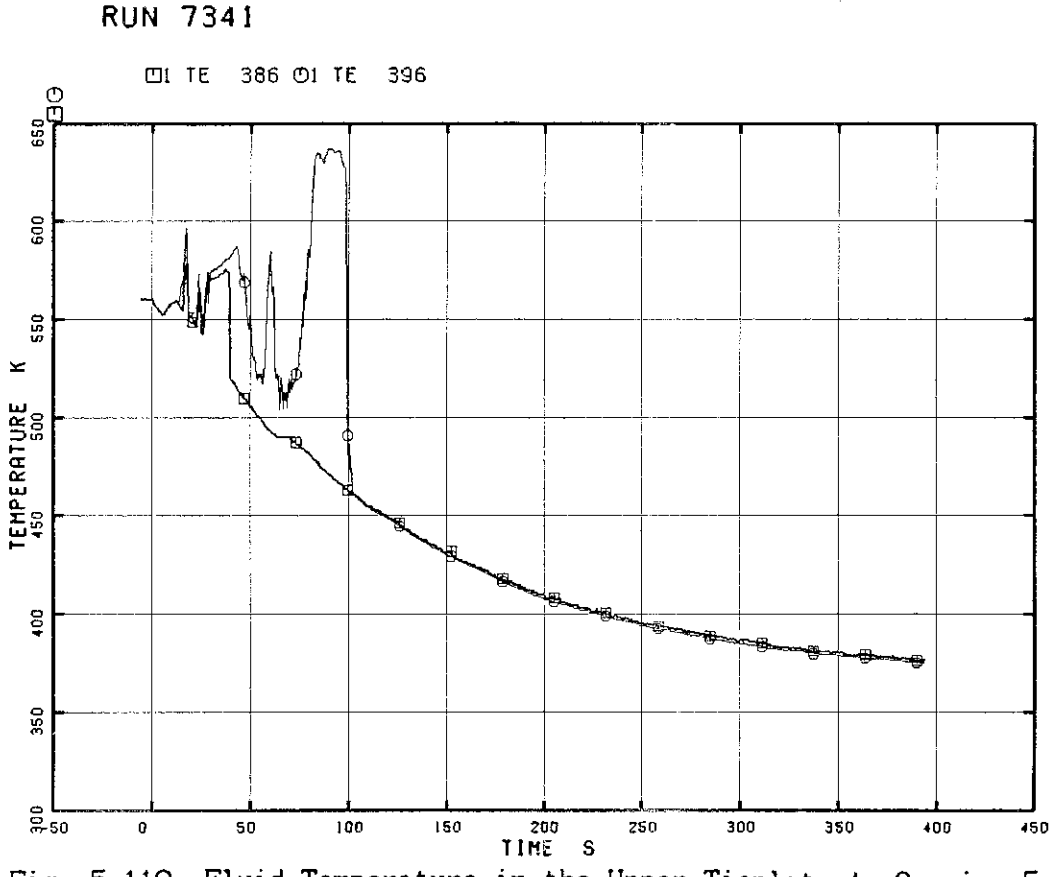

Fig. 5.119 Fluid Temperature in the Upper Tieplate A, Opening 5

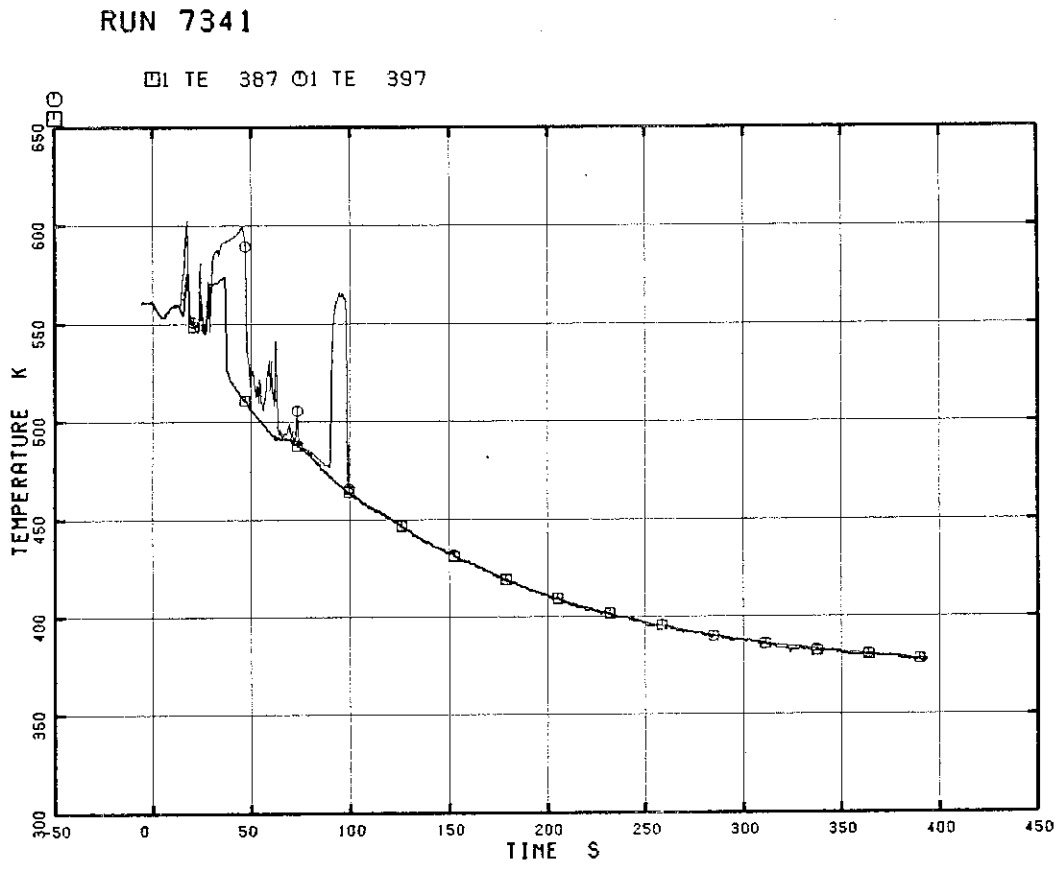

Fig. 5.120 Fluid Temperature in the Upper Tieplate A, Opening 6

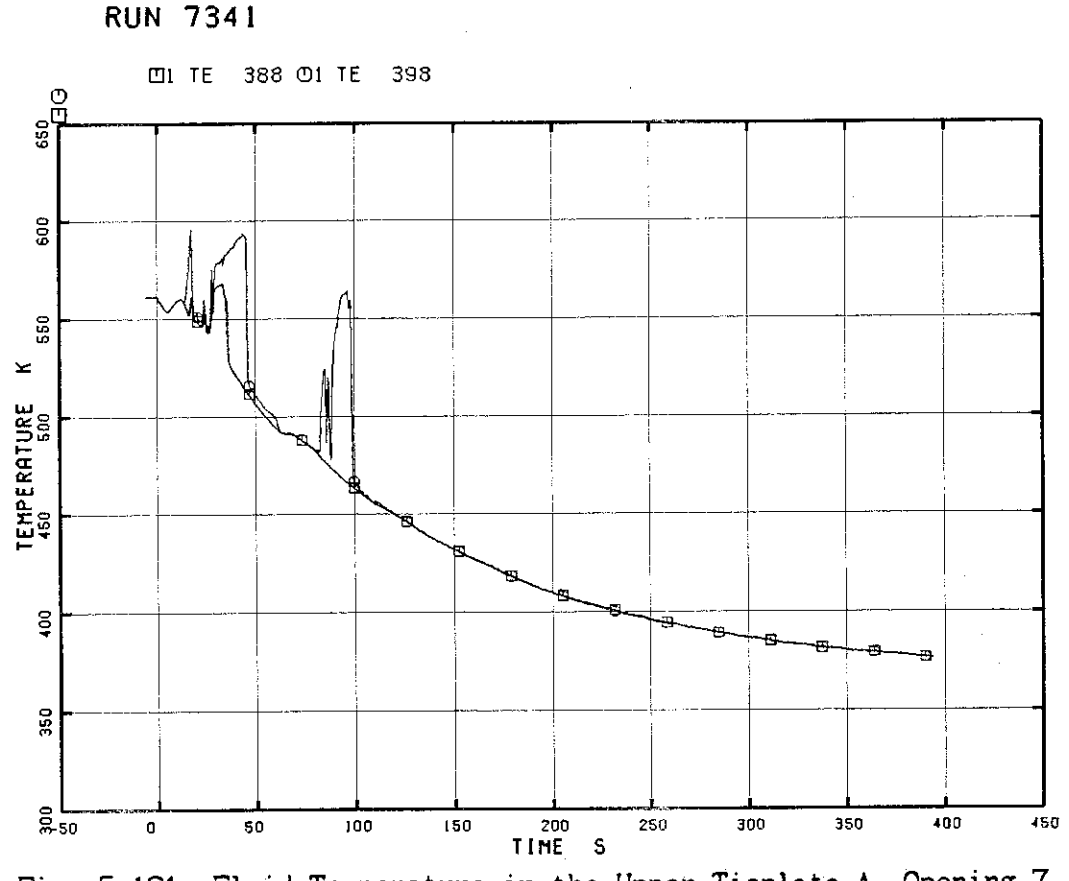

Fig. 5.121 Fluid Temperature in the Upper Tieplate A, Opening 7

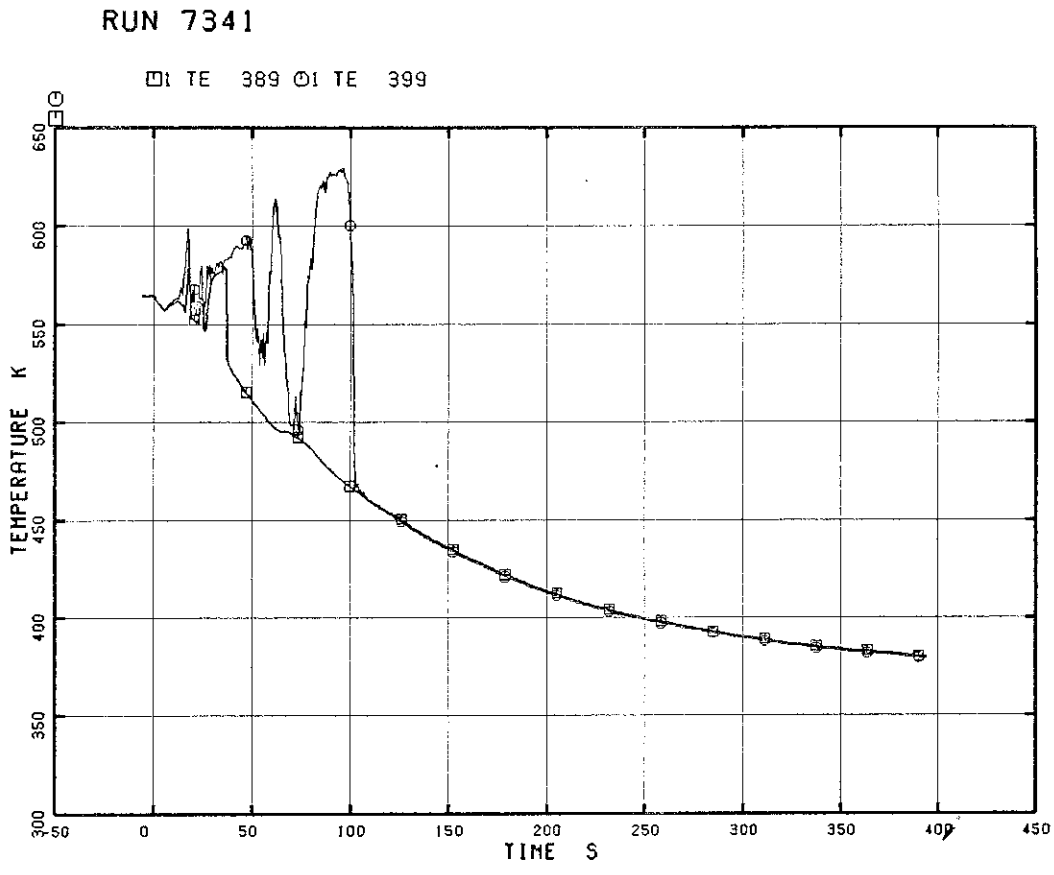

Fig. 5.122 Fluid Temperature in the Upper Tieplate A, Opening 8

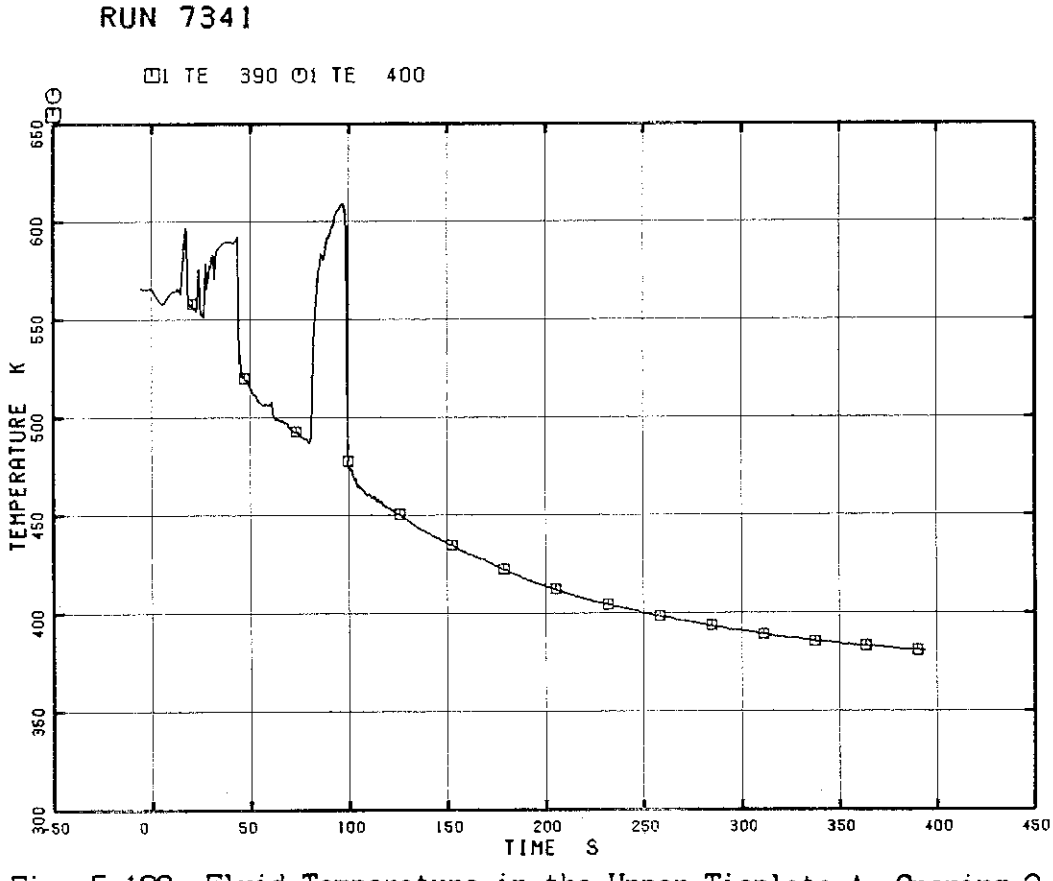

Fig. 5.123 Fluid Temperature in the Upper Tieplate A, Opening 9

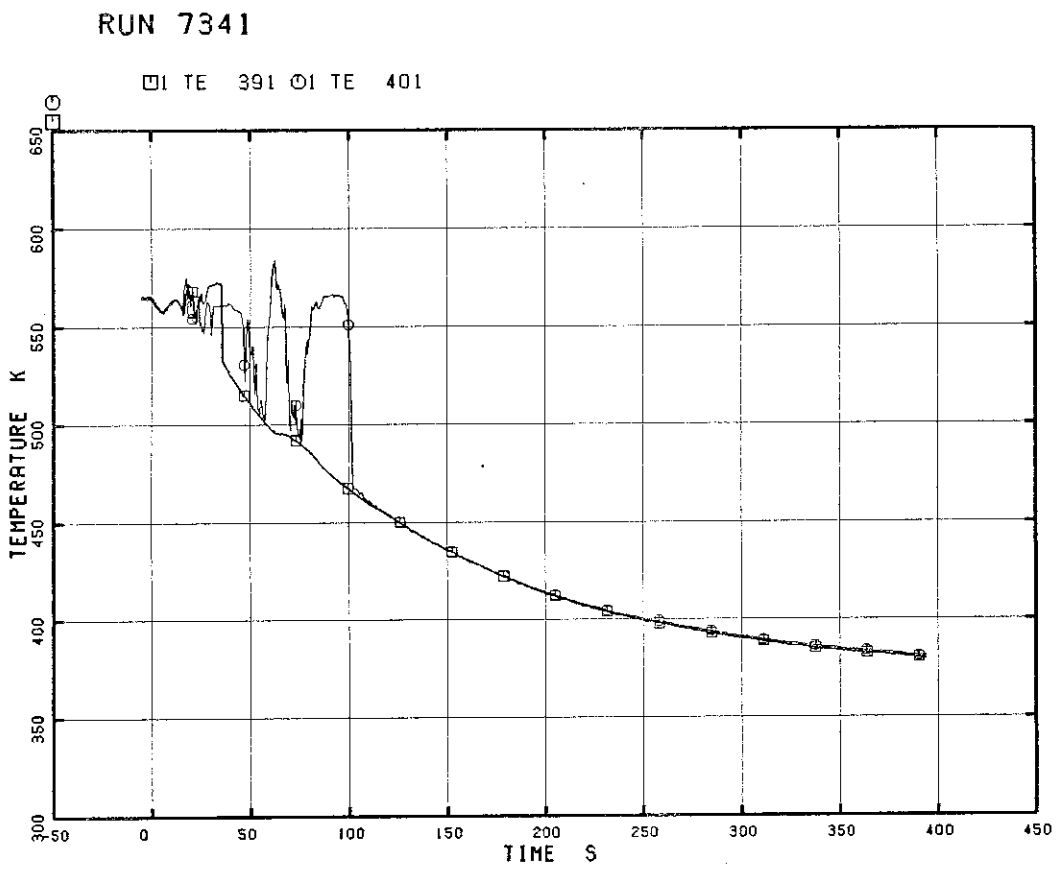

Fig. 5.124 Fluid Temperature in the Upper Tieplate A, Opening 10

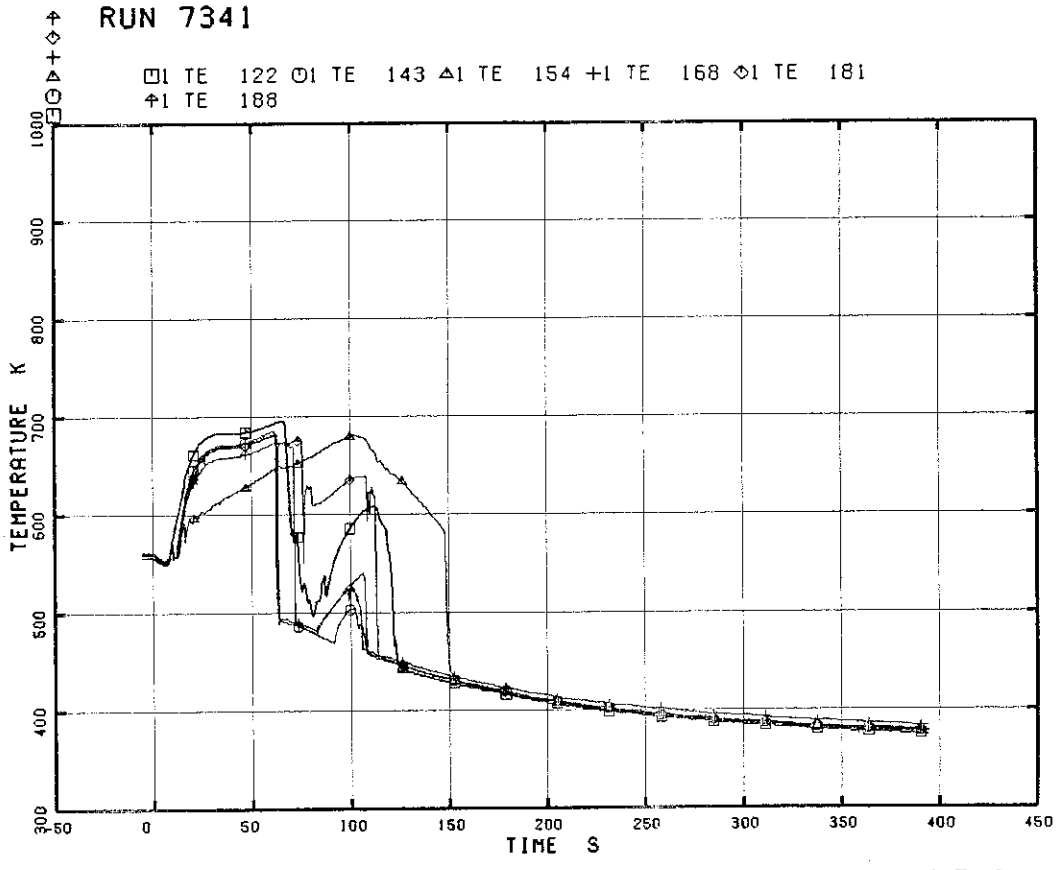

Fig. 5.125 Heater Rod Surface Temprature at Position 1 of Rods A22, A24, A33, A34

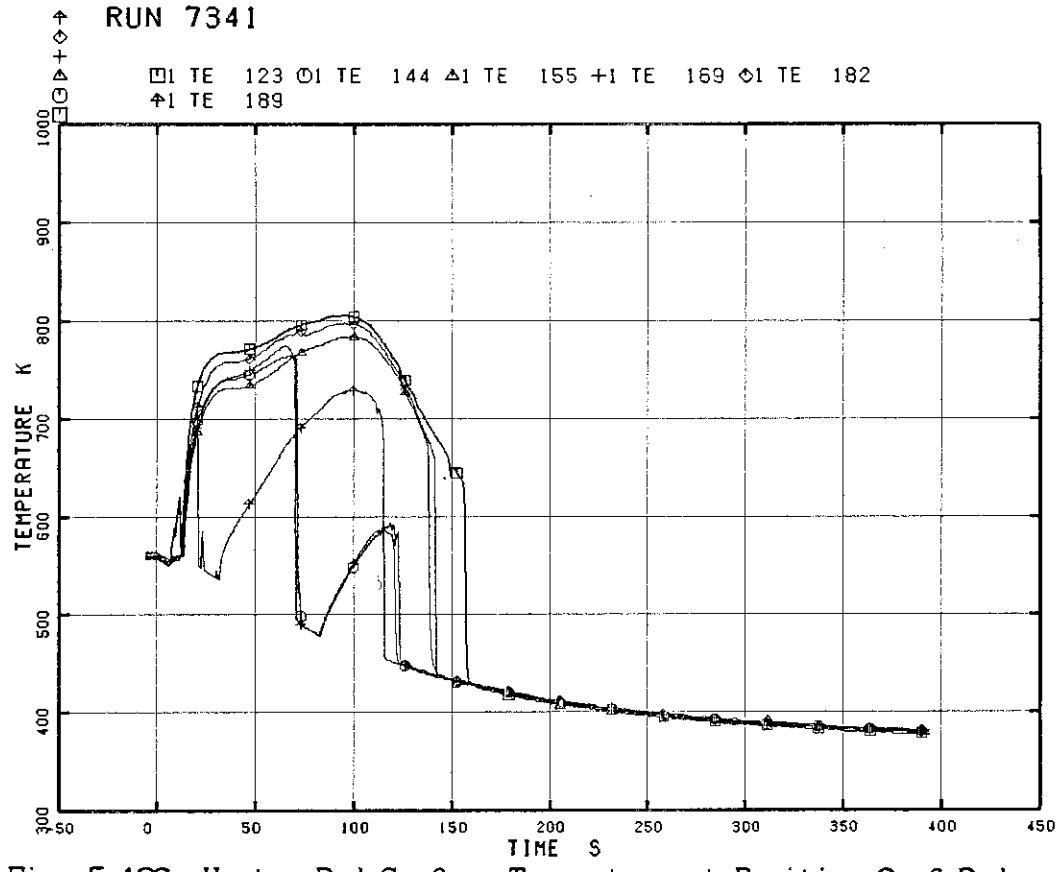

Fig. 5.126 Heater Rod Surface Temprature at Position 2 of Rods A22, A24, A33, A34

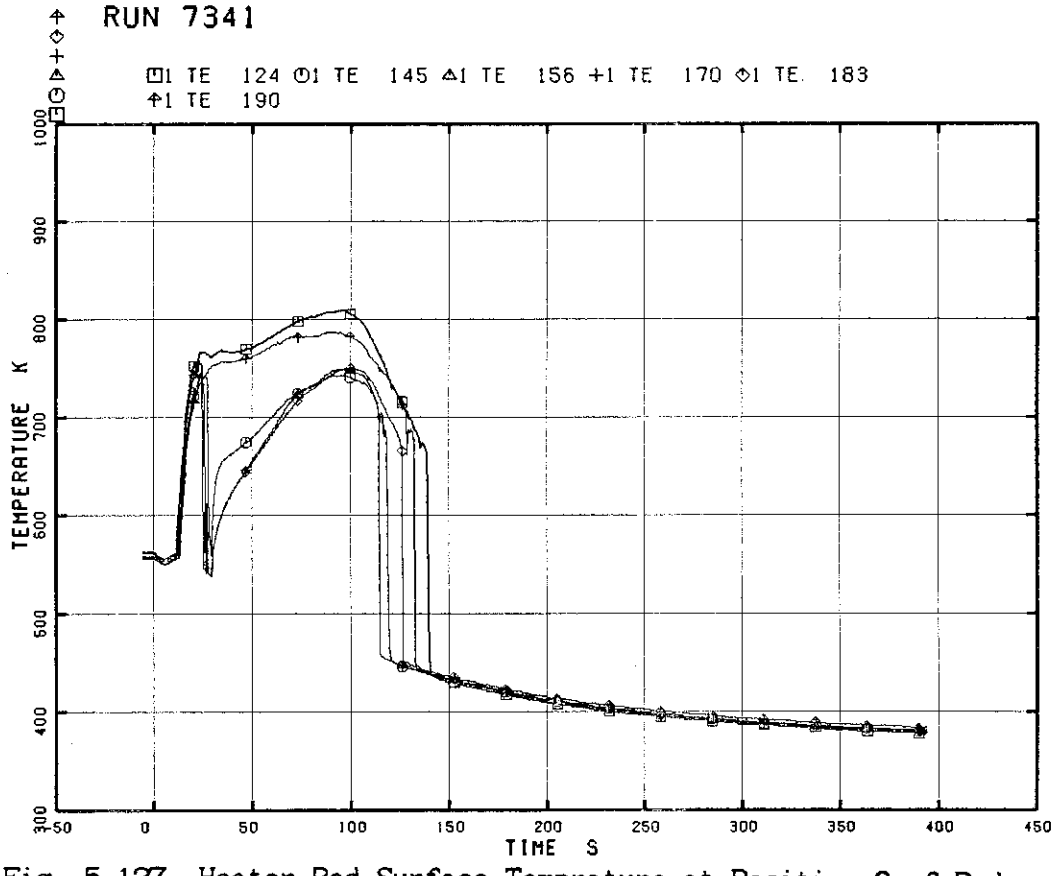

Fig. 5.127 Heater Rod Surface Temprature at Position 3 of Rods A22, A24, A33, A34

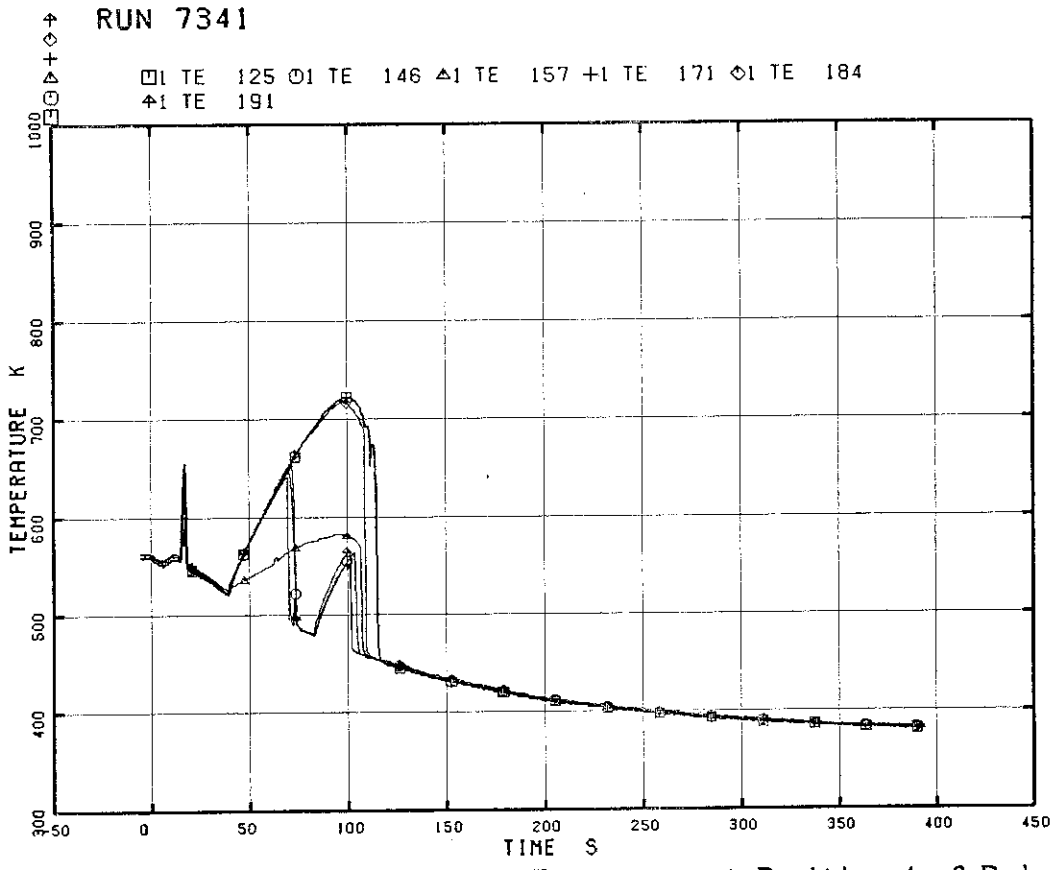

Fig. 5.128 Heater Rod Surface Temprature at Position 4 of Rods A22, A24, A33, A34

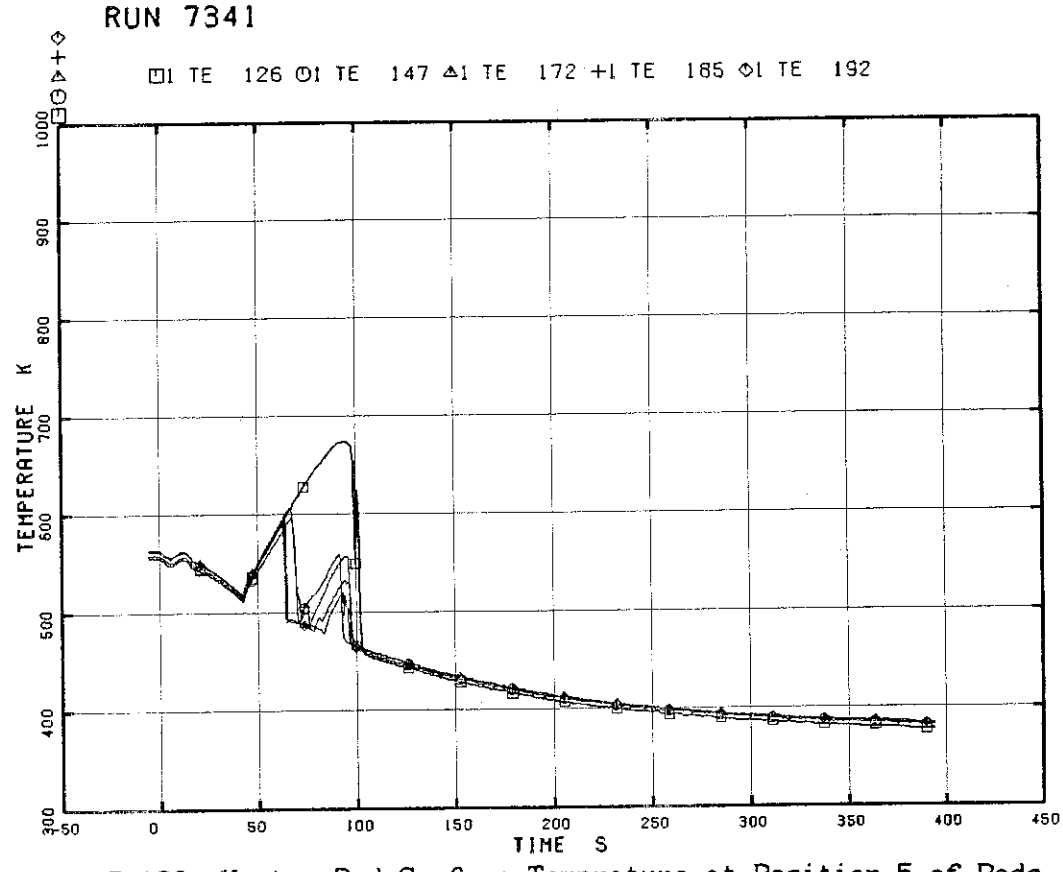

Fig. 5.129 Heater Rod Surface Temprature at Position 5 of Rods A22, A24, A33, A34

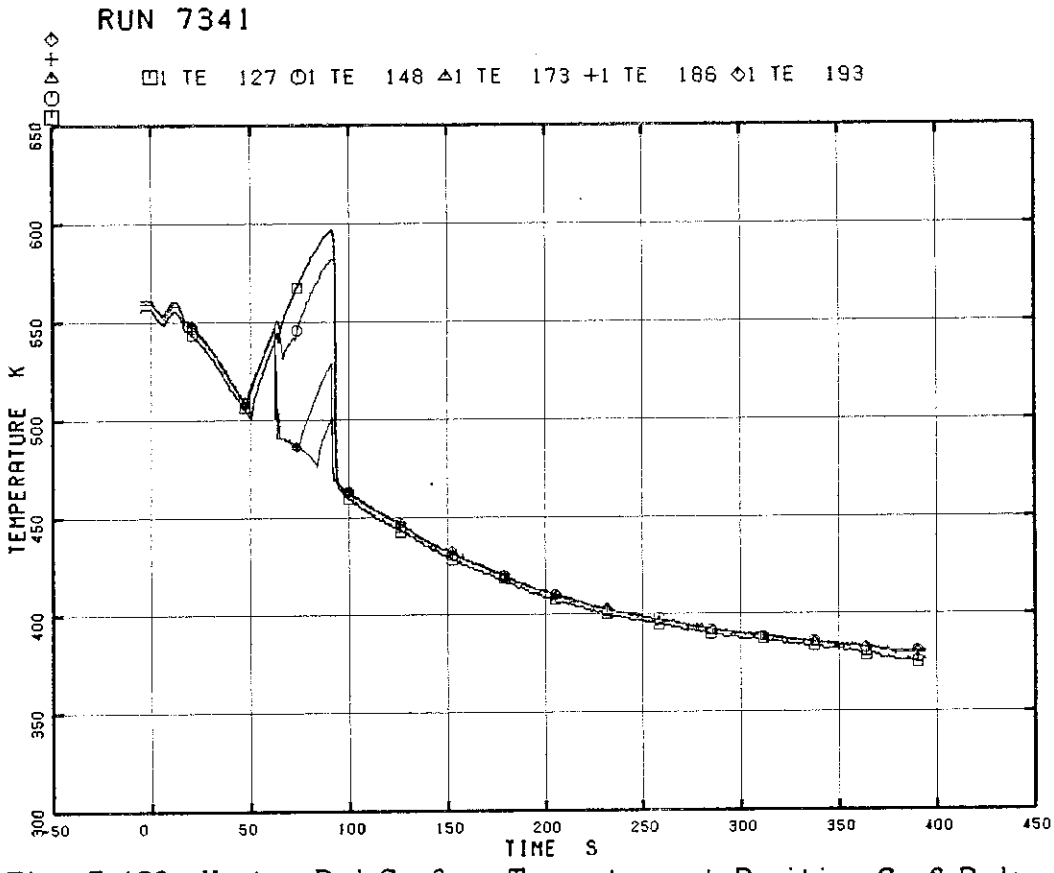

Fig. 5.130 Heater Rod Surface Temprature at Position 6 of Rods A22, A24, A33, A34

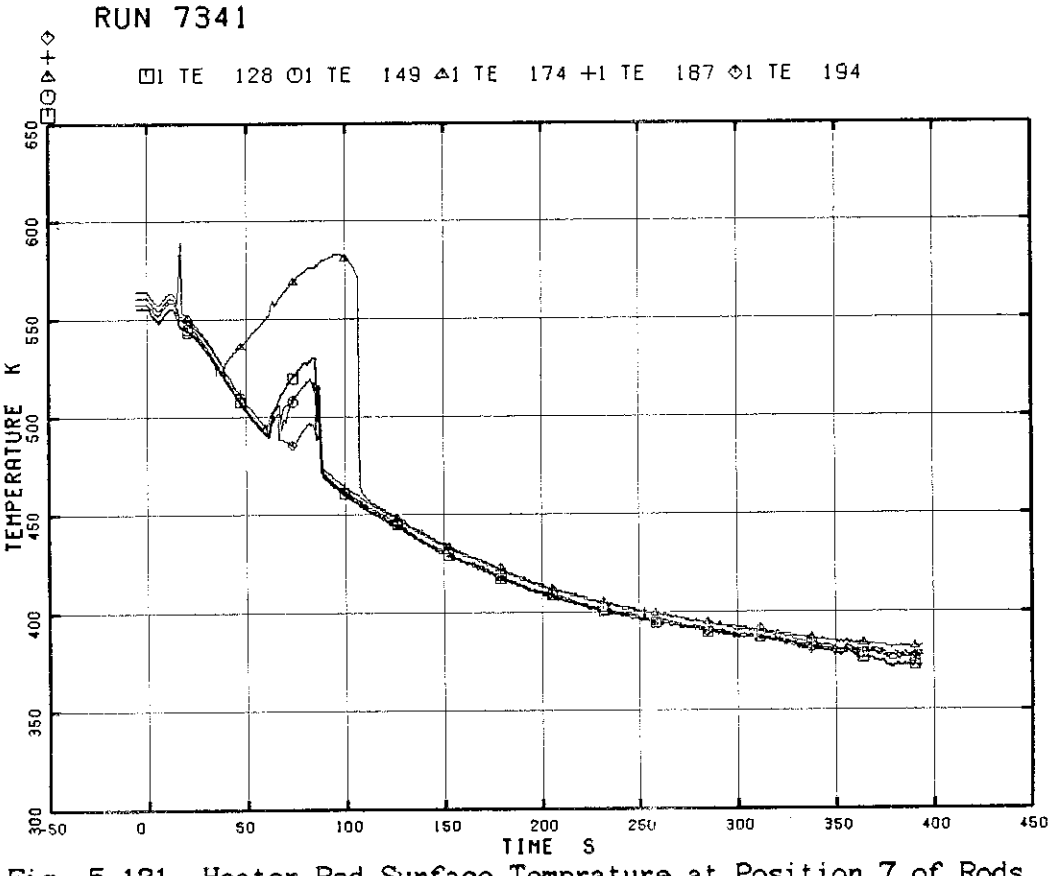

Fig. 5.131 Heater Rod Surface Temprature at Position 7 of Rods A22, A24, A33, A34

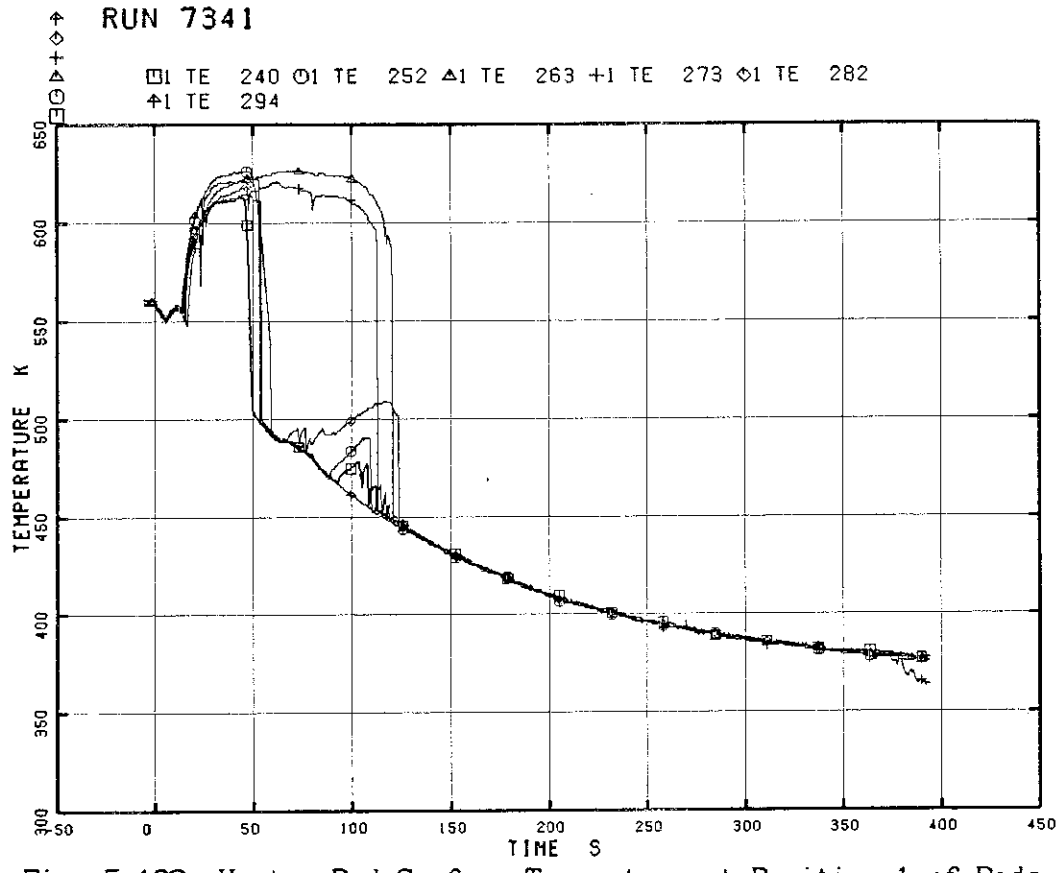

Fig. 5.132 Heater Rod Surface Temprature at Position 1 of Rods B15,B85,C33,C77,D27,D88

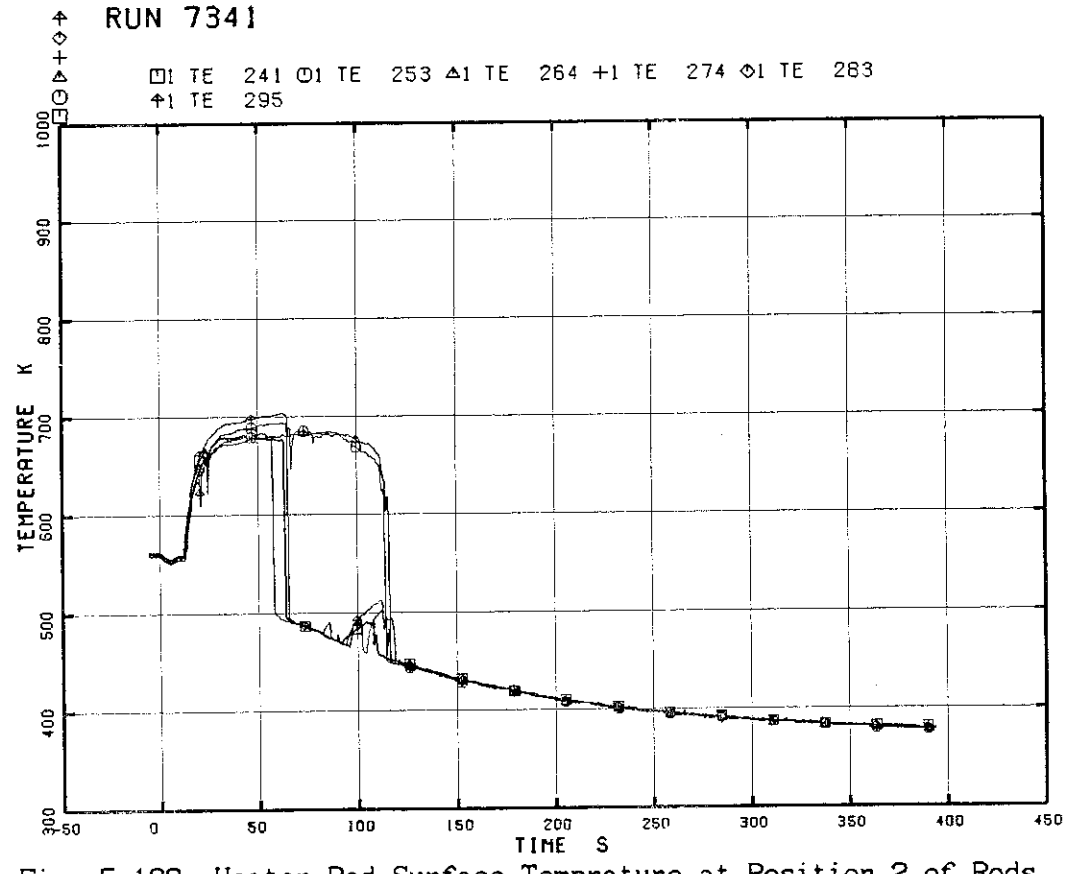

Fig. 5.133 Heater Rod Surface Temprature at Position 2 of Rods B15,B85,C33,C77,D27,D88

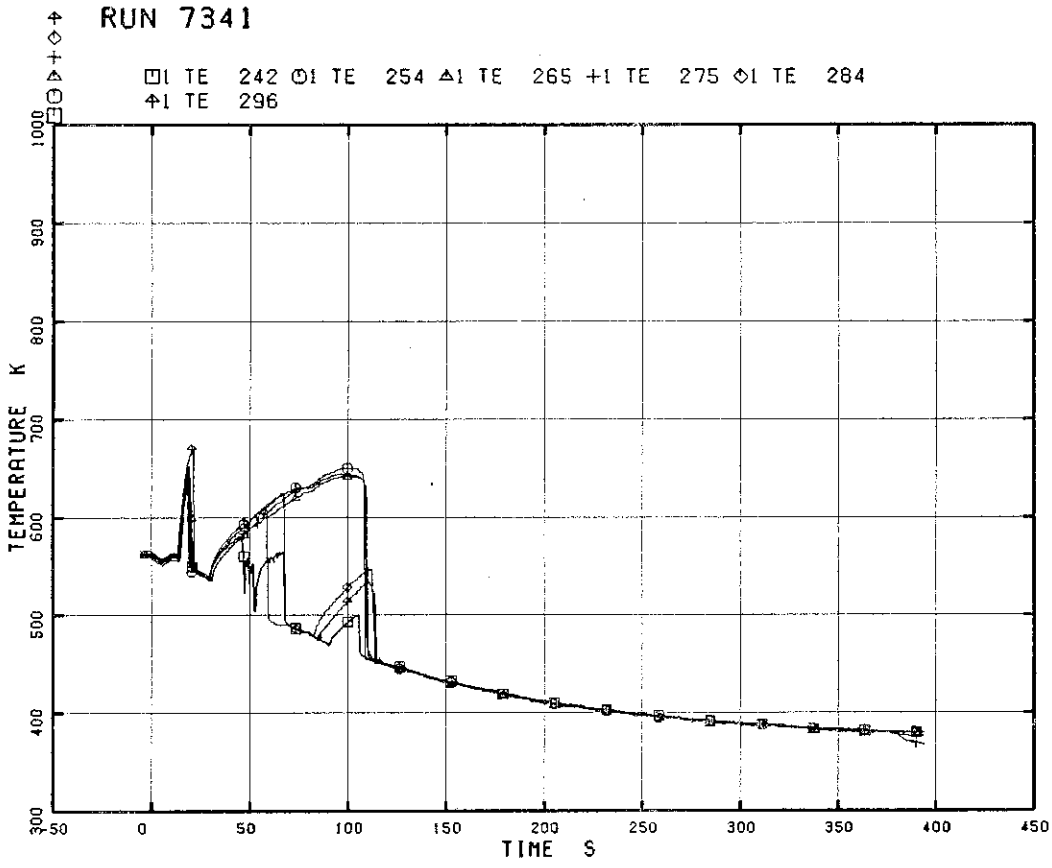

Fig. 5.134 Heater Rod Surface Temprature at Position 3 of Rods B15,B85,C33,C77,D27,D88

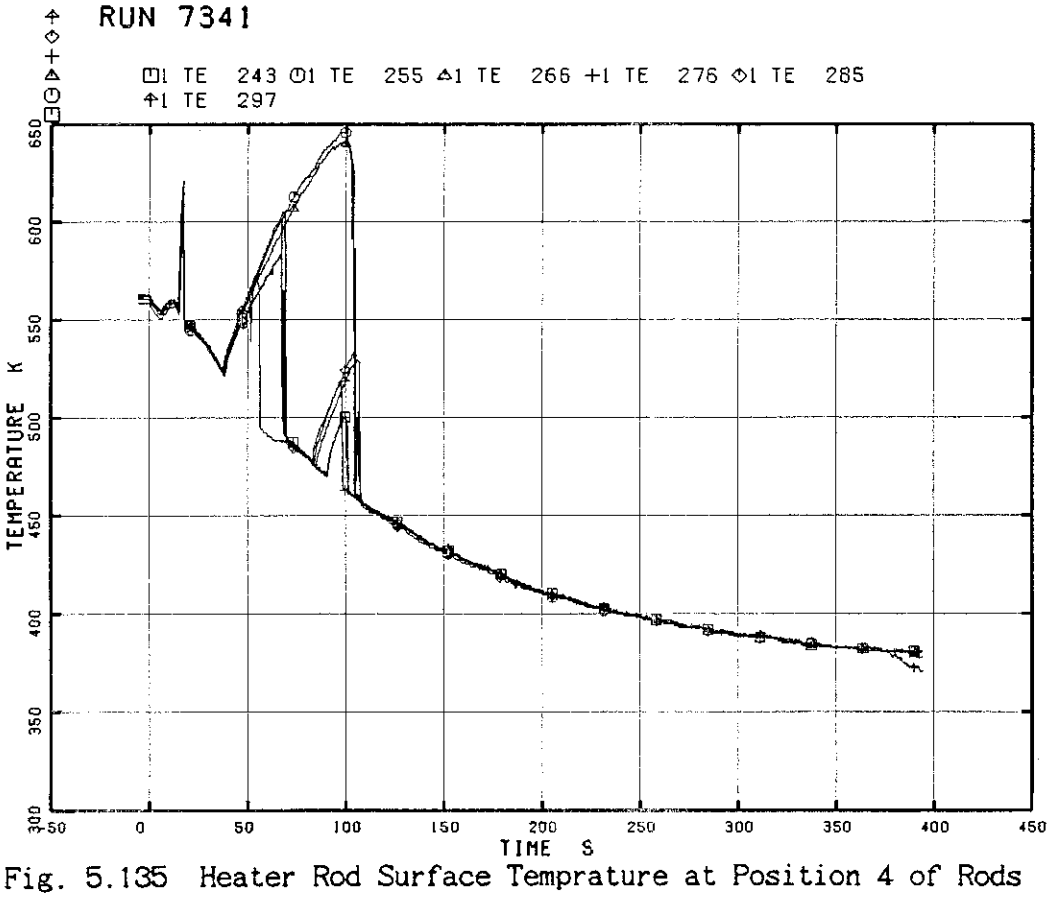

Fig. 5.135 Heater Rod Surface Temprature at Position 4 of Rods B15,B85,C33,C77,D27,D88

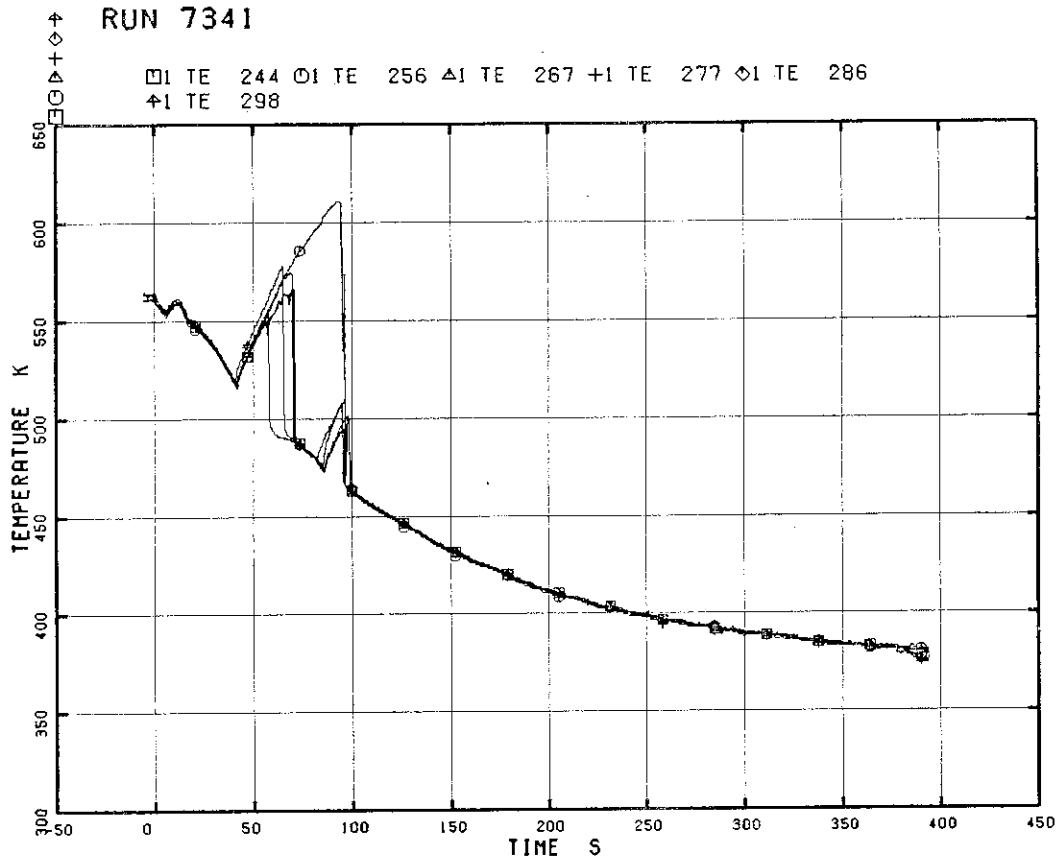

Fig. 5.136 Heater Rod Surface Temprature at Position 5 of Rods B15,B85,C33,C77,D27,D88

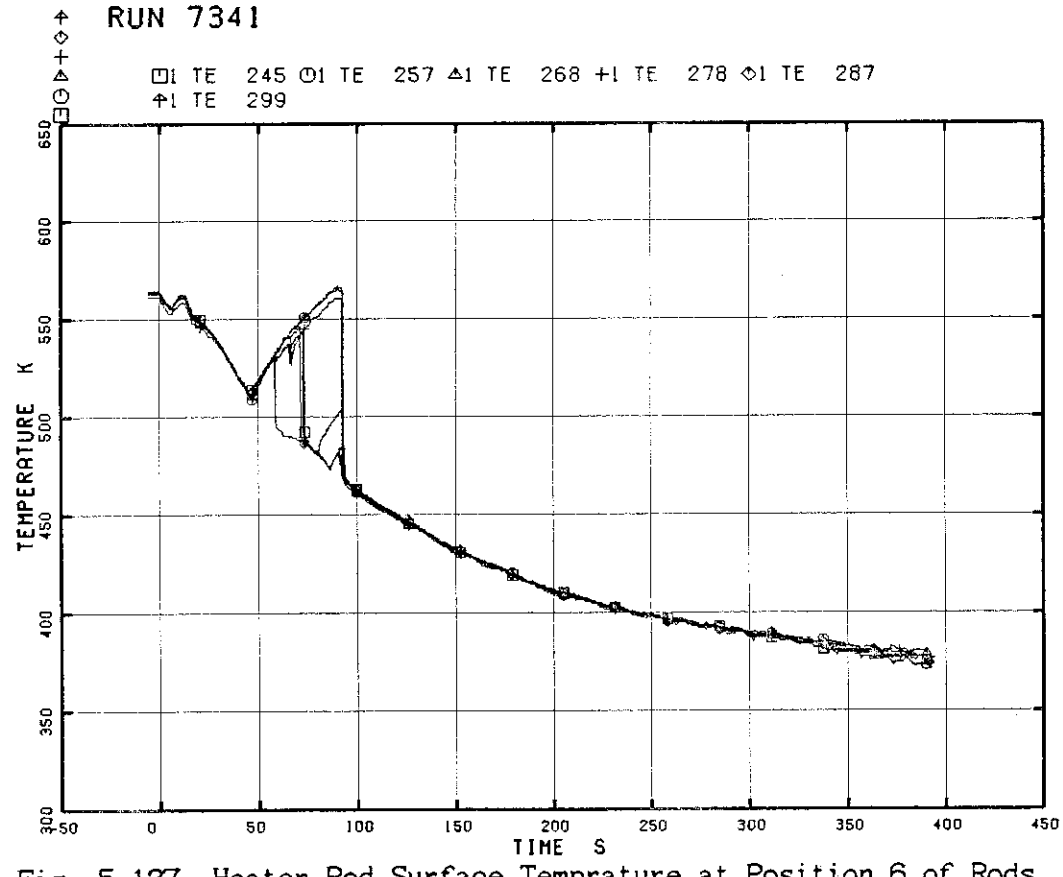

Fig. 5.137 Heater Rod Surface Temprature at Position 6 of Rods B15,B85,C33,C77,D27,D88

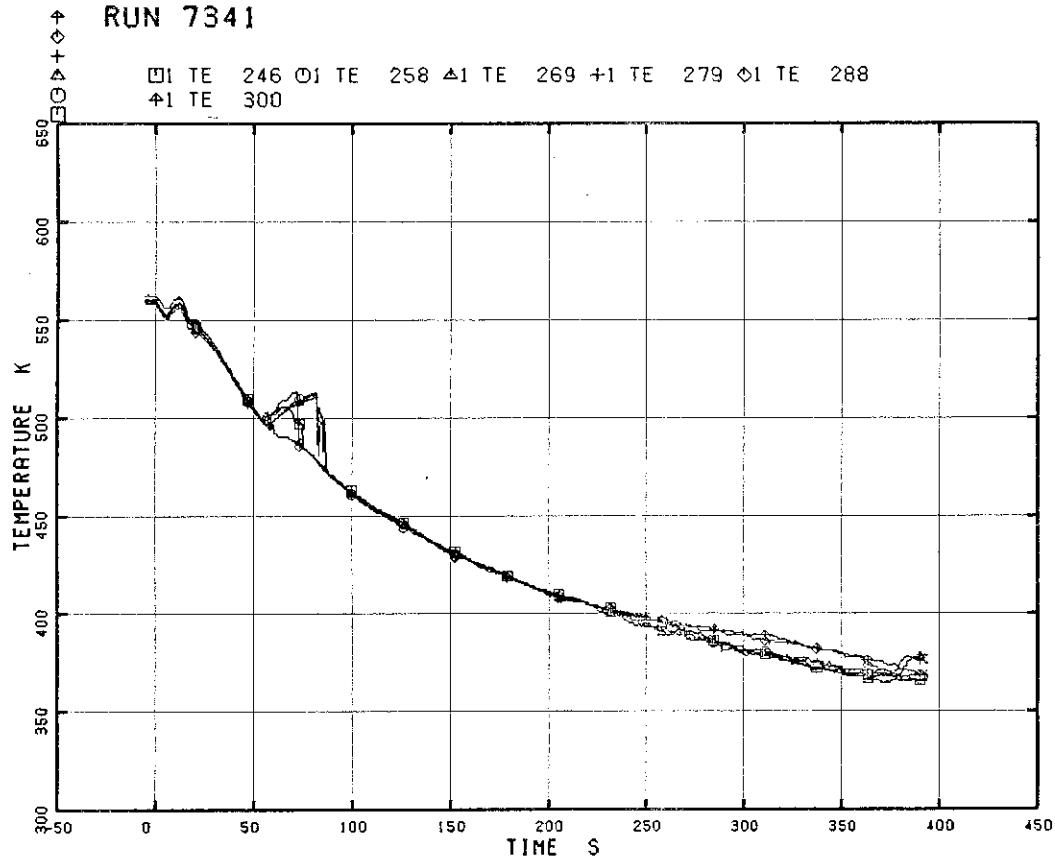

Fig. 5.138 Heater Rod Surface Temprature at Position 7 of Rods B15,B85,C33,C77,D27,D88

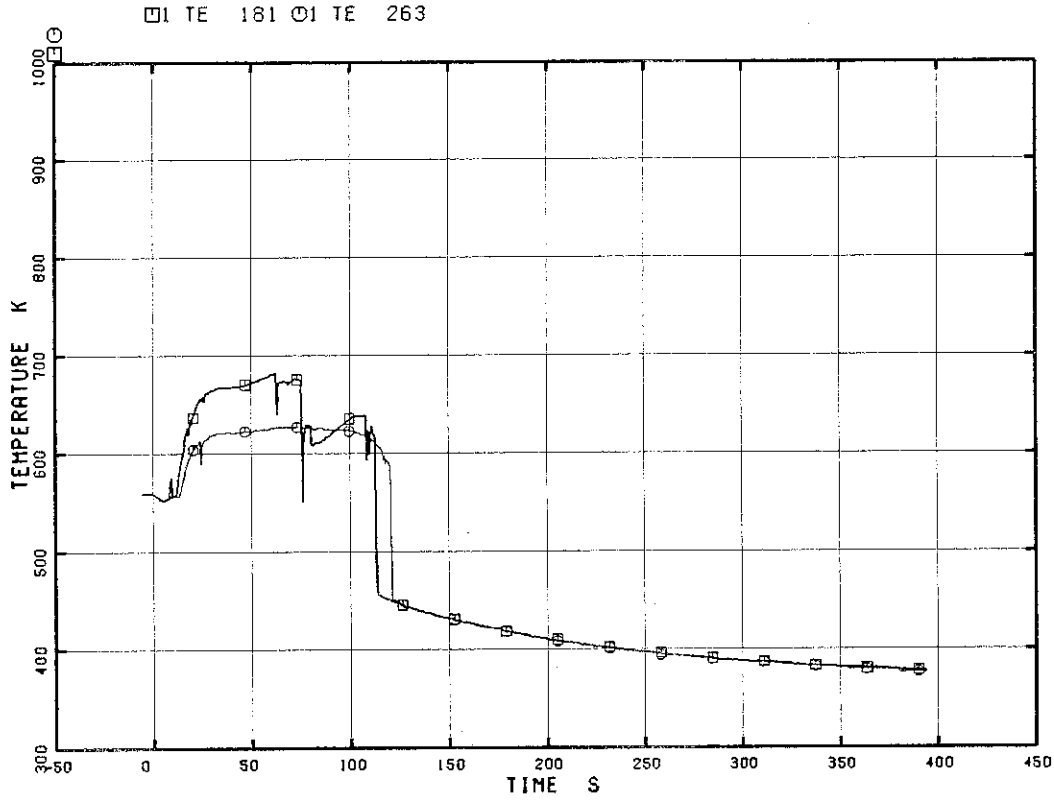

Fig. 5.139 Heater Rod Surface Temprature at Position 1 of Rods A33,C33

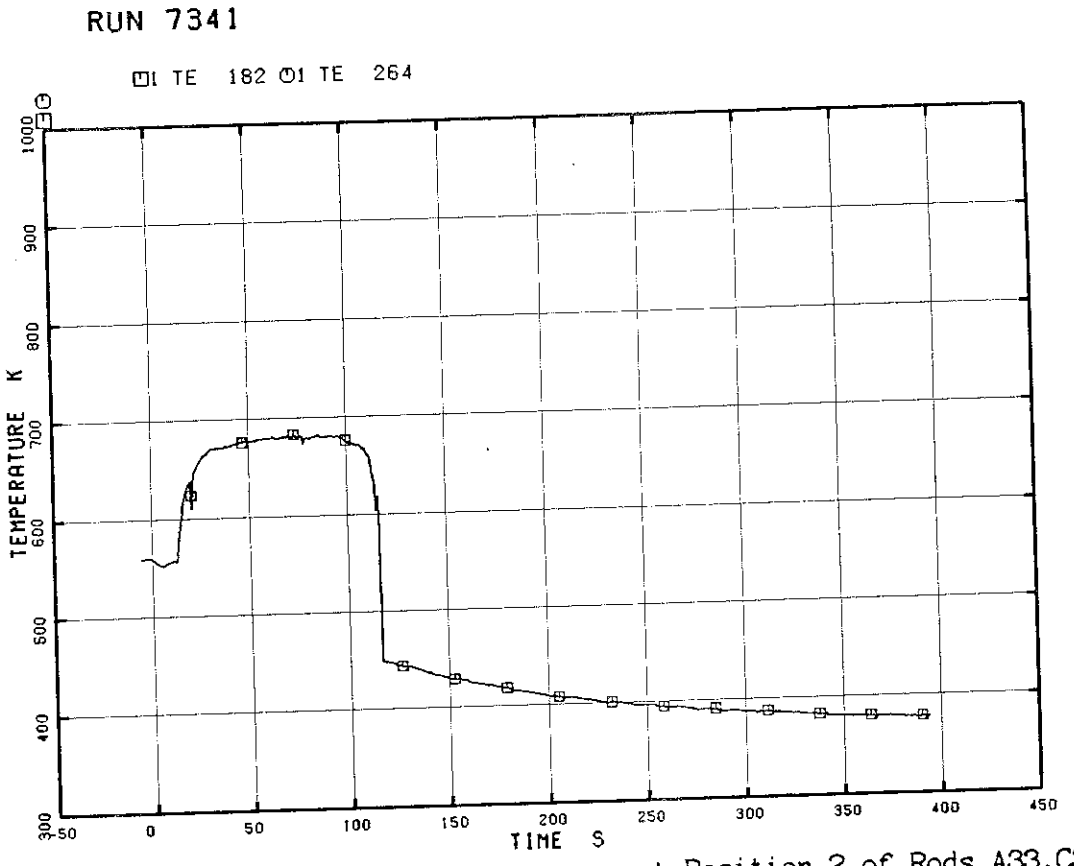

Fig. 5.140 Heater Rod Surface Temprature at Position 2 of Rods A33,C33

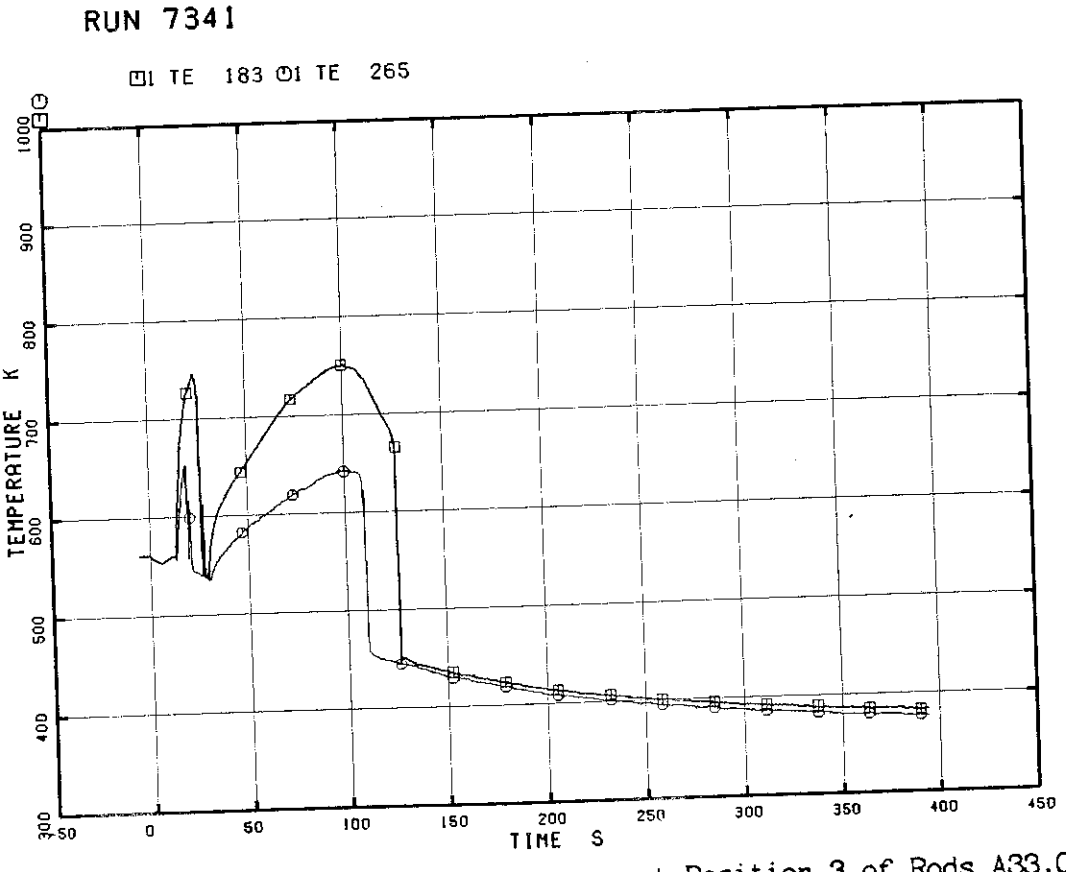

Fig. 5.141 Heater Rod Surface Temprature at Position 3 of Rods A33,C33

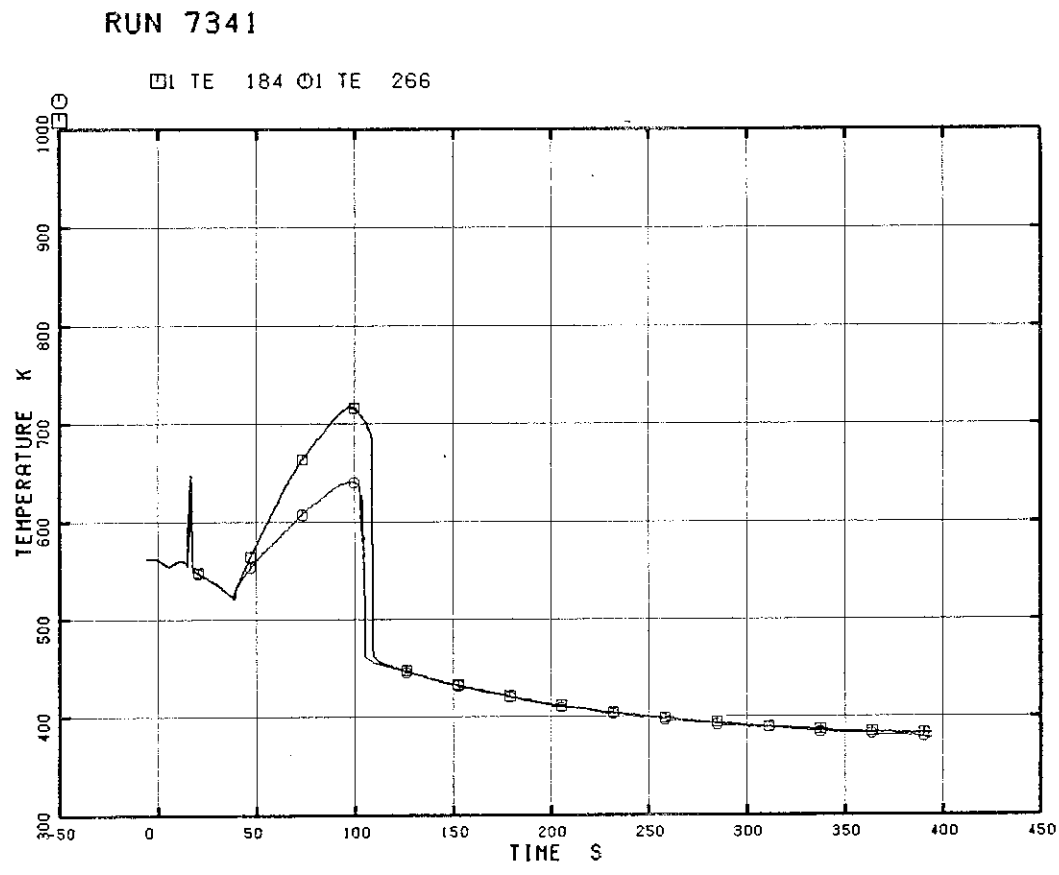

Fig. 5.142 Heater Rod Surface Temprature at Position 4 of Rods A33,C33

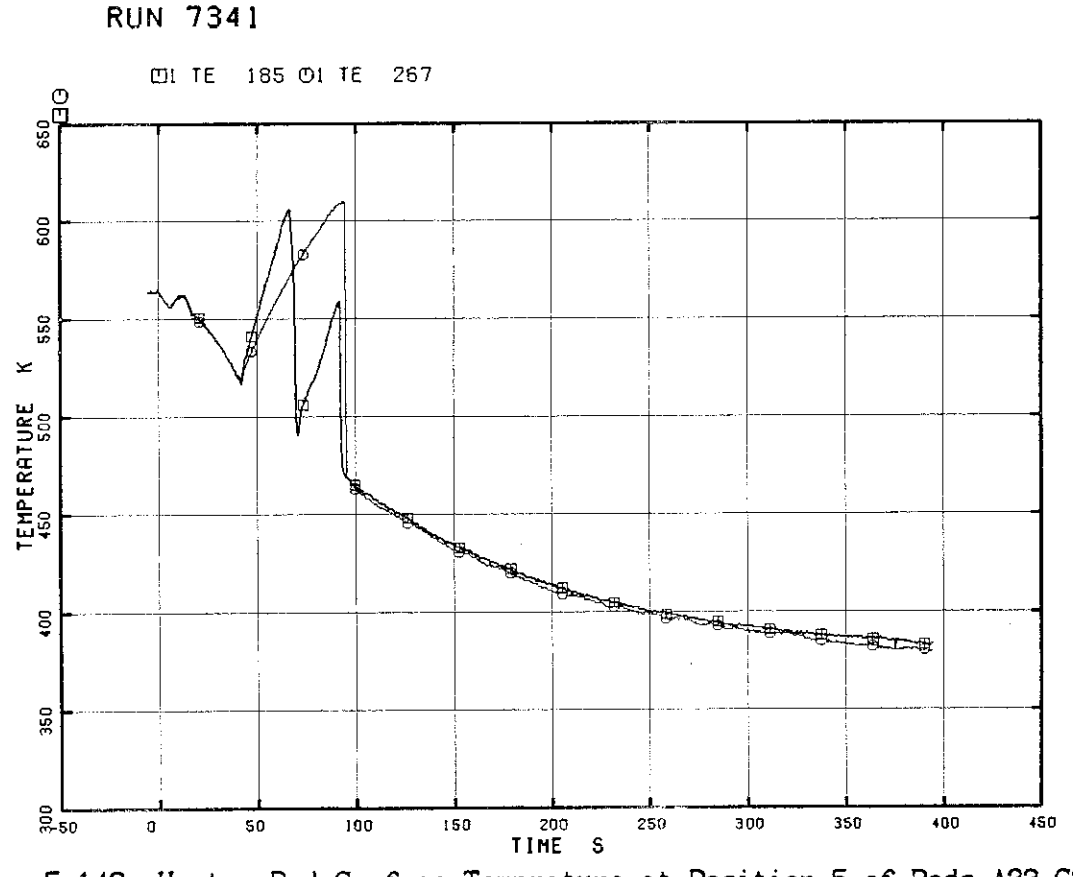

Fig. 5.143 Heater Rod Surface Temprature at Position 5 of Rods A33,C33

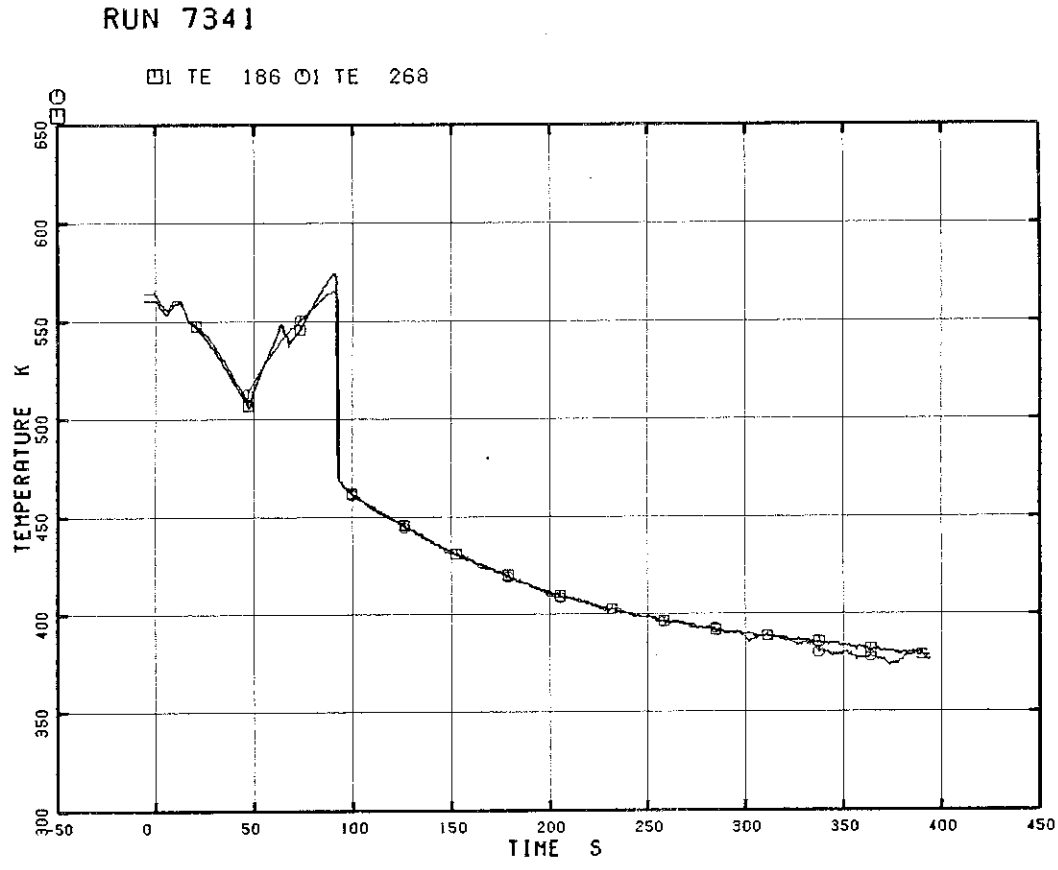

Fig. 5.144 Heater Rod Surface Temprature at Position 6 of Rods A33,C33

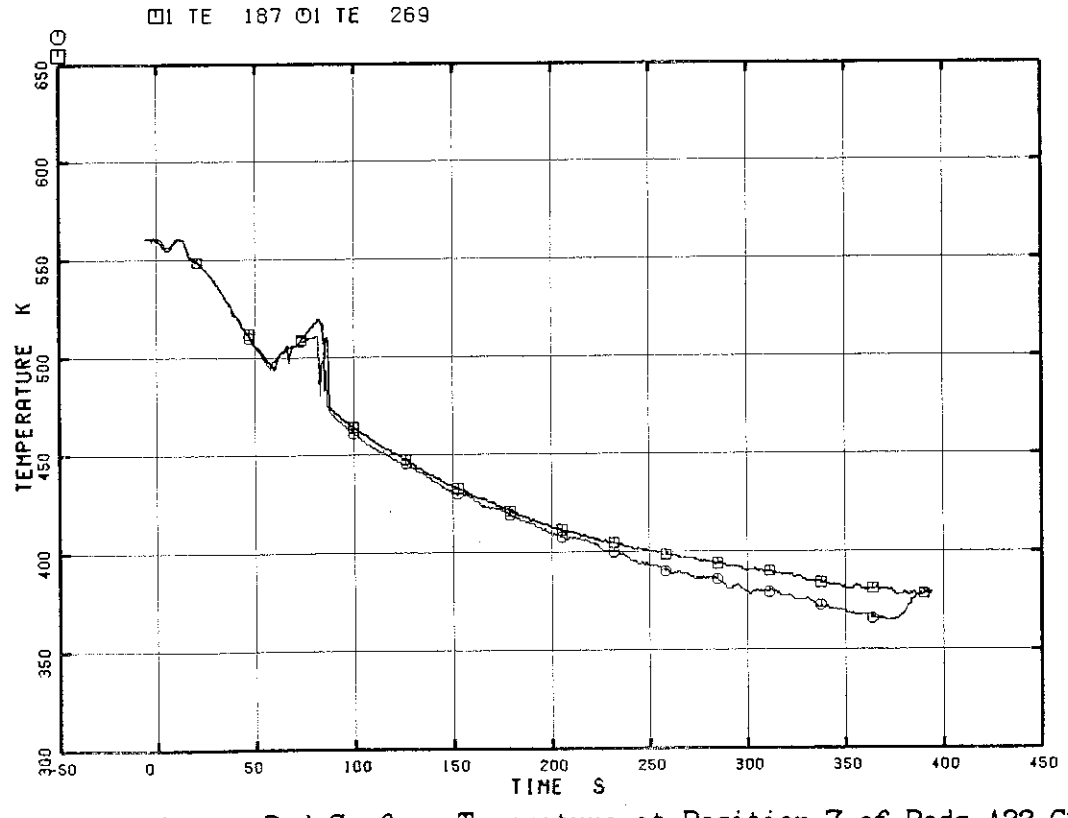

Fig. 5.145 Heater Rod Surface Temprature at Position 7 of Rods A33,C33

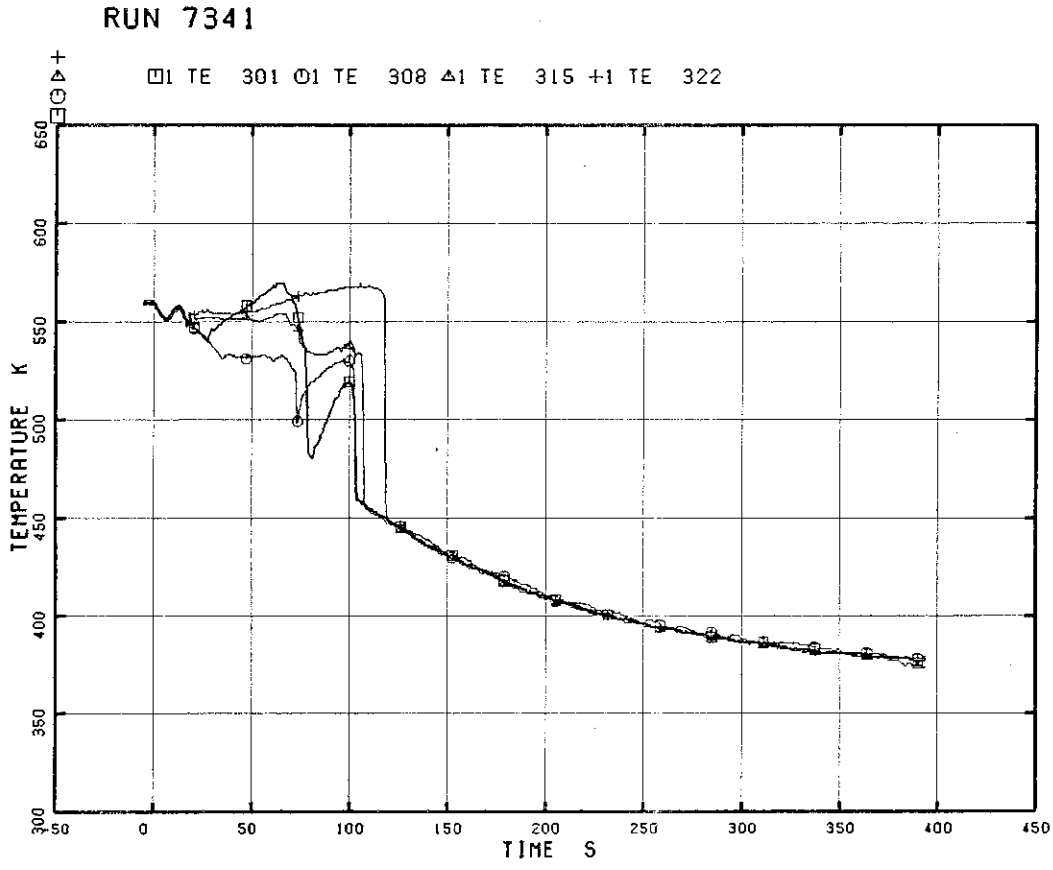

Fig. 5.146 Surface Temprature of Tie Rod at Position 1

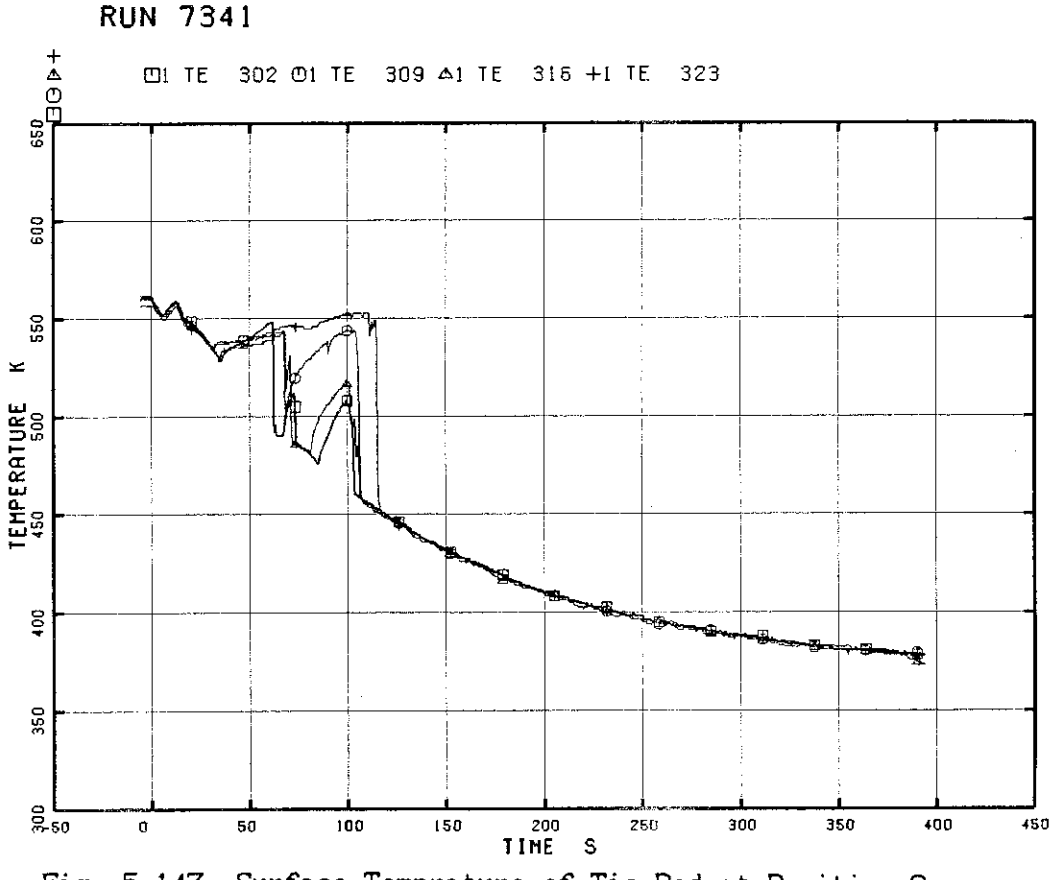

Fig. 5.147 Surface Temprature of Tie Rod at Position 2

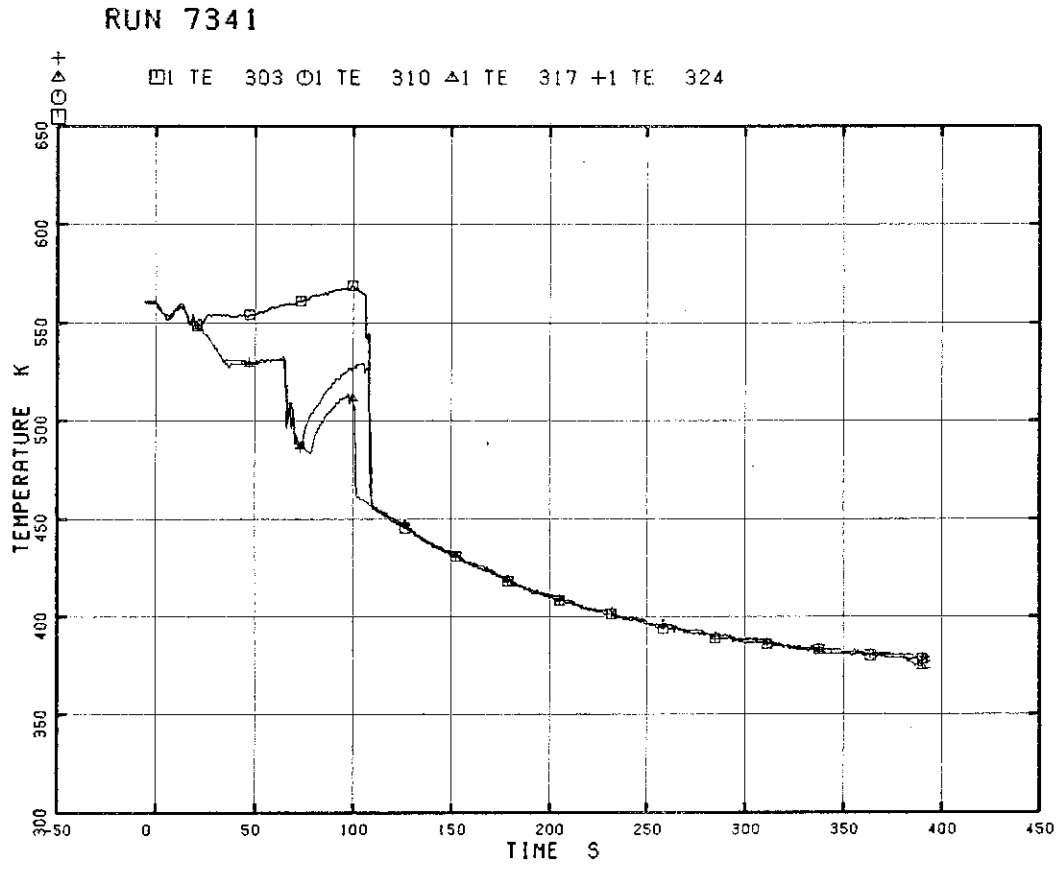

Fig. 5.148 Surface Temprature of Tie Rod at Position 3

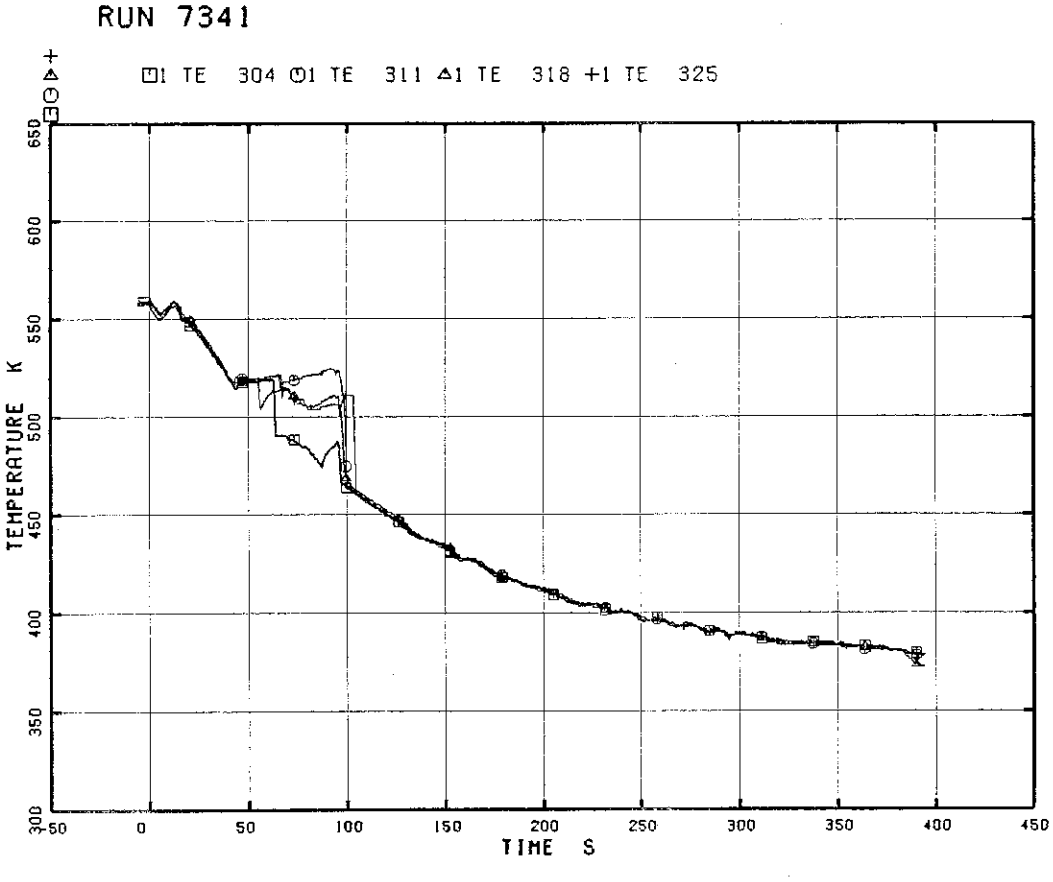

Fig. 5.149 Surface Temprature of Tie Rod at Position 4

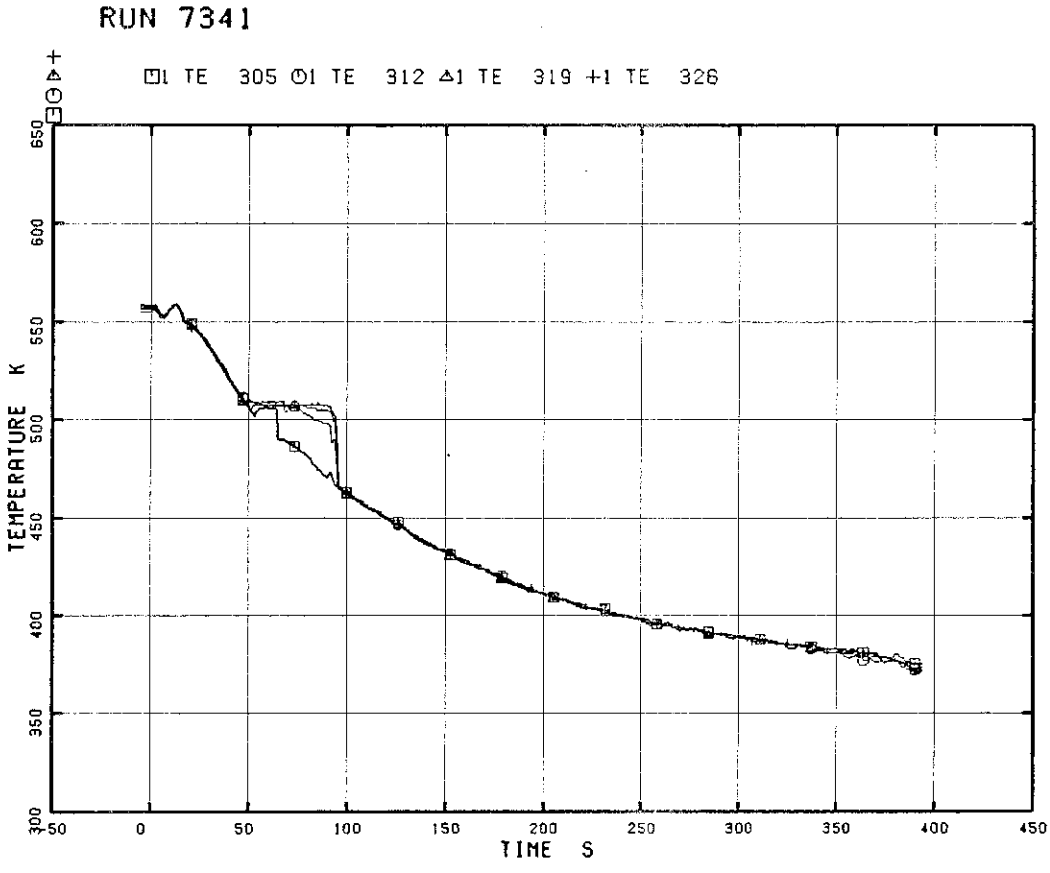

Fig. 5.150 Surface Temprature of Tie Rod at Position 5

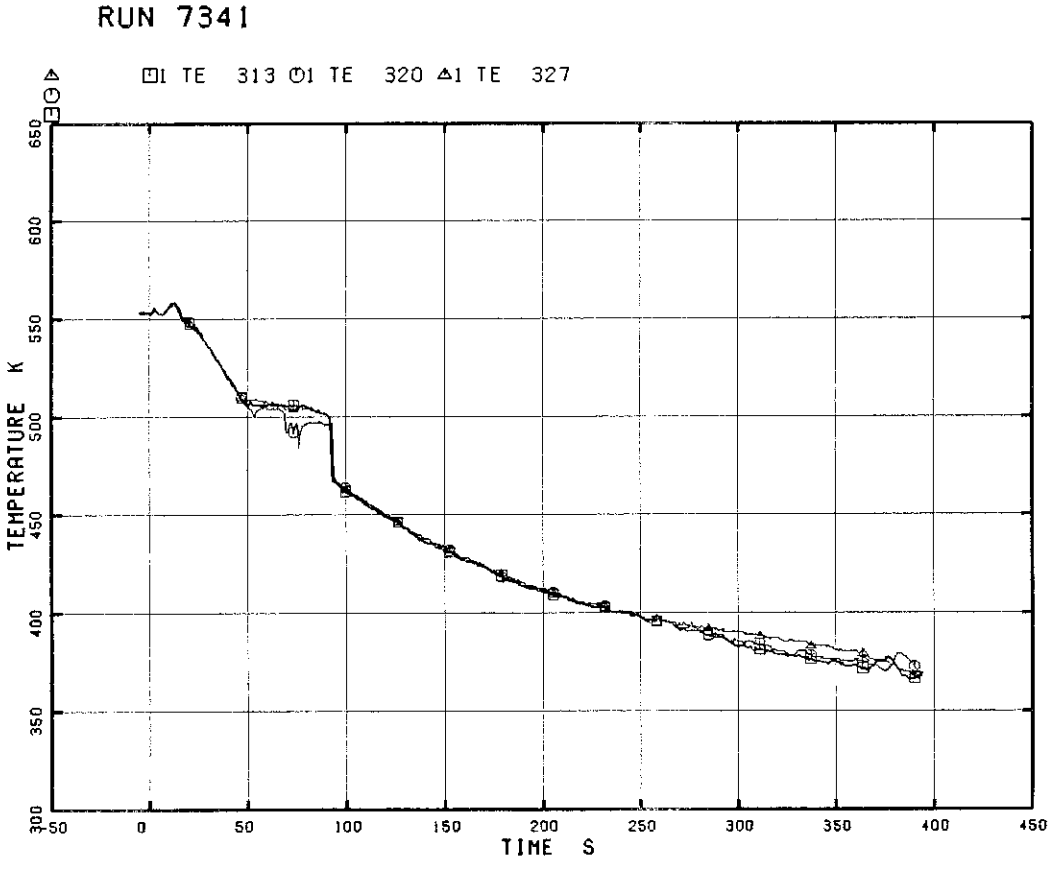

Fig. 5.151 Surface Temprature of Tie Rod at Position 6

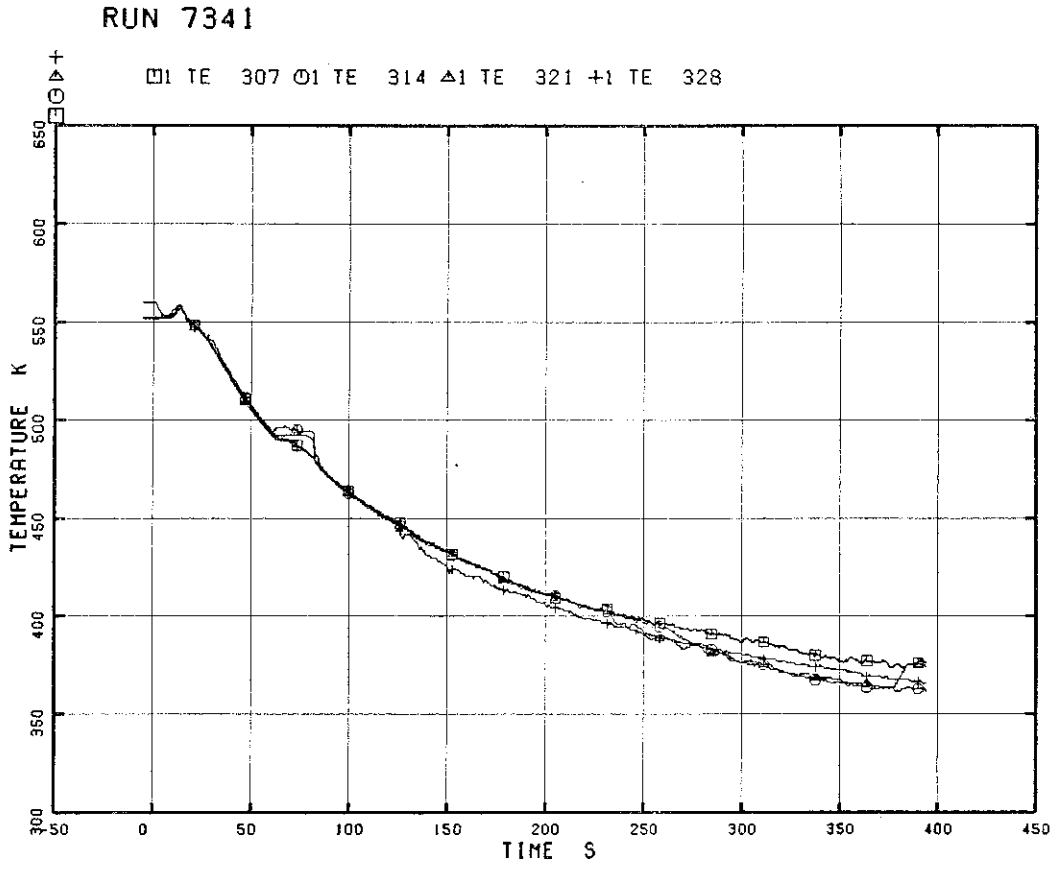

Fig. 5.152 Surface Temprature of Tie Rod at Position 7

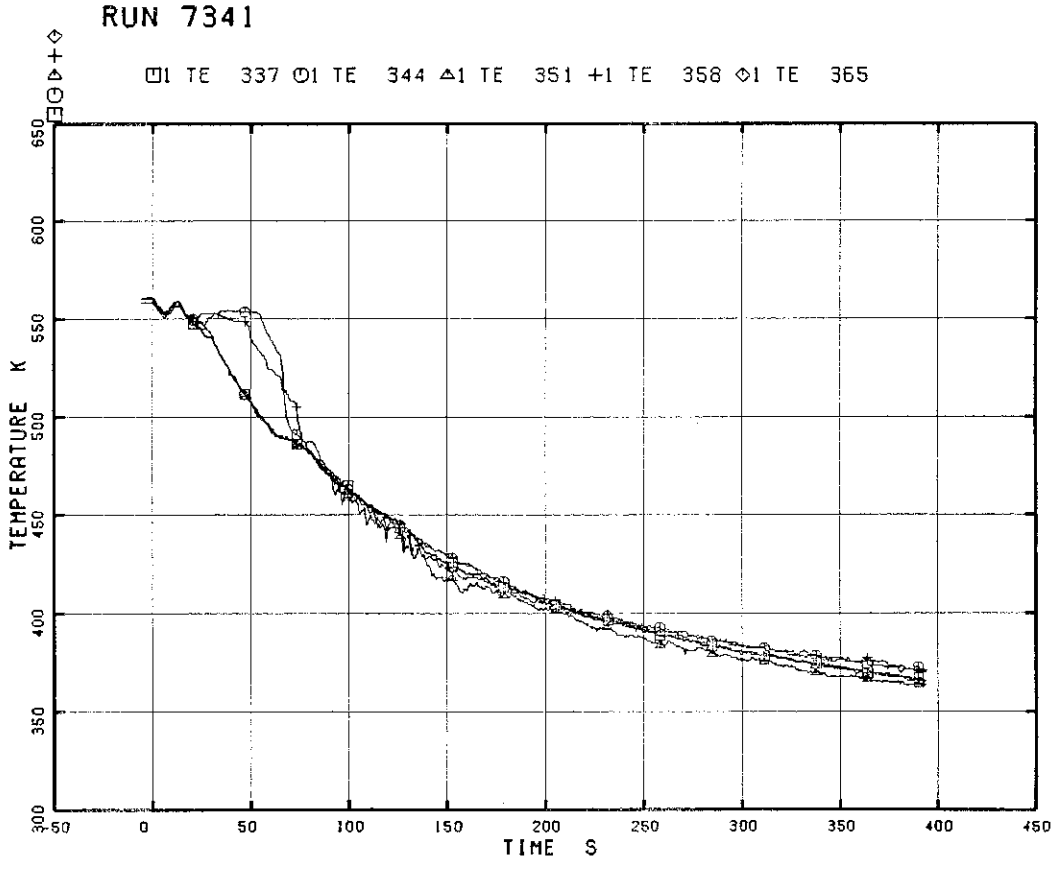

Fig. 5.153 Inner Surface Temprature of Channel Box at Position 1

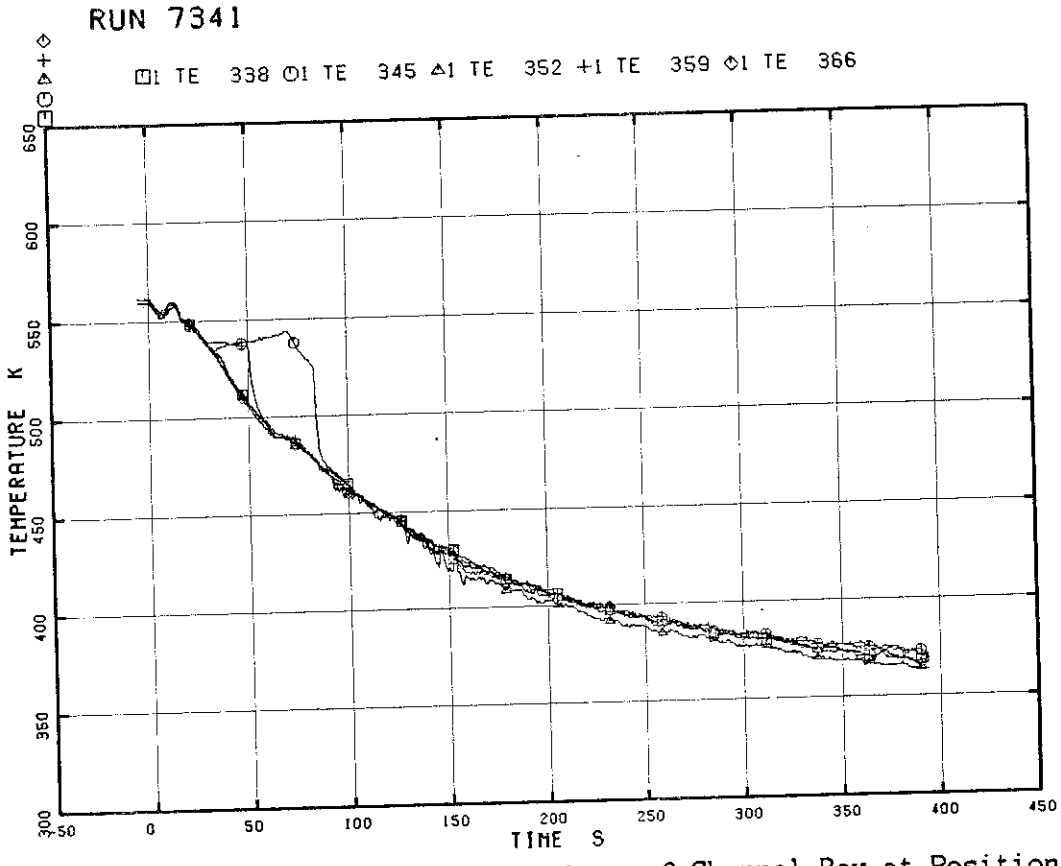

Fig. 5.154 Inner Surface Temprature of Channel Box at Position 2

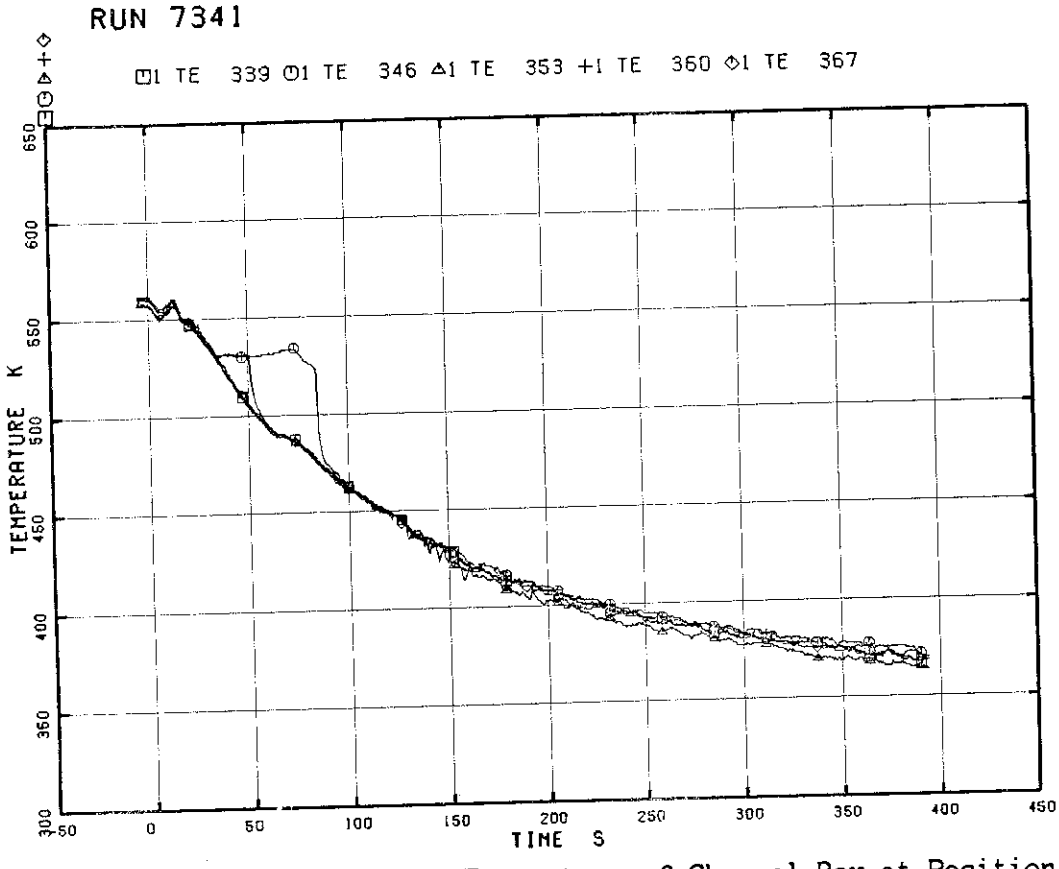

Fig. 5.155 Inner Surface Temprature of Channel Box at Position 3

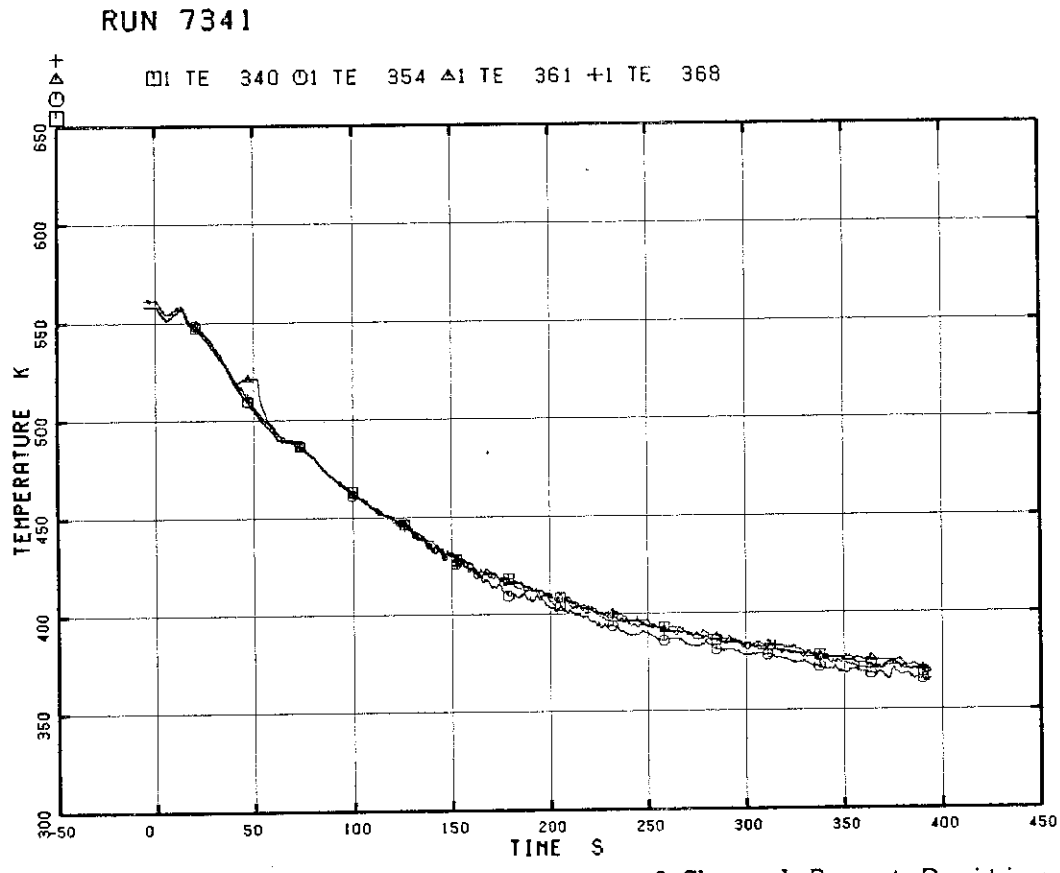

Fig. 5.156 Inner Surface Temprature of Channel Box at Position 4

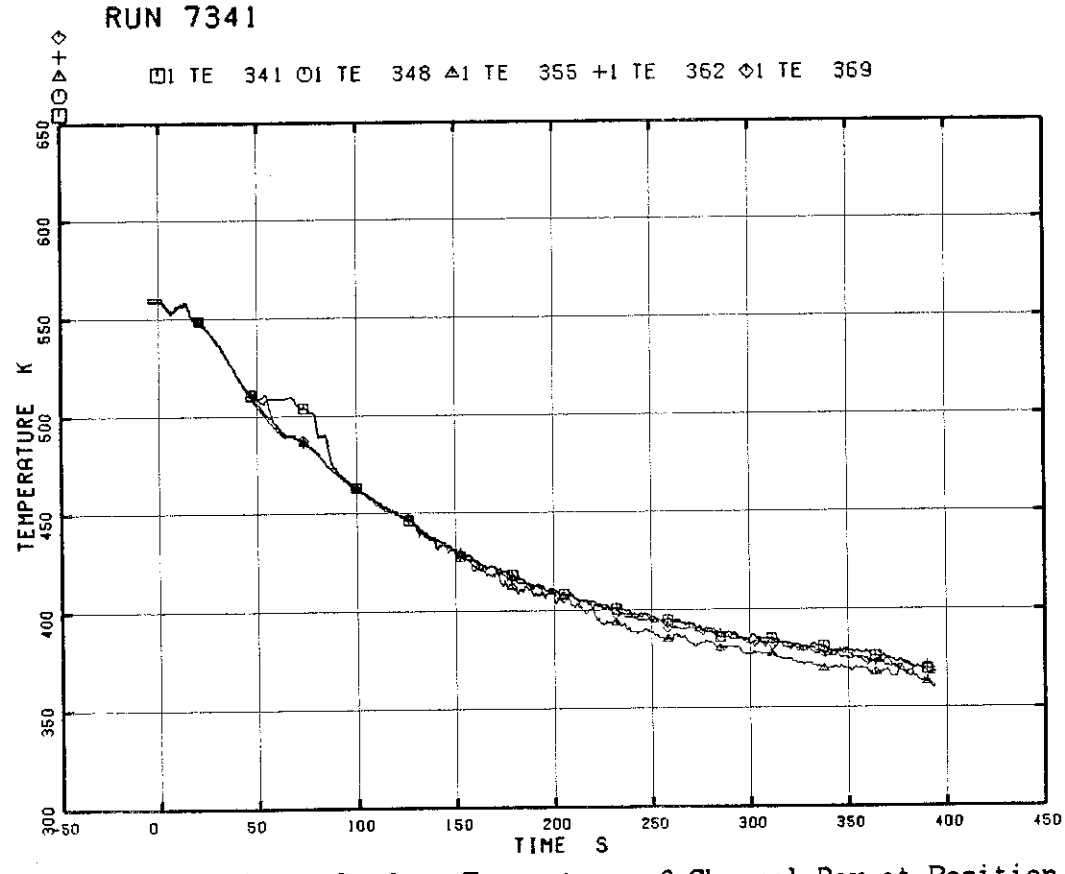

Fig. 5.157 Inner Surface Temprature of Channel Box at Position 5

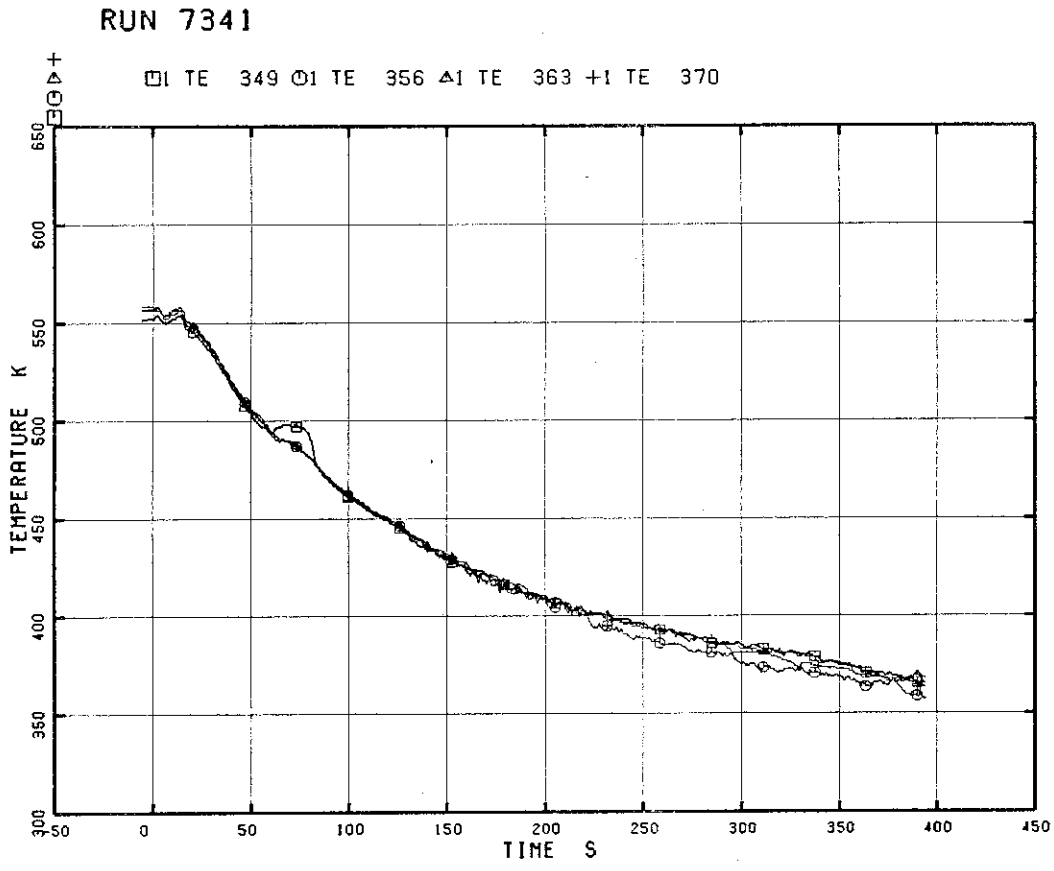

Fig. 5.158 Inner Surface Temprature of Channel Box at Position 6

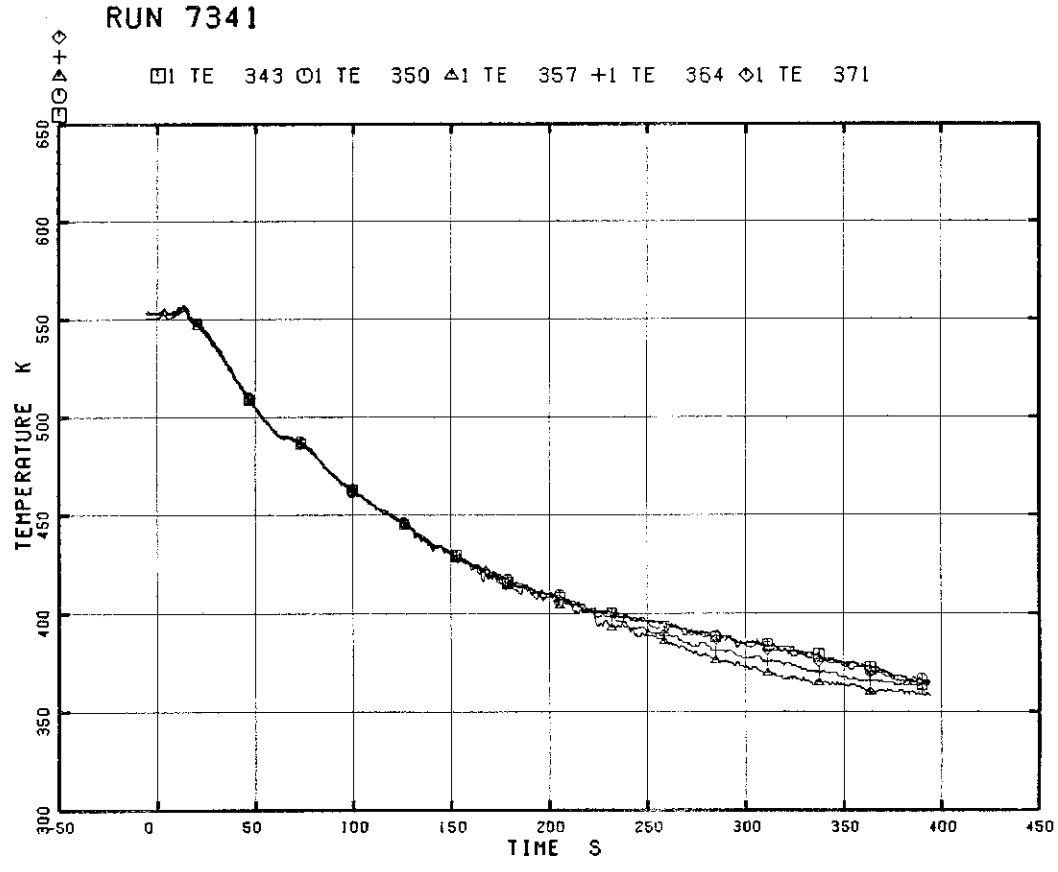

Fig. 5.159 Inner Surface Temprature of Channel Box at Position 7

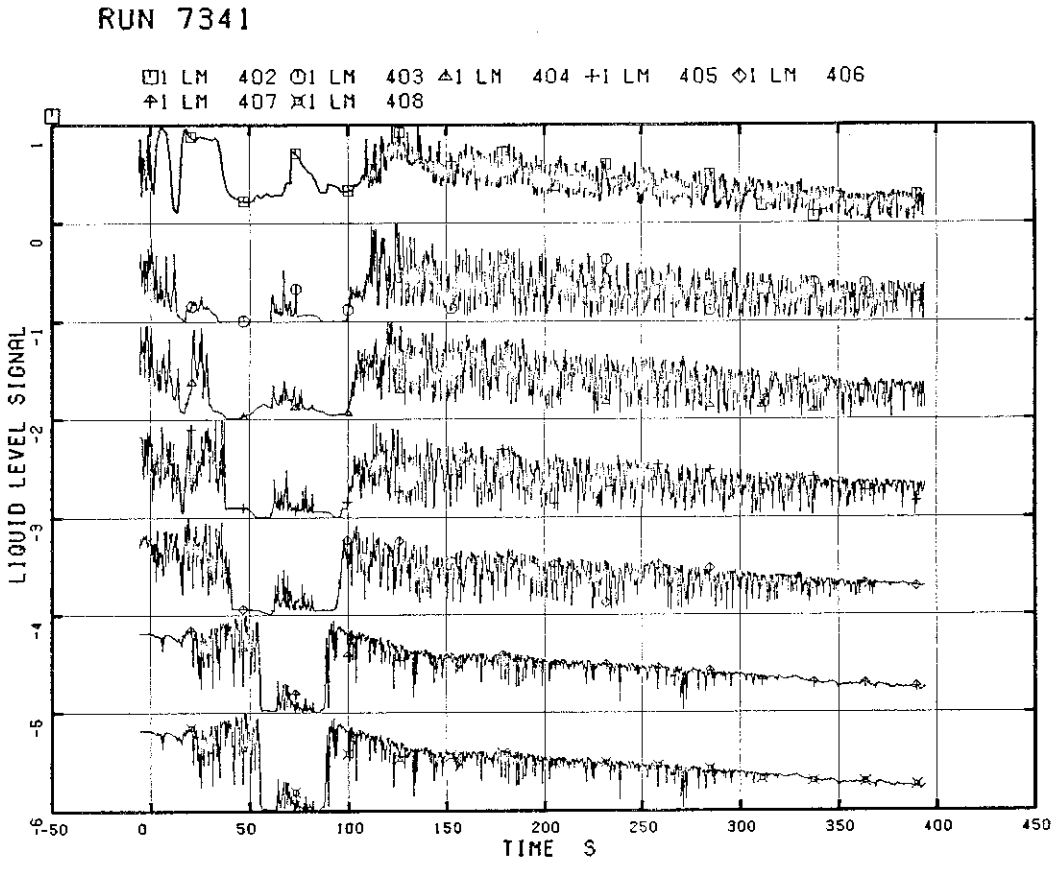

Fig. 5.160 Liquid Level in Channel Box A, A1 Location

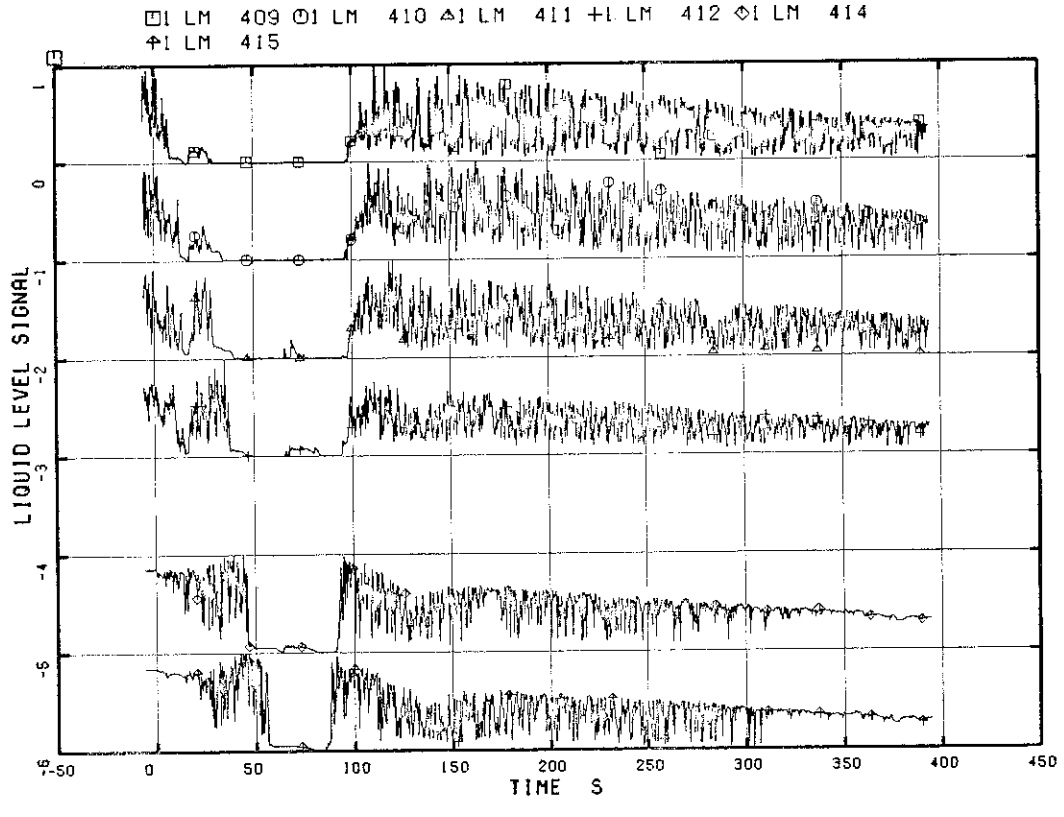

Fig. 5.161 Liquid Level in Channel Box A, A2 Location

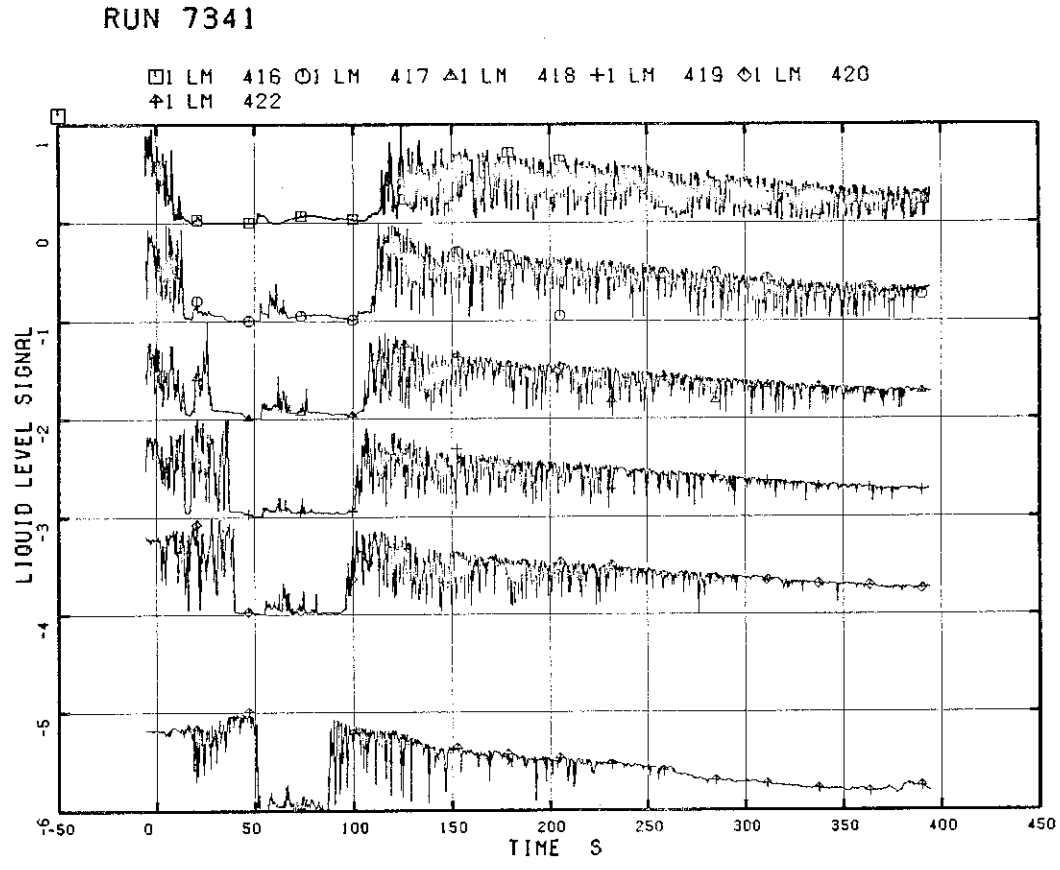

Fig. 5.162 Liquid Level in Channel Box B

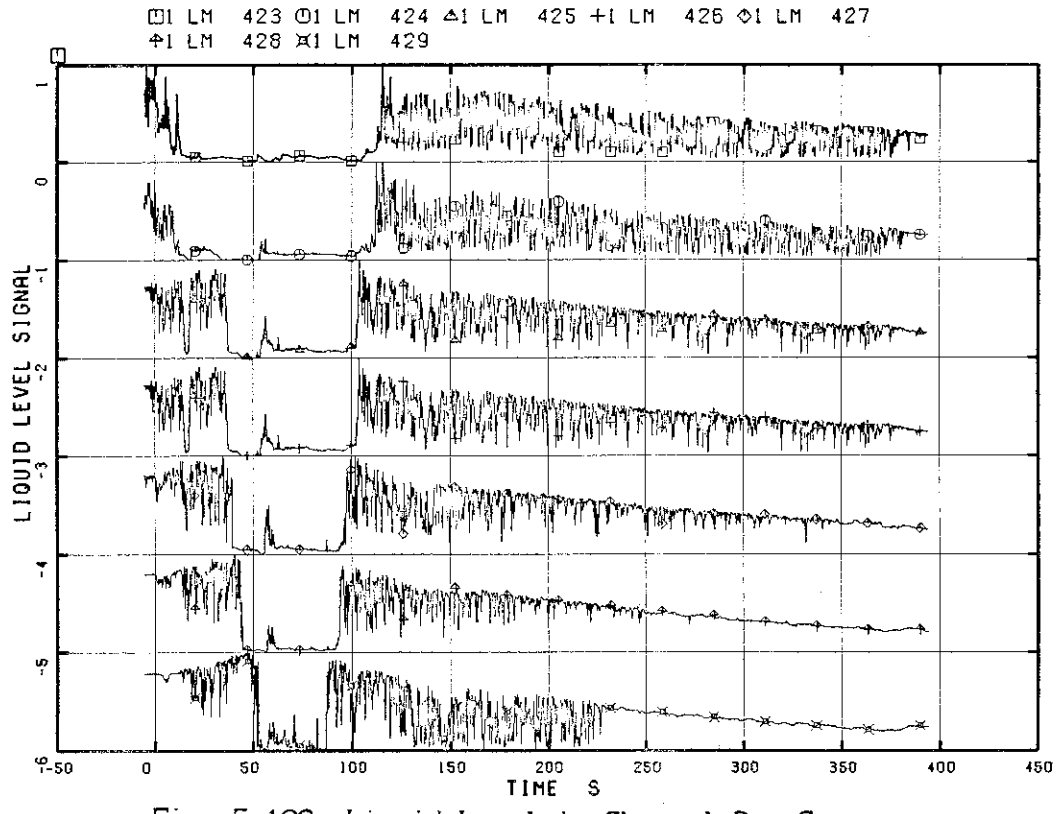

Fig. 5.163 Liquid Level in Channel Box C

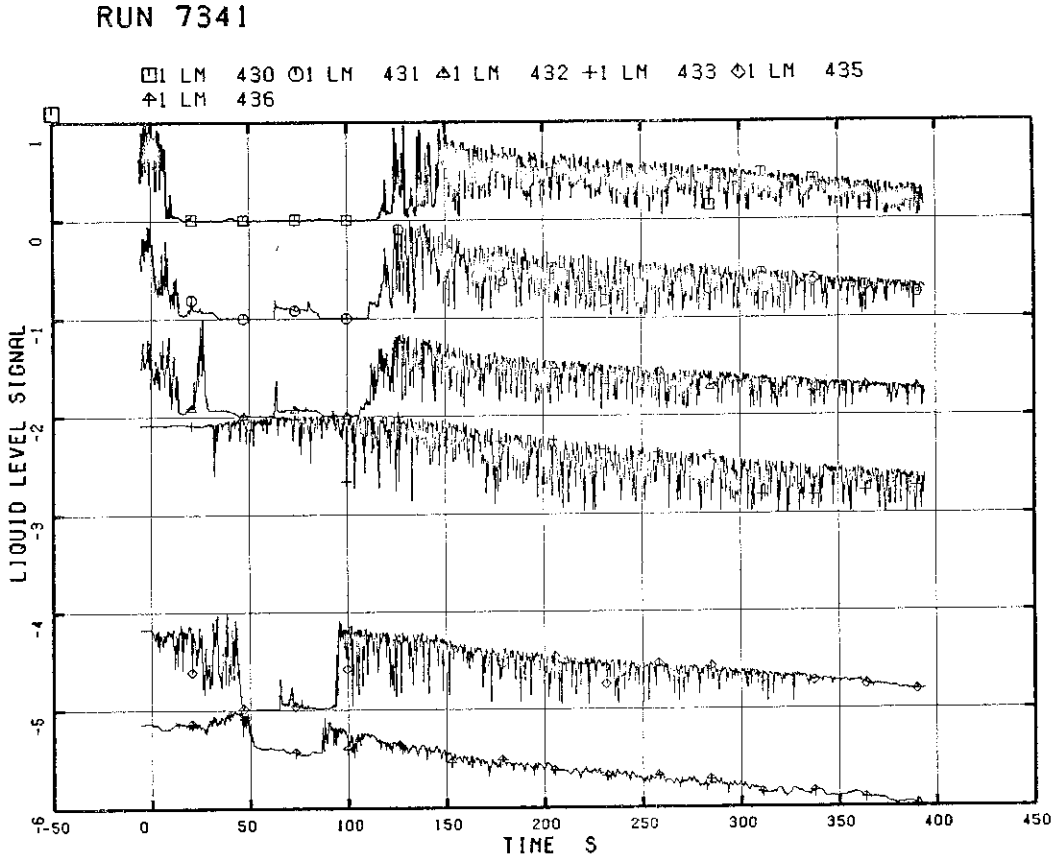

Fig. 5.164 Liquid Level in Channel Box D

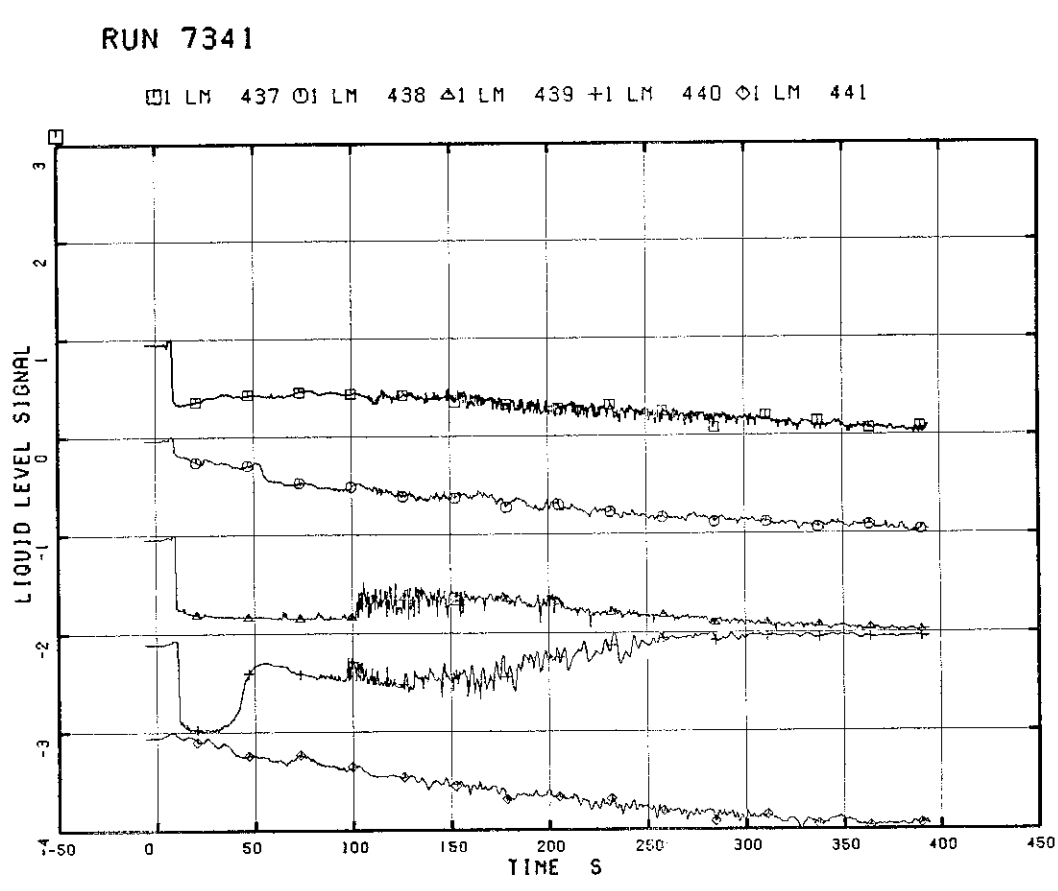

Fig. 5.165 Liquid Level in Downcomer

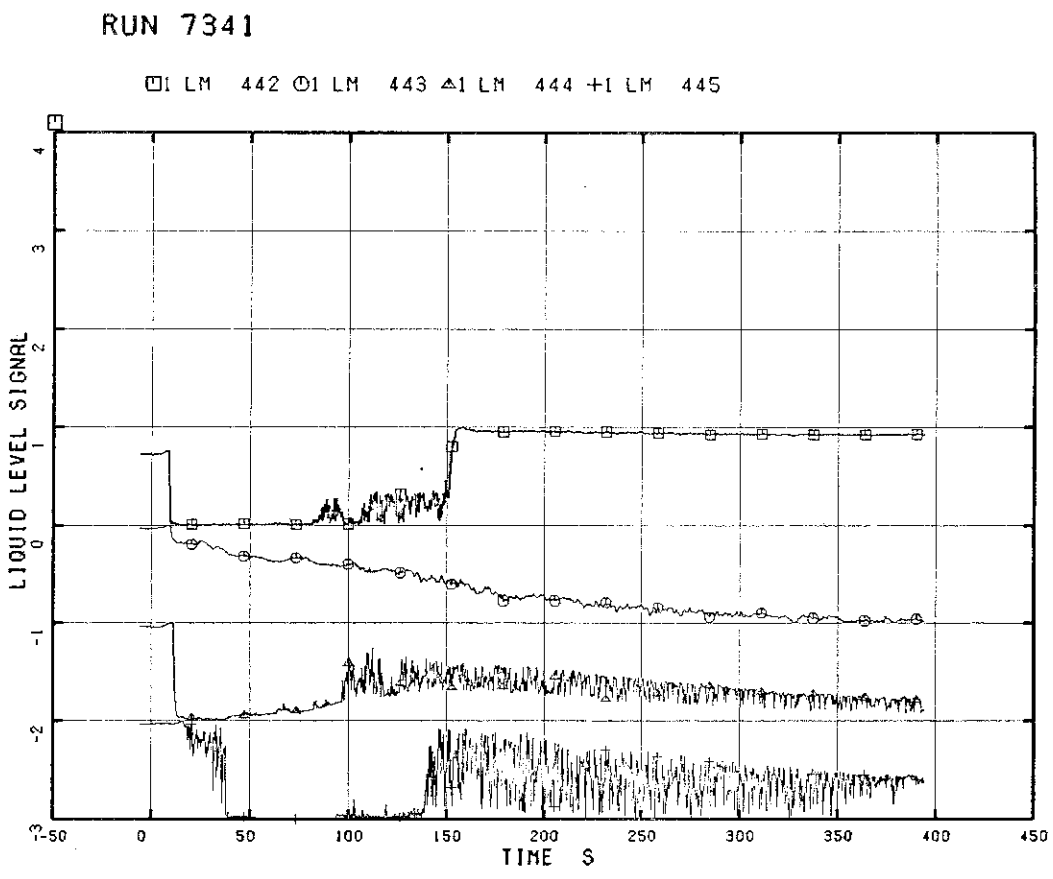

Fig. 5.166 Liquid Level in Downcomer

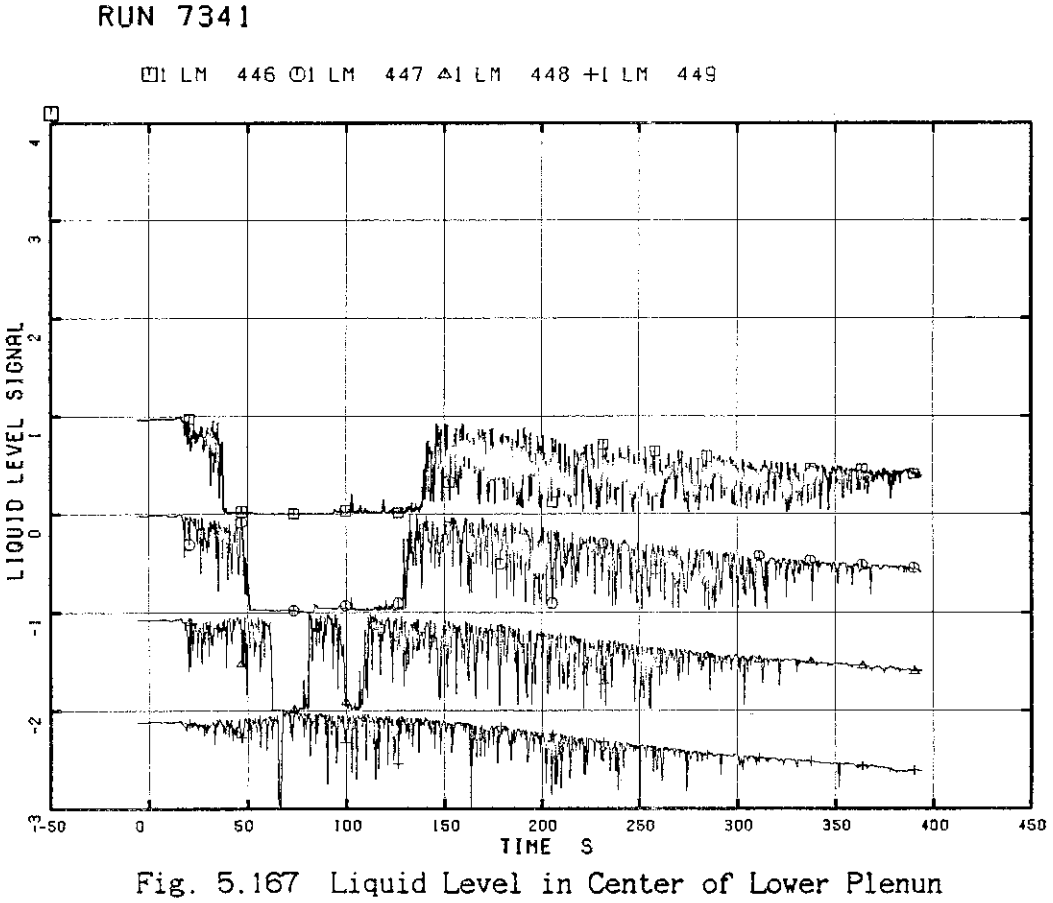

Fig. 5.167 Liquid Level in Center of Lower Plenun

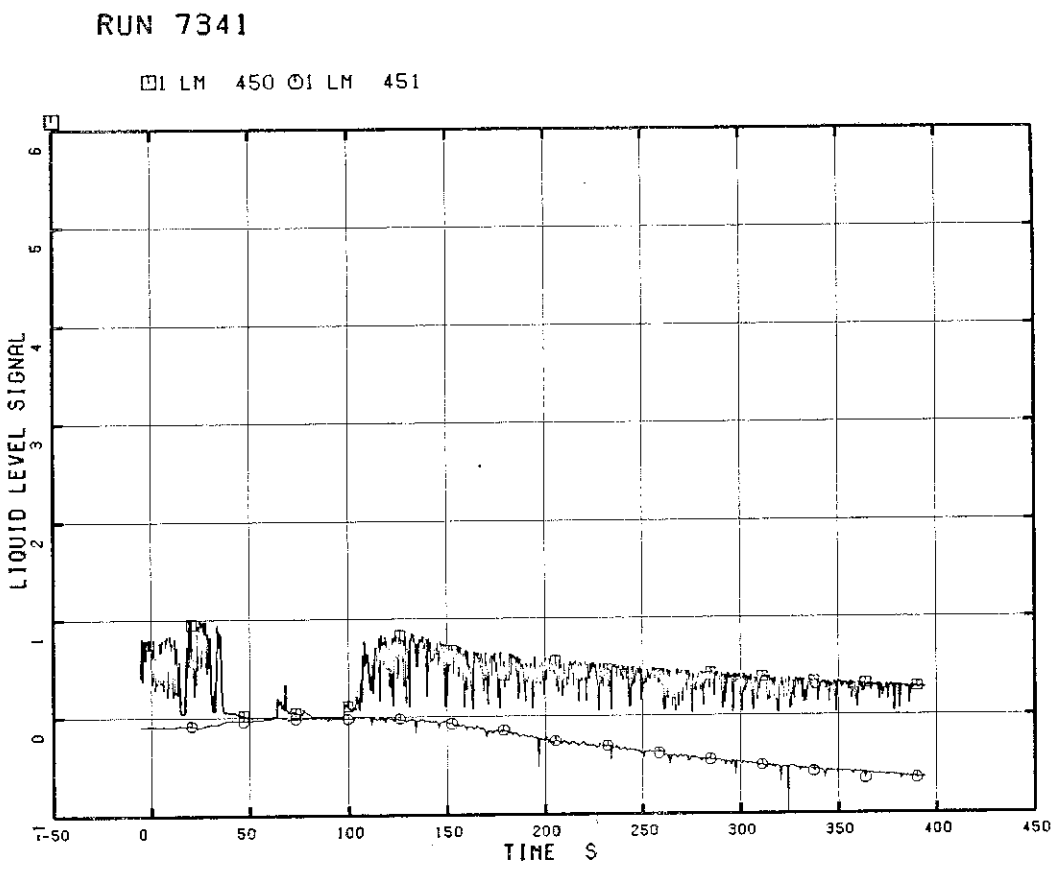

Fig. 5.168 Liquid Level in Lower Plenun, North

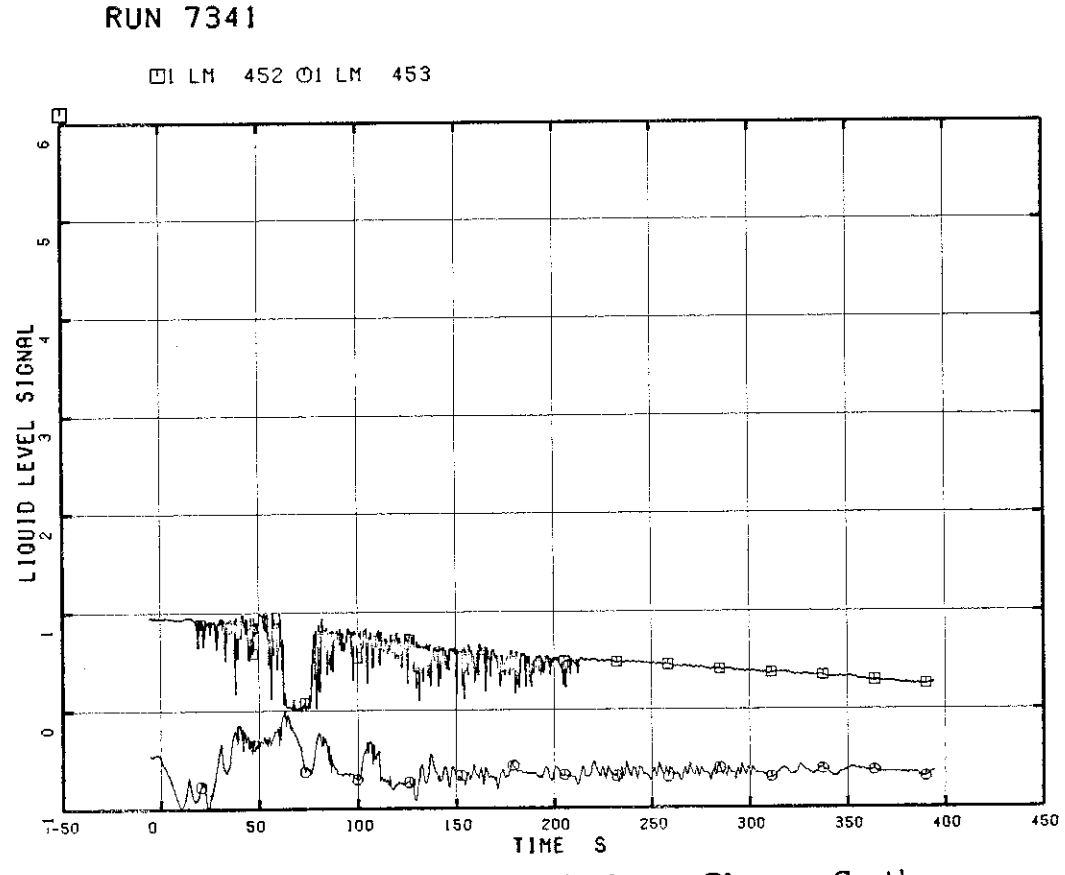

Fig. 5.169 Liquid Level in Lower Plenun, South

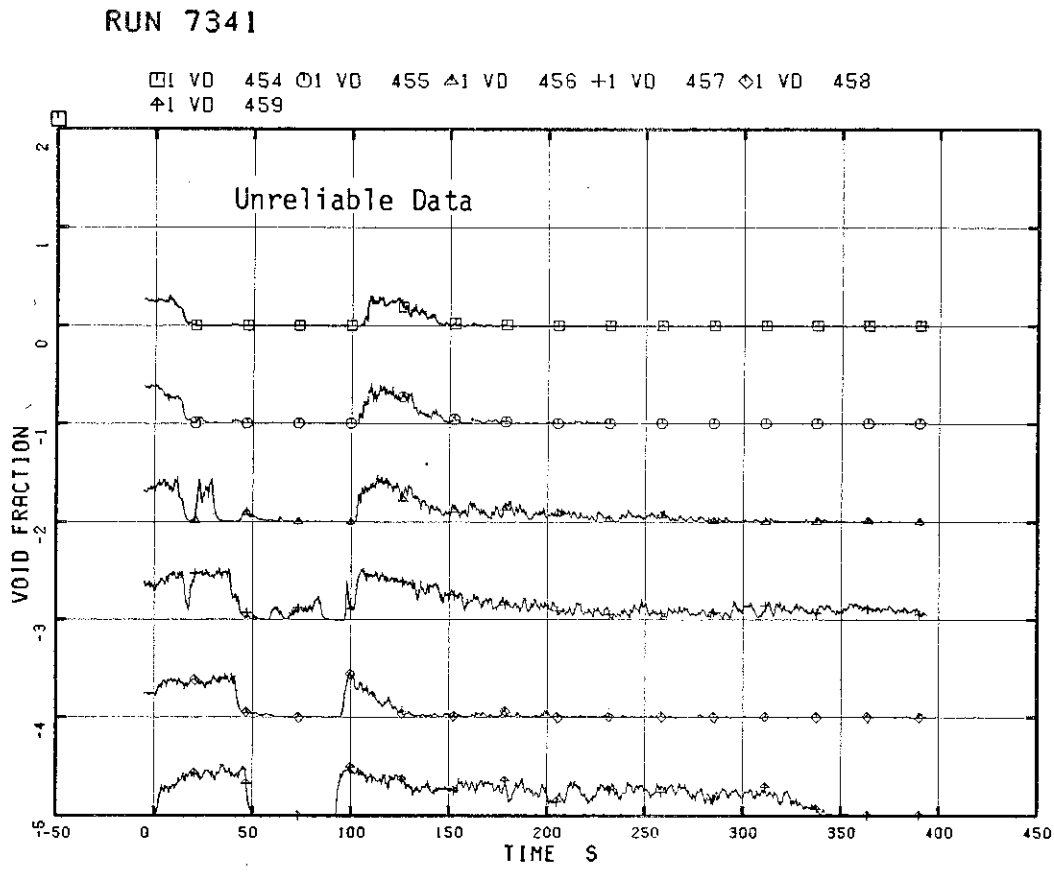

Fig. 5.170 Void Fraction, A55 Rod

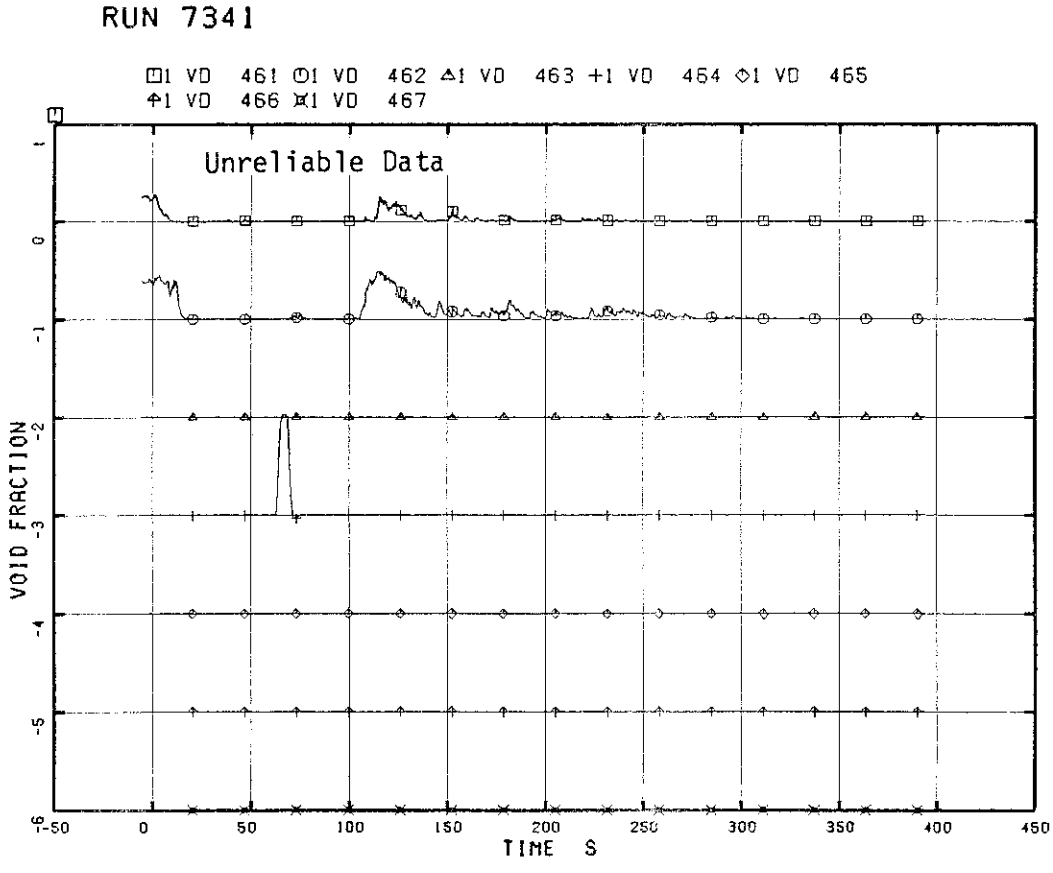

Fig. 5.171 Void Fraction, C55 Rod

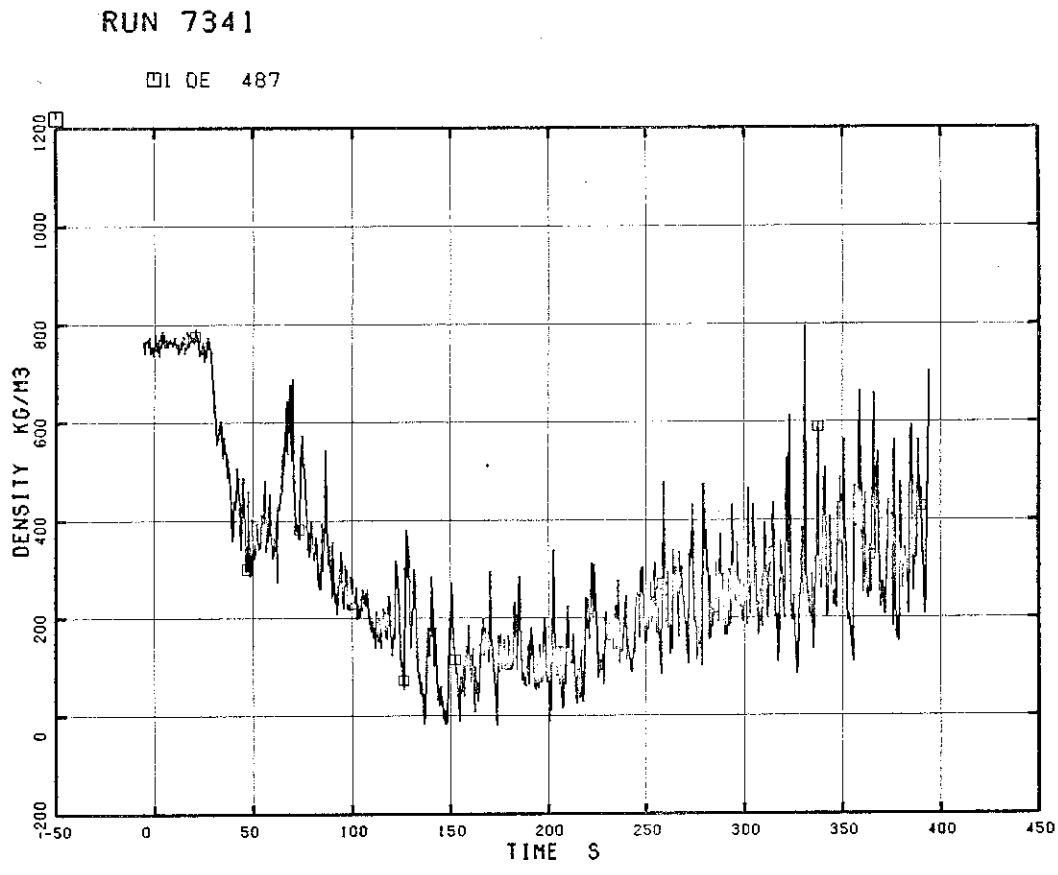

Fig. 5.172 Fluid Density at Intact Loop Jet Pump Outlet, Beam A

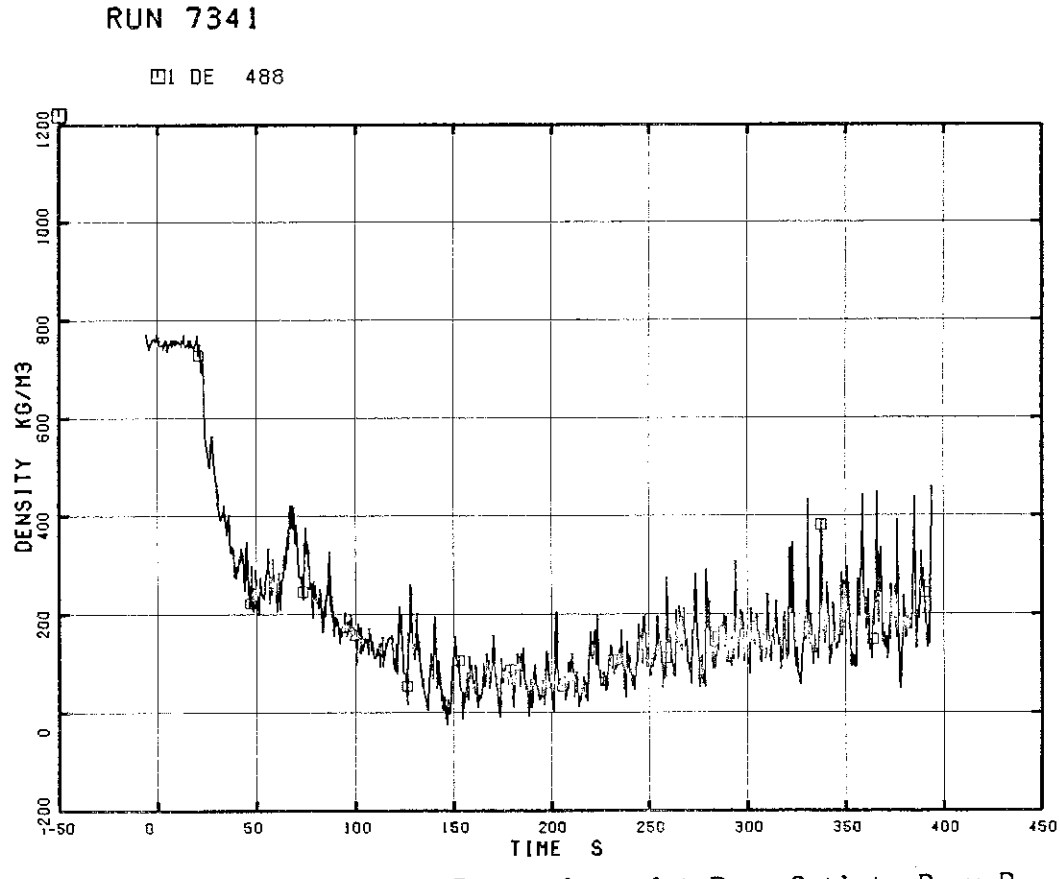

Fig. 5.173 Fluid Density at Intact Loop Jet Pump Outlet, Beam B

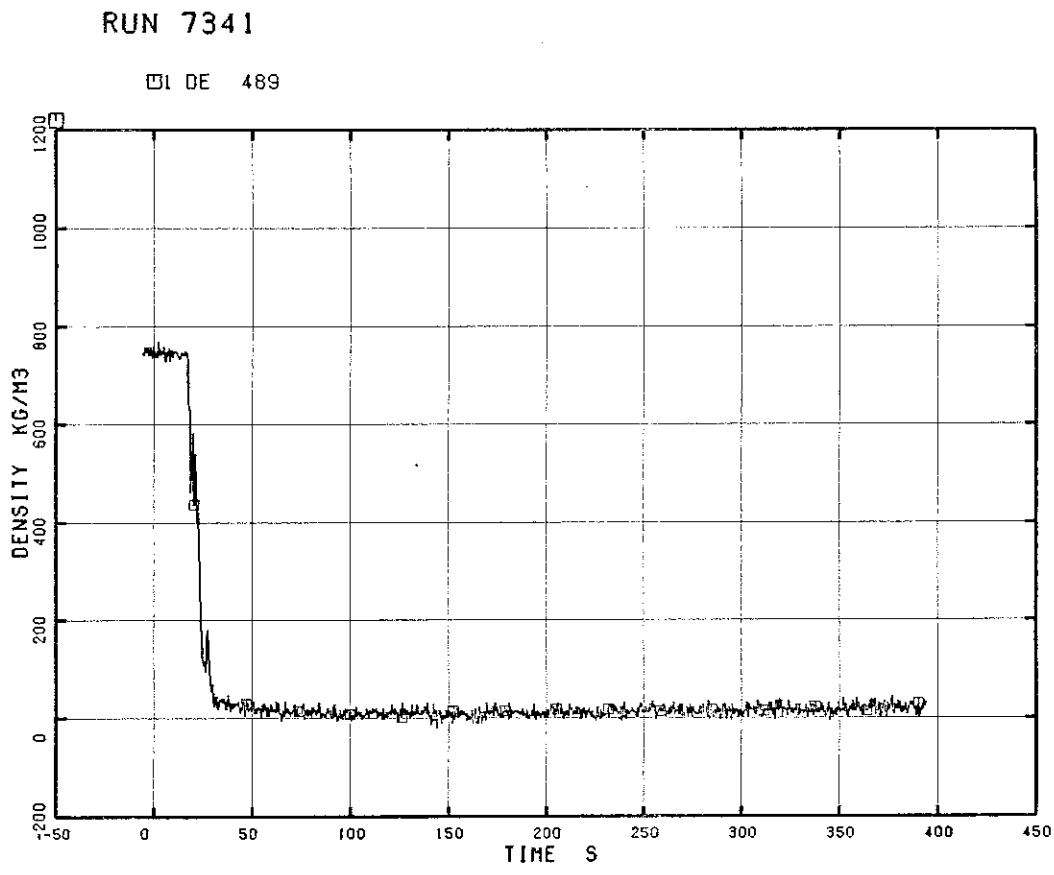

Fig. 5.174 Fluid Density at Intact Loop Jet Pump Outlet, Beam C

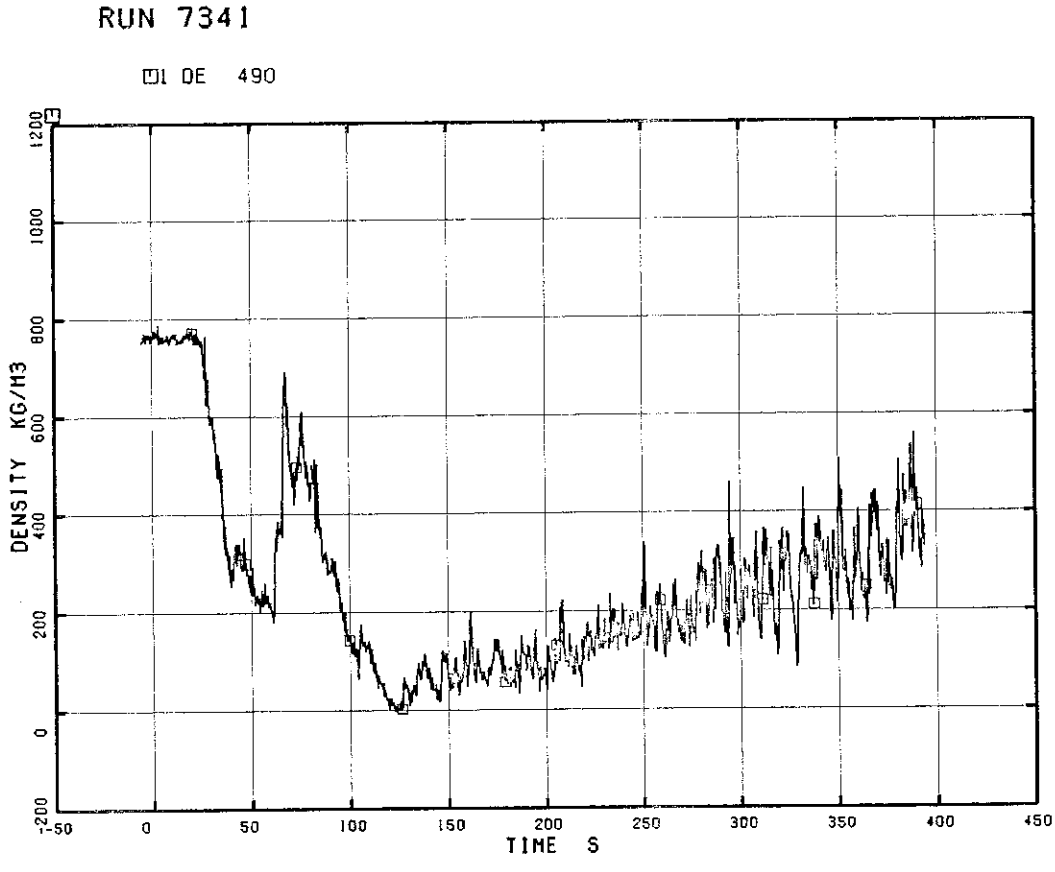

Fig. 5.175 Fluid Density at Broken Loop Jet Pump Outlet, Beam A

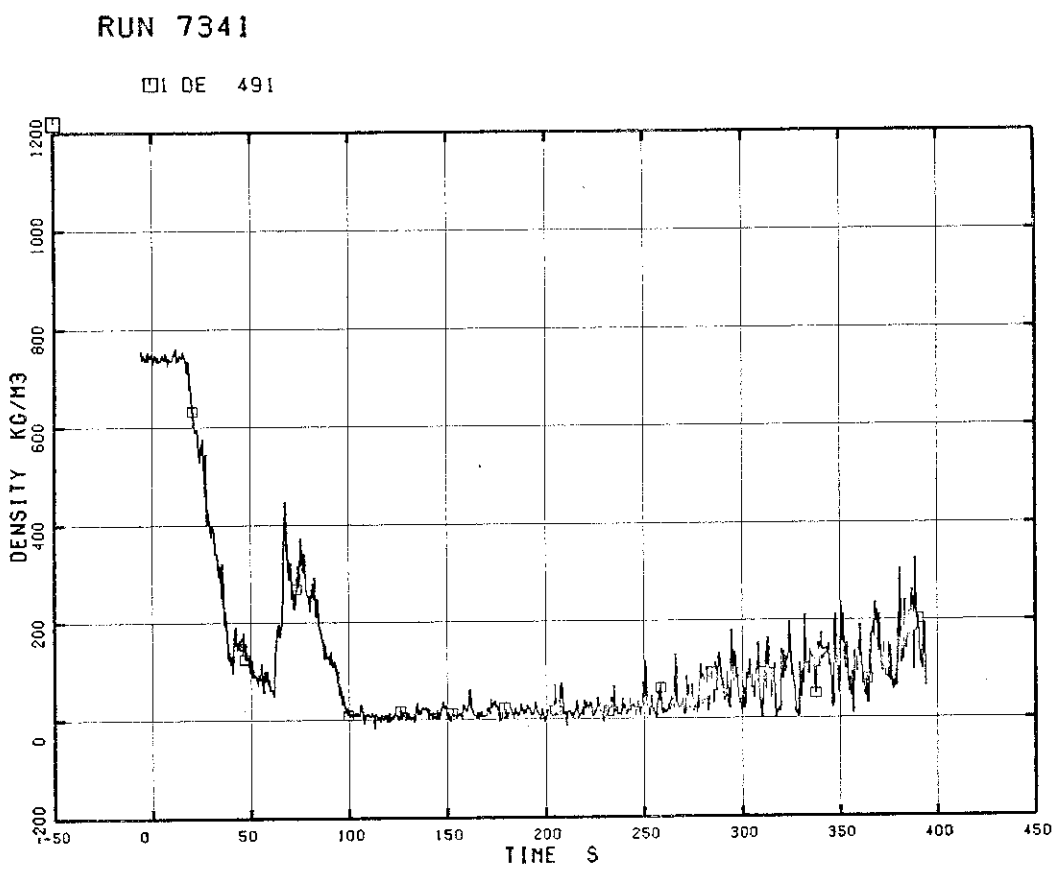

Fig. 5.176 Fluid Density at Broken Loop Jet Pump Outlet, Beam B

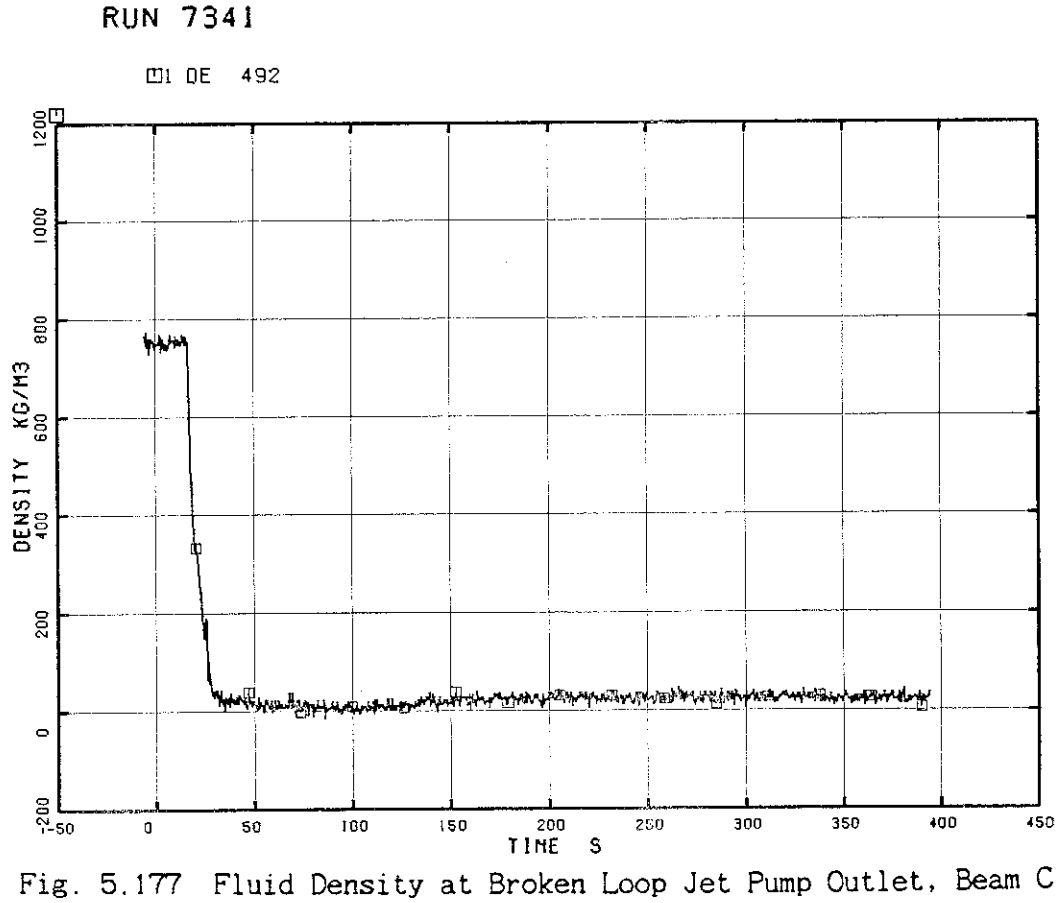

Fig. 5.177 Fluid Density at Broken Loop Jet Pump Outlet, Beam C

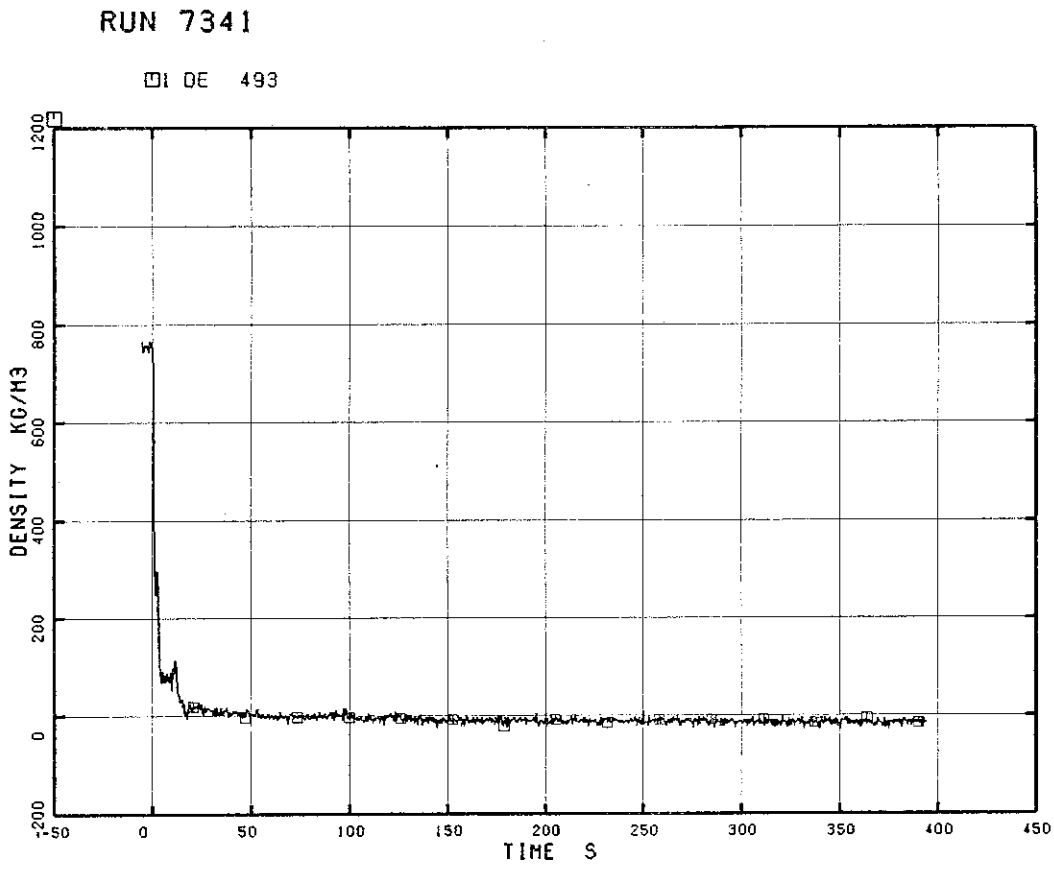

Fig. 5.178 Fluid Density at Pump Side Break, Beam A

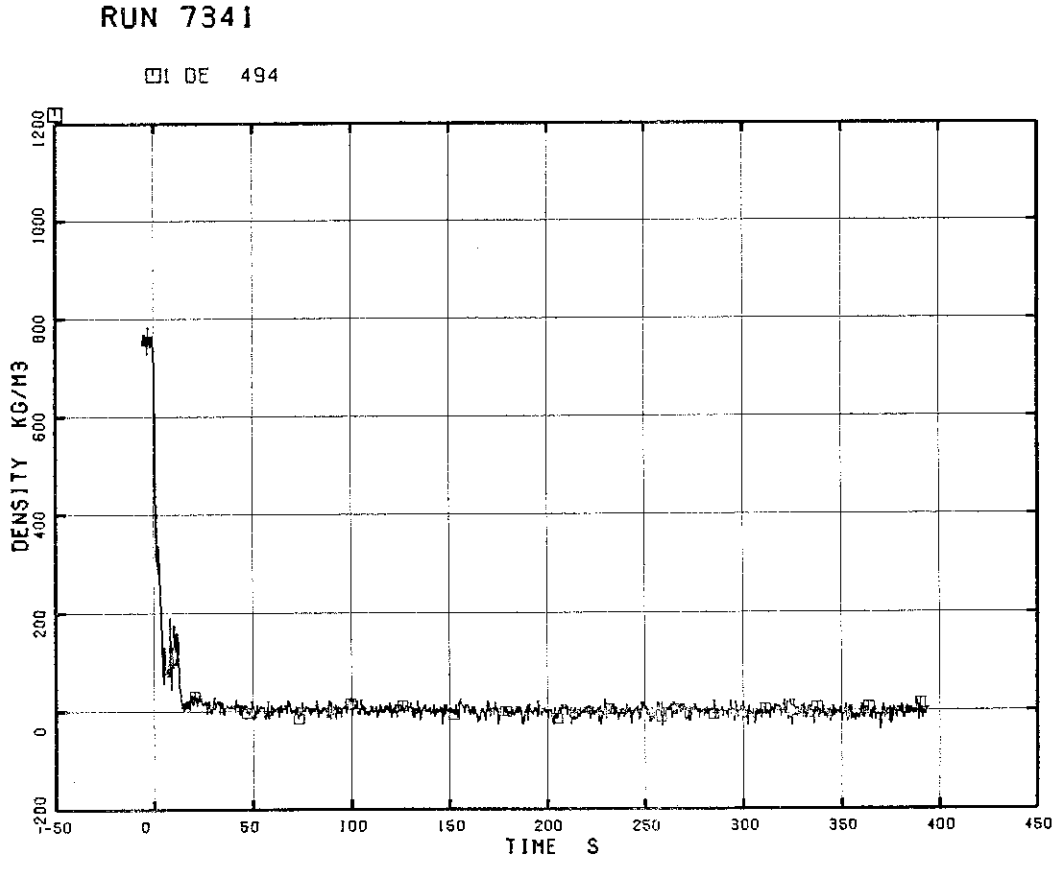

Fig. 5.179 Fluid Density at Pump Side Break, Beam B

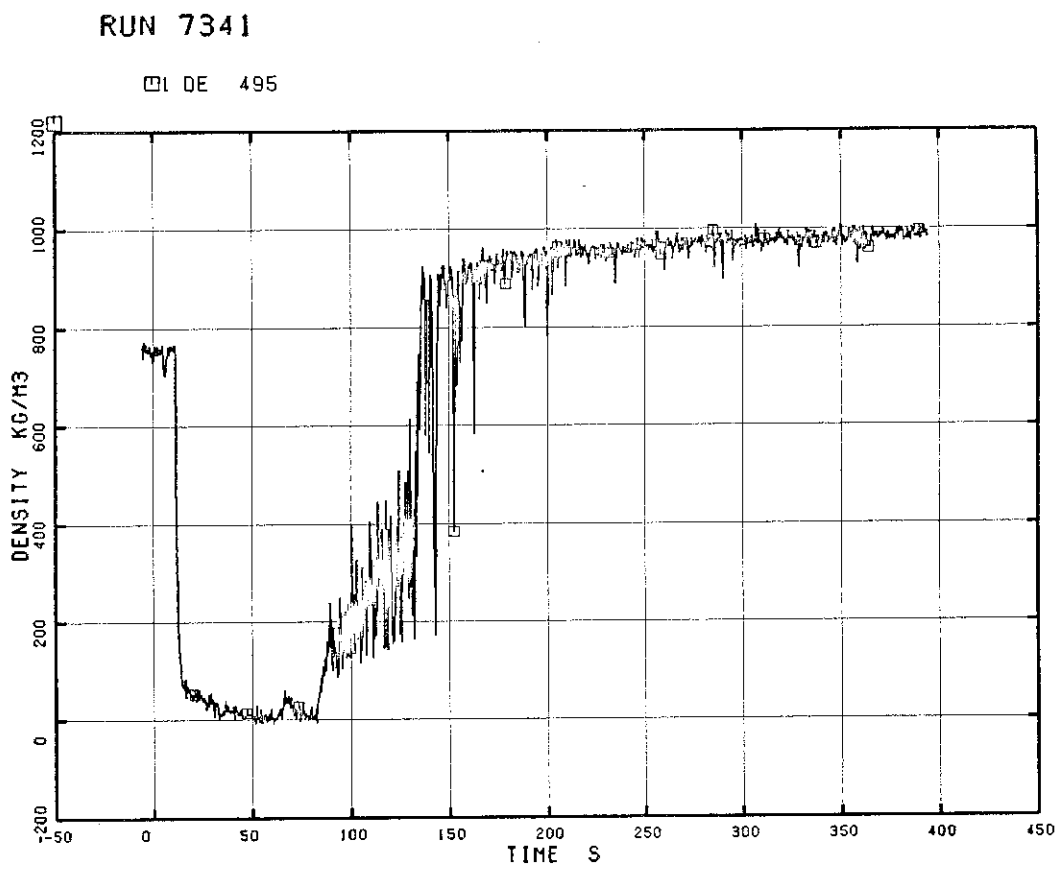

Fig. 5.180 Fluid Density at Vessel Side Break, Beam A

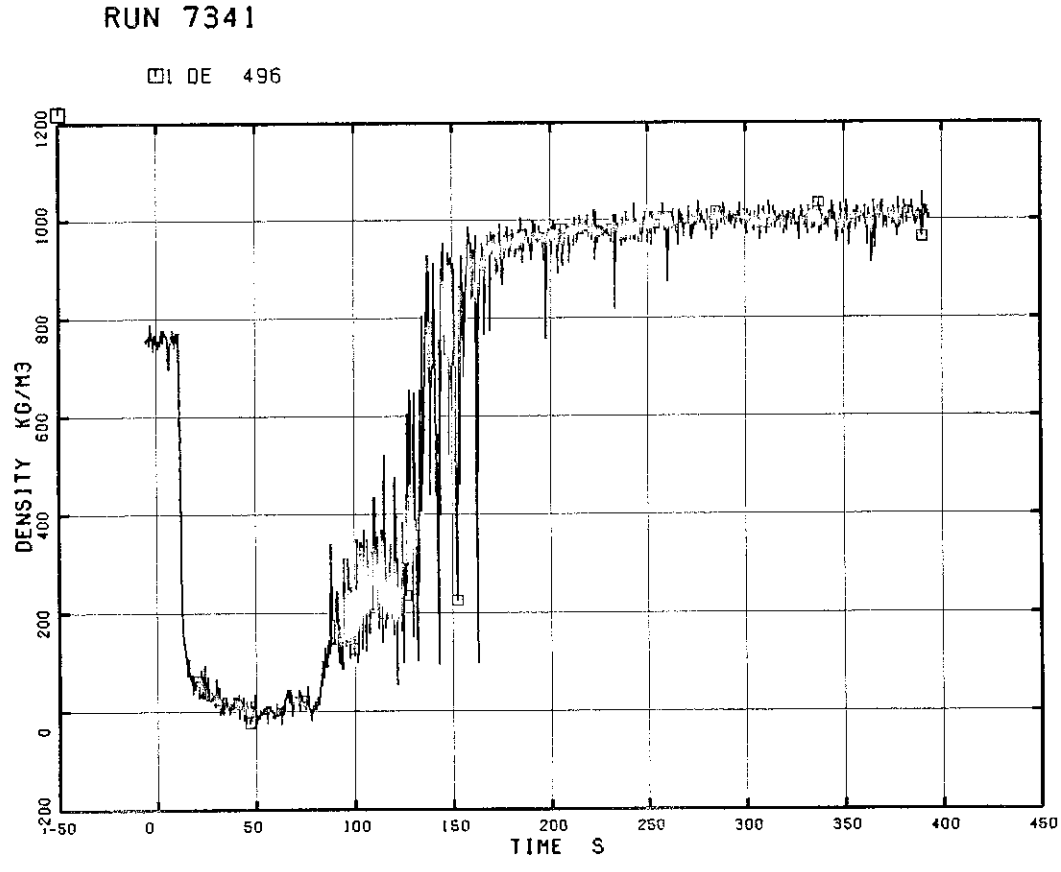

Fig. 5.181 Fluid Density at Vessel Side Break, Beam B

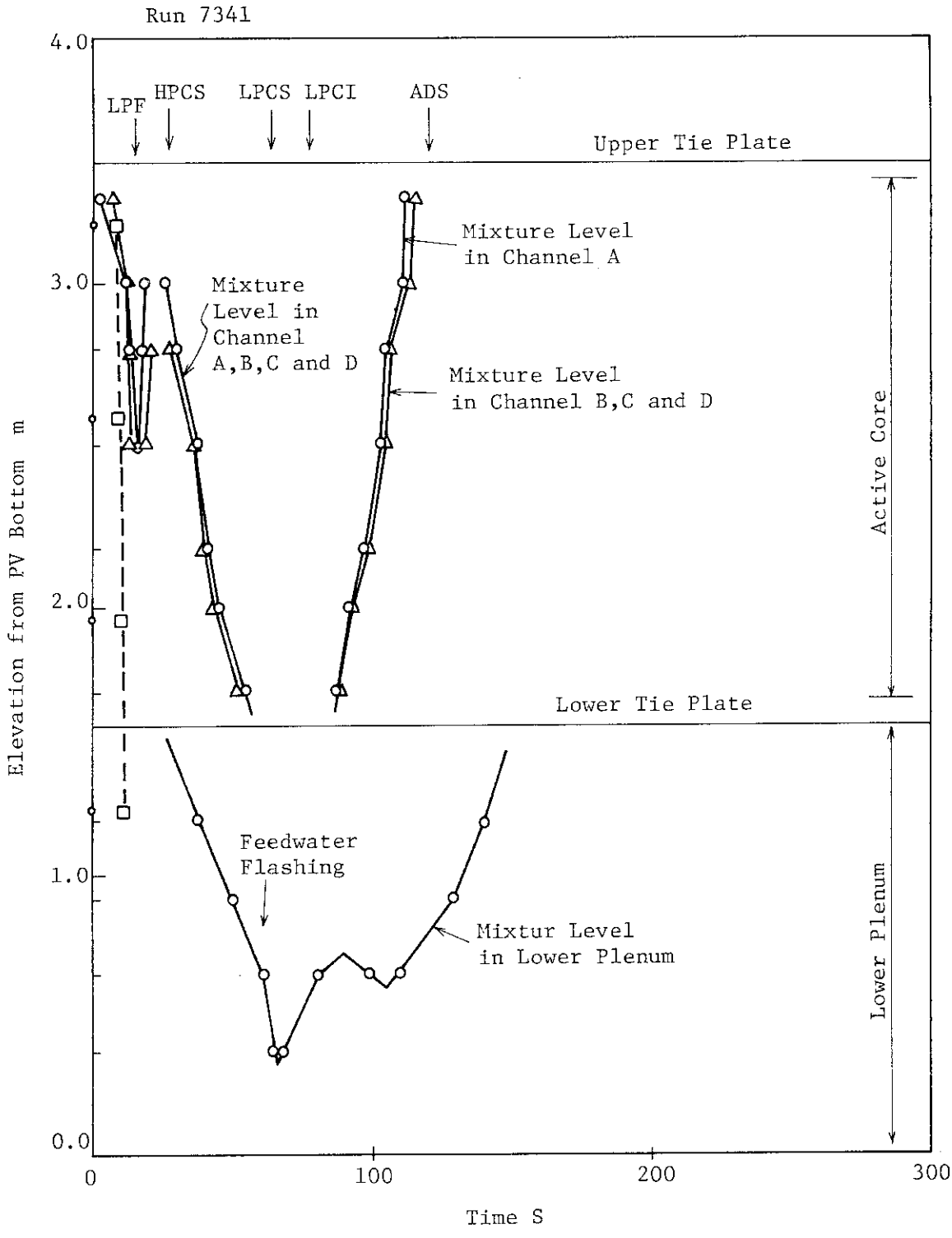

Fig. 5.182 Estimated Liquid Level in Pressure Vessel

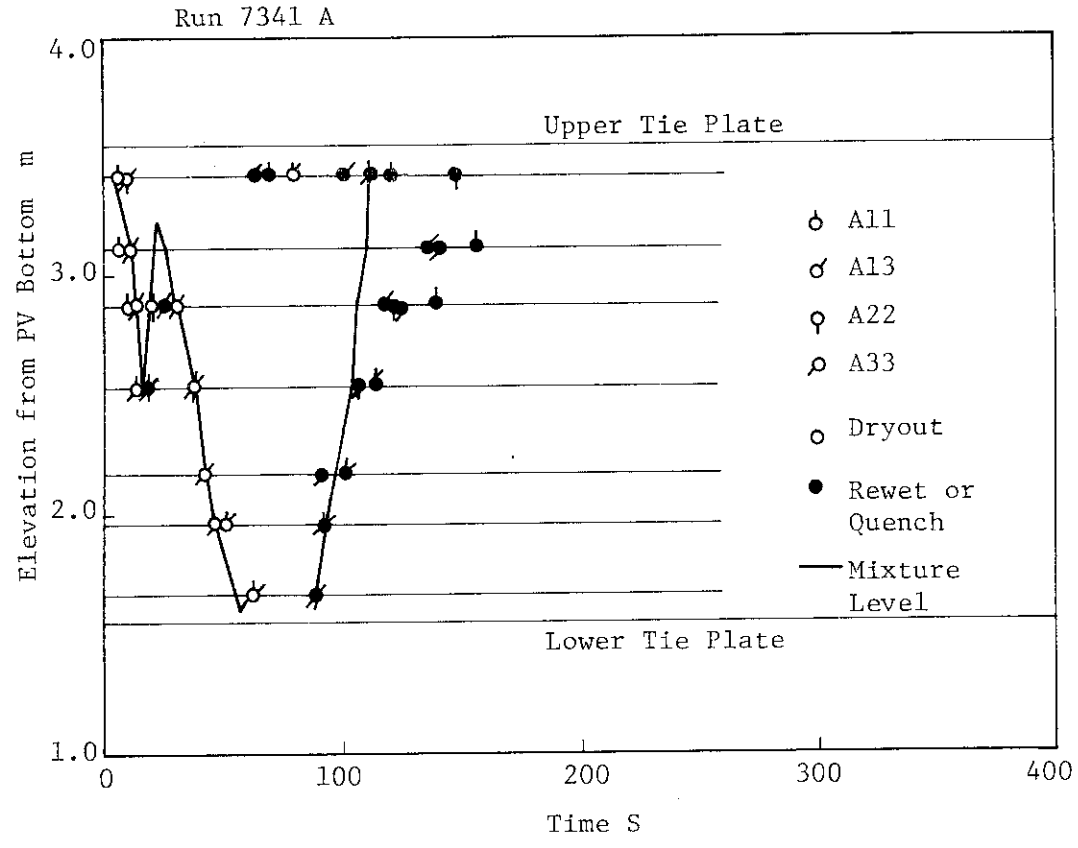

Fig. 5.183 Dryout and Quench Transients in Channel A

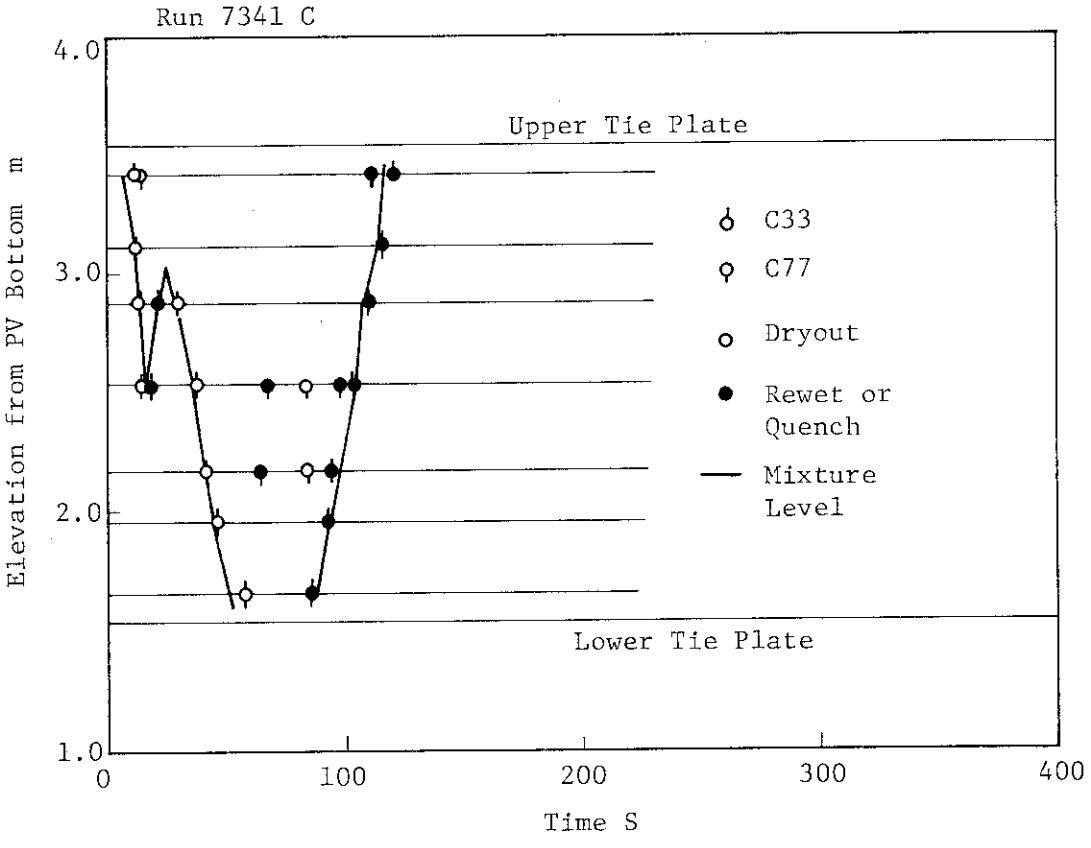

Fig. 5.184 Dryout and Quench Transients in Channel C

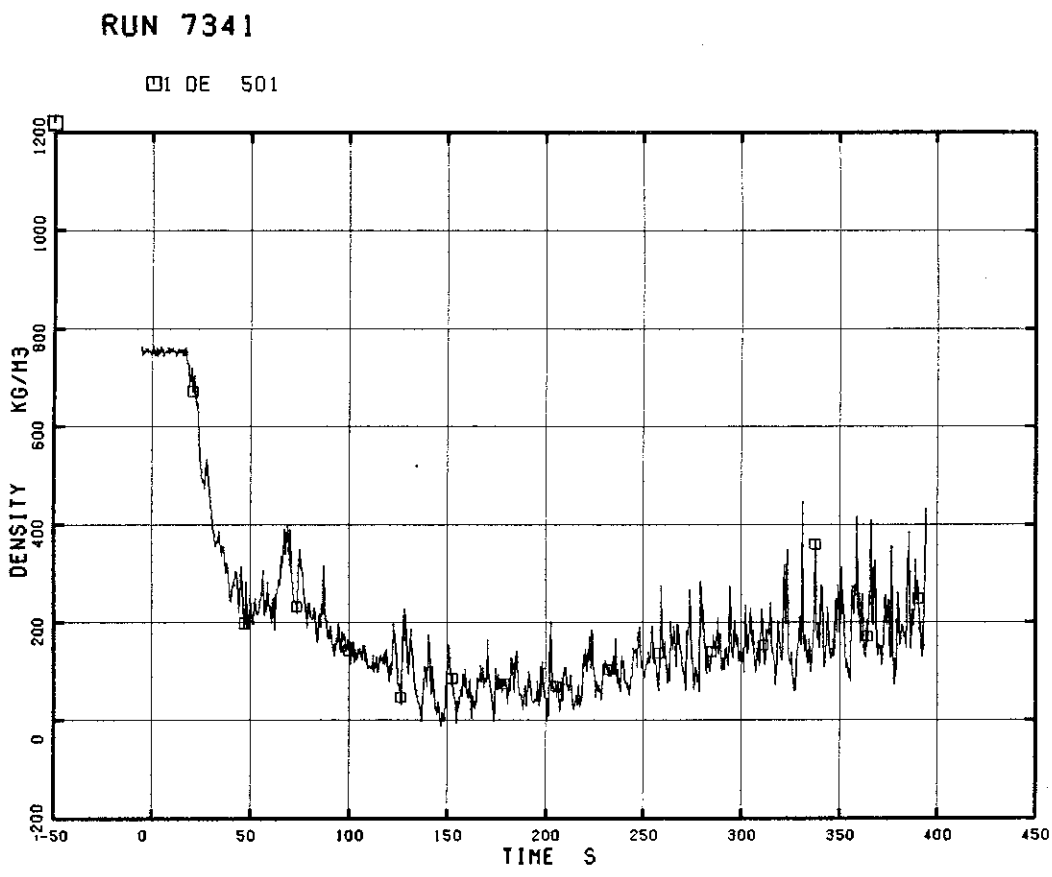

Fig. 5.185 Average Density at Intact Loop Jet Pump Outlet

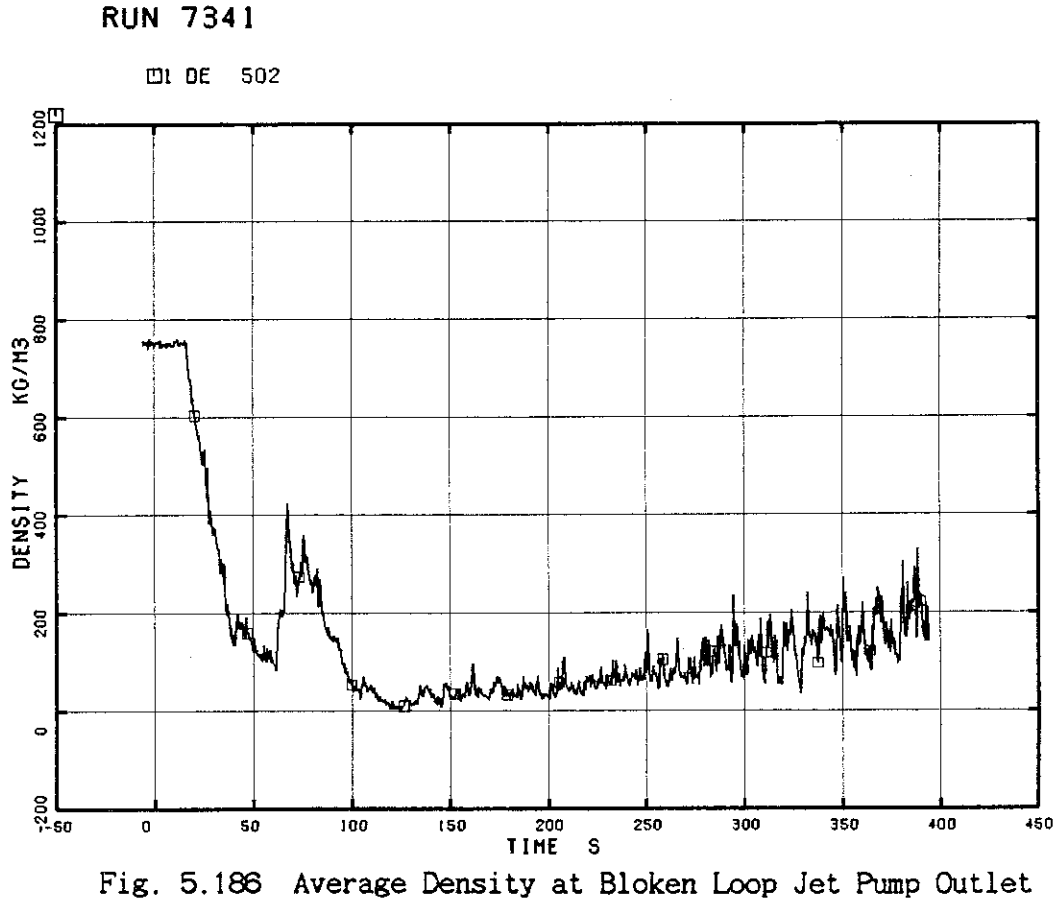

Fig. 5.186 Average Density at Bloken Loop Jet Pump Outlet

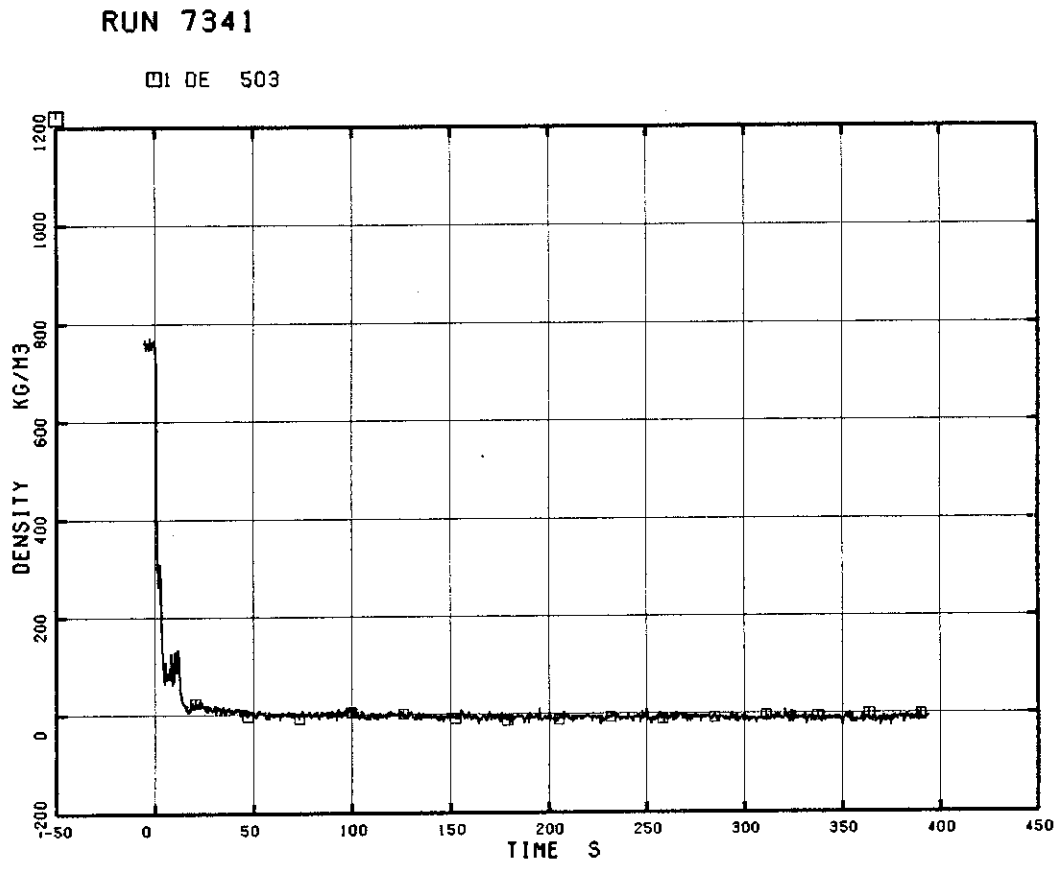

Fig. 5.187 Average Density at Pump Side Break

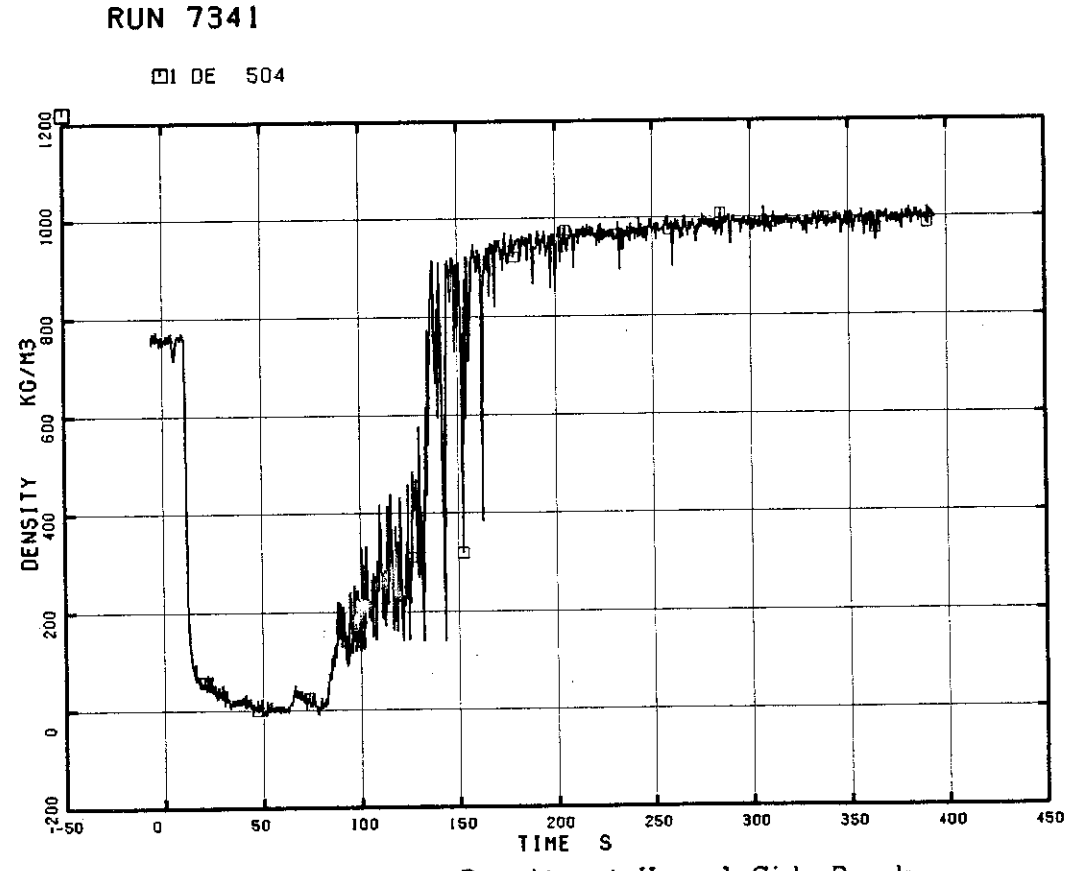

Fig. 5.188 Average Density at Vessel Side Break

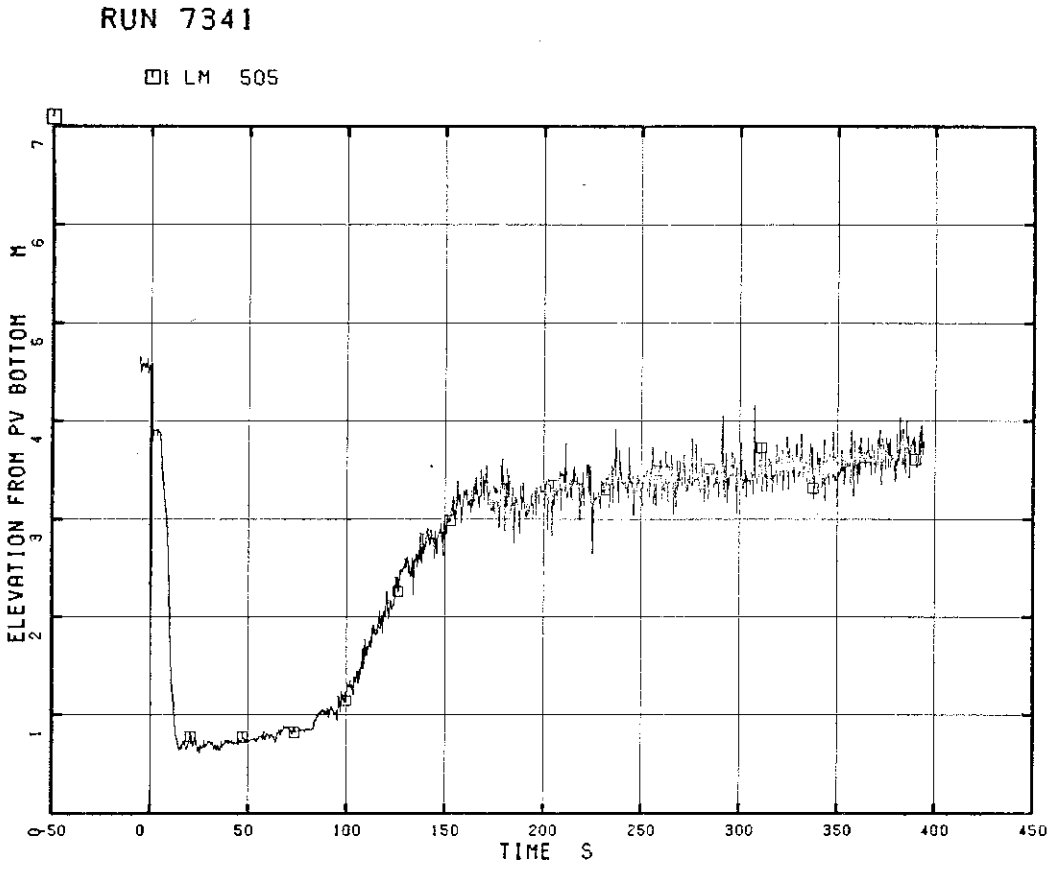

Fig. 5.189 Liqud Level Outside Shroud

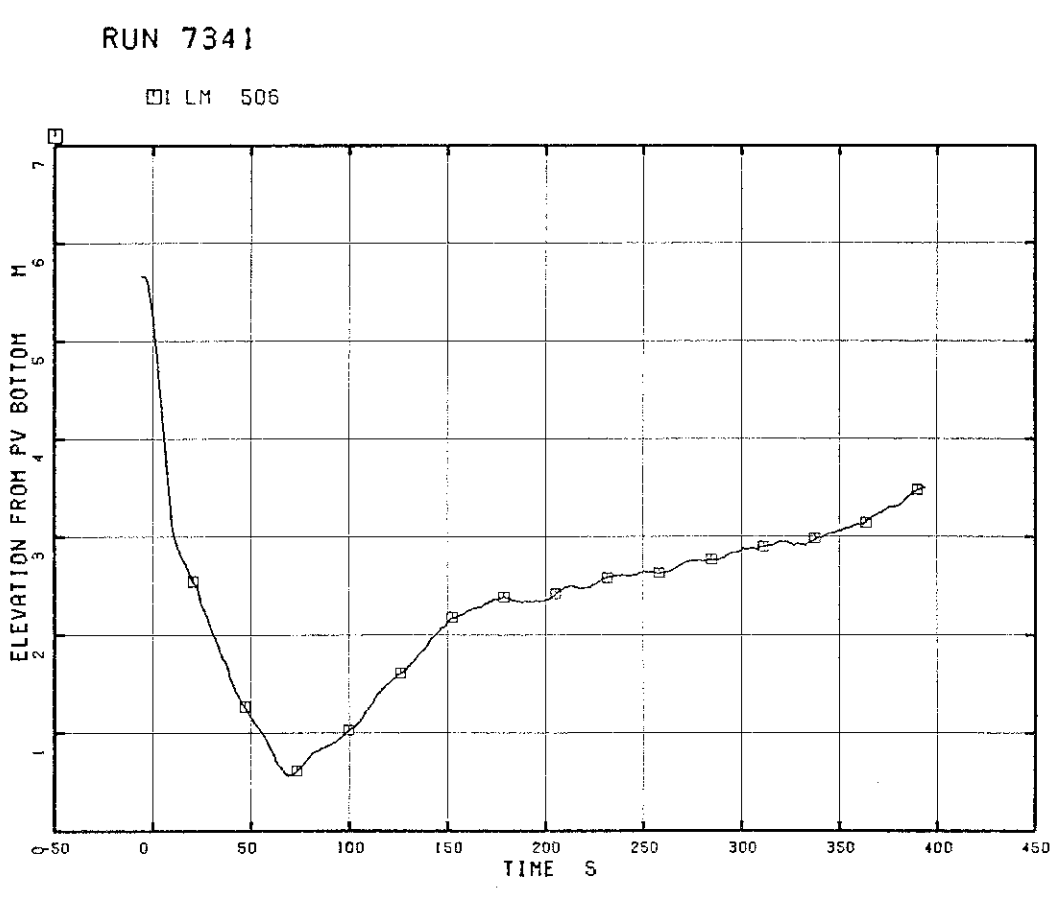

Fig. 5.190 Liqud Level Inside Shroud

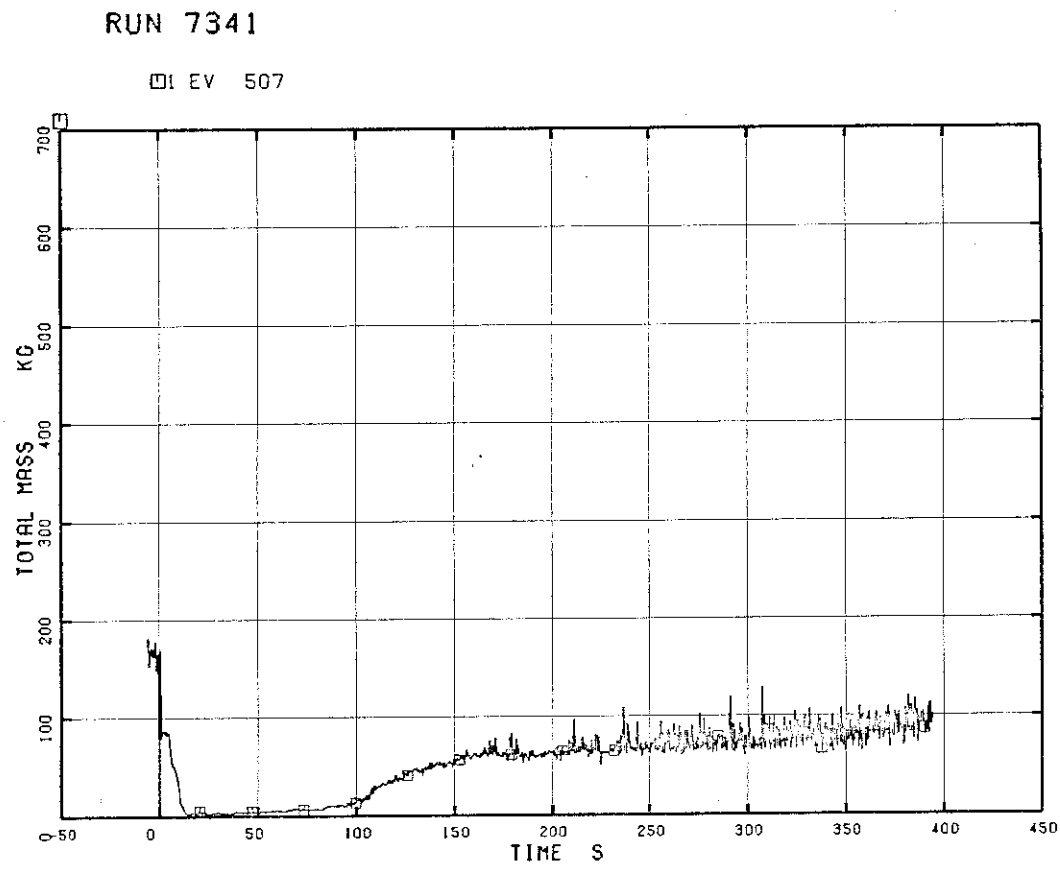

Fig. 5.191 Fluid Inventory Outside Shroud

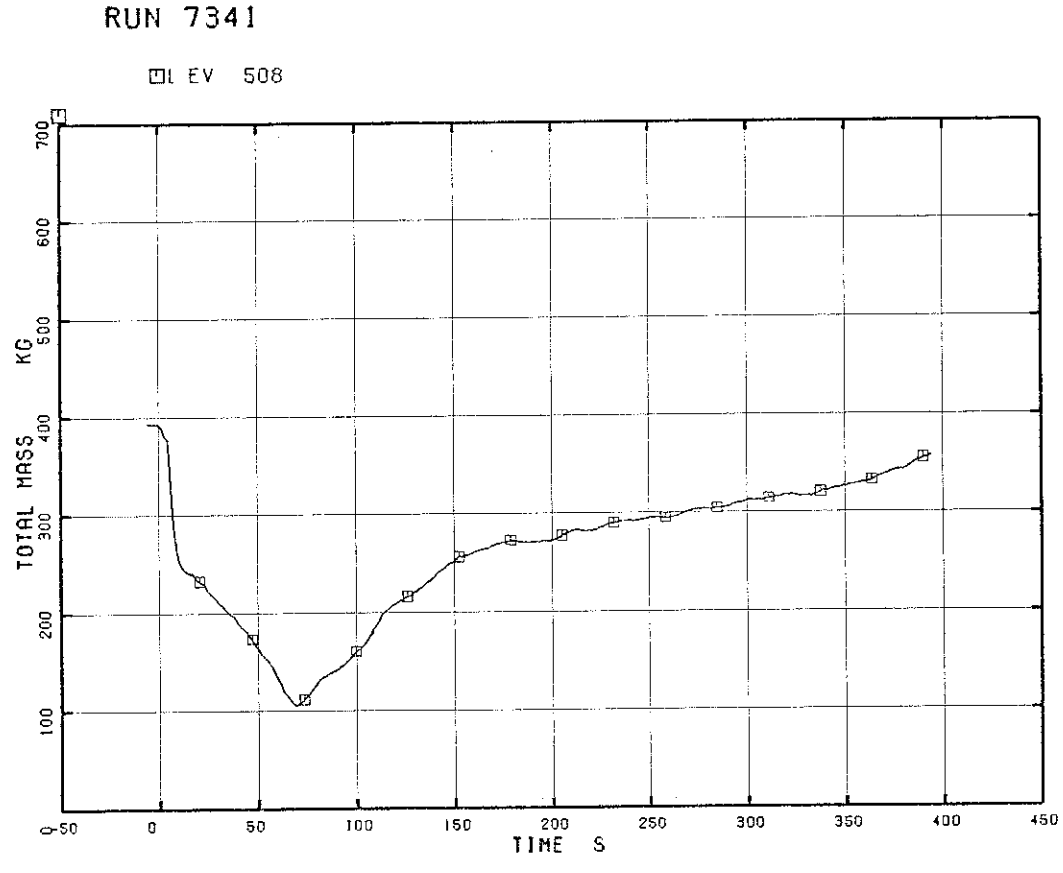

Fig. 5.192 Fluid Inventory Inside Shroud

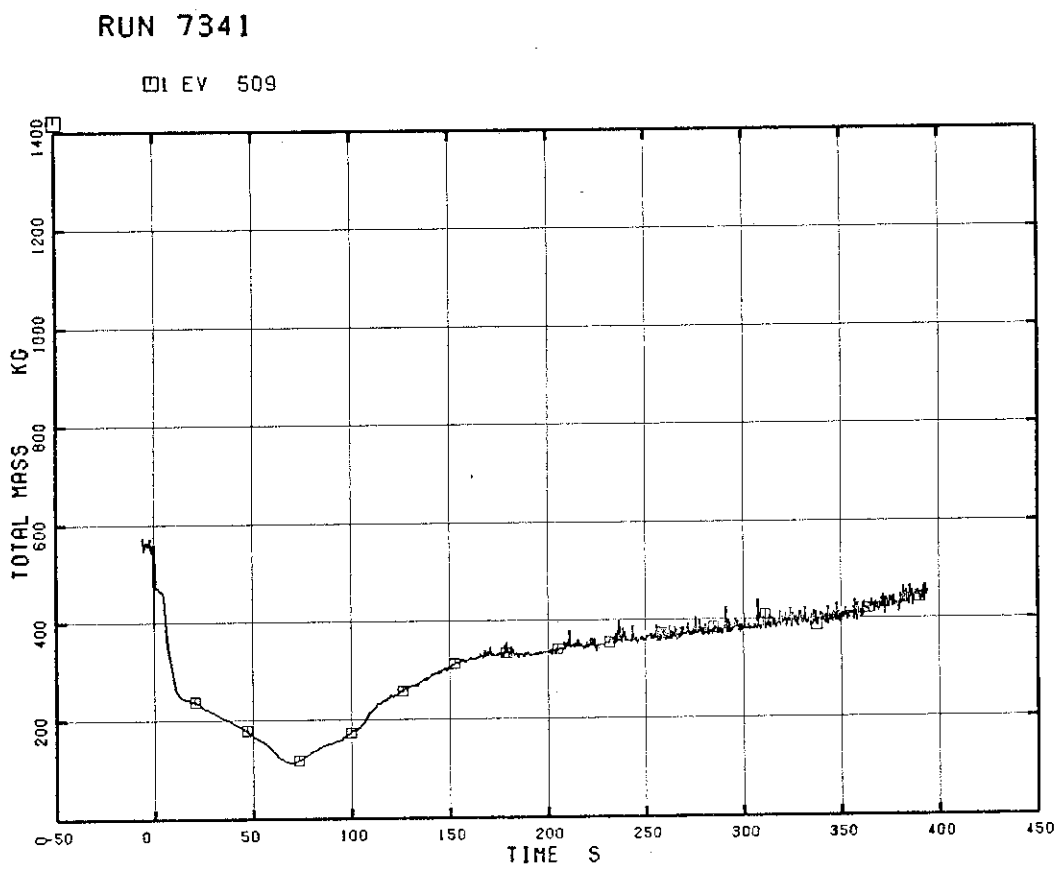

Fig. 5.193 Total Fluid Mass in Pressure Vessel

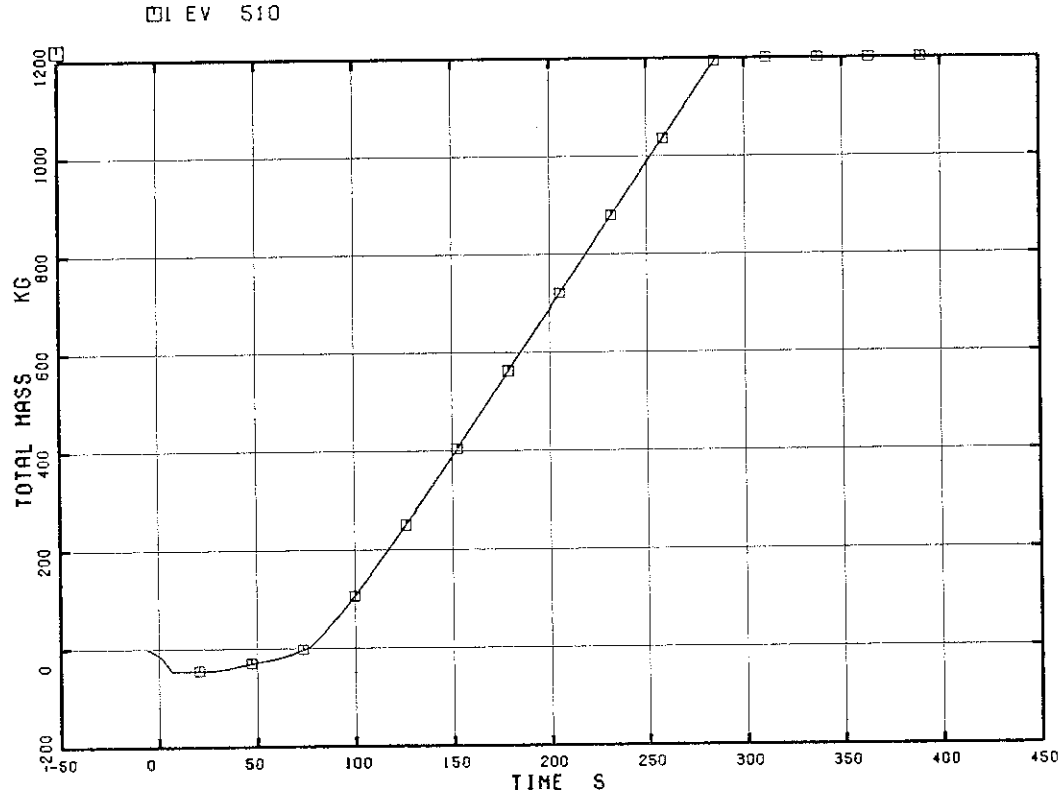

Fig. 5.194 Fluid Mass Increase by the ECCS and the Feedwater Flow and Decrease by the Steam Discharge Flow

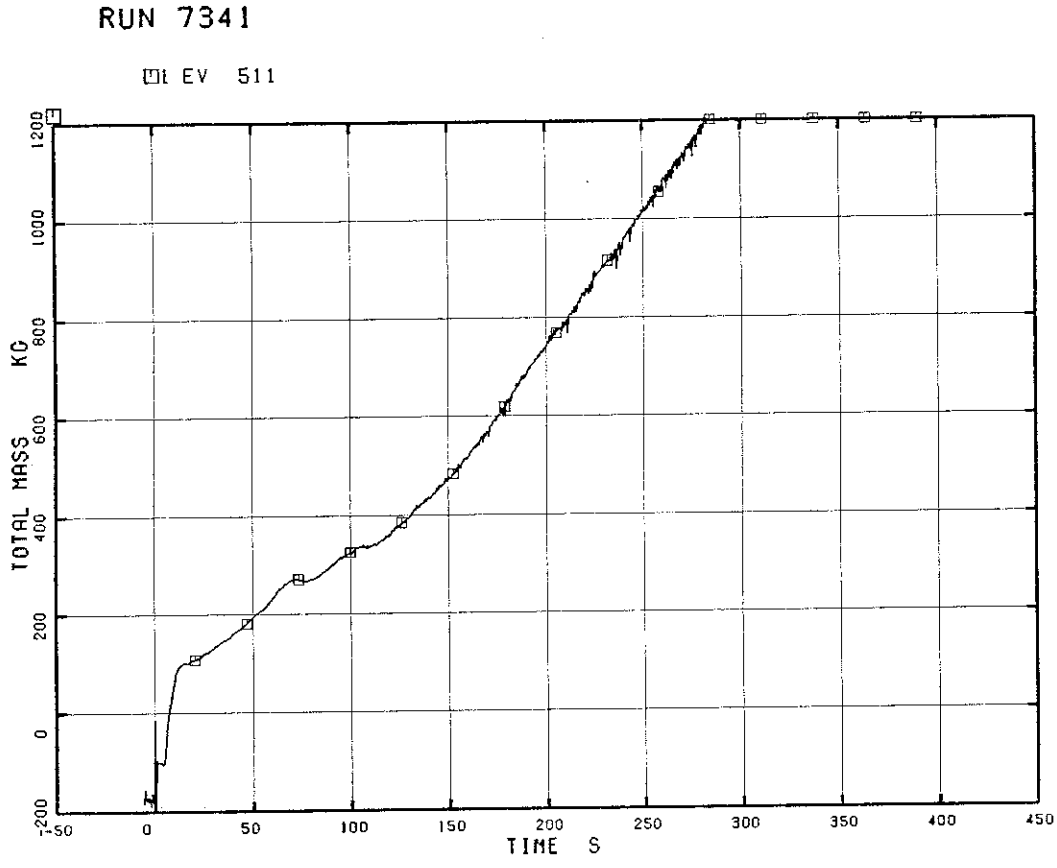

Fig. 5.195 Fluid Mass Discharged from the Break

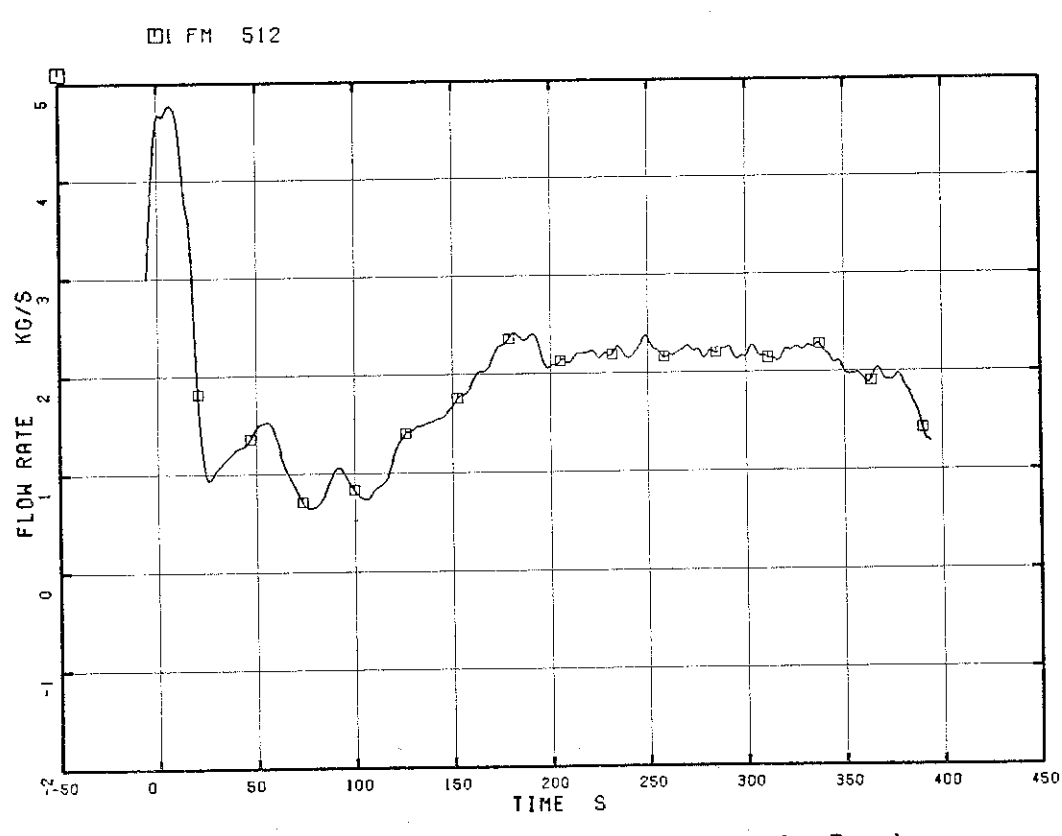

Fig. 5.196 Discharged Flow Rate from the Break